

# **Ephemeral river systems at the Skeleton Coast, NW-Namibia**

**Sedimentological and geomorphological studies on the braided river dominated Koigab Fan, the Cenozoic succession in the Uniabmond area and comparative studies on fluvio-aeolian interaction between ephemeral rivers and the Skeleton Coast Erg**

Dissertation zur Erlangung des  
naturwissenschaftlichen Doktorgrades der  
Bayerischen Julius-Maximilians-Universität Würzburg



vorgelegt von

**Carmen Krapf**  
aus Arnstein

**Würzburg 2003**

**Eingereicht am:**

**1. Gutachter:** PD Dr. Harald Stollhofen

**2. Gutachter:** Prof. Dr. Volker Lorenz

**1. Prüfer:** Prof. Dr. L Lorenz

**2. Prüfer:** Prof. Dr. D. Busche

**Tag der Prüfung (öffentlicher Vortrag und Disputation):** 18.06.2003

**Doktorurkunde ausgehändigt am:** \_\_\_\_\_

|   |           |
|---|-----------|
| <b>Table of contents</b> .....  | <b>1</b>  |
| <b>Acknowledgements</b> .....   | <b>5</b>  |
| <b>Abstract</b> .....   | <b>7</b>  |
| <b>German Summary</b> .....   | <b>9</b>  |
| <br>  |           |
| <b>1 Introduction</b> .....   | <b>11</b> |
| 1.1 Objective of the study .....  | 11        |
| 1.2 Overview of the study area .....  | 11        |
| 1.2.1 Location .....  | 11        |
| 1.2.2 Climate .....   | 13        |
| 1.2.2.1 Precipitation and temperature.....  | 13        |
| 1.2.2.2 Wind as a geological factor .....   | 15        |
| <br>  |           |
| <b>2 Geological setting</b> .....   | <b>18</b> |
| 2.1 Palaeo- to Middle Proterozoic rocks.....  | 20        |
| 2.2 Late Proterozoic Pan-African Damara metamorphic rocks.....                      | 20        |
| 2.3 Etendeka Group .....  | 21        |
| 2.3.1 Twyfelfontein Formation .....   | 21        |
| 2.3.2 The Etendeka Igneous Province.....  | 22        |
| 2.4 Cenozoic deposits .....   | 23        |
| 2.4.1 Red Canyon Formation: Tertiary Red-beds .....                                 | 23        |
| 2.4.2 Whitecliff Formation: Plio- to Pleistocene carbonate-cemented sediments ..... | 24        |
| 2.4.3 Uniabmond Formation: Pleistocene semi- to unconsolidated sediments.....       | 24        |
| 2.4.4 Skeleton Coast Erg (Late Pleistocene).....                                    | 25        |
| 2.4.5 Holocene deposits .....   | 26        |
| 2.4.5.1 Ephemeral river deposits .....  | 26        |
| 2.4.5.2 Aeolian sediments and landforms .....                                       | 26        |
| 2.4.5.3 Marine terraces and coastal sabkhas .....                                   | 28        |
| 2.5 Tectonic setting.....   | 28        |
| <br>  |           |
| <b>3 Methods</b> .....  | <b>30</b> |
| 3.1 Field studies .....   | 30        |
| 3.2 Remote sensing data, image processing and data interpretation .....             | 31        |
| 3.3 Laboratory analysis.....  | 31        |

|   |           |
|---|-----------|
| <b>4 The ephemeral braided river dominated Koigab Fan .....</b>                                 | <b>33</b> |
| 4.1 Significance and setting of the Koigab Fan system.....                                      | 33        |
| 4.1.1 Geodynamic framework, tectonic setting and drainage evolution.....                        | 35        |
| 4.1.2 Catchment and source area characteristics .....   | 35        |
| 4.1.3 Depositional site and climate .....   | 38        |
| 4.1.4 Drainage system of the Koigab Fan .....   | 38        |
| 4.2. Fan Morphology .....   | 39        |
| 4.2.1 Principal anatomy and dimensions of the Koigab Fan .....                                  | 39        |
| 4.2.2 Channel and surface characteristics of the Koigab Fan .....                               | 42        |
| 4.2.2.1 Koigab River and Koigab Canyon Poort .....  | 42        |
| 4.2.2.2 The lower Koigab River - active channel of the Koigab Fan.....                          | 43        |
| 4.2.2.3 Abandoned channels of the Koigab Fan.....   | 46        |
| 4.3 Sedimentological processes shaping the Koigab Fan.....                                      | 47        |
| 4.3.1 Sedimentological characteristics of the active channel .....                              | 47        |
| 4.3.2 Ancient fluvial sequences of the Koigab Fan .....   | 49        |
| 4.3.3 Fluvio-aeolian interaction affecting the Koigab Fan surface.....                          | 50        |
| 4.4 Interaction of the fan with the marine environment .....                                    | 56        |
| 4.4.1 Active channel and oceanic interaction .....  | 56        |
| 4.4.2 Flanking shoreline barriers and coastal sabkhas.....                                      | 57        |
| 4.5 The Koigab Fan compared to other fans and rivers along the Namibian coast.....              | 59        |
| 4.6 Classification of the Koigab Fan and comparison with worldwide fans and<br>fan systems..... | 61        |
| 4.6.1 Fan, terminal fan or fan-delta?.....  | 62        |
| 4.6.2 Position and contrasts within alluvial fan classifications .....                          | 62        |
| 4.7 Koigab Fan: significance for Precambrian and Early Palaeozoic fans.....                     | 65        |
| 4.8 Conclusion .....  | 66        |
| <br>  |           |
| <b>5 The Cenozoic succession in the Uniabmond area.....</b>                                     | <b>68</b> |
| 5.1 The Uniab River system and the Uniabmond area .....   | 68        |
| 5.1.1 Catchments and source area characteristics.....   | 69        |
| 5.1.2 Climate and flood characteristics.....  | 70        |
| 5.2 The lithostratigraphic framework of the Uniabmond area .....                                | 70        |
| 5.3 Red Canyon Formation.....   | 73        |
| 5.3.1 Waterfall Member .....  | 74        |
| 5.3.2 Bone-Area Member.....   | 76        |
| 5.3.3 Tectonic structures .....   | 77        |
| 5.3.4 Interpretation and age estimates.....   | 78        |
| 5.4 Whitecliff Formation .....  | 80        |
| 5.4.1 Facies of the Whitecliff Formation .....  | 82        |
| 5.4.1.1 Fluvial facies .....  | 82        |
| 5.4.1.2 Aeolian facies .....  | 85        |
| 5.4.1.3 Marine facies .....   | 86        |
| 5.4.2 Investigated sections and outcrops of the Whitecliff Formation .....                      | 90        |
| 5.4.2.1 Waterfall and C2 section .....  | 90        |
| 5.4.2.2 Red Canyon Exit section A .....   | 93        |



|  |            |
|--|------------|
| 5.4.2.3 Red Canyon Exit section B .....  | 95         |
| 5.4.2.4 Red Canyon Exit section C .....  | 95         |
| 5.4.2.5 Bivalves section.....  | 96         |
| 5.4.2.6 Whitecliff section in C5c.....   | 97         |
| 5.4.2.7 Palaeo-dunefield in the main channel .....   | 98         |
| 5.4.3 A combined litho- and cyclo-stratigraphic correlation approach for<br>the deposits of the Whitecliff Formation.....                | 101        |
| 5.4.4 Age estimate for the Whitecliff Formation .....  | 104        |
| 5.3.5 Red-beds and calcified sediments in the lower Kharu-Gaiseb River –<br>equivalents of the Red Canyon and Whitecliff Formation ..... | 105        |
| 5.5 Uniabmond Formation.....   | 107        |
| 5.5.1 Facies of the Uniabmond Formation.....   | 109        |
| 5.5.1.1 Fluvial Facies .....   | 109        |
| 5.5.1.2 Aeolian Facies .....   | 117        |
| 5.5.1.3 Marine Facies .....  | 121        |
| 5.5.2 Stratigraphic subdivision of the Uniabmond Formation.....  | 125        |
| 5.5.2.1 Unit 1 .....   | 125        |
| 5.5.2.2 Unit 2 & 3.....  | 126        |
| 5.5.2.3 Unit 4.....  | 130        |
| 5.5.3 Tectonic structures .....  | 131        |
| 5.5.4 A fan model for the continental deposits of the Uniabmond Formation .....  | 131        |
| 5.5.5 Age constrains for the Uniabmond Formation.....  | 136        |
| 5.6 Skeleton Coast Erg and Uniabpoort deposits .....   | 138        |
| 5.7 Modern day sediments.....  | 138        |
| 5.8 Summary and conclusions .....  | 139        |
| <br>   |            |
| <b>6 A comparison of fluvio-aeolian interactions between ephemeral rivers<br/>and the Skeleton Coast Erg .....</b>                       | <b>143</b> |
| 6.1 Varieties of ephemeral rivers and aeolian interaction .....  | 147        |
| 6.2 Koigab and the southern margin of the Skeleton Coast Erg.....  | 147        |
| 6.2.1 Koigab River and Koigab Fan .....  | 147        |
| 6.2.2 Southern margin of the Skeleton Coast Erg.....   | 150        |
| 6.3 Uniab .....  | 154        |
| 6.4 Hunkab.....  | 157        |
| 6.5 Hoanib .....   | 161        |
| 6.6 Hoarusib.....  | 164        |
| 6.7 The river systems and their settings compared .....  | 165        |
| 6.7.1 Similarities .....   | 165        |
| 6.7.1.1 Climatic setting .....   | 165        |
| 6.7.1.2 Wind regime .....  | 165        |
| 6.7.1.3 River style .....  | 166        |
| 6.7.2 Differences .....  | 166        |
| 6.7.2.1 Skeleton Coast Erg anatomy .....   | 166        |
| 6.7.2.2 The catchment areas of the investigated ephemeral rivers.....  | 168        |
| 6.7.2.2.1 The size of the catchment areas.....   | 169        |
| 6.7.2.2.2 Precipitation in the catchment areas .....   | 169        |

---

|  |            |
|--|------------|
| 6.7.2.2.3 The geology of the catchment areas .....                         | 169        |
| 6.7.2.2.4 Depositional architecture and longitudinal river gradients ..... | 170        |
| 6.8 Conclusions.....   | 172        |
| <br>   |            |
| <b>7 References .....</b>  | <b>174</b> |
| <br>   |            |
| <b>Appendix .....</b>  | <b>189</b> |
| <br>   |            |
| <b>Circulum Vitae .....</b>  | <b>201</b> |

**ACKNOWLEDGEMENTS**

I am grateful to many people who supported and encouraged me during my dissertation. To all of them I want to express a very special “THANK YOU”.

First of all, I would like to thank my supervisor PD Dr. Harald Stollhofen for the opportunity to carry out this study. He encouraged me right from the start to present the results of this study at national and international conferences and was the initiator of the international publications. I appreciate his motivating cooperation and his assistance whenever it was needed. I also want to thank him for his help and co-operation during fieldwork and for the many 'lekker potjies' cooked on the campfire!

My co-supervisor Dr. Ian Stanistreet (Liverpool) is gratefully thanked for numerous helpful and inspiring observations, discussions and suggestions throughout the entire study, especially during writing papers and field work in the remote, foggy Skeleton Coast.

I would like to thank Prof. Volker Lorenz for his support during office and field work and his open ‘volcanic’ mind for sedimentological and geomorphological problems.

I am very grateful to the rangers of the Skeleton Coast, John Paterson & Alwin Engelbrecht, for showing me the secret roads of the park, providing me with all kinds of information concerning weather data or driving techniques for traversing the dunes of the Skeleton Coast Erg. John and his wife Barbara are thanked for their hospitality and for many cups of rooibush-tea. Mareli Grobler (former ranger at Ugabgate) is thanked for her great hospitality during first years field work, for homelike evenings after the lonesome field campaigns and for her wonderful shower. Many thanks also to the staff at Ugabgate and Springbokwasser Gate, especially to Whity.

A very special thanks to Claus Zeller and Bernd Schlicker for joint work, great fellowship, laughing, talking, discussing, arguing, dancing and good music from Claus famous 'African tape' during and after field work. Many thanks also to Johan Svendsen for accompanying fieldwork and many helpful discussions about fluvio-aeolian interaction.

The Geological Survey of Namibia, in particular Gabi Schneider and Wulf Hegenberger, is thanked for logistical support during fieldwork. A special thanks to Holger Kolberg from the Ministry of Tourism and Environment providing the research permit and the free entry permit for the Skeleton Coast Park. Mr. Klöble (German Embassy in Windhoek) is thanked for organising the research visa for Namibia.

Many thanks to the staff from Terrace and Torra Bay, in particular to Werner and Daniel. They provided us with accommodation, showers, chocolate bars, cool drinks, African music and saved our car from being drowned in the Atlantic Ocean.

Thanks for weather data information, accommodation and fan belt rescue to the people of Wereldsend (it's definitely not the end of the world!).

I'm grateful for having the opportunity to spend two days at the Desert Research Foundation of Namibia in Gobabeb. John Henschel, his wife and the staff provided me with many helpful information about the Cenozoic deposits at the Kuiseb River and about the ecology of the Namib desert.

Many Namibians supported me logistically and with their friendship: Lucia Sheimi (Ombalantu), Frenus, Sybille and Raphael (owners of the most wonderful backpacker in the world situated in Swakopmund), Carlos Peres, his family, Pedro (the biggest Michael Schuhmacher fan in whole southern Africa!), Henny, Björn and the whole staff from the Provenance Camp (Noordoewer), Burger Oelofsen and his youngest son, Coenie Nolte and his family (Keetmanshoop), Thiunes Cotzeé (Khumib Camp), Robert (Toscanini), the staff from the Engen petrol station in Hentjes Bay, the 'pad scrubber team' from road C34, and finally Karl & Freda Steiner (Windhoek) who know everything about and almost everyone in Namibia.

The study was funded by the German Research Foundation (DFG) through the Postgraduate Research Project 'Geoscience research in Africa' and by the Bayerische Julius-Maximilians-Universität Würzburg through the HWP-programme ("Programm Chancengleichheit für Frauen in Forschung und Lehre). Special thanks to Prof. Dr. Martin Okrusch, who initiated the Postgraduate Research Project and to Prof. Dr. Reiner Klemd, who was the leader of this project for the last two years. Many thanks also to Gisela Kaiser (Frauen- und Gleichstellungsbüro der Universität Würzburg) who provided helpful information about the HWP-programme.

Angelika Kirchner, Jutta Lingstädt and Maike Dörnemann are thanked for their brilliant administrative support.

Hildegard Schöning and Klaus Weppeler are thanked for taking photographs of sand samples and thin sections. Many thanks to Peter Späthe and Brigitte Wienen (RWTH Aachen) for their excellent preparation of thin sections.

A special thank to Prof. Peter Kukla and the staff of the Department of Geology, RWTH Aachen for their support during the final phase of this thesis.

Many thanks for the assistance, help and friendship I received from my colleagues from the Postgraduate Research Project and from the Department of Geology/Univ. Würzburg: Heike Klock, Jürgen Kempf, Andreas Eizenhammer, Michael Schlirf, Stephen White, Ansgar Wanke, Matthias Kukulus, Iris Gehring, Frank Holzförster, Wilfried Joos, Martine Priens, Eberhard Rothfuß and Sandra Roos.

Silke, Moni, Maike, Christina, Johanna, Katja, Rainer, Dirk, Stefan, Astrid and all my other friends are gratefully thanked for many happy hours outside the department.

I'm also grateful to my parents, my sister and her family, my grandmother and my parents in law for their confidence and moral support.

Finally, I want to say thank you to the most important person in my life, my husband Majo. Thanks for your assistance 'round the clock and round the world', endless and most inspiring discussions, patience, freedom and love!

**Abstract**

The Skeleton Coast forms part of the Atlantic coastline of NW Namibia comprising several ephemeral rivers, which flow west-southwest towards the Atlantic Ocean. The area is hyper-arid with less than 50 mm average annual rainfall and a rainfall variability of 72%. Therefore, the major catchment areas of the rivers are about 100-200 km further inland in regions with relatively high annual rainfall of 300-600 mm. The coastal plain in the river downstream areas is characterized by a prominent NNW trending, 165 km long belt of 20-50 m high, locally compound, barchanoid and transverse dunes. This dune belt, termed Skeleton Coast Erg, starts abruptly with a series of barchans and large compound dunes 15 km north of the Koigab River and extends from 2-5 km inland sub-parallel to the South Atlantic margin of NW Namibia over a width of 3-20 km. As the SSE-NNW trending dune belt is oriented perpendicular to river flow, the dunefield dams and interacts with the west-southwestward flowing ephemeral river systems. This study focused on three main topics: 1) investigation and classification of the Koigab Fan, 2) the investigation of the Cenozoic succession in the Uniabmond area and 3) comparative studies of fluvio-aeolian interaction between five ephemeral rivers and the Skeleton Coast Erg.

Sedimentological and geomorphological investigations show that the Koigab Fan represents a yet undocumented type of a braided fluvial fan system, which operates in an arid climatic, tropical latitude setting, is dominated by ephemeral mixed gravel/sand braided rivers, lacks significant vegetation on the fan surface, has been relatively little affected by human activity, is a perfect study site for recording various types of fluvio-aeolian interaction and thereby acts additionally as a model for certain Precambrian and Early Palaeozoic fan depositional systems deposited prior to the evolution of land plants.

The Cenozoic succession in the Uniabmond area consists of three major unconformity-bounded units, which have been subdivided into the Red Canyon, the Whitecliff, and the Uniabmond Formation. The Tertiary Red Canyon Fm. is characterized by continental reddish sediments documenting an alluvial fan and braided river to floodplain depositional environment. The Whitecliff Fm. displays a wide variety of continental and marine facies. This formation provides the possibility to examine fluvio-aeolian interactions and spectacular, steep onlap relationships towards older sediments preserved in ancient seacliffs. The Whitecliff Fm. has been subdivided into four sedimentary cycles, which resulted from sea level changes during the Plio- to Middle Pleistocene. The following Uniabmond Fm. provides a unique insight into the depositional history of the NW

Namibian coast during the Last Pleistocene glacial cycle. The formation has been subdivided into four units, which are separated by unconformities controlled by sea level changes. Unit 1 represents deposits of an Eemian palaeo-beach. The overlying Units 2-4 build up the sedimentary body of the Uniab Fan, again a braided river dominated fan, which is nowadays degraded and characterized by deeply incised valleys, deflation surfaces and aeolian landforms. The Uniabmond Fm. is overlain by the dunes of the Skeleton Coast Erg, whose development is related to the Last Glacial Maximum (LGM).

The damming of river flow by aeolian landforms has been previously recognized as one of several principal types of fluvio-aeolian interaction. Five ephemeral rivers (from S to N: Koigab, Uniab, Hunkab, Hoanib, Hoarusib), which variously interact with the Skeleton Coast Erg, were chosen for the purpose of this study to consider the variability of parameters within these fluvio-aeolian systems and the resulting differences in the effectiveness of aeolian damming. The fluvio-aeolian interactions between the rivers and the dune field are controlled by the climate characteristics and the geology of the river catchment areas, the sediment load of the rivers, their depositional architecture, the longitudinal river profiles as well as the anatomy of the Skeleton Coast Erg. Resulting processes are 1) aeolian winnowing of fluvially derived sediments and sediment transfer into and deposition in the erg; 2) dune erosion during break-through resulting in hyperconcentrated flow and intra-erg mass flow deposits; 3) the development of extensive flood-reservoir basins caused by dune damming of the rivers during flood; 4) interdune flooding causing stacked mud-pond sequences; and 5) the termination of the erg by more frequent river floods.

## German Summary

Das hyperaride Gebiet der Skelettküste im NW Namibias ist durch eine Vielzahl ephemerer Flußsysteme und einen über 165 km langen, NNW-streichenden Dünengürtel, den Skelettküsten-Erg, charakterisiert. Der Erg verläuft nahezu orthogonal zu den westwärts, zum Atlantik entwässernden ephemeren Flußsystemen, deren Haupteinzugsgebiete etwa 150-300 km östlich der Küste liegen. Bei ihrem unregelmäßigen Abkommen auf dem Weg zum Atlantischen Ozean müssen die meisten dieser westwärts entwässernden Riviere den Dünengürtel passieren. Aus diesem Grund wurde dieses Gebiet ausgewählt, um vergleichende sedimentologische und geomorphologische Studien durchzuführen, die sich auf folgende drei Schwerpunkte konzentrierten: 1) die Untersuchung und Klassifizierung des Koigab Fans und dessen Rolle für den Sedimenteintrag in den Skelettküsten Erg; 2) die detaillierte Aufnahme und Untersuchung der känozoischen Sedimente im Mündungsbereich des Uniab Riviers und deren Rolle bei der Interpretation von Plio- und Pleistozänen Meeresspiegelschwankungen; und 3) die Erlangung eines grundlegenden Verständnis der zugrundeliegenden Kontrollparameter für die Variabilität von fluvio-äolischen Interaktionen und der daraus resultierenden Sedimentkörpergeometrien.

Im Mündungsbereich des Koigab Riviers befindet sich der Koigab Fan. Dieser ist mit einer Länge von 15 km und einer Breite von 21 km der größte aktive Fan der Skelettküste, der durch einen der westsüdwestwärts entwässernden ephemeren Flußsystemen gebildet wurde. Sedimentologische und geomorphologische Studien an dessen Ablagerungen ergaben, dass es sich bei ihm um einen bis jetzt noch nicht dokumentierten Fan-Typ innerhalb der bestehenden Fan-Klassifikationen handelt. Der Koigab Fan repräsentiert einen von verflochtenen ephemeren Flußrinnen aufgebauten Fan, der keine Anzeichen von Schuttstößen (debris flows) oder mäandrierenden Flußrinnen aufweist. Der Koigab-Fan stellt daher ein Endglied innerhalb des von Stanistreet & McCarthy (1993) zur Fan-Klassifikation aufgestellten Dreieckdiagramms dar. Dem Koigab-Fan kommt eine besondere Bedeutung zu, da er in Bezug auf Größe und Gradienten eine Brücke zwischen der Gruppe kleiner, steil abfallender Fans und den mit nur geringem Gefälle versehenen Mega-Fans schlägt. Trotz seiner Position in den Tropen liegt der Koigab-Fan in einem ariden Gebiet und ist durch eine ausgeprägte Vegetationsarmut gekennzeichnet. Sedimentologische Untersuchungen an seinen Ablagerungen können daher auch als Analogbeispiele für vegetationsfreie früh-proterozoische und früh-paläozoische Fan-Systeme verwendet werden. Zudem stellt der Koigab Fan eine wesentliche Sedimentquelle

für den Skelettküsten Erg dar, was mit Hilfe von Schwermineral- und Korngrößenanalysen nachgewiesen werden konnte.

Die im Mündungsbereich des Uniab Riviers anstehenden Sedimente stellen die am vollständigsten erhaltene und am besten aufgeschlossene känozoische Sedimentabfolge entlang der Küste NW-Namibias dar. Im Rahmen des Promotionsprojektes wurde diese Abfolge erstmals vollständig sedimentologisch bearbeitet und anhand markanter Diskordanzen in drei Formationen unterteilt: die Red Canyon, Whitecliff und Uniabmond Formation. Die tertiäre Red Canyon Fm. ist durch Rotsedimente charakterisiert, die in einem alluvial-fluvialen Milieu abgelagert wurden. Die überlagernde Whitecliff Fm. wird aus vier sedimentären Einheiten aufgebaut. Die älteste und die jüngste Einheit enthalten marine und äolische Ablagerungen, in denen fossile Strandniveaus überliefert sind. Diese können herangezogen werden um die Whitecliff Fm. in das späte Pliozän bis ins mittlere Pleistozän einzustufen. Mit den Sedimenten der Uniabmond Fm. ist höchst wahrscheinlich der letzte glaziale Zyklus des Pleistozäns überliefert. Die jüngsten Sedimente der Uniabmond Fm. werden direkt von dem Skelettküsten Erg überlagert, dessen Bildung mit dem letzten glazialen Meeresspiegel-Tiefstand zusammenfällt.

Das Aufstauen von Flüssen durch Dünen stellt einen Haupttyp fluvio-äolischer Interaktion dar. Fünf ephemeren Flusssystemen, die unterschiedlich mit dem Skelettküsten Erg in Interaktion treten, wurden innerhalb dieser Studie eingehend untersucht, um die Bandbreite fluvio-äolischer Interaktionen und deren zugrundeliegenden Kontrollparameter zu erfassen. Die fluvio-äolischen Interaktionen zwischen den Flüssen und dem Dünenfeld werden kontrolliert durch Klimacharakteristika, die Geologie des Einzugsgebietes, die Sedimentfracht der Flüsse, ihre Ablagerungsarchitektur und die Anatomie des Skelettküsten Ergs. Die zu beobachtenden Prozesse sind 1) äolische Verfrachtung von fluvial antransportiertem Sediment und dessen Ablagerung in dem Erg; 2) die Erosion und Aufarbeitung von Dünen während Durchbruchereignissen; 3) die Bildung ausgedehnter Stauseen; 4) die Flutung von Interdünenbereichen mit der Ablagerung von Ton-Silt-Abfolgen; und 5) die Termination des Ergs durch häufiger auftretende Fluten.



## **1 Introduction**

### **1.1 Objectives of the study**

The hyper-arid coastal area of the Skeleton Coast in NW Namibia is characterized by several ephemeral river systems and an impressive, 180 km long dune belt termed Skeleton Coast Erg. On their way to the Atlantic Ocean, most of these westward draining ephemeral river systems have to pass through the erg, which is arranged perpendicular to them. Therefore, this area provides a perfect site to study modern day fluvio-aeolian interactions between ephemeral rivers and dunes. Comparative studies of five ephemeral rivers at the Skeleton Coast (Koigab, Uniab, Hunkab, Hoanib and Hoarusib) aim to enhance knowledge of the variability of parameters within fluvio-aeolian systems and the resulting differences in the effectiveness of intermittent aeolian dune damming. These interactions play an important role in the shaping of dryland environments. In addition, understanding these processes will help to develop and to improve models for ancient fluvial-aeolian deposits, many of which form important reservoirs for hydrocarbons and groundwater.

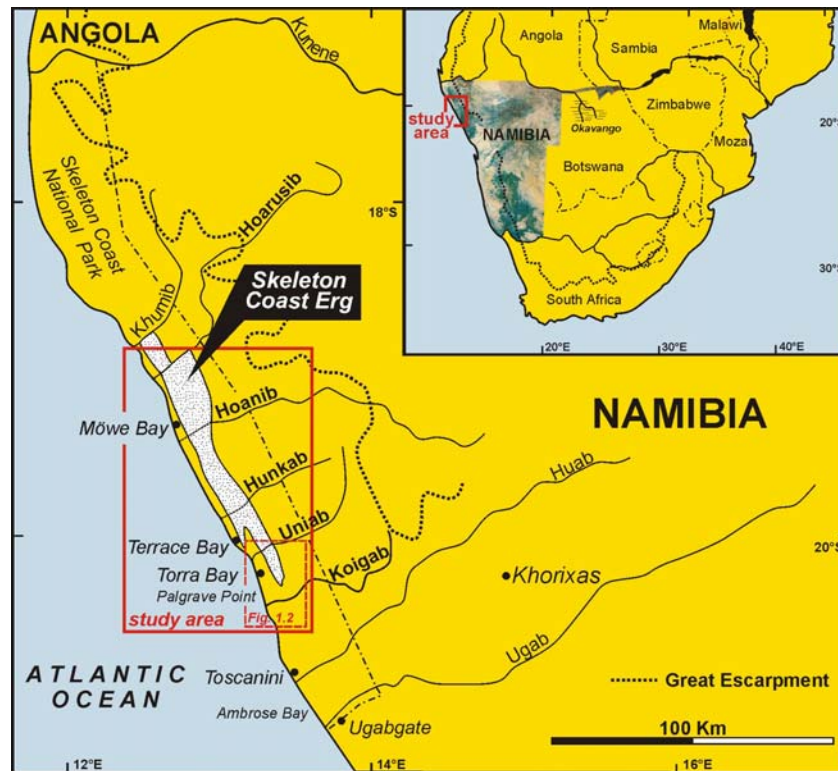
In addition, two of these ephemeral river systems - the Koigab and the Uniab River - have been chosen for detailed sedimentological and geomorphological studies. In the mouth area of the Koigab River the Koigab Fan has developed. It represents a suitable site to describe the morphology and processes of this braided river dominated fan and therefore to widen the knowledge of this barely described fan type. In the mouth area of the Uniab River, the Uniabmond area, various Cenozoic sediments crop out, which have not yet been described in detail. These deposits are considered to provide important information about the Cenozoic evolution of the coastal strip of NW Namibia and to reflect local and possible global climatic and sea-level changes during the Plio- and Pleistocene.

### **1.2 Overview of the study area**

#### **1.2.1 Location**

The study area is situated in NW Namibia at the Skeleton Coast between 19°05' to 20°35' S Latitude and 12°30' E to 13°30' E Longitude. It extends over a distance of 180 km from the Koigab River catchment in the S to the Hoarusib River catchment in the N (Fig. 1.1). The majority of the study area belongs to the Skeleton Coast National Park. Main focus lies on the mouth areas of both the Koigab and Uniab River between 20°05' S to 20°35' S Latitude and 13°05' E to 13°30' E Longitude, with Torra Bay National Campground situated between the two mouth areas of the Koigab and Uniab River (Fig. 1.2). Outcrops suitable for sedimentological studies are located in the variable incised river valleys

themselves and along the microtidal South Atlantic coastline where several seacliffs developed landward of the backshore.



**Fig. 1.1:** Location map of the study area in southern Africa (upper right) and NW Namibia. Frame shows the area of the lower reaches of the Koigab and Uniab River where detailed investigations were carried out.



**Fig. 1.2:** Landsat TM-5 scene 181-074 (30.03.1995; 7-3-1 RGB) showing the main study area at the lower reaches and mouth areas of the Koigab and Uniab River.

## 1.2.2 Climate

The study area is located within southern African tropical latitudes in the western continental, coast-parallel arid zone of the Namib Desert. Within the Namib Desert two main sand seas occur, the main Namib Sand Sea in the southern part and the Skeleton Coast Erg in the northern part. The study areas position within the Skeleton Coast Erg is characterized by the hyperarid but foggy coastal Namib desert climate (LANCASTER, 1982; LANCASTER et al., 1984). The regional climate is strongly influenced by the cool northward flowing Benguela Current and its associated cold-water upwelling systems off the Namibian coastline, causing low humidity of southerly to south southwesterly winds. Additional impact on the regional climate has the subtropical south Atlantic anticyclone and particularly monsoonal influences from the northeast which are associated with disturbances of the intertropical convergence zone (VAN ZINDEREN BAKKER, 1984; TYSON, 1986; BARNARD, 1989; LINDESAY & SEELY, 1989; JURY, 1996; WARD & SWART, 1997; STOLLHOFEN et al., 1999; MCCARTHY et al., 2000; STANISTREET & STOLLHOFEN, 2002). Climatic effects resulting from variable strength of the Benguela Current are analogous with effects of the Humboldt Current on the Atacama Desert arid zone of Chile (cf. MESSERLI et al., 1993).

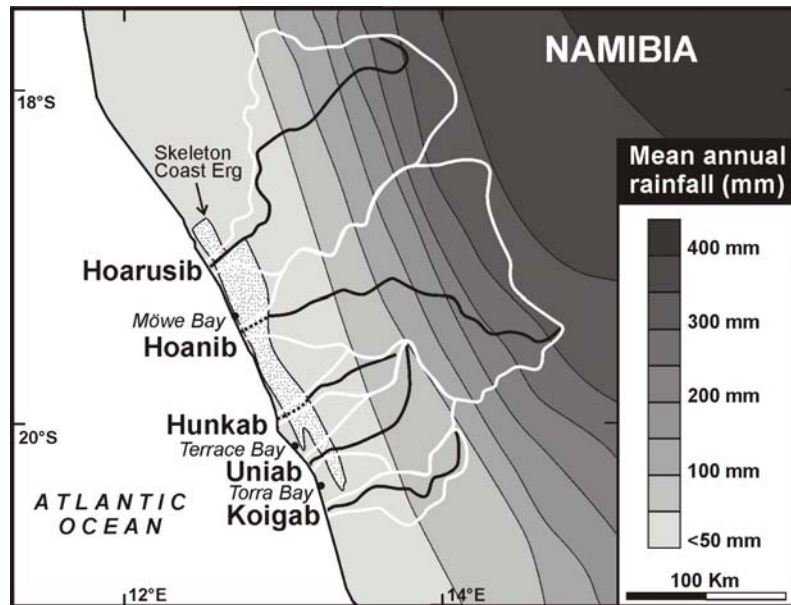
With the exception of the perennial Kunene River, all other rivers of the Skeleton Coast are ephemeral ones (JACOBSON et al., 1995). Experiencing flood pulses of short duration, typically a few days only, the rivers flow towards the South Atlantic coast across a considerable climatic gradient from Summer rainfall in the semi-humid to semi-arid mountainous catchment area (150-600 mm/a) to arid (<50 mm/a) in the coastal areas over a distance of merely 150 km (JACOBSON et al., 1995). Because of the remote setting and flashy nature of the flooding no discharge records are available. Minor river flows normally occur between November and April, during the annual rainy season of the southern hemisphere summer whereas high-magnitude floods have been observed at an average interval of nine years during the past 63 years, preferentially between February and April (cf. SHANNON et al., 1986; JACOBSON et al., 1995; STOLLHOFEN et al., 1999). Considerable precipitation can then supply large volumes of water and sediment discharge from the mountainous hinterland catchment (Fig. 1.3). The rivers may rarely undergo such a major flooding and frequently experience several consecutive years of drought.

### 1.2.2.1 Precipitation and temperature

The main study area is situated in the hyper-arid but cool foggy coastal zone of the northern Namib Desert (LANCASTER, 1982) which extends from the coast about 20 km

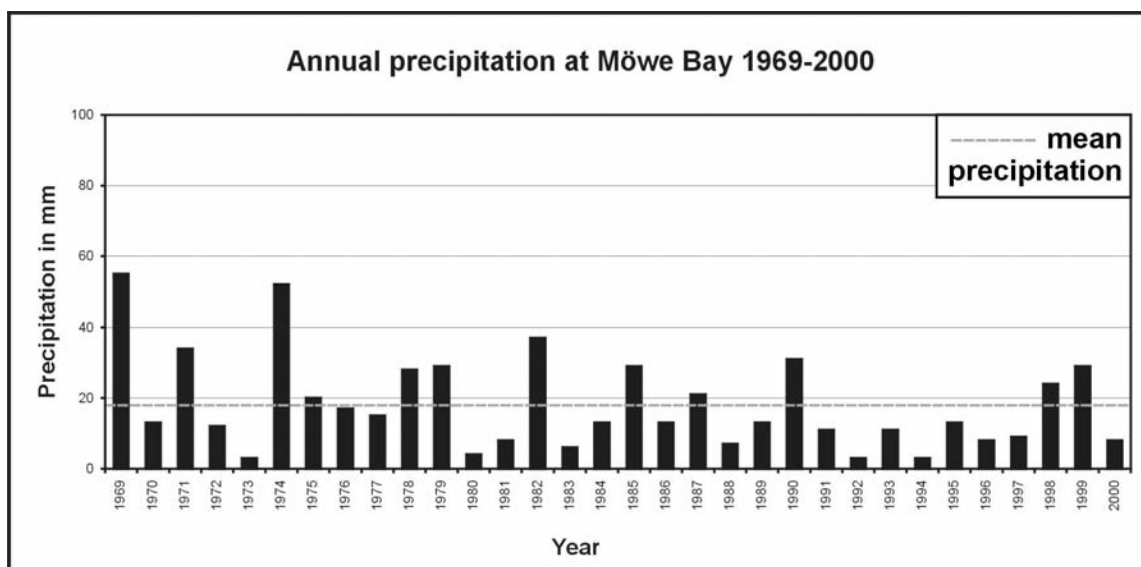
inland. Only little reliable information is available regarding rainfall, temperature, wind direction, wind intensity and the occurrence of fog. Most information concerning climate is available - on a regional scale - from the weather station at Möwe Bay (see Fig. 1.1), and on a supra-regional scale from detailed climatic studies of the northern part of the main Namib Sand Sea (Gobabeb weather station; LANCASTER et al., 1984).

At Möwe Bay the annual rainfall is less than 50 mm (JACOBSON et al., 1995) with an average of 18 mm during the period 1969-2000 and an annual variability of more than 70% (Tab. 1.1). Fog precipitation is more than twice the annual rainfall and is one of the most important moisture sources for the Namib biota (SEELY, 1978).



**Fig. 1.3:** River catchment and mean annual rainfall in the study area (compiled after: JACOBSON et al., 1995).

Furthermore, it also contributes to rock weathering - especially salt cracking of rocks - and mineral breakdown (GOUDIE, 1972; SWEETING & LANCASTER, 1982; GOUDIE et al., 1997; ECKHARDT & SCHEMENAUER, 1998; LANCASTER, 2002).

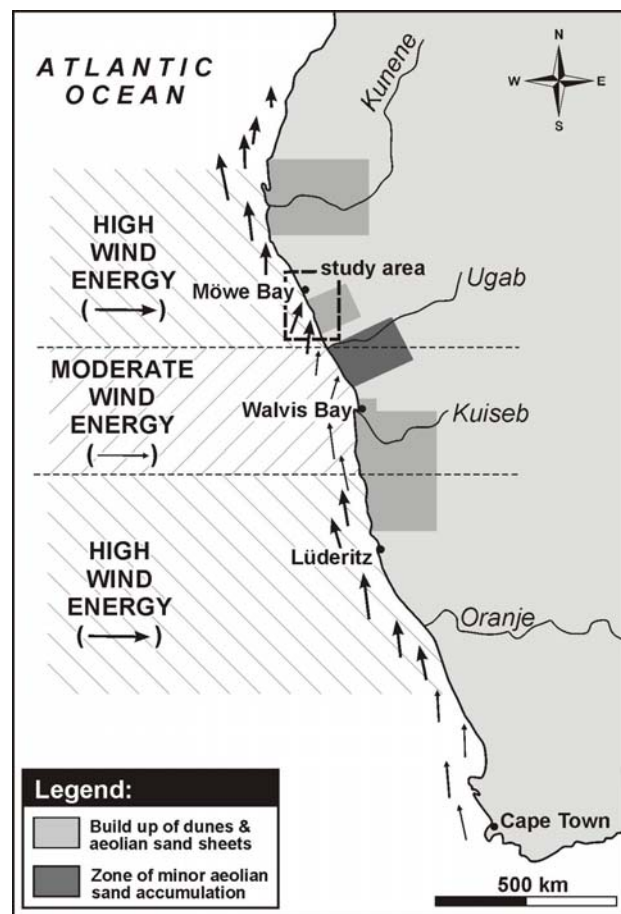


**Tab. 1.1:** Annual precipitation at Möwe Bay (compiled from: LEGGETT, 1998).

The annual mean temperature is around 16°C at the coast but increases inland towards the eastern part of the catchment areas. Along the coast mean daily maximum temperatures range during the year between 13-24° C and mean daily minima temperatures range seasonal from 9-15°C (LANCASTER, 1982). Fog occurs frequently in the late afternoon, night and early morning during 11-25 days per month with a maximum frequency during southern hemisphere winter and early spring (July/October) (LANCASTER, 1982).

### 1.2.2.2 Wind as a geological factor

Wind is a key factor for fluvio-aeolian interaction (see Chapter 6). Published wind data derived from LANCASTER (1982), from the weather station at Möwe Bay and from own measurements on aligned tails from shrub coppices during field work substantiate the knowledge of the wind regime in the research area. Strong all-year onshore south to south-southwesterly winds dominate the coastal area (Fig. 1.4; LANCASTER, 1982; BARNARD, 1989; WARD, 1989), whereas the 'Bergwind' from easterly direction blows only during several days between April and July (TYSON, 1969, KEMPF, 2000). LANCASTER (1982) observed in the period between 1973-1977 that 98% of the

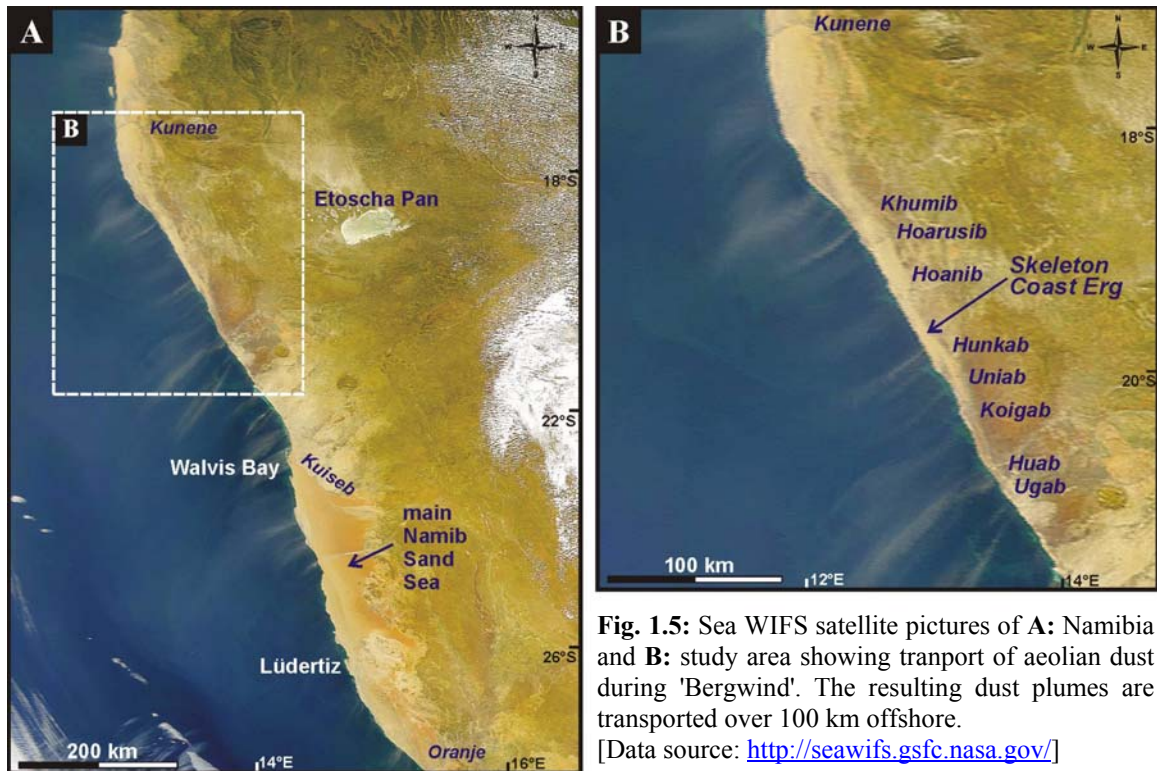


**Fig. 1.4:** Schematic sketch of relative strength and direction of the coastal wind regime along the western coastline of Southern Africa (compiled from: WARD, 1989; SHANNON et al., 1989).

annual sand flow was from directions between south-southeast and south-southwest and that wind velocity was able to move sand for almost 50% of the time. Maximum sand flow takes place during August and October (LANCASTER, 1982). Average wind speed measured at Möwe Bay weather station during periods 10/1994-03/1995 and 09/2000-03/2001 is 4.34 m/s, with a maximum of 31 m/s (Namibian Weather Bureau, Windhoek). The 'Bergwind' from easterly direction achieve wind speeds of up to 17 m/s. Such winds play

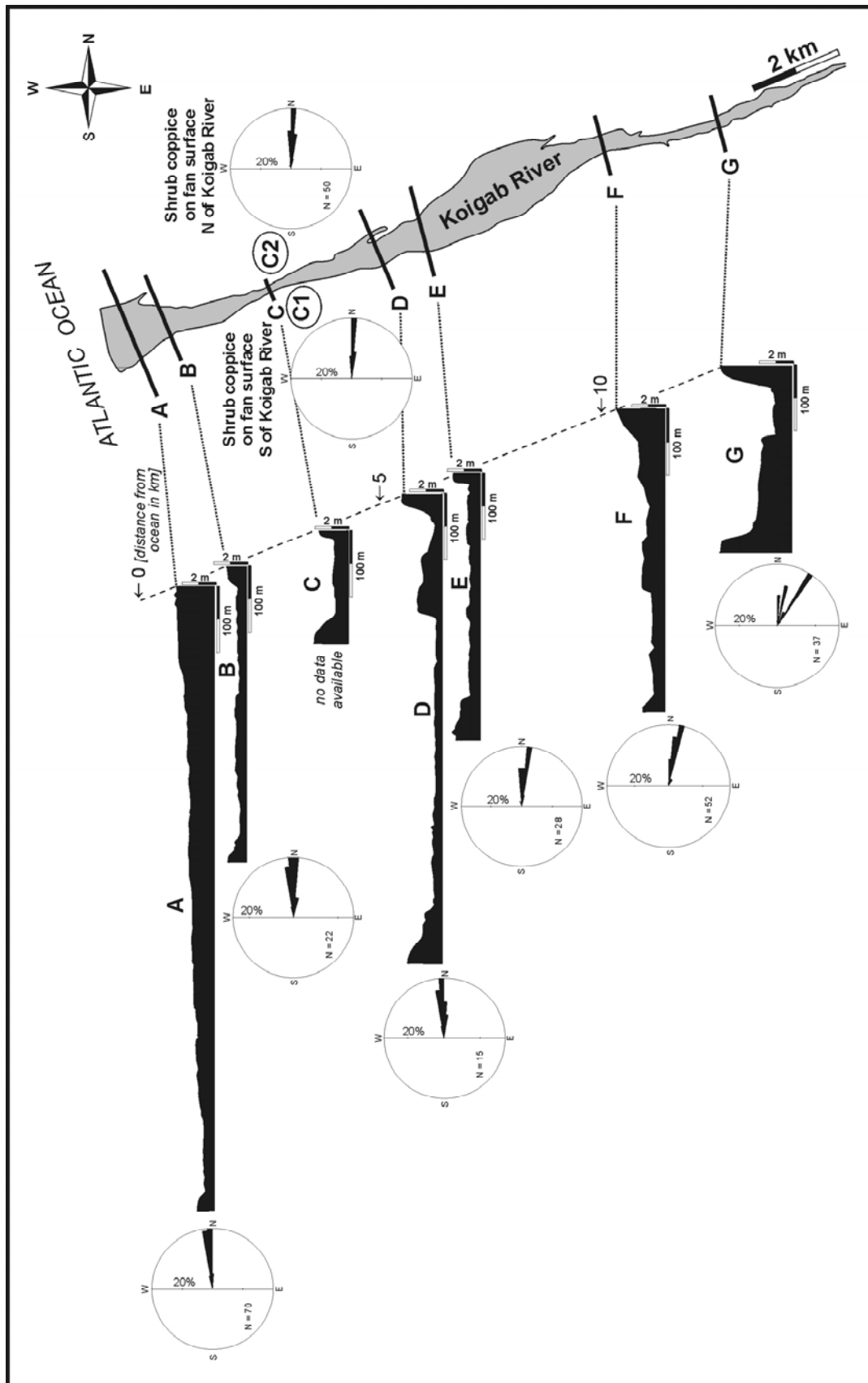


an important role in the transport of aeolian dust (WHITAKER, 1984) and resulting 'dust plumes' can be transported over 100 km offshore (Fig. 1.5). However, because of the dominance and persistence of the southerly winds, effects of 'Bergwinds' do not seem to have a major influence on the sedimentological record in the study area in contrast their effects in the main Namib Sand Sea (LANCASTER et al., 1984; KEMPF, 2000).



North of the Ugab River the strength and dominance of the SSW wind direction increases significantly (Fig. 1.4; WARD, 1989). However, first onshore movement of sand-sized sediment from the beach is observable about farther south of the study area at Ambrose Bay (Fig. 1.1), and about 15 km north of Ambrose Bay a small barchan field is developing out of the Huab River (WARD, 1989). 15 km north of the Koigab a combination of topographic funnelling, a change in coastline orientation, wind strength and increased sediment supply resulting from aeolian winnowing of fluvial and marine/beach sediments leads to the onset of the Skeleton Coast Erg. In the lee-side of several up to 60 m high basement outcrops, 5 km north of the Koigab River, several barchan trains have developed feeding the southern margin of the Skeleton Coast Erg.

Topographic funnelling of wind has also been observed within the ephemeral river valleys themselves. Measurements from aligned tails of shrub coppices within the Koigab River and from the Koigab Fan surface illustrate this effect (Fig. 1.6), causing eastward aligned tails of the shrub coppices approximately perpendicular to the general SSW wind direction.



**Fig. 1.6:** Effects of topographic funnelling illustrated by the Koigab River. Data derived from measurements of aligned shrub coppice tails within the Koigab River itself. Sections A-G showing measured topographic cross sections of the Koigab River. The river is less incised into the fan surface towards the coast (cross sections A+B). The deeper the river is incised into the fan (cross sections D to G) the higher is the deviation from the overall major SSW wind direction. In comparison, measurements on shrub coppice located on the adjacent fan surface (C1 & C2) show that there is no change in wind direction compared to the overall SSW wind direction.

## 2 Geological setting

The river catchment areas of NW Namibia are developed largely outboard of the Great Escarpment (see Fig. 1.1), a pronounced rise in topography, which separates in NW Namibia the Skeleton Coast area, varying in height between sea-level and 400 m, from a mountainous hinterland, typically ranging between 900 m and 1300 m. The Great Escarpment fronts the 'highveld' of the continental interior, the latter maintaining heights between 1300 m and 1700 m, and encircles the entire southern African continent (KING, 1951; ABEL, 1959; HÜSER, 1989; BRUNOTTE & SPÖNEMANN, 1997; PARTRIDGE & MAUD, 2000). The geology of the river catchments of the study area comprises rocks of Vaalian to recent age, which can be subdivided into 1) Pre-Damara rocks, 2) Damara rocks, 3) Etendeka rocks and 4) Cenozoic rocks (Fig. 2.1).

Pre-Damara crystalline rocks occur only in the northern and easternmost part of the study area, while most other parts are underlain by Late Proterozoic Damara basement rocks (Fig. 2.2). They form part of the Pan-African orogenic belts of Namibia and adjacent parts of Western Gondwana (HOFFMANN, 1983). Following with a distinct hiatus of about 400 Mio. years are deposits of the Etendeka Group, which cover the complete hinterland of the Koigab and Uniab River in the southern part of the study area (Fig. 2.3). The basal parts of the Early Cretaceous tholeiitic basalts and basaltic andesite lavas with intercalated silicic rheoignimbrite sheets are underlain and interlayered by sedimentary rocks of the Twyfelfontein Formation.

In addition, numerous sedimentary rocks of various Cenozoic age occur

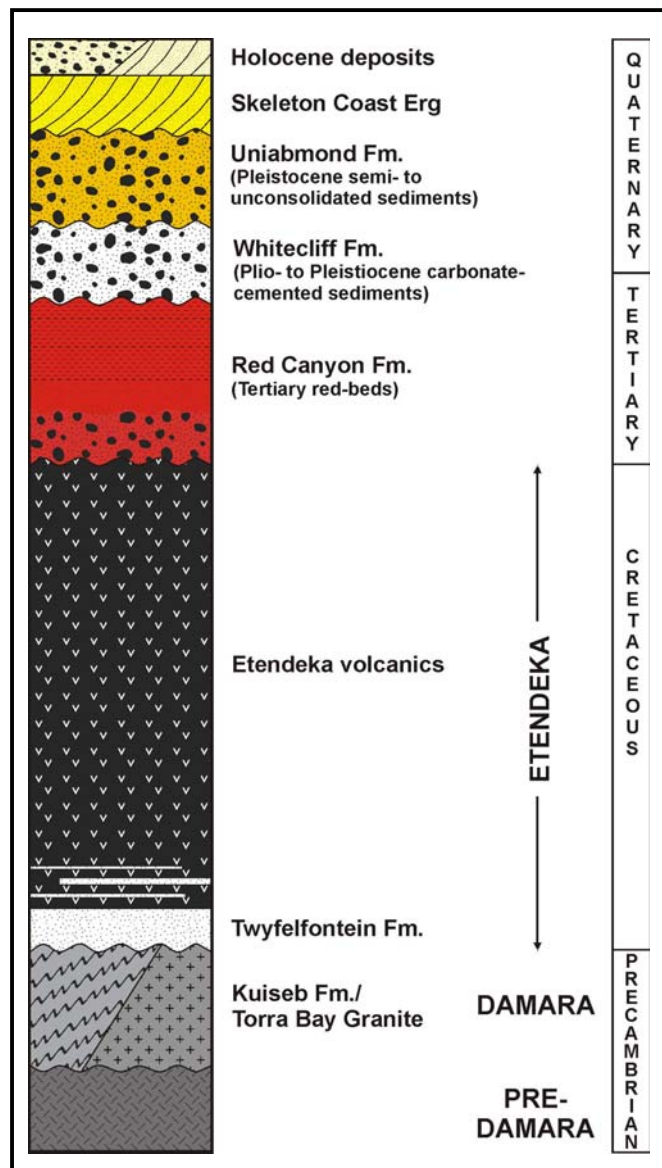


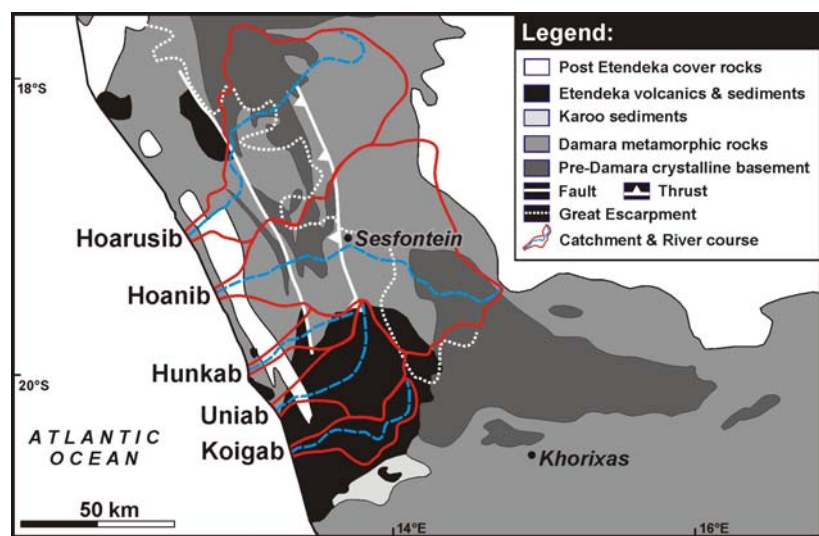
Fig. 2.1: Overview of the stratigraphic succession in the study area (not to scale).



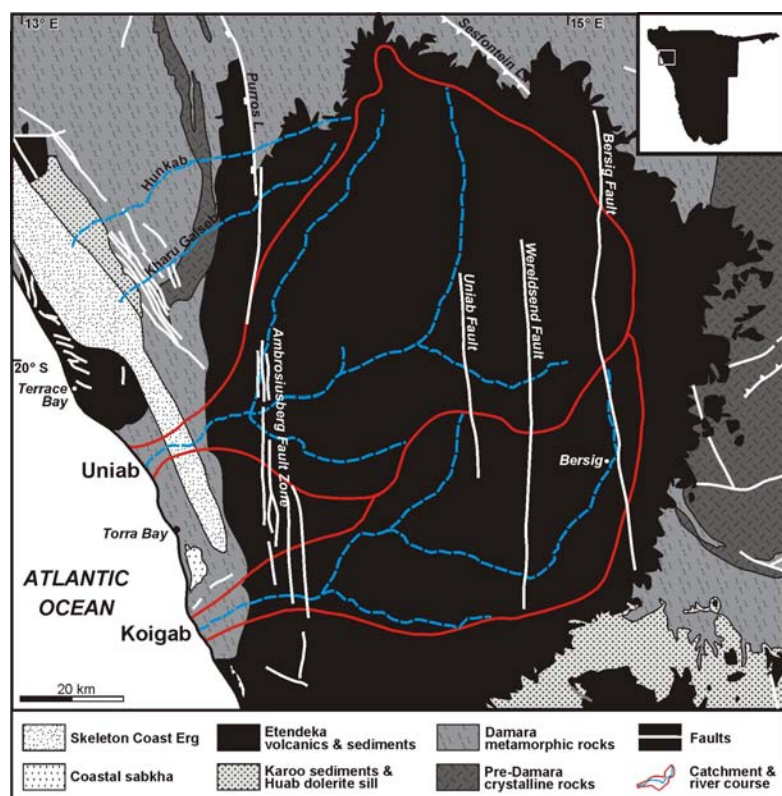
widespread in the whole study area. In the mouth area of the Uniab River one of the best preserved Cenozoic successions along the Namibian coast is exposed. This succession has been studied in detail (see Chapter 5) and has been subdivided into the Red Canyon, Whitecliff and Uniabmond Formations. The latter represents a part of the Pleistocene gravel accumulation which overlies the coastal plain west of the Great Escarpment. On these deposits sits the Skeleton Coast Erg. It is arranged as a 165 km long and 3-15 km wide, S-N trending dune belt, which runs 2-5 km inland parallel to the coastline.

The Holocene sediments in the study area are represented by ephemeral river deposits and various aeolian deposits. In addition, Quaternary marine gravel terraces and coastal sabkhas are quite common along the coastline.

**Fig. 2.2:** Simplified geological map of the study area (modified after SETH, 1999; STANISTREET & CHARLSWORTH, 2001; PASSCHIER et al., 2002).



**Fig. 2.3:** Geological map of the catchment areas of the Koigab and Uniab River (modified after: MILLER, 1988).



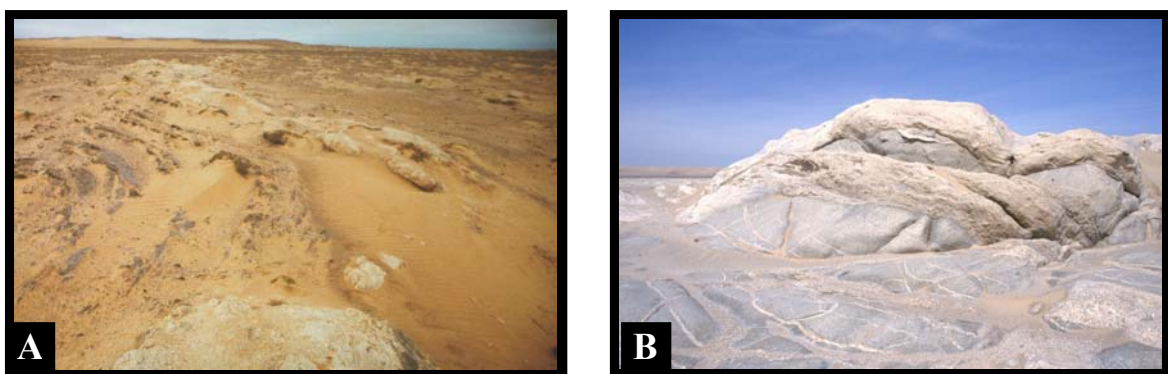
## 2.1 Palaeo- to Middle Proterozoic rocks

Crystalline rocks of Vaalian (> 2000 Ma) and Mokolian (1000-2000 Ma) age are exposed as several small inliers in the catchment areas of the Hoanib and Hoarusib River. They are composed of meta-volcanics, quartzites, pelites, augen gneisses and meta-sediments (STANISTREET & CHARLSWORTH, 2001).

## 2.2 Late Proterozoic Pan-African Damara metamorphic rocks

Wide parts of the study area are underlain by Late Proterozoic Pan-African Damara metamorphic rocks. Essentially they are schists (Fig. 2.4 A), migmatitic gneisses and granites, which are mainly composed of quartz, feldspar and mica. The paragenetic (sedimentary origin) rocks are assigned to the Kuiseb Fm. (MILLER, 1988) whereas the orthogenetic (magmatic origin) are represented by the Torra Bay Granite and associated garnetiferous pegmatites (Fig. 2.4 B). The heavy mineral suite comprises garnet, epidote, amphibole, apatite, chloritoid, staurolithe, gypsum, mica and tourmaline (SCHLICKER, 2000b).

The metamorphic basement rocks exposed in the study area belong to the N-S striking Kaoko Belt (HOFMANN, 1983) which represents the northern coastal branch of the Pan-African Late Proterozoic Damara Orogen (AHRENDT et al. 1983). The Kaoko Belt is subdivided into three tectono-stratigraphic zones, the Eastern, Central and Western Kaoko Zone (MILLER, 1983). The study area lies within the Western Kaoko Zone (WKZ), which extends from the Purros Lineament (Fig. 2.3) to the Atlantic Coast (STANISTREET & CHARLSWORTH, 2001).



**Fig. 2.4:** **A:** Typical schist outcrop (ca. 7 m long) of the Kuiseb Fm. in the Uniabmond area. **B:** Ca. 3 m large outcrop of Torra Bay Granite (bluish-grey) intruded by garnet-bearing pegmatites (whitish-grey) 500 m ESE of Torra Bay close to the main road C34.

## 2.3 Etendeka Group

The Lower Cretaceous Etendeka Group overlies the Proterozoic metamorphic rocks with a major unconformity. The Etendeka Group comprises mainly volcanic and subordinate sedimentary rocks and reaches a thickness of more than 2000 m. It is subdivided into three formations: the sedimentary Twyfelfontein Formation and the volcanic Awahab and Tafelberg Formations, the latter two forming the major part of the Etendeka Plateau (MILNER et al., 1994; STOLLHOFEN, 1999).

### 2.3.1 Twyfelfontein Formation

The deposits of the Twyfelfontein Formation represent the basal, sedimentary part of the Etendeka Group and is composed of aeolian, fluvial and mass flow deposits (WANKE, 2000). Due to the predominance of aeolianites within these sediments, they were formerly erroneously correlated with the Jurassic Etjo Formation (MILLER & SCHALK, 1980; SACS, 1980; MILNER et al., 1994). However, Early Cretaceous K/Ar and Ar/Ar ages for the basal Etendeka lavas point to a substantial younger age for the Etendeka sediments than the Etjo sediments in their Mt. Etjo and Mt. Waterberg type locality (SIEDNER & MITCHELL, 1976; RENNE, 1997 [pers. comm. in WANKE, 2000]). In addition, sedimentological investigations on the Twyfelfontain Fm. sediments showed marked palaeoenvironmental differences to sediments of the Etjo Fm. and, therefore, STOLLHOFEN (1999) and STANISTREET & STOLLHOFEN (1999) introduced the term Twyfelfontein Formation.

The Twyfelfontain Fm. is characterized by aeolian sandstones with minor fluvial and debris flow deposits intercalated in its basal parts. The succession shows complex spatial and temporal variations in depositional style controlled by a gradual transition from semi-arid to hyper-arid climatic conditions and by syn-sedimentary tectonic faulting. The Twyfelfontain Fm. subdivides into four units starting with the basal alluvial-fluvial Krone Member, followed by the Mixed Aeolian-Fluvial Unit, the Main Aeolian Unit and the Upper Aeolian Unit, with the last two units becoming inundated by Etendeka lavas (MOUNTNEY et al., 1998).

Sediments of the Twyfelfontein Fm. are best exposed in the Huab area, but single scattered outcrops also occur up to 20 km north of Terrace Bay (WANKE, 2000). In the southernmost part of the study area only one outcrop west of the main road was known so far (MILLER, 1988) but another small outcrop has been newly discovered during fieldwork east of the main road (S 20°35.24'/E 13°21.86'). There, sediments interfinger with basal Etendeka basalts and may belong to the Upper Aeolian Unit of the Twyfelfontein Formation. The

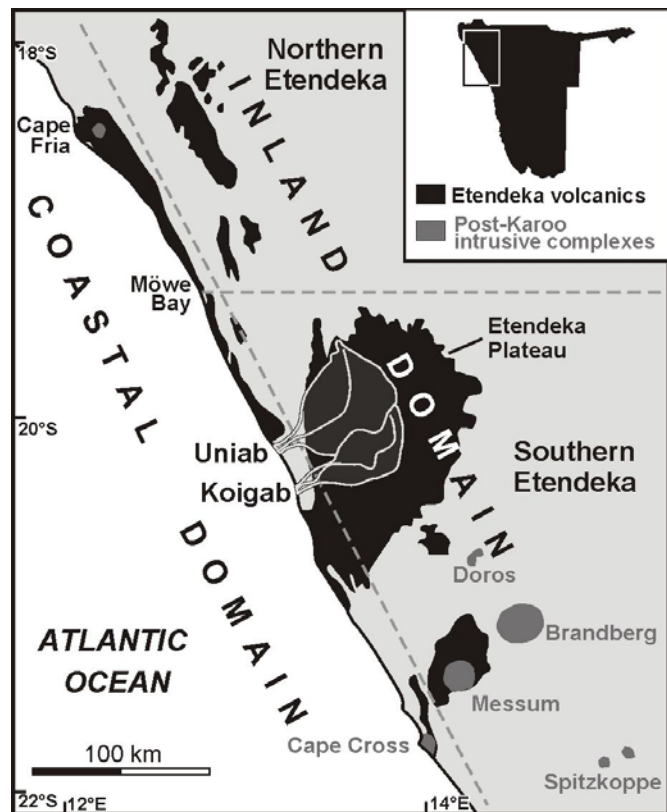
sandstones in the outcrop west of the main road are intensively silicified and have a silcrete-like appearance. Only in a few places bedding is visible. Locally the moderately to well sorted, medium-grained aeolian sandstones show low-angle cross bedding, some with coarser grained bottom-set layers.

### 2.3.2 The Etendeka Igneous Province

The Etendeka Igneous Province forms part of the giant Paraná-Etendeka Flood Basalt Province (MILNER et al., 1995) and comprises all Lower Cretaceous extrusives and intrusives found in NW Namibia (Fig. 2.5). Volcanic deposits of the Etendeka Group are related to a mantle plume and the break-up of western Gondwana between Africa and South America, and the subsequent opening of the South Atlantic (MILNER et al., 1994, 1995; RENNE et al., 1996). Ages and geochemical characteristics of the Etendeka volcanics correlate with the volcanics of the Serra Geral Formation in the South American Paraná Basin (HAWKESWORTH et al., 1992; MILNER et al., 1995).

Recently the Etendeka Province has been subdivided by MARSH et al. (2001) into two structural domains and two geochemical subprovinces. Based on a structural interpretation MARSH et al. (2001) defined a 15-20 km wide coastal domain characterized by tilted blocks bounded by closely spaced listric faults. The structural nature of the inland domain is characterized by horizontal layering of the volcanic succession and widely spaced N-S trending faults with downthrows to the west. A Northern and a Southern Etendeka subprovince was identified by geochemical provinciality within both mafic and silicic volcanic rocks (MARSH et al., 2001).

Deposits of the Etendeka Province are exposed in the study area as



**Fig. 2.5:** Distribution of the main volcanic and intrusive rocks of the Etendeka Igneous Province including the geographical and structural subdivision into the coastal and inland domain (compiled from: MARSH et al., 2001). The catchment areas of the Koigab and Uniab River are indicated.



eroded remnants of an up to 2000 m thick pile of tholeitic basalts and basaltic andesite lavas and intercalated quartzlatitic rheoignimbrite sheets (MILNER, 1988). The volcanics of the Etendeka Group are mainly composed of plagioclase and clino-pyroxene. Minor components are magnetite, ortho-pyroxene, epidote, chlorite and olivine-psenomorphs. In the rheoignimbrites also quartz occurs in various amounts.

Except for the last kilometres towards the Atlantic coastline the volcanics of the Etendeka Group completely occupy the catchment area of the Koigab and the Uniab River. The source region for the catchment of the two investigated rivers is located exclusively within the Etendeka Plateau (Fig. 2.5). The basalts build up a hilly low rising topographic landscape which is associated with vast deflation surfaces. The basalts are deeply, crumbly weathered and only in a few

places, like the Koigab Canyon Poort, relatively fresh sections are exposed. The quartz latites represent only ~25% of the extruded lavas of the Etendeka Group but due to their high weathering resistance cover more than 60% of the surface (MILNER, 1988). They also form the top of the prominent table mountains of the Etendeka Plateau (Fig. 2.6).



**Fig. 2.6:** The Etendeka Plateau in the middle reaches of the Koigab River near Wolfswasser. Weathering-resistant quartz latites build up the top of the table mountains. View towards ESE.

## 2.4 Cenozoic deposits

Along the courses of the ephemeral rivers and their tributaries, in their mouth areas and along the coastal strip a wide variety of Cenozoic sediments are exposed. Most of them are still undated but from correlations with dated equivalents from the main Namib Sand Sea and the Sperrgebiet area in southern Namibia an age estimation can be given.

### 2.4.1 Red Canyon Formation: Tertiary red-beds

Red-coloured sediments occur only at two localities within the study area: in the mouth area of the Uniab River (see Chapter 5.3) and in the Kharu Gaiseb River directly E of the Skeleton Coast Erg (see Chapter 5.4.5).

In the Uniabmond area the term Red Canyon Formation was introduced for these reddish sediments (see also Chapter 5.3). It represents a lithostratigraphic unit consisting predominantly of reddish terrestrial, mainly fluvial sediments, showing an overall upward fining trend from dominantly coarse-grained, feldspar-rich conglomerates and sandstones to mainly fine-grained, clay-rich silt- and sandstones. These weakly consolidated sediments overlie Pan-African Damara metamorphic rocks with a major unconformity and are unconformably overlain by sediments of the Whitecliff Formation (see Chapter 2.3.2). The Red Canyon Fm. has a cumulative thickness of approximately 60 m and is subdivided into the lower Waterfall Member and the upper Bone-Area Member. The deposits of the Red Canyon Fm. are markedly affected by tectonic activity resulting in faulting, tilting and jointing. The occurrence of strongly weathered clasts of Etendeka basalts and quartzites in all stratigraphic units of the Red Canyon Fm. implies a post-Early Cretaceous Etendeka age. A recently discovered fossil bovid bone clearly indicates a post-Upper Cretaceous age of the Bone-Area Member.

#### **2.4.2 Whitecliff Formation: Plio- to Pleistocene carbonate-cemented sediments**

Carbonate-cemented sediments are quite common along and in the ephemeral rivers and their tributaries as well as in the mouth area of the Uniab River. RUST (1987) summarized these sediments in the Ogams Formation.

In the Uniabmond area a wide variety of these sediments have been studied in detail (see Chapter 5.4) and have been summarized into the Whitecliff Formation. The Whitecliff Fm. represents a litho-stratigraphic unit consisting of light coloured, indurated, carbonate-cemented sandstones and conglomerates, which overlie both the sediments of the Red Canyon Fm. and the Pan-African Damara metamorphic rocks with a major unconformity. The Whitecliff Fm. has a maximum cumulative thickness of about 23,5 m and displays a wide variety of continental and marine facies (KRAPP et al., 2002; ZELLER, 2000).

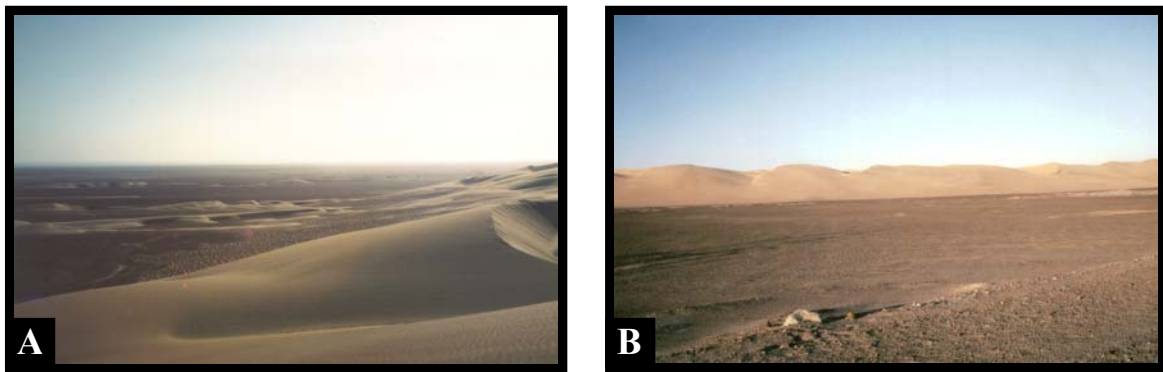
#### **2.4.3 Uniabmond Formation: Pleistocene semi- to unconsolidated sediments**

Semi- to unconsolidated sediments build up the area between the coastal plain and the Great Escarpment. In the Uniabmond area thick gravel and sand accumulations are exposed. These deposits have been summarized in the Uniabmond Formation (see Chapter 5.5). The Uniabmond Fm. overlies the sediments of the Whitecliff Fm. and Damara metamorphic rocks with a major unconformity. The up to 35 m thick deposits of the

Uniabmond Fm. display a wide variety of continental and marine facies and are characterized by drastic vertical and lateral facies changes. Within this formation four main sedimentary units were determined (see Chapter 5.5).

#### 2.4.4 Skeleton Coast Erg (Late Pleistocene)

About 15 km north of the Koigab River the Skeleton Coast Erg starts with a series of barchans and large compound barchan dunes (Fig. 2.7 A). The erg covers an area of ~2.000 km<sup>2</sup>. Five kilometers north of the Uniab River mouth a second dune-branch developed near to the coast NE of a coastal sabkha. This second branch merges with the main branch north of Terrace Bay. Transverse, compound crescentic and barchanoid dunes (LANCASTER, 1982) constitute the roughly S-N trending, 165 km long and 3-15 km wide dune belt, which runs 2-5 km inland parallel to the coast.



**Fig. 2.7 A:** The southern outlet of the Skeleton Coast Erg with single barchan trains in the back (view toward WSW). **B:** Photograph showing the dune wall at the western margin of the Skeleton Coast Erg near Torra Bay (view towards E).

At the western, windward margin of the erg transverse and compound crescentic dunes are coalescing to form a prominent 'dune wall' between 20-80 m high (Fig. 2.7 B) whereas the eastern margin of the erg is not so well confined (LANCASTER, 1982). Because of less sand supply only simple crescentic and barchan dunes have developed there on the coastal plain. In contrast to the orange to red colouration of the main Namib Sand Sea dunes, resulting from iron coatings around the quartz grains, the dunes of the Skeleton Coast Erg are generally much lighter in colour and their flanks are draped by red to purple and black veils of heavy mineral layers composed of garnets and magnetites. The Skeleton Coast Erg is supposed to have been developed after the Last Glacial Maximum (BARNARD, 1989).

### 2.4.5 Holocene deposits

Due to the ephemeral nature of the rivers in the study area deposition of fluvially generated sediments takes place only episodically during flood events, whereas aeolian processes operate almost continuously throughout the year.

#### 2.4.5.1 Ephemeral river deposits

The modern day river beds are characterized by a network of shallow braided channels and longitudinal gravel- and sand bars. The deposits are composed of moderately sorted sands and gravels, which are often draped by thin mud-layers of waning flood stages. Sandramps are often developed at the channel margins. Rivers, which traverse the Skeleton Coast Erg, frequently flood interdune areas adjacent to the main river course depositing mud layers of up to 15 cm thickness (STANISTREET & STOLLHOFEN, 2002).

#### 2.4.5.2 Aeolian sediments and landforms

##### Barchans

15 km north of the Koigab River the Skeleton Coast Erg starts with a series of single barchans (Fig. 2.8) and barchan trains (see Fig. 2.7). One such isolated barchan was studied in detail, to achieve a better understanding of sediment transport and barchan movement rates at the southern margin of the Skeleton Coast Erg (see Chapter 6.2.2). In addition to areas S of the erg abundant barchans move over the coastal plain at the western and eastern margins of the N-S trending erg.



**Fig. 2.8:** Moving barchan directly at the T-junction of the two main roads C34/C39 15 km S of Torra Bay. View towards SSW.

##### Shrub coppice

Shrub coppices are extensively distributed in the whole study area and can be found as single isolated coppice or as complex shrub coppice fields. They can reach heights of up to 4 m by the interplay of plant growth and associated lee-side accumulation of aeolian sand.



In the Skeleton Coast area, various species of *Salsoa spp* and *Zygophyllum Stapffii* (CRAVEN & MARAIS, 1998) provide the most efficient sediment traps. The tails of shrub coppices are aligned parallel to the prevailing modern day south-southwesterly wind direction. Because of the lack of detailed wind direction data for the study area, the orientation of coppice tails was used to obtain additional wind data information about the regional sand transport pattern, especially for the Koigab Fan area and the southern margin of the Skeleton Coast Erg (see Chapter 1).

### Sand ramps

Sand ramps are a common feature in the ephemeral rivers. They drape the sidewalls of the channels. During floods these sand ramps are eroded (Fig. 2.9) but shortly afterwards they reestablish.

**Fig. 2.9:** Sand ramp on the southern sidewall of channel C6 in the Uniabmond area eroded on its foot during the April 2000 flood.



### Deflation surfaces

Deflation surfaces are a dominant feature in the coastal regions adjacent to the Skeleton Coast Erg resulting from aeolian winnowing. Ventifacts are irregularly distributed on these deflation surfaces (Fig. 2.10). These ventifacts are developed almost exclusively from nearly unweathered and relatively solid quartz latites. In many places the ventifacts are cracked as a result of salt



**Fig. 2.10:** Typical appearance of deflation surfaces in the study area. Note the quartz latite rocks which are cracked by salt weathering (hammer for scale).

weathering. Frequent fog also contributes to rock weathering and mineral breakdown (see Chapter 1; GOUDI, 1972; SWEETING & LANCASTER, 1982; GOUDI et al., 1997; ECKHARDT & SCHEMENAUER, 1998). In places where basement and Etendeka rocks crop out, wind abrasion polished the rock surfaces.

### 2.4.5.3 Marine terraces and coastal sabkhas

Marine terraces and coastal sabkhas occur widespread in the coastal areas of the study area. In the mouth areas of the ephemeral rivers marine terraces often separate the fluvial from the oceanic regime (see Chapter 4). Crests heights of levelled marine terraces ranges between +2 and +6 m asl. and can be correlated with heights of Pleistocene raised marine complexes from the Sperrgebiet area in southern Namibia (PICKFORD & SENUT, 1999).

## 2.5 Tectonic setting

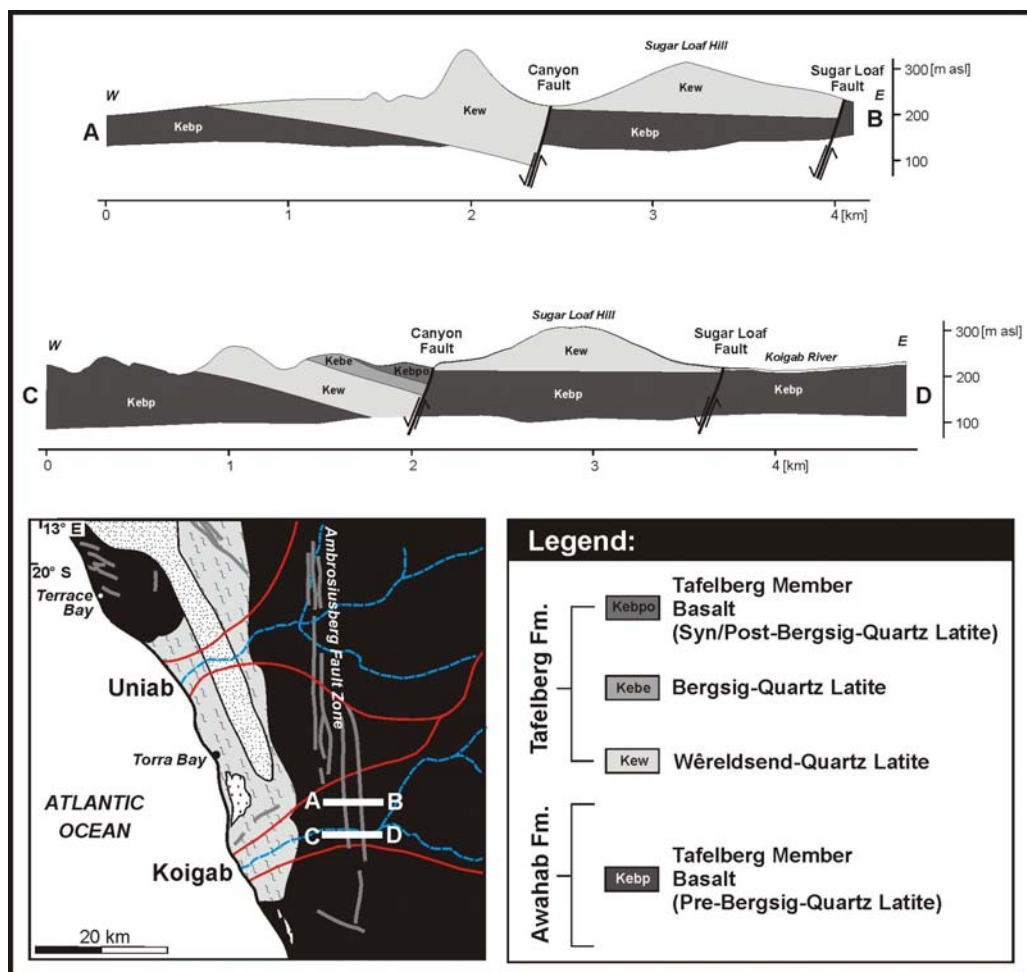
The catchments of the ephemeral rivers in the study area have developed largely outboard of the Great Escarpment. The initiation of the Great Escarpment followed the "unzipping" of the oceans that presently surround southern Africa: the Indian Ocean to the east during Late Jurassic and the Atlantic Ocean to the west during the Early Cretaceous (DINGLE, 1992/1993). Subsequent uplift has affected the Namibian coastal tract, enhanced particularly during the Upper Cretaceous (WARD, 1987; BROWN et al., 2000; COCKBURN et al., 2000; RAAB, 2000), followed by less well-known phases of uplift during the Cenozoic (KLEIN, 1980; WARD, 1987; HARTNADY & PARTRIDGE, 1995; PARTRIDGE & MAUD, 2000). Such phases of uplift have been accompanied by the headward incision of deep canyons of westward draining river systems such as the Kuiseb (KORN & MARTIN, 1957; WARD, 1987) and the Omaruru (KLEIN, 1980) in central Namibia.

Following the Atlantic opening along the northern Namibian continental margin, braided rivers, such as the Krone River (MOUNTNEY et al., 1998; HOLZFÖRSTER, 2002), were initiated flowing westwards off the newly defined continent into the neighbouring ocean. Successor Tertiary rivers continued to flow also westwards off the interior (WARD, 1987, 1988). Subsequent aggradational and degradational cycles have been interpreted to reflect an overall but fluctuating decrease in hydrological competency from the Early to Middle Pleistocene (Oswater Conglomerate) to the present day (WARD, 1987). Of the rivers running off the western margin of southern Africa only the Orange and Kunene River catchments progressed substantially into the continental interior to the east, its headwaters capturing river systems throughout the subcontinental interior (DE WIT et al., 2000; JACOB, 2001).

The research area is situated on the rift shoulder of a passive continental margin (STOLLHOFEN, 1999). The tectonic setting of the study area is determined by the rifting and break-up of Western Gondwana before and during the opening of the southern South-

Atlantic Ocean. The Late Cretaceous rift geometry of the South-Atlantic is strongly preset by basement structures (DALY et al., 1989; LIGHT et al., 1993; CLEMSON et al., 1997), which trace reactivated Pan-African suture zones (PORODA, 1989; STANISTREET et al., 1991; LEDENDECKER, 1992).

The Ambrosiusberg Fault Zone which pursues the Purros Fault Zone southwards, traverses the study area from N to S (Figs. 2.3 & 2.11). This structure acted as a thrust fault during the Pan-African orogeny and later became reactivated as a normal fault confining the rift shoulder of the South Atlantic rift prior to continental break up (STOLLHOFEN, 1999; WANKE, 2000). The Purros/Ambrosiusberg Fault Zone separates two areas with contrasting layering and geometries. West of the fault zone closely spaced, coast-parallel, listric, NNW-SSE trending faults with downthrows of several tens of meters towards W occur, whereas east of the fault zone widely spaced faults appear (see Fig. 2.11) (STOLLHOFEN, 1999). The architecture of the Etendeka volcanics records the activity of the Purros/Ambrosiusberg Fault Zone. Highest lava thicknesses can be observed W of the fault but decreasing thicknesses towards the east (MILNER & DUNCAN, 1987; STOLLHOFEN, 1999).



**Fig. 2.11:** Geological W-E sections across the Ambrosiusberg Fault Zone in the lower reaches of the Koigab River (compiled from: SCHLICKER, 2000a). [Legend for overview map see Fig. 2.2]

### 3 Methods

Selected field, remote sensing and sediment petrographic methods have been used to build up a data base for approaching the tasks of this study (see Chapter 1).

#### 3.1 Field studies

A level meter, provided by the Geological Survey of Namibia, was used to map precisely the topography of river channels, obtain detailed information about:

- the incision rate of river channels into the surrounding land surface
- the morphology and location of the rivers thalweg
- the distribution of channels
- the width and length of channels
- the shape, size and height of channel bar forms
- the accurate height information of marine terraces and palaeo-seacliffs in the rivers mouth areas
- measurement of river gradients and river cross-sectional profiles

A plane table, also provided by the Geological Survey of Namibia, was used to obtain accurate data of the morphology of barchans and their changing morphology through time (see Chapter 6.2.2).

Furthermore, detailed field mapping of the Uniabmond area have been undertaken in cooperation with C. Zeller (University of Würzburg/Germany).

The sedimentological data base for this study was mainly obtained by :

- sedimentological logging of vertical and cross sections
- sampling of sand-sized material from various facies and localities
- large, intermediate and small axis size measurements on basalts and quartz latite clasts from gravel bars and from the Koigab Fan surface

During field work, climate data such as amount and distribution of precipitation, wind direction and wind speed and the magnitude and duration of flood events were collected from the Governments weather stations at Möwe Bay and Springbokwater and from the private weather station in Wêreldsend, as well as from the Namibian Weather Bureau/ Windhoek. Own observations and measurements were added to these data sets.

### **3.2 Remote sensing data, image processing and data interpretation**

Because of the restricted accessibility of some areas within the Skeleton Coast Park and relatively scarce information concerning both the ephemeral rivers and the Skeleton Coast Erg remote, sensing data were chosen as a as a helpful tool for monitoring fluvio-aeolian interaction during the last four decades in this area (see also Chapter 6).

#### ***Landsat TM-5 data***

Landsat TM-5 scenes 181-073 and 181-074 are showing the area between the Koigab and the Hoarusib River on the 22.08.1984, half a year after a moderately strong flood event, whereas the more recent Landsat TM-5 scene 181-074 from the 30.03.1995 shows the area between the Koigab and the Hoanib River only one month after the huge floods of 1995. The Landsat data sets were processed with the software-package ENVI 3.2. Different channel combinations, contrast linear stretching and the applications of various digital filters have been used to visualize particular features.

Printouts of the satellite images were used for orientation in the field because of the lack of detailed topographic maps.

#### ***CORONA Satellite Photos***

CORONA Satellite Photos have been ordered through the NASA Eros Data Centre - Boulder/USA recording the ephemeral rivers and the Skeleton Coast Erg in 1965.

#### ***Aerial photographs***

Aerial photographs taken in 1973 were available for most part of the lower reaches of the Koigab and Uniab River from the Surveyor General – Windhoek/Namibia. In addition, three photographs of the Koigab and Uniab River mouth and the southern margin of the Skeleton Coast Erg from a new flight mission in 1996 have been acquired.

Areas of particular interest then were photographed in April 2000 from a chartered plane.

### **3.3 Laboratory analysis**

Sand samples of various facies and localities have been analysed for:

- grain-size
- heavy mineral spectrum
- carbonate content
- major and minor element geochemical composition by XRF
- petrographic composition through optical microscopy

### ***Grain-size analysis***

Dry sieving has been applied to samples taken from 1) channels and sand ramps in the Koigab River, 2) from shrub coppices, sand ribbons and barchans on the Koigab Fan surface as well as for samples from 3) various facies of the sedimentary succession exposed in the Uniabmond area. Dry sieving was chosen because of the low silt and mud contents of the samples (< 1 wt %). A sieving column consisting of 6 (10 for channel samples) sieves with mesh sizes of (-5, -4, -3, -2) -1, 0, 1, 2, 3 and 4 phi were used. Sediment parameters (mean, median, standard deviation, skewness, kurtosis) have been calculated after FOLK & WARD (1957) using a MS-Excel spreadsheet.

### ***Heavy mineral analysis***

Heavy mineral analysis has been tested as a tool to reconstruct the amount of aeolian material input into the Koigab River system as well as the amount of fluvial material output by the aeolian system (see Chapter 4). Heavy minerals from aeolian and fluvial deposits of the Koigab River have been separated from three grain size fractions (<1, <2, <3 phi by using a polytungstate heavy liquid. The heavy mineral separates were then grain mouted and from each sample 200 grains have been point-counted to obtain a reliable statistical data base on the spectrum of heavy minerals (cf. MANGE & MAURER, 1991).

Grain-size and heavy mineral analysis have been undertaken in cooperation with B. Schlicker (Diploma thesis, University of Würzburg/Germany).

### **Carbonate content**

The CaCO<sub>3</sub>-content from samples of the Whitecliff Formation (see Chapter 5, Tab. 5.2) was determined volumetrically after Scheibler (BASCOMB, 1974).

### **XRF-analysis**

X-ray fluorescence analysis has been applied to determine the chemical composition of whole rock sediment samples of the Uniabmond Formation (see Chapter 5) and was tested as a tool to discriminate between different facies. These data were mainly used for a joint research project with J. Svendsen (Aarhus-University/Denmark) (SVENDSEN et al., in press).

## 4 The ephemeral braided river dominated Koigab Fan

### 4.1 Significance and setting of the Koigab Fan system

The Koigab Fan has been deposited within the coast-parallel arid zone of the Skeleton Coast about 20 km south of Torra Bay (Fig. 4.1). The fan (Figs. 4.1 & 4.2), first referred to by VAN ZYL & SCHEEPERS (1993), is intermediate in size for braid dominated alluvial fans (cf. STANISTREET & MCCARTHY, 1993), with lateral dimensions 15 km from apex to toe and 23 km across its maximum lateral extent (KRAPP *et al.*, in press). It is the largest of fan systems, formed by a few of the WSW flowing ephemeral braided rivers, issuing from the Etendeka Plateau, that intermittently traverse the northern Namib Desert to reach the Skeleton Coast. The Koigab Fan is traversed along its central axis by the ephemeral Koigab River, which also represents the present day active channel of the fan. The fan surface bears little surface vegetation, the latter being restricted to shrubby vegetation near the fan toe, associated mainly with small-scale aeolian bedforms such as coppice dunes. This scarce peripheral vegetation relies upon the fog of the Skeleton Coast which drift in almost daily, especially during winter months (LANCASTER, 1982), and are caused by the cold Benguela Current offshore from the Atlantic coastline of Namibia (see Chapter 1.3).

The Koigab Fan was chosen for a detailed study because it differs from many described systems in that it:

- operates at low, tropical latitudes in an arid climatic setting
- lacks significant surface vegetation
- is dominated by mixed gravel/sand ephemeral braided river channels
- is a perfect study site for recording various types of fluvio-aeolian interaction
- thereby acts additionally as a model for certain Precambrian and Early Palaeozoic fan systems deposited prior to the evolution of land plants

In comparison to other fans e.g. the Kosi Fan/India (WELLS & DORR, 1987a, b; GOHAIN & PARKASH, 1990) or the Yallah Fan/Jamaica (BURKE, 1967; WESCOTT & ETHRIDGE, 1980; WESCOTT, 1990) the Koigab Fan has been relatively little disturbed by human activity. In pre-recorded times it was solely the aridity of the area that deterred human exploitation of the region. The fan is enclosed within the Skeleton Coast Park and access has been effectively controlled by the Ministry of Environment & Tourism. Only within a small section of the shoreline of the northern half of the fan and the mouth area of the Koigab River access is allowed for anglers via Koigabmond and Torra Bay. For these reasons the



fan surface and the active channel have been preserved in a relatively pristine condition and allow sedimentological and geomorphological analysis.

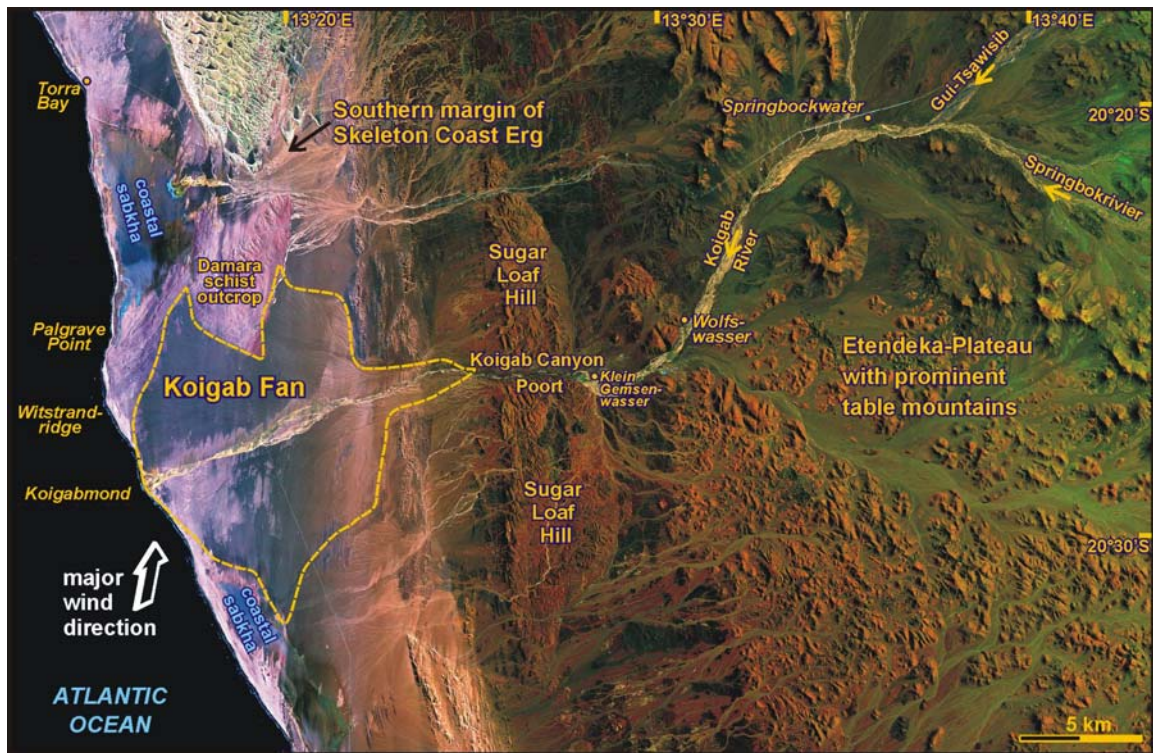


Fig. 4.1: The appearance of the Koigab Fan and parts of its Etendeka Plateau catchment area shown in a Landsat TM-5 image 171-074 (7-4-1 R-G-B; acquisition date 31.03.1995).

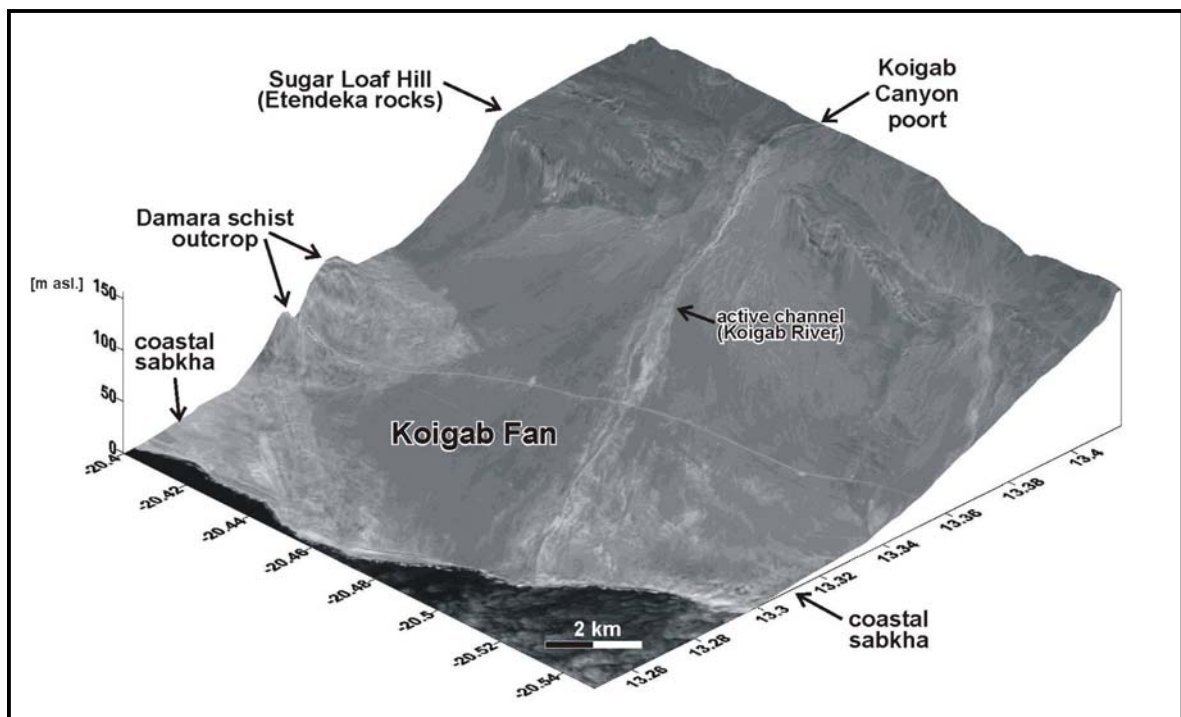


Fig. 4.2: 3-D upstream view from Koigabmond towards ENE illustrating the geomorphological and geological elements of the Koigab Fan and adjacent areas.



#### 4.1.1 Geodynamic framework, tectonic setting and drainage evolution

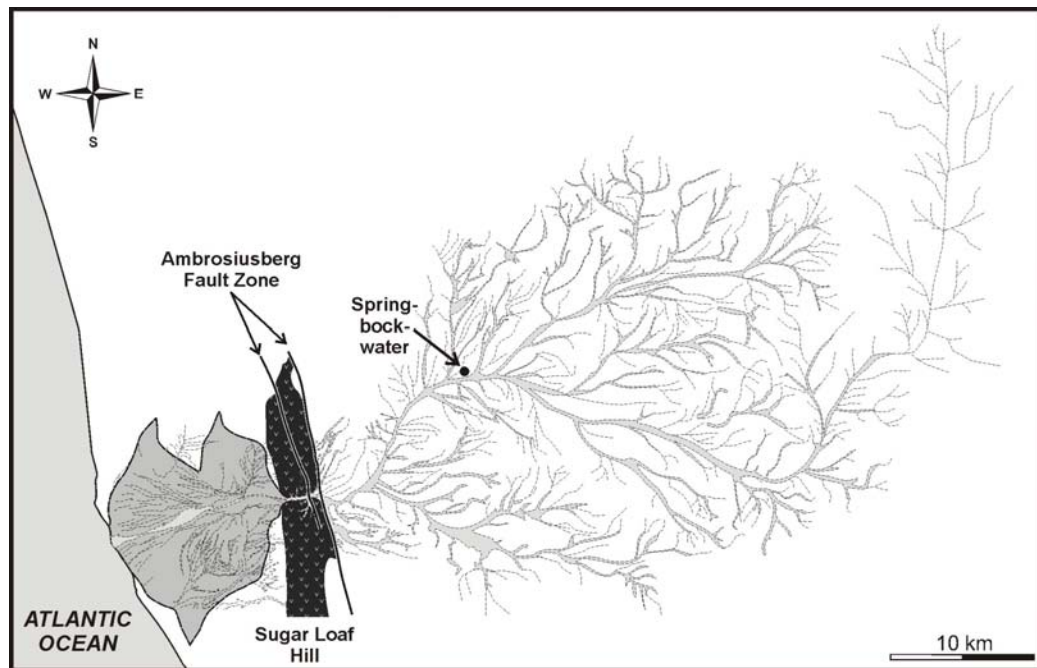
Unlike some other rivers of the northern Namibian coastal strip (e.g. Hoanib, Hoarusib), the Koigab River did not succeed in making a major breach back through the Great Escarpment region (VAN ZYL & SCHEEPERS, 1993; JACOBSON et al., 1995), giving significantly different characteristics to the river channel and its accumulated deposits (see Chapter 4.1.2 and Chapter 6). In particular the system is aggradational in character in its lower course, despite widespread uplift of the coastal region during the Quaternary (KLEIN, 1980). The presently active Koigab channel extends headwards into the Etendeka Plateau and generated a pronounced gorge incision of about 24 m at Koigab Canyon Poort, 20 km east of the coast. The area through which the poort is cut (Figs. 4.1 & 4.2) comprises a series of down-to-the-west imbricate fault blocks (Fig. 4.3) which relate to the major north-south trending Ambrosiusberg Fault Zone (MILNER, 1986; see Chapter 2). Cretaceous volcanics exposed in the fault blocks dip between 5° and 30° towards the east (MILNER, 1986; SCHLICKER, 2000a) whereas capping terraces of Early to Middle Pleistocene (WARD, 1987) Oswater-equivalent conglomerates (VAN ZYL & SCHEEPERS, 1993) have not been tilted (see chapter 4.2.2.1; Fig. 4.9 C) indicating a pre-Quaternary age of the main tectonic movements.

#### 4.1.2 Catchment and source area characteristics

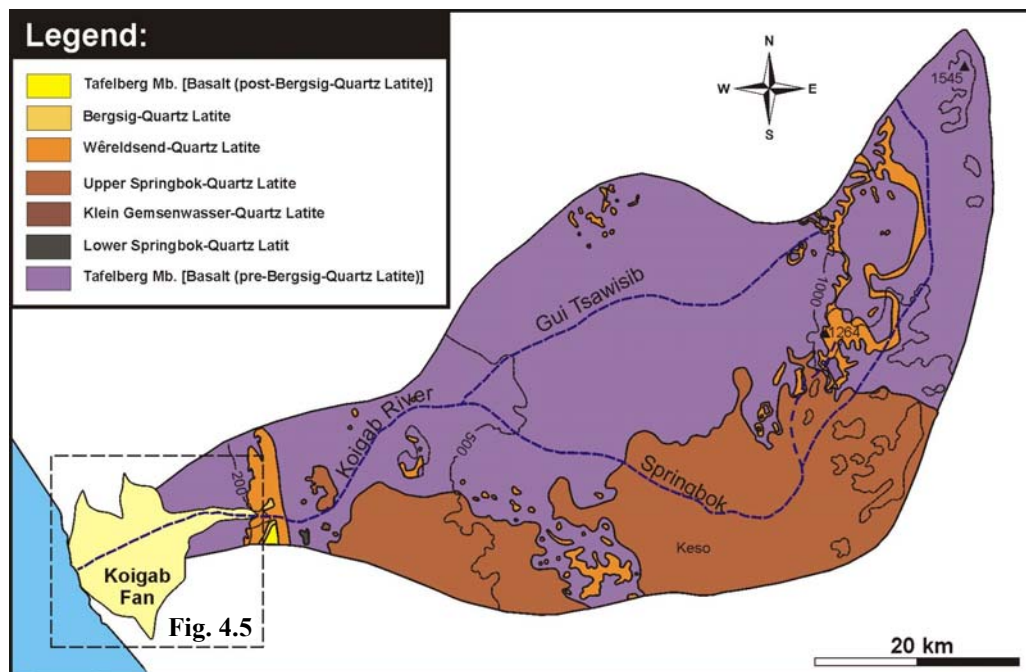
The catchment area of the Koigab River has a size of 2.400 km<sup>2</sup> (JACOBSON et al., 1995) and is one of the smallest of the ephemeral rivers of the Skeleton Coast. The maximum E-W extension of the catchment area is about 95 km, from N-S about 55 km (JACOBSON et al., 1995; SCHLICKER, 2000b). The highest elevation point within the hinterland catchment is 1571 m asl. situated on the top of one of the table mountains of the Etendeka Plateau in the Khorixas District. Nominally the Koigab River starts at the point where the Gui Tsawisib and the Springbok River unite about 3 km E of Springbokwater (Fig. 4.1).

The hinterland catchment area of the Koigab Fan is developed in particularly mountainous terrain of the Etendeka Plateau (Figs. 4.1, 4.3), comprising a thick sequence of flood basalts and interbedded quartz latites by the effusion of which between 131 and 133 Ma immediately preceded final South Atlantic Oceanic rifting and onset (RENNE et al., 1996; see also Chapter 2.2.2). The Etendeka Plateau represents an eroded remnant of a thick volcanic succession, rising to heights of about 2000 m. The catchment area is exclusively build up by tholeiitic basalts, basaltic andesites and quartz latitic rheoignimbrites (MILNER

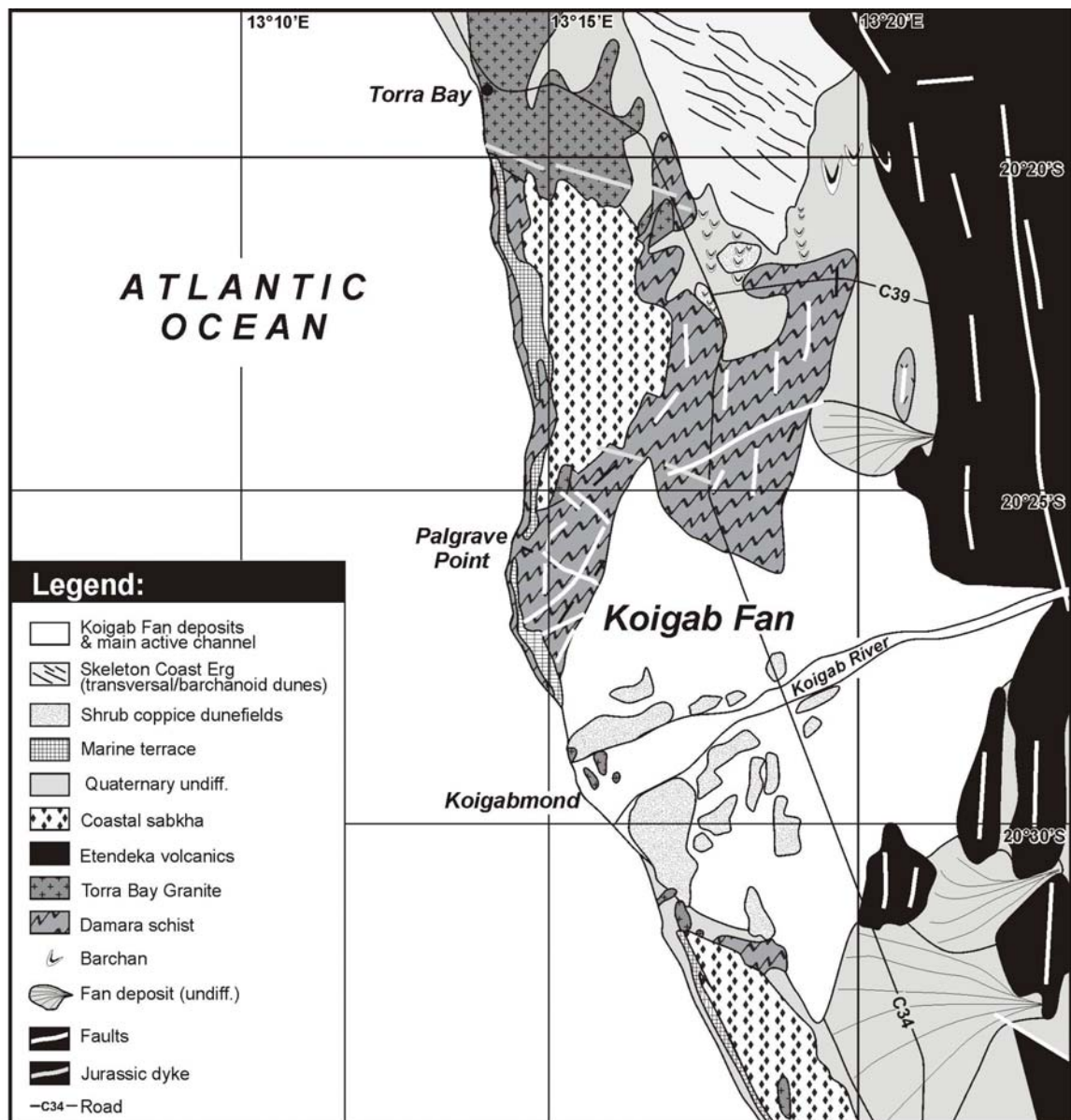
et al., 1992; MARSH et al., 2001; see also Chapter 2.2.2). Weathering products of the Etendeka volcanics comprise dominantly volcanoclastic lithics, plagioclase and clinopyroxene besides minor amounts of volcanic magnetites, orthopyroxenes and epidote. Also some quartz and agate derive from amygdales or vugs in the volcanics. Therefore, the bedload and the sediment transported by the Koigab River onto the Koigab Fan is exclusively composed of the Etendeka volcanics and their weathering products.



**Fig. 4.3:** Drainage system of the Koigab River (modified after SCHLICKER, 2000a; Topographic maps 1:50.000 2013 AC & AD Torraabai & 2013 BC).



**Fig. 4.4:** Geological map of the catchment area of the Uniab River (modified after MILLER, 1988; SCHLICKER, 2000a). [Box indicating position of Fig. 4.5]



**Fig. 4.5:** Detailed geological map of the Koigab Fan and adjacent area (compiled from: Landsat TM-5 scene 181-074; aerial photos 22.11.1973 & 26.08.1996; MILLER, 1988)

In the coastal area near Koigabmond Late Proterozoic Damara metamorphic basement rocks crop out within the active Koigab channel and the adjacent fan areas (Fig. 4.5). Essentially these are schists, migmatitic gneisses and granites, composed mainly of quartz, feldspar, biotite and garnet (AHRENDT et al., 1983). The Torra Bay Granite is intruded by pegmatites composed of quartz, feldspar and garnets.

These contrasting source rock types are important for the understanding of fluvio-aeolian processes which have been observed in the Koigab Fan area (see Chapter 4.3.3).

### 4.1.3 Depositional site and climate

Traversing the fan surface, the gravelly Koigab braided river is ephemeral (JACOBSEN et al., 1995), experiencing flood pulses of short duration, typically of a few days only. Because of the remote setting and flashy nature of the flooding no discharge records are available. Floods normally happen during November to February, during the annual rainy season within the Southern Hemisphere summer (see Chapter 1.3). The Koigab River flows to the South Atlantic coast across considerable climatic gradient from summer rainfall in the semi-arid mountainous catchment (~125 mm/a) to arid (0-25 mm/a) over a distance of merely 150 km (JACOBSON et al., 1995). Considerable precipitation can supply large volumes of water and sediment discharge from the mountainous hinterland catchment. In the years 1999, 2000 and 2001 most of the rain that caused runoff of the ephemeral rivers in the Skeleton Coast Park fall during the months of March and April (own observations in all three years during own fieldwork). Thus the Koigab River may undergo major flooding once or twice a year, or at lower frequencies if precipitation in the hinterland catchment is insignificant during one or several years of drought. Such bursts of significant rainfall can be extremely localised, often affecting only two or a few neighbouring river catchments that parallel one another and are characteristic for the coastal strip of north-western Namibia.

### 4.1.4 Drainage system of the Koigab Fan

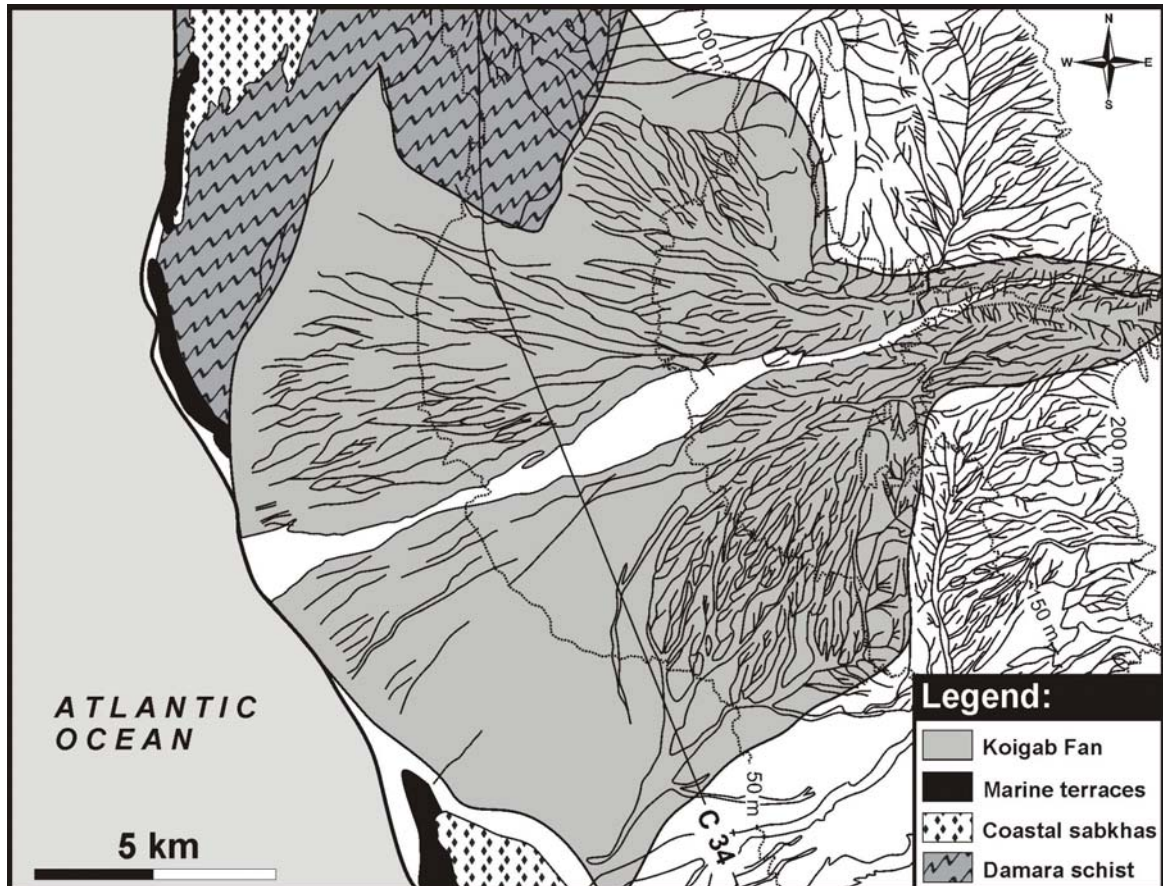
The drainage system of the Koigab Fan is dominated by the main active channel, the Koigab River, which traverses the fan on its central axis and divided it into a northern and southern part.

On its 130 km long way to the Atlantic Ocean the Koigab River drop over a height of about 1200 m resulting in an overall river gradient of about 0.9%. In comparison to the river gradient the regional gradient is about 1.7 % (SCHLICKER, 2000b).

The Koigab River, leaving the area of the Etendeka Plateau, enters onto the fan surface through an entrenched fan apex (Fig. 4.6) at a height of 200 m asl. and thence grades at 1:89 (Fig. 4.6) down to sea-level over a distance of 15 km. Beside the Koigab River a radial-like drainage system of slightly incised abandoned channels is clearly visible on the fan surface (Fig. 4.6). However, this radial-like drainage pattern differs from the common pattern of most other known alluvial fans (e.g. Death Valley fans: BLAIR & MCPHERSON, 1992, 1994a, b; glacial outwash fans: BOOTHROYD & ASHLEY, 1975). Commonly, the



channel pattern spreads radially away from the apex (NEMEC & STEEL, 1988; CHAMLEY, 1990) and results in building up the typical fan shape form. The drainage pattern of abandoned channels on the southern fan surface merges towards the distal part of the fan, whereas on the northern part the channel pattern has a typical braided form (Fig. 4.6).



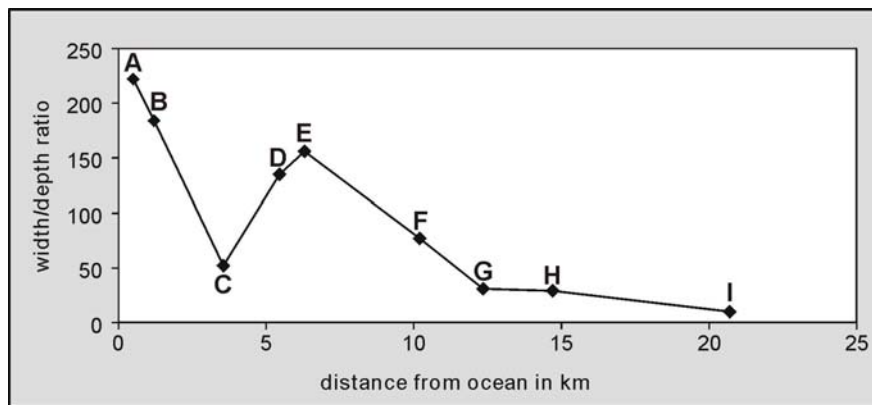
**Fig. 4.6:** Drainage pattern of the Koigab Fan. [Data derived from Topographic map 1:50.000 2013 AC & AD Torrabaai)

## 4.2. Fan Morphology

### 4.2.1 Principal anatomy and dimensions of the Koigab Fan

The Koigab Fan area has a size of about 345 km<sup>2</sup> (VAN ZYL & SCHEEPERS, 1993) and has lateral dimensions of 15 km from apex to toe and 23 km across its maximum lateral extent. The fan has a typical semi-conical shape showing a plano-convex cross profiles (Fig. 4.8 C). The gradients of the Koigab River and the adjacent fan surface (Fig. 4.8 B) are approximately the same. In comparison to many other described fans the gradient profiles of the fan surface and the river channel do not indicate an intersection point. This is usually the point, where the slope of a fan surface decreases and becomes less than the slope of the channel (HOOKE, 1967). Below this point a depositional lobe develops. This has not been the case at the Koigab Fan.

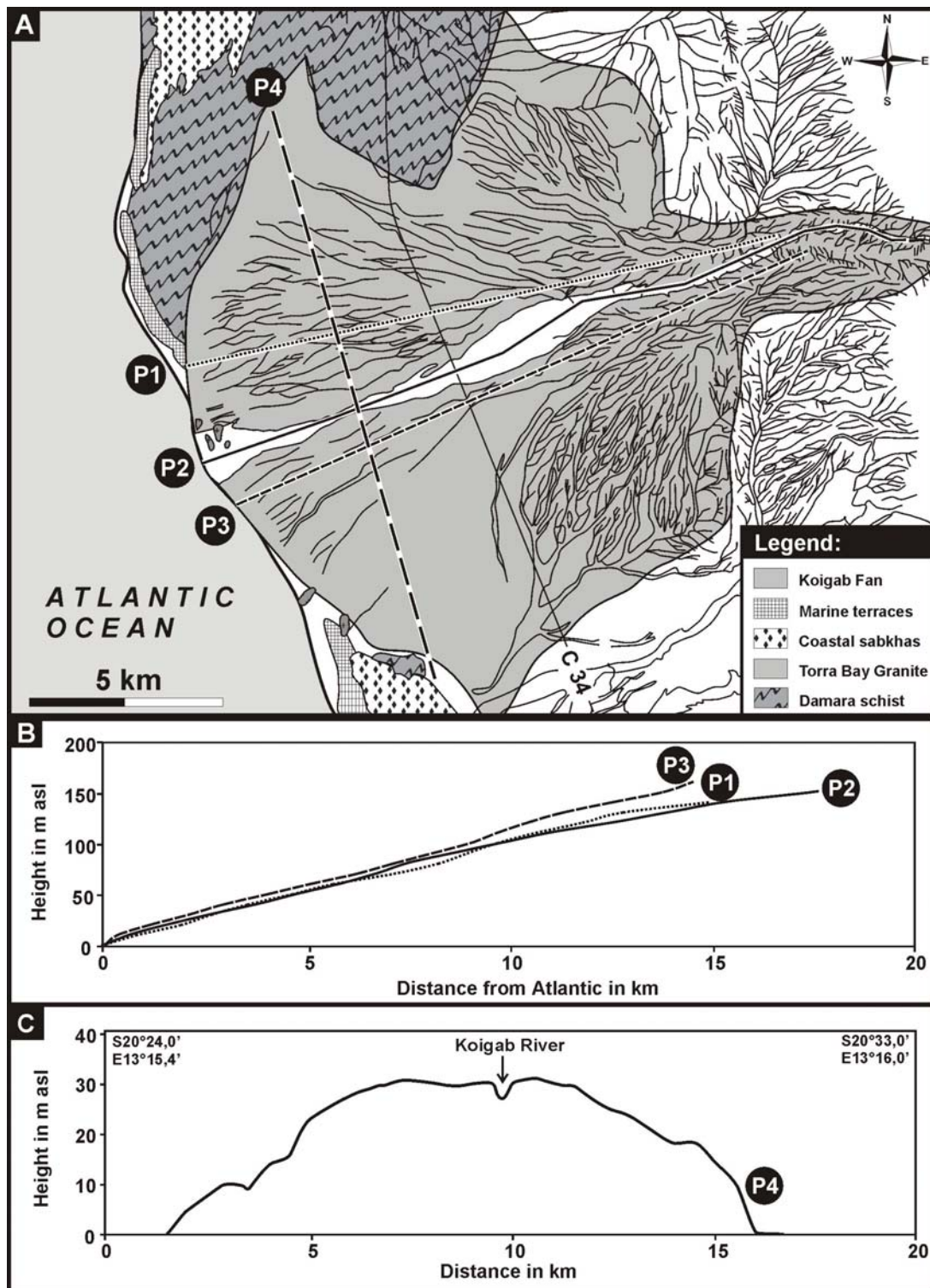
Width/depth ratios of the Koigab River (Fig. 4.7) show that the channel widens towards the middle part of the fan (I to E in Fig. 4.7) but becomes narrower again between 6.5 to 3.5 km away from the coast (D & C in Fig. 4.7). From there onwards the river starts to widen again and incision decreases (A & B in Fig. 4.7). The narrowing of the river between E and C (see Fig. 4.7) is not yet understood. As the Koigab River is incised into former fan deposits and not into the underlying bedrocks, an influence of changing bedrock geology like the change from strongly weathered basalts into more resistant Torra Bay Granite cannot be used for an interpretation. Due to limited outcrops of the fan deposits themselves, which are widely covered by sandramps, it was not possible to investigate the sediments in respect to different degrees of lithification. Further investigations applying e.g. Ground Penetrating Radar (GPR) might be helpful for getting more information about the underlying fan sediments and underlying bedrock topography resulting in a better understanding for the dramatic downstream changes of width/depth ratios.



**Fig. 4.7:** Width/depth ratios of the Koigab River (for localities see Fig. 4.11).

The fan base has a width of 15 km, sectorially encompassing an angle of  $110^\circ$  (Fig. 4.6). The base of the fan system only partly progrades into the Atlantic Ocean, however only a central sector of 15% actually debouches directly into the sea through an area of active beach berm, backshore and foreshore (Fig. 4.8). Thence the channel passes into the ocean, to feed an area of offshore shoal 5 km by 4 km (see Chapter 4.4, Fig. 4.21). On either side of the river mouth the foreshore is sandy and scattered with articulated shells and shell debris, including shells of inarticulate brachiopods.

Two fan-base areas on either side of the central sector pass into different settings. To the north the fan base is set upon a basement area of Damaran schists, itself backed by the area of a large coastal sabkha that floods occasionally (Fig. 4.8 A).



**Fig. 4.8:** A: Drainage network of the Koigab Fan with locations of the downchannel profiles. B: illustrates the slight contrast between downchannel profiles of the Koigab River (P2) and the adjacent fan surfaces to the north (P1) and to the south (P3). C: transverse section across the lower part of the Koigab Fan showing the convex shape of the fan (25x exaggeration).

To the south the fan base debouches not into the ocean but into coastal sabkhas (Fig. 4.8), where fine marine-flood sediments are heavily indurated by subsurface precipitation of salts, particularly gypsum. The coastal sabkhas are separated from the ocean over large

areas by shore-parallel beach ridges (see also chapter 4.4). The beach ridges back onto presently active beach berm, backshore and foreshore systems similar to that of the actual river mouth.

#### **4.2.2 Channel and surface characteristics of the Koigab Fan**

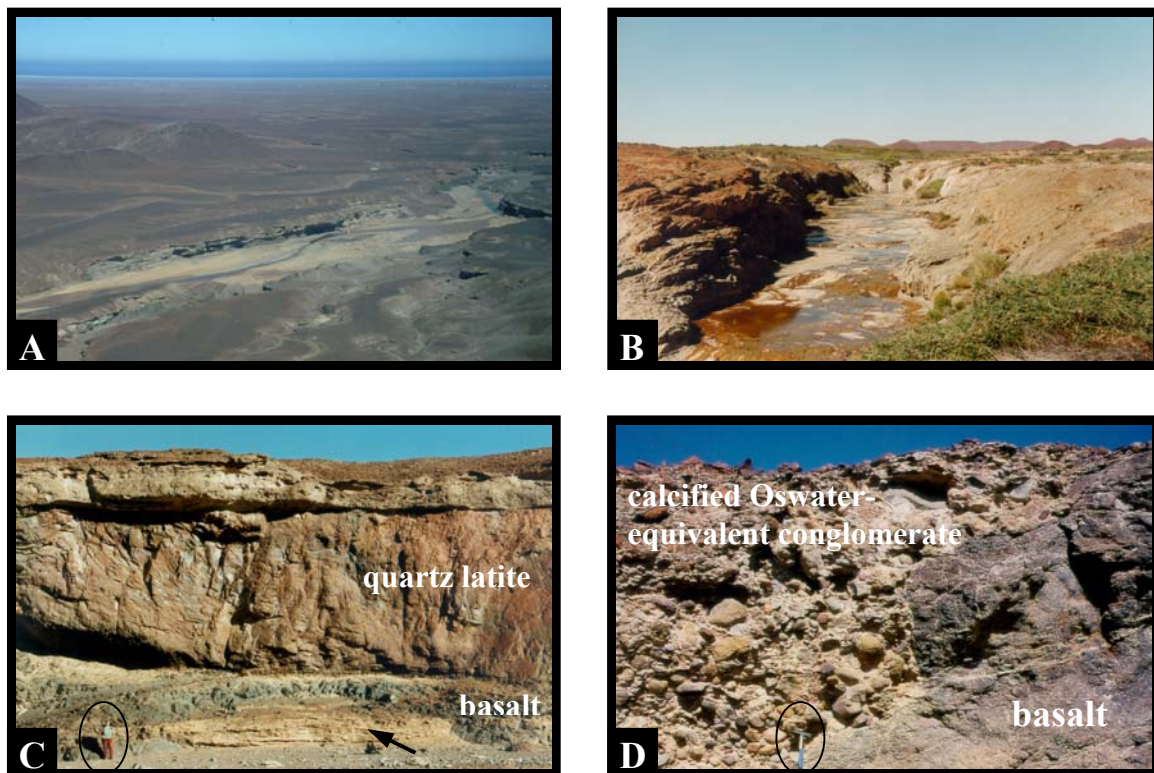
Sections across active and abandoned channels of the Koigab Fan were surveyed at various positions along the length of the channel (Fig. 4.11) in its traverse of the fan surface, using survey level and tape. These surveys were undertaken in order to collect information concerning channel geometry, bar and depositional forms within the channel, clast textural data, and to locate samples of sand-sized material deposited during waning floods. Where sample sites allowed the measurement of ancient river deposits, exposed in side walls or isolated terraces, partial down-channel and cross-channel sectional profiles were recorded. Such profiles allowed comparison between modern and ancient Koigab River deposits.

##### **4.2.2.1 Koigab River and Koigab Canyon Poort**

40 km east of the Atlantic Ocean the Gui-Tsawisib and the Springbock River flow together and become the Koigab River, which traverses the westernmost part of the Etendeka Plateau and reaches the coastal plain via the impressive Koigab Canyon Poort (see Figs. 4.9A-C). There, the Koigab River cuts a gorge up to 24 m deep over a distance of more than 1.5 km into the resistant quartz latitic rocks of the Sugar Loaf Hill (Figs. 4.9 A-C). The gorge is termed the Koigab Canyon Poort. VAN ZYL & SCHEEPERS (1993) suggested a Tertiary age for the development of the Koigab Canyon Poort.

After the gorge had been incised the whole river valley and its tributary systems were buried during the Early to Middle Pleistocene by Oswater-equivalent deposits (Figs. 4.9 C & D), which is comparable to the situation described from the lower Kuiseb River by WARD (1987). Most of these calcified sediments have been eroded probably during the sea level lowstand in the Last Glacial Maximum (LGM, c. 18 Ka BP). Remnants of these Oswater-equivalent sediments can still be found forming and underlying the present day river floor in the gorge, on terraces and in tributary channels (Fig. 4.9 D). However, investigations from the Uniabmond area (see Chapter 5) show, that comparable calcified sediments (there termed Whitecliff Fm.) are probably of Late Pliocene to Middle Pleistocene age.





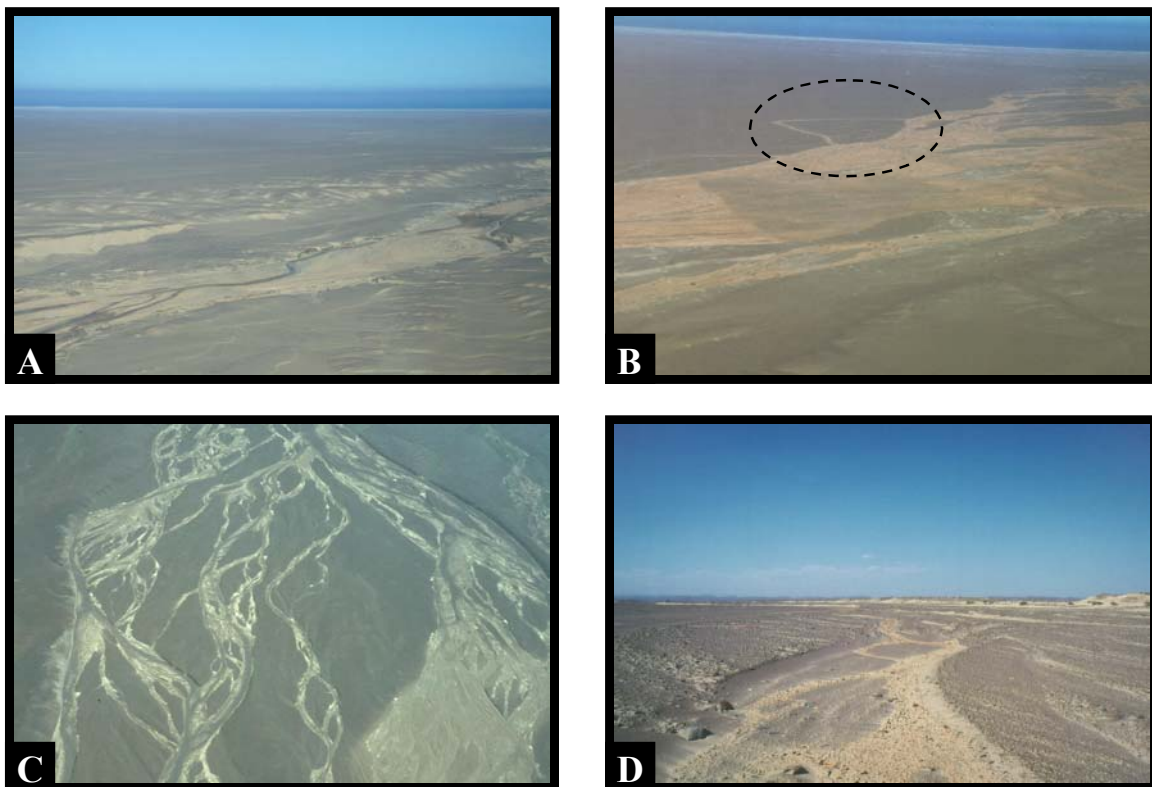
**Fig. 4.9:** **A:** Oblique view of the Koigab Canyon Poort (view towards WSW). **B:** The eastern part of the Koigab Canyon Poort. **C:** Southern cutwall in the Koigab Canyon Poort (person for scale). The Etendeka volcanics (black: basalt, brown/red: quartz latites) are overlain by calcified Oswater-equivalent conglomerates. Attached to the canyon walls are remnants of ancient flood deposits (arrow). **D:** Oswater-equivalent sediments buried also tributaries of the Koigab River, which have been later cut off by subsequent erosion of the Koigab River (hammer for scale).

#### 4.2.2.2 The lower Koigab River - active channel of the Koigab Fan

The head of the Koigab Fan is heavily entrenched by the active river channel -the Koigab River- which presently only approaches height parity with the fan surface near the outermost fan perimeter (Fig. 4.8). Midway up the fan the Koigab River channel cuts down 3-6 m metres into the fan surface (Fig. 4.10 B), while at the apex the channel is entrenched to a depth of 10-15 m metres (Figs. 4.10 A & 4.11). Upstream from the apex, downcutting into bedrock has developed the Koigab Canyon Poort which cuts back as a major nick-point (Figs. 4.9 A & B) into the faulted Etendeka Plateau to a maximum depth of 24 m.

On its way through the fan area, the Koigab River shows the characteristics of a low-relief, braided river with longitudinal bars separating medium to low flow channels (Figs. 4.10 C & D). The channels are filled with medium sand to gravel, usually up to 50-60 cm in size, and the uppermost parts of the channel surface are modified during long lasting interflood periods by wind deflation of finer grains. Only during extreme flood events like 1995

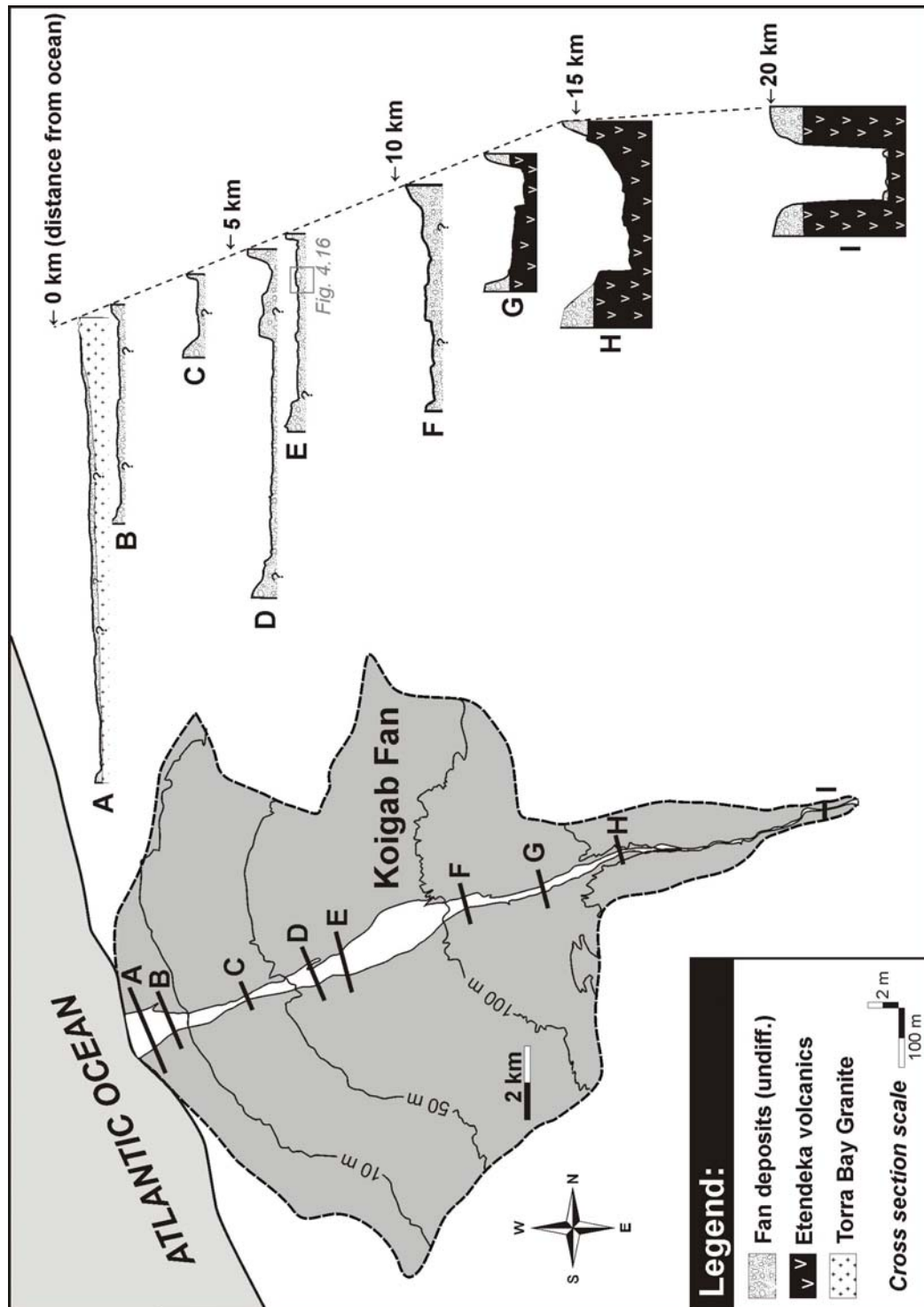
(JACOBSON et al., 1995) the whole channel will be filled and in some parts also overtopped by the running water. For the duration of the flood aeolian generated sediments and sedimentary structures but also former fluvial forms are eroded and destroyed. Also channel avulsion has been observed during flood events (Fig. 4.10 B). As such mega-floods do only occur averagely once a decade (SHANNON et al., 1986; JACOBSON et al., 1995; STOLLHOFEN et al., 1999) and usually last only for several hours to a couple of days, the actual dominant process in the Koigab Fan area is aeolian winnowing and deposition resulting e.g. in vast deflation surfaces, shrub coppices or sandramps.



**Fig. 4.10:** **A:** Oblique view towards WSW of the area where the Koigab River enters the fan. **B:** Oblique view towards WSW of the Koigab River in the mid part of the fan two weeks after the April 2000 flood. The flood followed the main channel, signs of avulsion can be seen on the southern banks which are locally overtopped (circle). **C/D:** The typical field appearance of the ephemeral braided Koigab River: small, slightly incised channels with longitudinal gravel bars. The thalweg is partly covered by thin waning flood stage sand and mud layers (D).

The most common bar form in the active channel is that of vegetation-free longitudinal gravel bars (averaging 100 to 300 m long and 20-50 m wide) composed of subangular to subrounded quartz latite and basalt clasts. They are poorly to non-sorted, comprising a large variety of grain sizes from fine sand to boulders. Slight imbrication, caused by the westerly flow direction, is recognisable in some places. Aeolian winnowing of finer material causes the development of a deflation surface on the top of the bars (Fig. 4.10 D). Bar height decreases towards the river mouth from about 70 cm at the fan apex to less than

10 cm and the difference in height between bars and channels decreases towards zero. After a flood event small sand ramps form in the lee of the bar flanks. Fluvially generated sandy bar forms tend to be eroded and reworked by the strong southerly winds, a factor contributory to the relative lack of sandy bars documented in the cross channel sections and also in the ancient fan sequences (see Chapter 4.3.2).



**Fig. 4.11:** Locations of cross-sectional profiles surveyed by theodolite level and tape. Sections to the right of the figure were measured at various positions down the Koigab River from the fan apex to the river mouth with numbers to the right of the sections indicating their distance from the Atlantic Ocean.

### 4.2.2.3 Abandoned channels of the Koigab Fan

Variably discernible within the whole fan surface is the morphology of abandoned channels (Fig. 4.12). The presently active Koigab channel more or less bisects the fan surface along its central axis. To the north, channels are the least modified by subsequent flooding and aeolian fill. The most recently abandoned channel is immediately north of the presently active channel and channels become progressively less well defined the further they are situated northward away from the active channel. South of the present Koigab channel, the abandoned channels are far less well preserved and only defined as shallow troughs in the surface (Fig. 4.13).

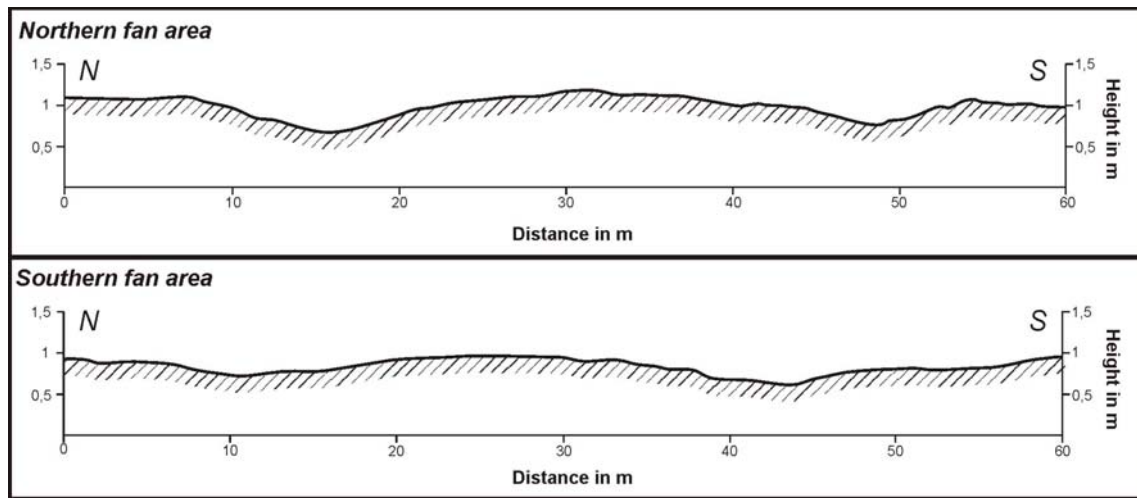


**Fig. 4.12:** Oblique view towards WSW illustrating the drainage network on the surface of the Koigab Fan. The fan surface in the foreground displays less active and/or abandoned channels, centre-ground shows the main channel (Koigab River) two weeks after a smaller flood event in April 2000. The southern part of the fan surface is characterized by shrub coppice fields (white spots).

Therefore, it can be deduced that the active channel is in the process of migrating southwards through successive lateral avulsion (see Fig. 4.10 B), slowly reworking an earlier fluvially generated surface, in which only rather ancient channel remnants are preserved. This reasoning also explains why aeolian bedforms (shrub coppices, sand ribbons, sand ramps and barchanoid forms) are also best represented within the southern half of the fan. In the northern fan area such forms have been reworked by lateral migration



of channels. Furthermore, the northern fan area acts today as a sediment bypass surface, where aeolian winnowing is the dominant process during the long lasting inter-flood periods. There is clearly a relationship between the setting of the Koigab Fan and the southern margin of the Skeleton Coast Erg (see Chapter 4.3.3). To a large extent the fluvial disturbance and windblown reworking of large volumes of sand from the northern half of the fan represents an important source, in addition to that of the shoreline, for sand provided to that part of the erg.



**Fig. 4.13:** Comparison of two measured channel-cross profiles surveyed by theodolite level and tape on the northern and southern fan area. On the northern fan area the morphology of abandoned channels is still more obvious than on the southern fan area.

### 4.3 Sedimentological processes shaping the Koigab Fan

#### 4.3.1 Sedimentological characteristics of the active channel

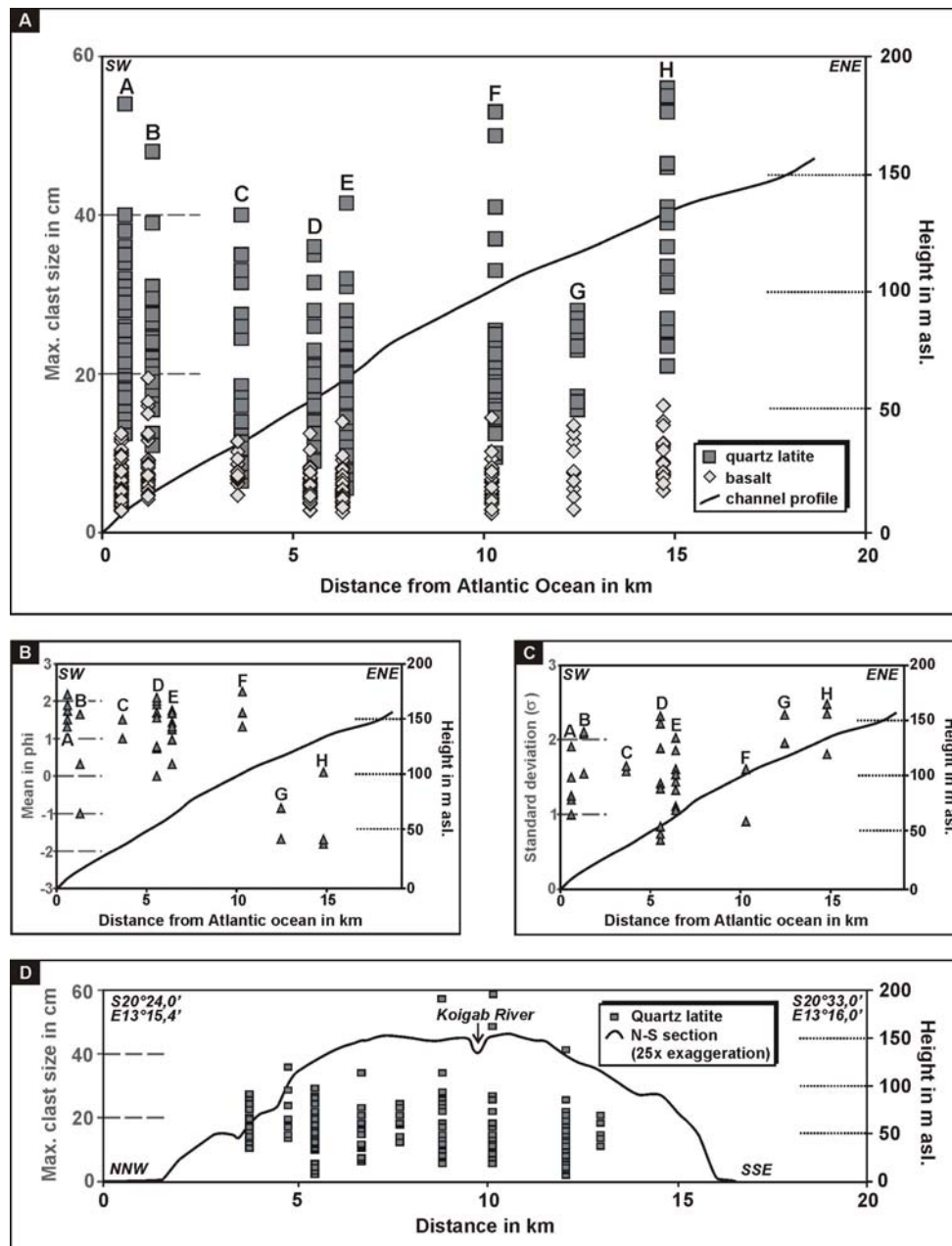
The restricted source terrain is of considerable advantage in assessing down-channel variation in clasts entrained by Koigab River floods. Only two types of clasts are apparent, those composed of massive or vesicular, but intensively weathered basalt and those composed of varieties of quartz latite. Data derived from different clast types were collected separately, so that comparative assessments could be made from one cross-sectional profile to the next.

Fig. 4.14 shows graphs of various clast and grain-size parameters of gravel and sand samples measured at specific cross-sectional profiles down the Koigab channel and across the fan surface. The analysis of the maximum clast size indicates that there is little significant reduction in clast size downstream (see also SCHLICKER, 2000b). This differs from other described fans like the Scott and Yana braided outwash fans (Alaska) described

by BOOTHROYD & ASHLEY (1975), where maximum clast size decreases in downfan direction (see their Fig. 8C, p. 200) and only sand-sized material occur at the fan toe.

If grain size parameters from channel samples are compared, changes neither in mean (Fig. 4.14 B) nor in sorting (standard deviation; Fig. 4.14 C) are significant. This reflects the ephemeral flash flood style of the active river system on the fan.

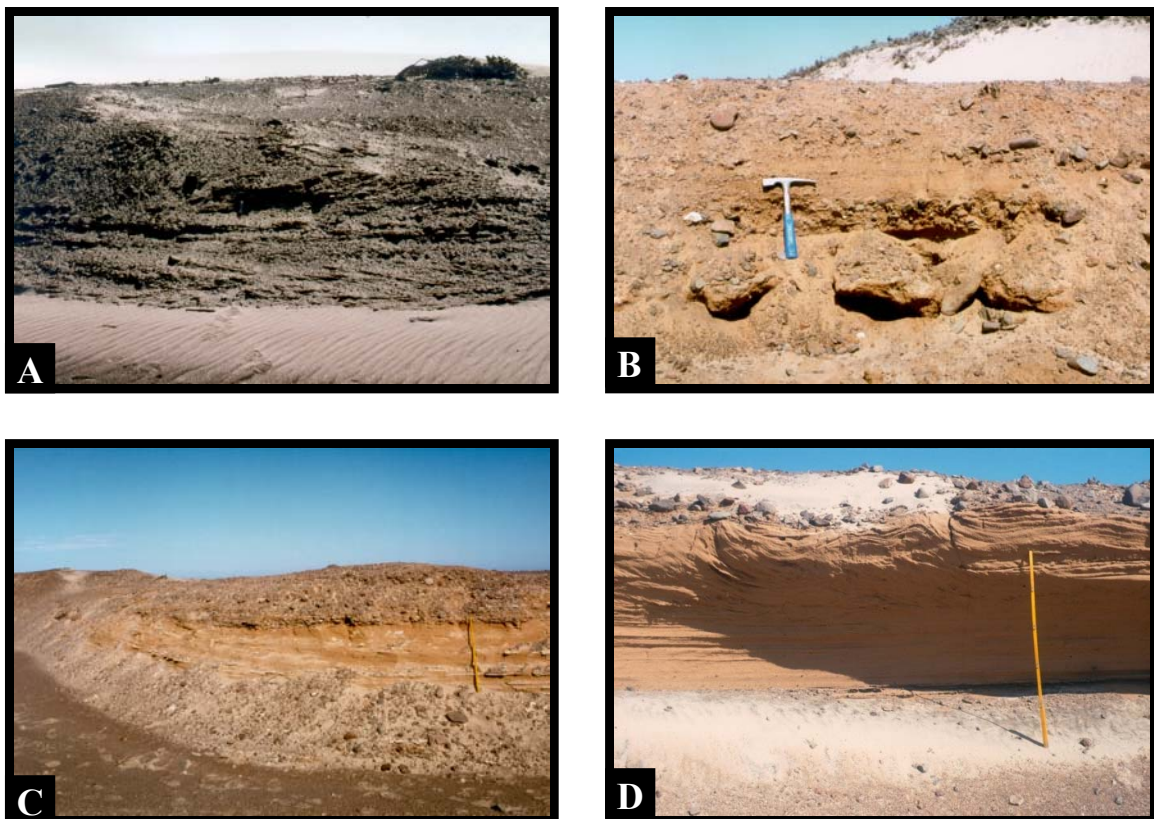
Furthermore, no maximum clast size variation is obvious along a NNW-SSE section across the central part of the fan parallel to the main road C 34 (Fig. 4.14 D).



**Fig. 4.14:** **A:** Clast size measurements (in cooperation with B. Schlicker) on basalts and quartz latites from gravel bars in the Koigab River showing that there is no decrease in clast size in down-fan direction. **B/C:** Variation of the mean (**B**) and sorting (**C**) of samples derived from channel sands (in cooperation with B. Schlicker). Sample locations in Figs. 4.14 A-C are shown in Fig. 4.9. **D:** Showing maximum clast size variations along NNW-SSE section across the central part of the fan parallel to the main road C 34 (see Fig. 4.8 C).

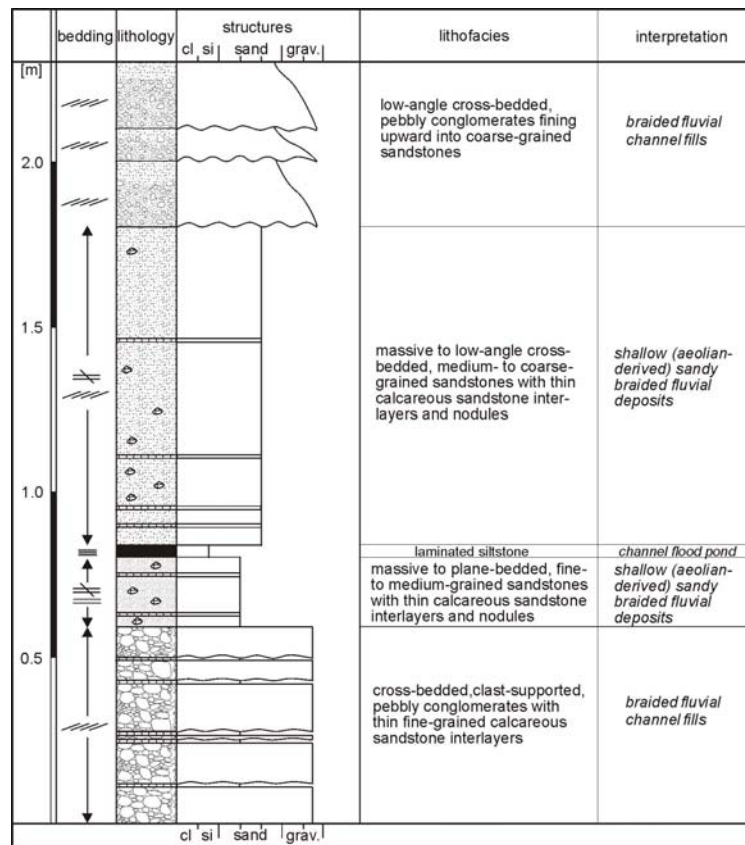
### 4.3.2 Ancient fluvial sequences of the Koigab Fan

Because of the deflationary nature of the fan surface (Fig. 4.17 A & B), it is difficult to record the depositional style of abandoned channel systems. The fan deposits are only exposed in cut-walls of the main active channel and terraces isolated within them, but most are covered by sand which is blown from the beach over the fan surface (Fig. 4.17 D). These fan deposits consist mostly of cobble to boulder gravel and display well-developed low-angle planar cross-bedding (Figs. 4.15 A, 4.16) and plane-bedded stratification (Fig. 4.15 B) related to longitudinal gravel bar migration. The gravel is dominated by quartz latite clasts, basalt clasts are of minor abundance. The gravels are interbedded with medium-grained sand layers (Figs. 4.15 B & C) representing waning flood stage deposits of eroded aeolian sands and sandramps. These fine- to coarse-grained sand layers (<1.20 m) show transitional flow plane lamination to low-angle cross-bedding in the lower parts and climbing ripple cross-lamination with convolute deformation structures in the uppermost part (Fig. 4.15 D). Thus braided fluvial processes deposited gravels and sands to cause the overall aggradation of the Koigab Fan in a manner similar to those of the modern Koigab River.



**Fig. 4.15:** Photographs of terraces and cut-walls showing ancient sequences of fan sedimentation. **A:** Low-angle cross-bedded gravel fill of a river channel. **B:** Plane laminated sand channel fill above a channel gravel bar deposit. **C:** Shallow sandy braided fluvial deposits in between braided fluvial channel fills. **D:** Plane-laminated fluvially reworked aeolian sand deposits with convolute deformation structures at the top.



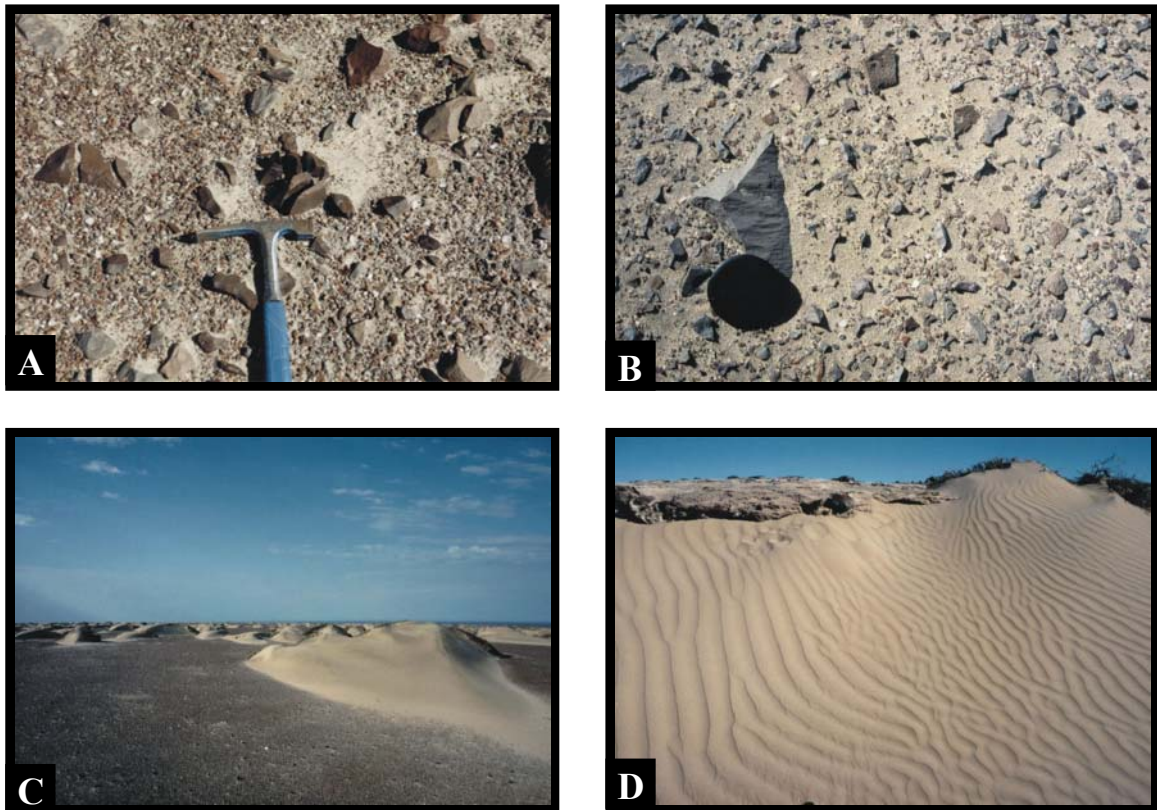


**Fig. 4.16:** Typical profile of an ancient sequence of the Koigab Fan deposits documenting the braided fluvial origin of the sedimentary environment. Position of profile see Fig. 4.11. For explanation of symbols see Appendix 1.

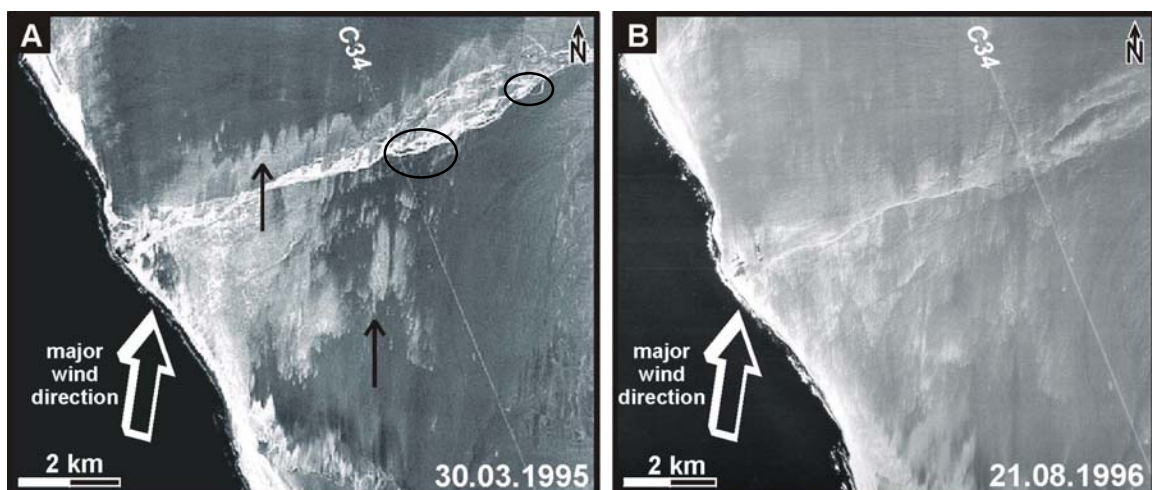
### 4.3.3 Fluvio-aeolian interaction affecting the Koigab Fan surface

Longlasting interflood periods, the hyper-arid setting and permanently strong south-southwesterly onshore winds provide a setting where aeolian processes operate throughout the year causing deflation, particularly of sand-sized material on the fan surface. At an advanced stage, this finally leaves behind a serir-like lag deposit of coarse pebbles (Fig. 4.17 A & B). The rate, nature and spatial characteristics of such transport processes are controlled by various factors like the moisture availability, magnitude and frequency characteristics of flood events and the nature of the sediment (BULLARD & LIVINGSTONE, 2002; KRAPF et al., 2003). The provision of abundant sand during ephemeral river flooding is usually followed by enhanced aeolian winnowing of sand out of dry channelways at the fan surface (KRAPF & STOLLHOFEN, 2000). These sands either accumulate as sandramps within another downwind channel, preferentially at its leeward side, or they form shrub coppices (Fig. 4.17 C), sand ribbons, and barchan trains which add material continuously to the Skeleton Coast Erg, developed about 6 km farther downwind of the active Koigab channel. Such winnowing out of a fluvial channel is well illustrated in Fig. 4.18 A where

the bright greyish shading shows the widespread development of shrub coppices and small sandsheets. An additional, more constant source of aeolian sand is provided in the coastal areas by a sandy backshore strip of several 10's to 100's metres in width.

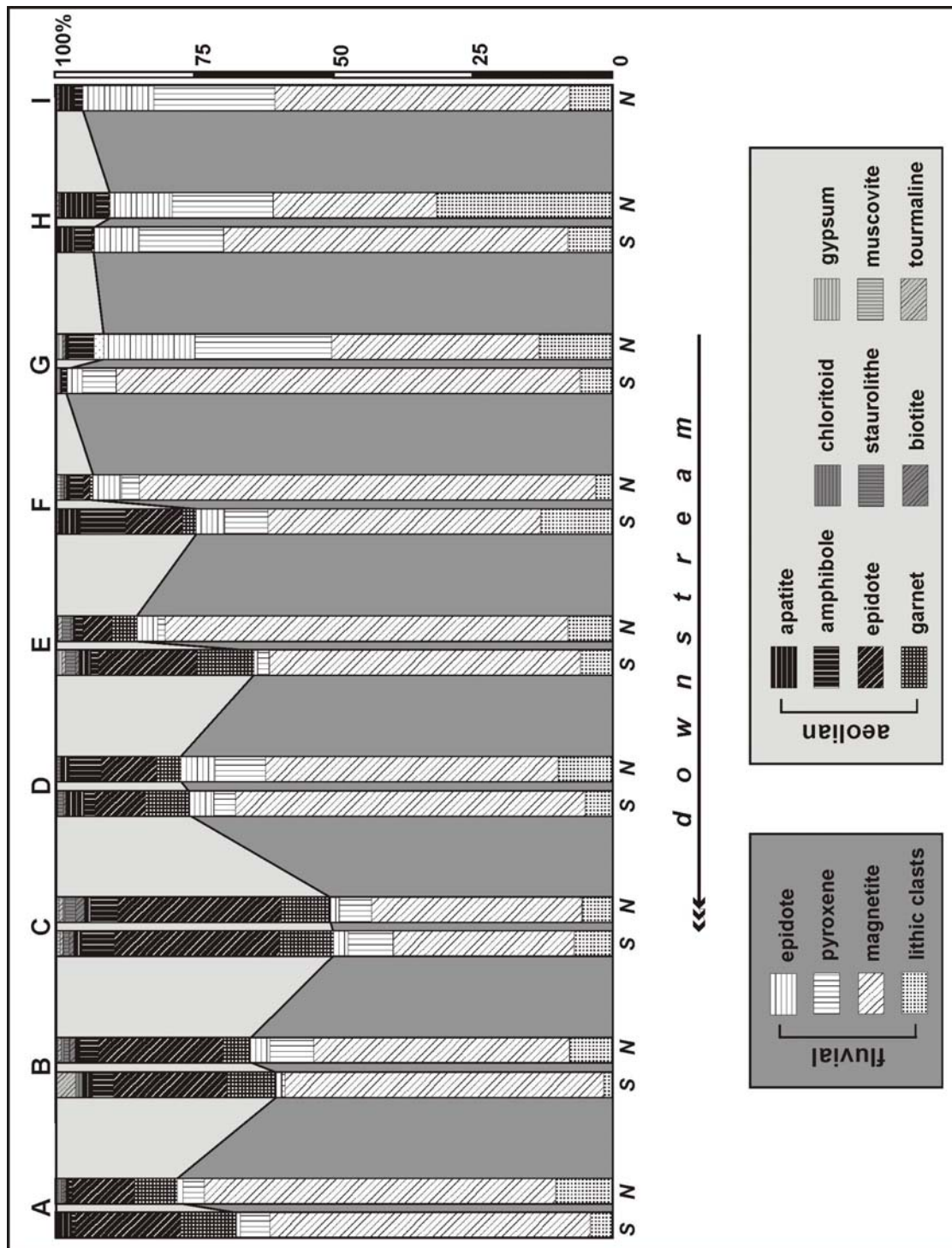


**Fig. 4.17:** **A & B:** Typical deflation surface developed on the Koigab Fan surface. **C:** Photograph of a typical shrub coppice field developed on the deflated fan surface on the southern part of the Koigab Fan (view towards S in upwind direction). Tails of the shrub coppices are aligned to the dominant SSW winds. **D:** Typical sandramp developed in the lee-side of the southern bank of the Koigab River channel.



**Fig. 4.18:** **A:** Landsat TM-5 image of the western part of the Koigab Fan one month after a major flood event of February, 1995. The floods run of the main channel, overtopping the banks locally (circles). After the flood the channel was subjected to aeolian winnowing (arrows) and sediment was blown out of the dried-up river bed onto the northern part of the fan by the dominantly SSW winds. In addition, aeolian sand is provided in the coastal areas constantly by the sandy backshore strip. **B:** Aerial photo from August, 1996, showing that most of the fluvially derived material from the last flood event in February, 1995 is already winnowed out of the Koigab River channel.

River flooding not only transports "juvenile" material from inland volcanic source rocks but also reworks and mixes with aeolian sands which are accumulated within the river channels. This may result finally in multiple cycles of fluvial and aeolian recycling of sand in the fan area, which is also recorded by the ancient Koigab Fan sequences (Figs. 4.15, 4.16).



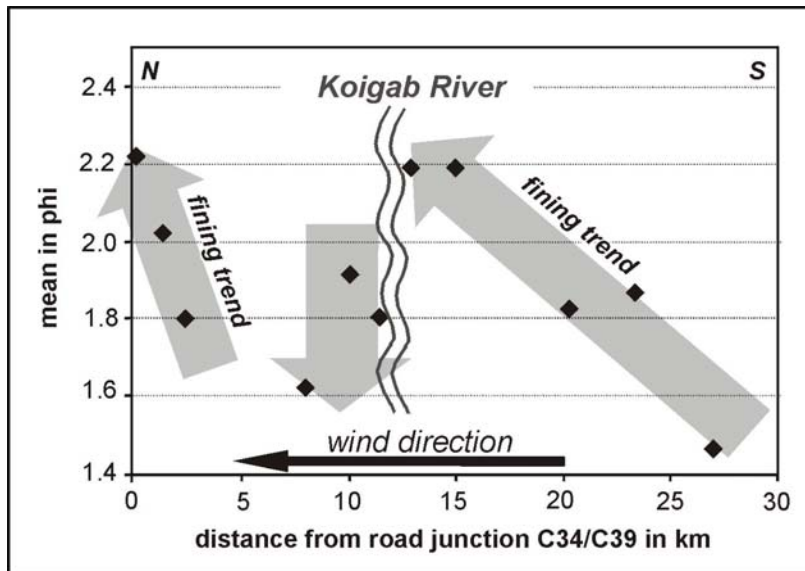
**Fig. 4.19:** Downstream variation of fluvially versus aeolian derived heavy mineral spectra of Koigab River deposits (63-125  $\mu$  fraction). Sampling locations A-I are shown in Fig. 4.9. Left columns represent heavy mineral assemblages from upwind southern and right columns from downwind northern channel flanks. See text for further explanations (compiled after SCHLICKER, 2000b).

Heavy mineral assemblages within fluvial deposits at sampling localities A to I (cf. Fig. 4.11) downstream along the Koigab River have been tested as a tool to demonstrate the amount of aeolian material input into the river system and the amount of fluvial material output by the aeolian system (SCHLICKER, 2000b). Components, which unequivocally relate to a volcanic source (e.g. volcanic lithics, Ti-magnetite, pyroxenes and epidote) can be distinguished from grains which require a metamorphic basement source (e.g. garnet, biotite, muskovite, staurolite, chloritoid, tourmaline, titanite). As no metamorphic rocks occur in the Koigab River catchment, the latter suite of heavy minerals reflects the minimum amount of aeolian input which increases from 5 % in the fan apex area (Fig. 4.19, section I) to as much as 50 % in the distal fan reaches (Fig. 4.19, section C). In fact, the true amount of material added to the river deposits by aeolian processes may be even higher if the amount of aeolian recycling of fluvial sands is considered. However, this process could not be accounted for on the basis of petrographic data.

Figure 4.19 distinguishes fluvial sand samples taken at the downwind (northern) flank (right column of each pair) from those derived from the upwind (southern) side of the channel (left column of each pair) with most of the latter recording a higher degree of "aeolian" material input. This illustrates that fluvial deposits at the southern channel margin eroded and incorporated those aeolian sands, which originally accumulated as sandramps in the lee-side of channel cut walls during interflood episodes.

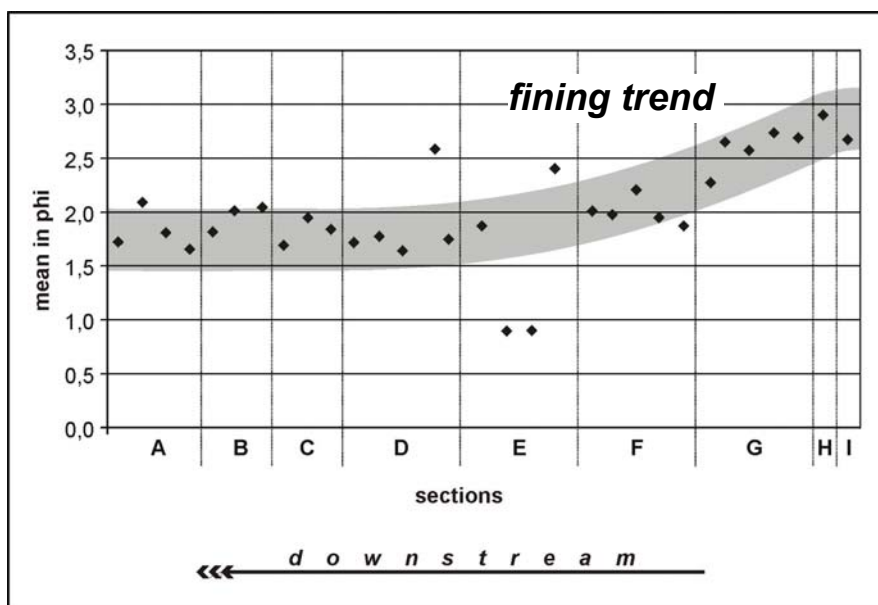
There is also good evidence from grain size data that supra-fan aeolian deposits frequently involve grains winnowed out of fluvial deposits. Figure 4.20 demonstrates that the mean grain size of aeolian sediments (samples of shrub coppices and sandsheets) varies considerably along a N-S oriented section across the Koigab Fan but relies on a general trend: at the southern margin of the fan, the majority of aeolian deposits is composed of medium- to coarse-grained sand (mean: 1,45 phi) that fines over 15 km distance downwind to fine-grained sand (mean: 2,2 phi). This development is disturbed by the provision of coarser, "juvenile" material through the active Koigab channel which records a downstream fining trend running oblique to the aeolian trend. Aeolian sands sampled immediately downwind of the Koigab River channel are markedly coarser-grained again (mean: 1,6-1,9 phi) but show another downwind fining trend to reach a mean of 2,2 phi towards the southern margin of the Skeleton Coast Erg.





**Fig. 4.20:** Mean grain size trends (based on Folk & Ward parameters) showing downwind fining in aeolian sand accumulations (shrub coppices and sand ribbons) along a N-S section across the Koigab Fan surface parallel to the main road C34. Downwind fining trends are interrupted by fluvial input of 'juvenile', less mature grains.

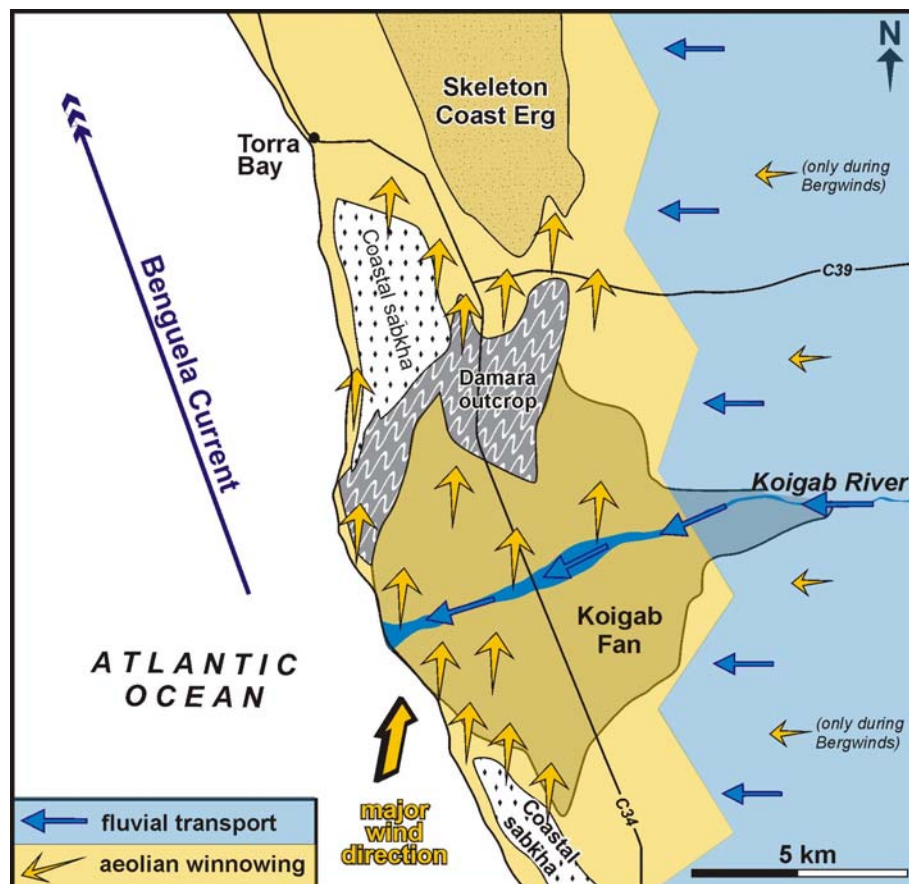
Aeolian sand accumulations like shrub coppices and dunes can only be found in a strip between the coast and about 30 km inland. Aeolian deposits in the Koigab River itself have also only been observed between the river mouth up to the western margin of the Koigab Canyon Poort. The amount of aeolian deposits also decrease towards the poort. An interesting observation can be deduced from grain size data of aeolian sand accumulations (e.g. shrub coppices and sand ribbons) sampled in the Koigab River (Fig. 4.21). Mean grain size data showing an overall upstream fining trend. This can be interpreted as a reduction of wind speed landward. If wind speed decreases, less and only finer-grained material can be transported.



**Fig. 4.21:** Mean grain size trends (based on Folk & Ward parameters) showing an overall upstream fining in aeolian sand accumulations (shrub coppices and sand ribbons) in the Koigab River from the coast towards the Koigab Canyon Poort indicating reduction of wind-speed landward. For locations of sections see Fig. 4.11.

Both, fluvial and aeolian processes have been observed in the Koigab Fan area. Rainfall in the catchment area provides enough water for floods reaching and affecting the Koigab Fan. These moderate to high intensity fluvial events occur at low frequency in the fan area due to the hyper-aridity in the coastal region. In addition, this area also represents an environment where aeolian processes operate at high frequency with moderate intensity throughout the year.

The investigation of the Koigab Fan thus compares well to studies of BULLARD & LIVINGSTONE (2002) where moderate to high intensity (fluvial) events occur at low frequency whereas aeolian processes operate at high frequency but with moderate intensity. Sand-sized material is provided sufficiently from inland by the ephemeral Koigab River after flood events but the beach acts as a more permanent source. However, the Koigab Fan itself acts as a huge sediment bypass surface and provides efficiently new sand-sized material for the southern margin of the Skeleton Coast Erg. Fig. 4.22 shows a summarized schematic sketch of fluvial and aeolian processes operating in the Koigab Fan area deduced from remote sensing data, heavy mineral and grain size analysis.

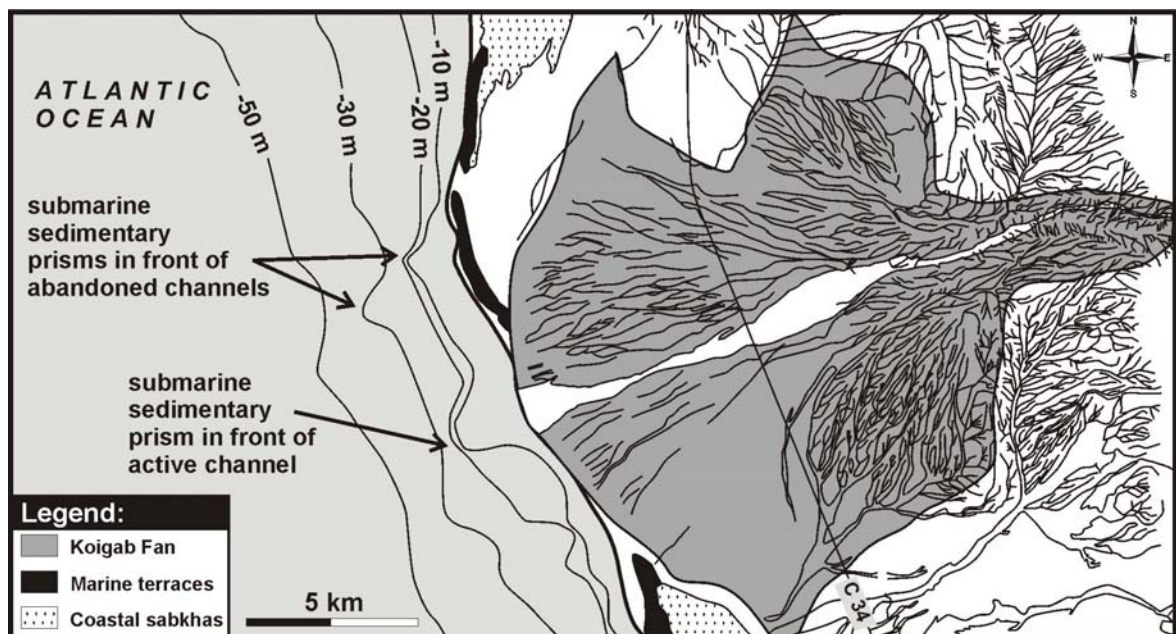


**Fig. 4.22:** Schematic sketch of fluvial and aeolian processes operating in the Koigab Fan area. Blue arrows indicate fluvial sediments, which are transported by ephemeral streams during flood events. These moderate to high intensity flood events operate at low frequency, whereas aeolian processes (indicated by yellow arrows) dominate throughout the year at moderate intensity.

## 4.4 Interaction of the fan with the marine environment

### 4.4.1 Active channel and oceanic interaction

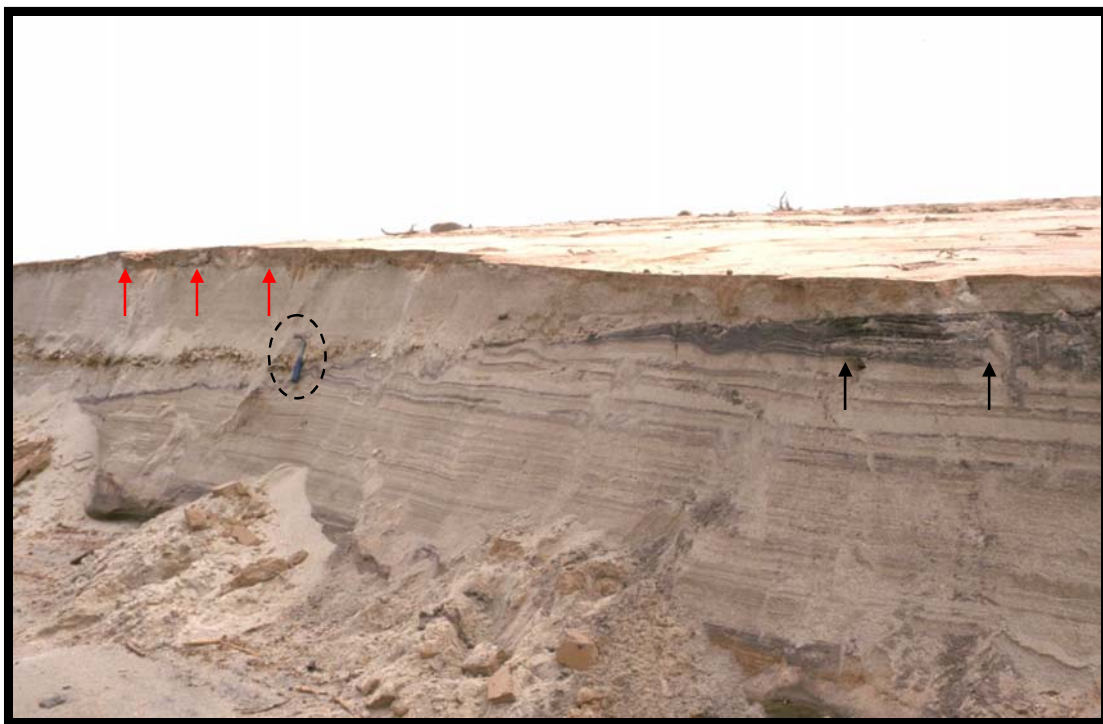
Only a small sector of the fan 2 km to either side of the presently Koigab River interacts directly with the South Atlantic Ocean. Ephemeral floods operating along the channel clearly deposit a small sedimentary prism onto the adjacent shelf area, directly in front of the Koigab River mouth (Fig. 4.23). Also visible on Figure 4.23 are the positions of previous prisms at the mouth of the previously abandoned channel, although not as well defined as the most recent one. Thus, reworking of these prisms seem to be a relatively slow process, surprisingly, considering the high wave energy nature of the Namibian coastline is considered, along with the narrowness of the shelf and the storm-prone nature of the region. It is tempting to speculate that boulders of Etendeka volcanics are transported that far offshore to form the frame of the offshore flood prism, in order to explain its longevity as a topographic feature. The abandoned flood prisms also support the notion that the Koigab River is migrating southwards. Firstly the topographic form of the prisms becomes less pristine moving northwards away from the active channel. Secondly, and in contrast, the shelf to the south of the active channel shows no prisms, interpreted to indicate that this area has had the longest opportunity to be resculpted by wave and storm energies.



**Fig. 4.23:** Bathymetric map and profiles showing the area offshore in front of the Koigab Fan. [Data derived from SAN 103, 1:150,000, Hydrographic Office, South African Navy].



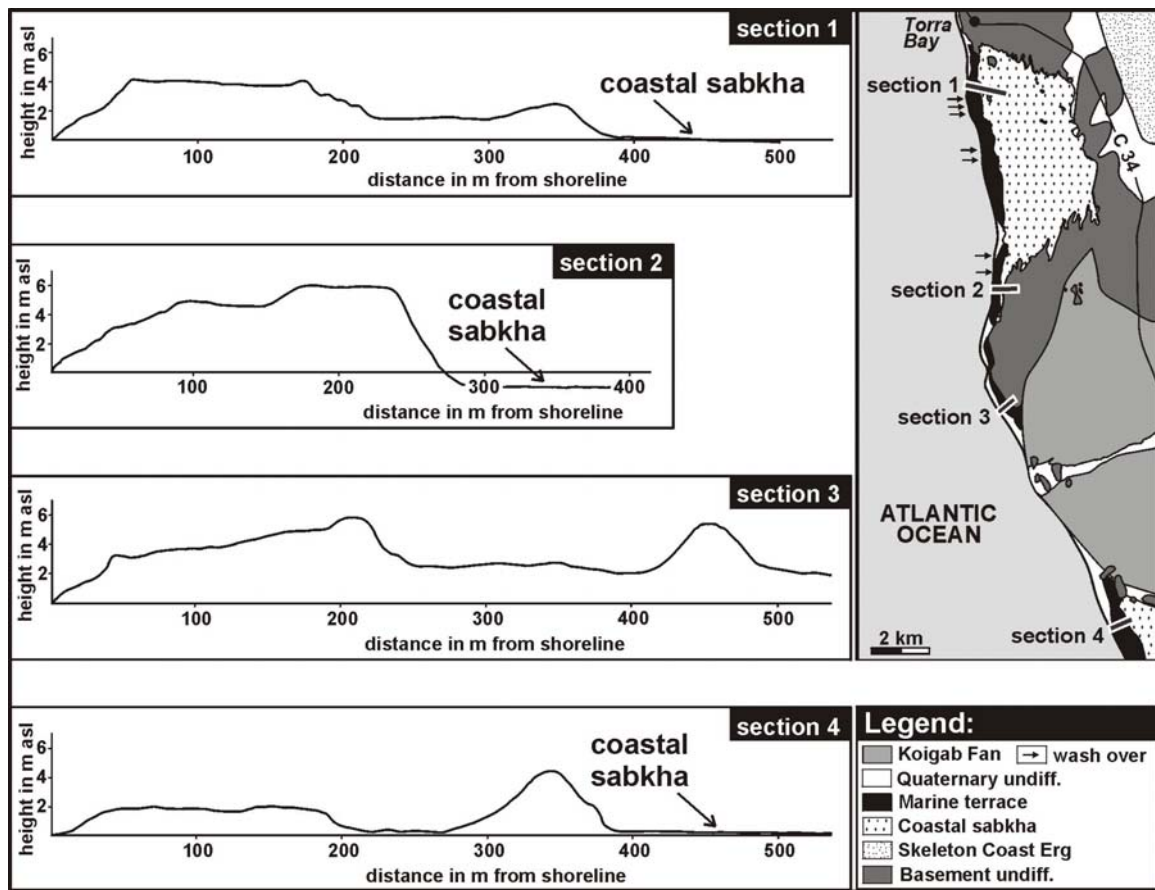
Directly at the present river mouth marine beach and washover sediments occur (Fig. 4.24). The low-angle cross-bedded foreshore sediments are characterised by heavy mineral-rich laminae consisting mainly of concentrated garnet and magnetite grains. Often driftwood of sizes up to 1 m with a thickness of up to 20 cm and single beach cobbles of quartz latites with sizes up to 30 cm are imbedded in the very well sorted fine- to coarse-grained sand. These sediments are draped by thin mud layers of less than 3 cm thickness, documenting the very last stage of a fluvial flood event. Up to 10 cm thick single layers of shell beds, mainly comprising inarticulate brachiopod shells, are good indicators of marine washover at the river mouth.



**Fig. 4.24:** Photograph of marine beach and washover sediments at the present day river mouth. The low-angle cross-bedded, well sorted, fine- to coarse-grained foreshore sands are characterised by heavy mineral-rich laminae consisting mainly of concentrated garnet and magnetite grains (black arrows). The sediments are draped by a thin less than 3 cm thick mud layer (red arrows), documenting the very last stage of the fluvial flood event of April 2000. The hammer (circle) shows the position of a <10 cm thick single layer shell bed, mainly comprising inarticulate brachiopods, interpreted as marine washover.

#### 4.4.2 Flanking shoreline barriers and coastal sabkhas

Separating the fluvial and oceanic regimes, shoreline barrier systems and large coastal sabkhas front broad areas of the Koigab Fan (Fig. 4.25). The highest barrier crest ranges between +4 and +6 m asl and could be correlated with heights of Pleistocene beaches from the Sperrgebiet area in southern Namibia (PICKFORD & SENUT, 1999).



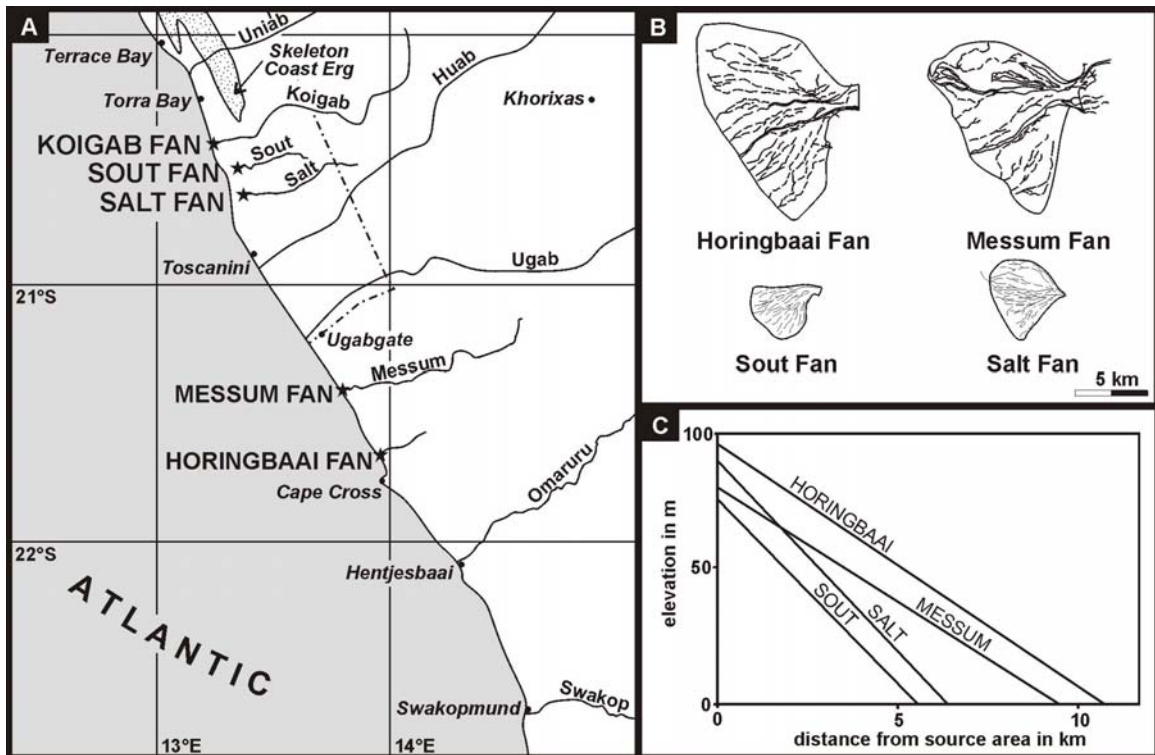
**Fig. 4.25:** Topographic profiles (1) to (4) measured by survey level and measuring tape through barrier systems and continuing onto the (1 & 2 northern, 4 southern) sabkha sediment surface. In (1) and (4) the sabkha surface relates to modern sea-level due to recent washover effects and subaerial fans. In (2) the barriers partially protect the coastal sabkha from marine inundation.

There, younger marine deposits occur between +6-8 m asl indicating palaeo-strandlines of the Middle Pleistocene 'C' beach, and at +4 m asl representing the Eemian 'B' beach (PETHER et al., 2000).

The most recent barrier occurs on a wave cut rock pediment about +2-3 m above present sea-level, which could be correlated with the Holocene +2 m raised 'A' beach in southern Namibia (DAVIES, 1959; PICKFORD & SENUT, 1999; PETHER et al., 2000). Only the most recent barrier in a position farthest away from the fan has washover channels incised through it, feeding subaerial washover fans which have aggraded to present day sea-level in that area. In contrast the multi-barrier system which developed closer to Kuiseb-schist outcrop and the northern fan base acts as a permanent barrier, and the coastal sabkha area there, representing an earlier sabkha sediment/water interface, has been surveyed at a level 1 m below present sea-level (Fig. 4.25, section 2). This height difference perhaps reflects the isolation of this part of the sabkhas from marine flooding during the present interglacial sea-level rise.

#### 4.5 The Koigab Fan compared to other fans and rivers along the Namibian coast

To the south of the Koigab Fan four similar fan systems have been recognized (Fig. 4.26 A), two of which are deposited by shorter headed streams issuing from the Etendeka Plateau and neighbouring areas, and subsidiary to the Koigab catchment. It is important to describe these separately in order to establish the size and gradient range that can be achieved by this type of braided river dominated alluvial fan system.

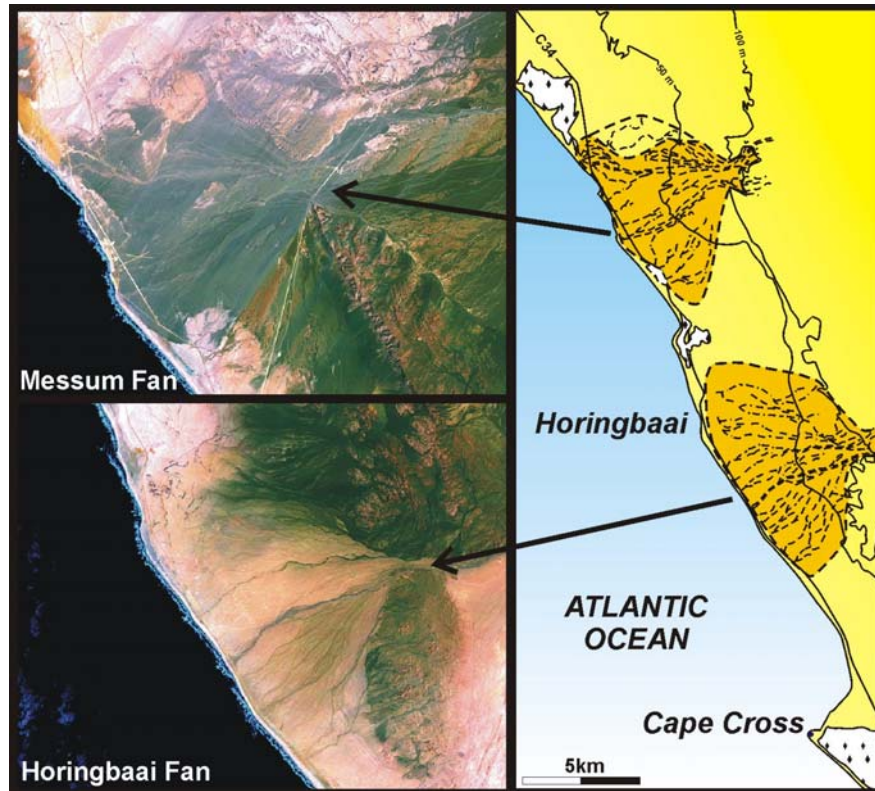


**Fig. 4.26:** A: Map locating the Horingbaai, Messum, Sout and Salt Fan systems south of the Koigab Fan. These fans are similar in order of magnitude to the Koigab Fan in terms of their size (B) and their downfan gradients (C).

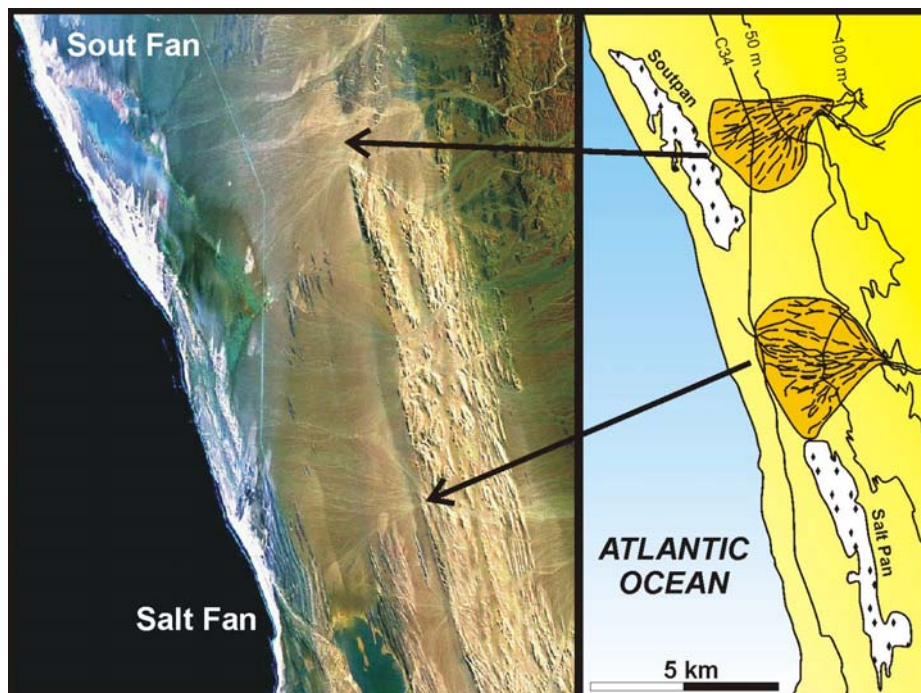
Directly south of the Koigab Fan two smaller fan systems, the Sout and the Salt Fans can be identified. Two other fan systems have been recognized south of the Skeleton Coast Park between Mile 108 and Cape Cross. The Horingbaai and the Messum Fans have similar dimensions to the Koigab Fan, but they differ in river length and size of the catchment area (Fig. 4.26 B & C). All the above fans are characterized by gradients between 1:63 and 1:108. They are all fed by braided ephemeral streams and the deposits consist predominantly of gravels. The catchment areas of the Horingbaai and Messum Fans are not restricted to the Etendeka Plateau, parts of the catchments are situated in Damaran basement rocks. In contrast to the Koigab, Messum and Horingbaai Fans (Fig. 4.27), the



Sout and Salt Fans do not debouch into the ocean but into the lagoonal system 1.5 to 2.5 km east of the Atlantic Ocean (Fig. 4.28).



**Fig. 4.27:** Right map giving an overview of the Messum and the Horingbaai Fan (modified after Topographic map 1:250.000 2013 Kaapkruijs). Left picture show the two Landsat TM-5 images of the fans (Landsat TM-5 scene 181-074; 7-4-1 RGB; 30.03.1995).



**Fig. 4.28:** Right map giving an overview of the Salt and the Sout Fan (modified after Topographic map 1:250.000 2013 Kaapkruijs). Left picture show the two fans in a Landsat TM-5 images (Landsat TM-5 scene 181-074; 7-4-1 RGB; 30.03.1995).

#### 4.6 Classification of the Koigab Fan and comparison with worldwide fans and fan systems

Considering morphological properties of alluvial fans (after: BULL, 1963, 1968, 1977; HOOKE, 1967; CHAMLEY, 1990; LECCE, 1990; COOKE et al., 1993; STANISTREET & MCCARTHY, 1993; BLAIR & MCPHERSON, 1994a, b; GALLOWAY & HOBDA, 1996) the Koigab Fan can be classified as one. The fan has a typical semi-conical shape (Fig. 4.1, 4.2), a restricted radial length of about 15 km, a plano-convex cross profile (Fig. 4.8 C) and has comparative values of radial slopes. The fan-radii extend outward from the apex and the mountain front (Sugar Loaf Hill) in all possible directions at a relatively similar slope of about 0.9% to form an arc of 110°. Furthermore, BLAIR & MCPHERSON (1994a, b) distinguish alluvial fans from rivers on the basis of hydraulic characteristics. Hydraulic effects taking place on a fan are connected with the presence of steep slopes, occurrence of rapid rainfall or snowmelt and catastrophic nature of water and sediment discharge. Due to these hydraulic characteristics, after BLAIR & MCPHERSON (1994a, b) primary sedimentary processes and resultant facies of alluvial fans are dominated by sediment gravity processes like colluvial slides and debris flows and fluid gravity processes like sheetfloods and incised-channel floods. The surface of these primary deposits are reworked and remolded by secondary processes, such as overland flow of braided river channels or wind erosion (BLAIR & MCPHERSON, 1994a, b). Studies from the Kosi Fan/India-Nepal (WELLS & DORR, 1987a, b; GOHAIN & PARKASH, 1990) and from glacial outwash fans like the Yana Fan, Alaska (BOOTHROYD & ASHLEY, 1975) have shown, that also channelized flow processes can be dominant processes on alluvial fans (GALLOWAY & HOBDA, 1996). These streamflow-dominated fans have been distinguished by other workers from alluvial fans. RUST (1978) termed them braided alluvial plains and BLAIR & MCPHERSON (1994a, b) distinguish them from alluvial fans *sensu stricto* and classified them as rivers or fan deltas.

The study on the Koigab Fan has shown that the dominating process on the fan is characterized by channelized flow and the ancient sedimentary fan sequences are also exclusively dominated by braided river deposits. Therefore, the Koigab Fan can be classified as an ephemeral braided river dominated alluvial fan.

#### **4.6.1 Fan, terminal fan or fan-delta?**

The Koigab Fan has formerly been described as a coastal terminal fan by VAN ZYL & SCHEEPERS (1993). Terminal fans occur in semi-arid basins of inland drainage and are fed by ephemeral streams (MUKHERJI, 1976; ABDULLATIF, 1989; KELLY & OLSEN, 1993). They are formed where topographically confined rivers drain into an unconfined lowland (GALLOWAY & HOBDAI, 1996) and are characterized by reduction of water discharge through evaporation and infiltration so that they simply cease to exist in downfan direction. Ephemeral flows down the Koigab channel frequently reach the fan perimeter and debouch through it into the Atlantic Ocean. This denies its designation as a typical terminal fan (cf. KELLY & OLSON, 1993).

The barrier/coastal sabkha system and basement outcrop near the coast separates most of the outer fan perimeter entirely from marine processes. The effects of fan sedimentation on the adjacent shelf are minimal and ultimately ephemeral. Flood prisms are of the same dimensions as the width of the active channel and do not survive under the high wave energy conditions much beyond the following succeeding channel abandonment (Fig. 4.23). On the other hand the area of the Koigab River mouth does provide a small prism of sediment to the neighbouring shelf (Fig. 4.23). STANISTREET & MCCARTHY (1993) have suggested that for every fan type there is a corresponding fan-delta. However, on balance the Koigab Fan system exhibits the characteristics of a fan (STANISTREET & MCCARTHY, 1993; BLAIR & MCPHERSON, 1994a, b) rather than those of a fan-delta (BULL, 1977; GLOPPEN & STEEL, 1981, MCPHERSON et al., 1987; NEMEC & STEEL, 1988).

#### **4.6.2 Position and contrasts within alluvial fan classifications**

In terms of subaerial fan types, the Koigab Fan classifies as a braided alluvial fan, showing no evidence of debris-flows or sheetfloods (BLAIR & MCPHERSON, 1994a, b) nor of meandering or low sinuosity river channels typical of another fan type (STANISTREET et al., 1993). It is therefore a ternary point end member in the classificatory triangle proposed by STANISTREET & MCCARTHY (1993) (Fig. 4.29). In terms of size within the braided alluvial fan class, the Koigab Fan is intermediate between small-scale braided river dominated systems e.g. the Yana Fan, Alaska (BOOTHROYD & ASHLEY, 1975), and braided dominated mega-fans, such as the Kosi Fan developed south of the Himalayas (GOHAIN & PARKASH, 1990; WELLS & DORR, 1987a, b) (Fig. 4.30). The four other described fan systems from the Skeleton Coast (Fig. 4.26) are of a similar order of magnitude as the larger Koigab Fan

system, but show variations from 5 to 15 km from apex to periphery and 4.25 to 23 km across their broadest dimension.

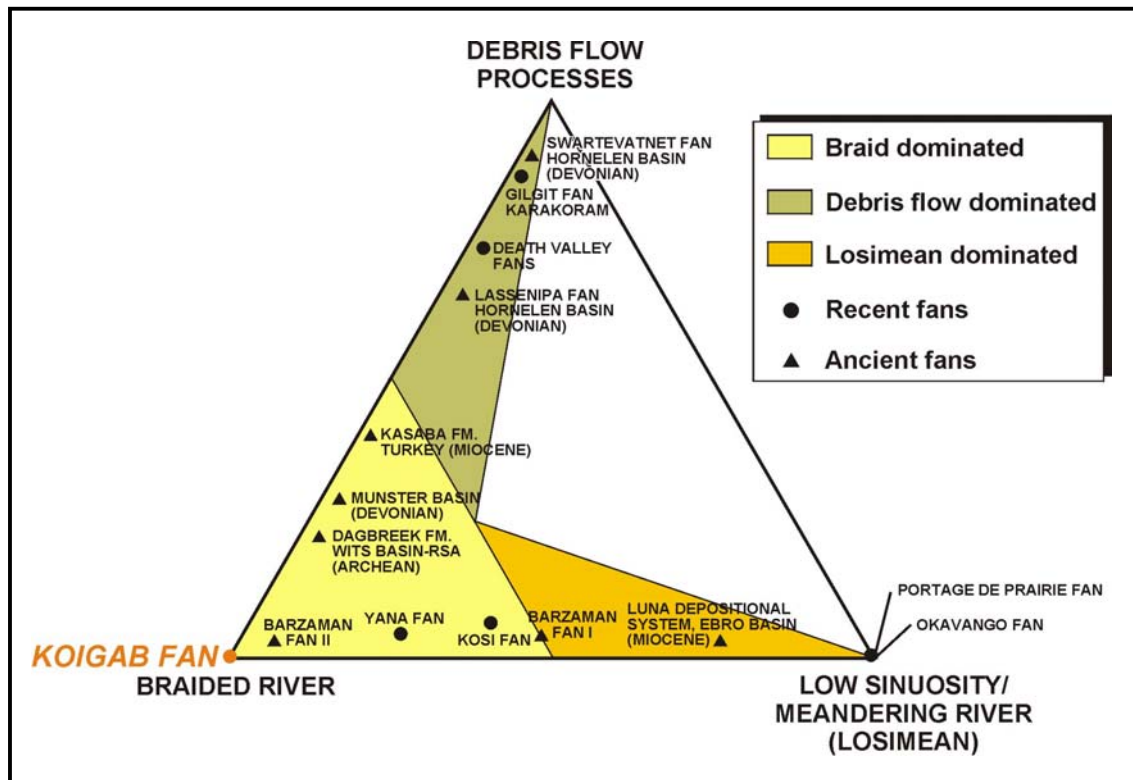


Fig. 4.29: The position of the Koigab Fan in the triangle field for subaerial fan types of STANISTREET & MCCARTHY (1993).

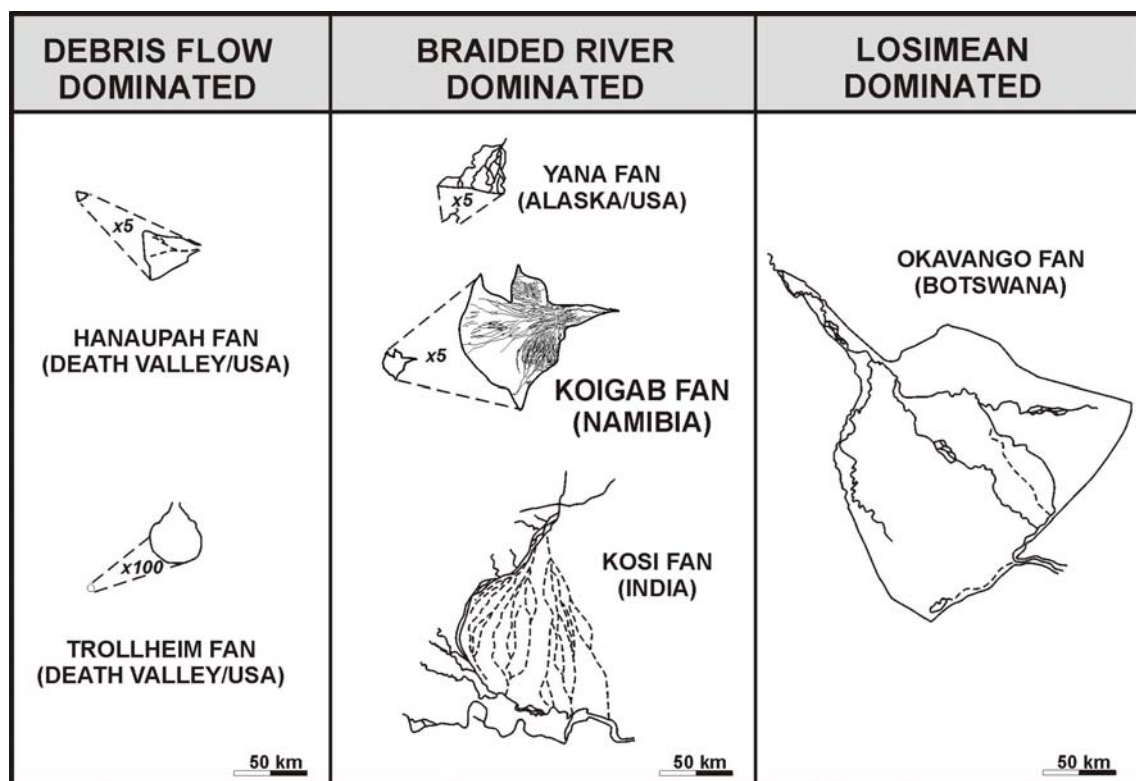
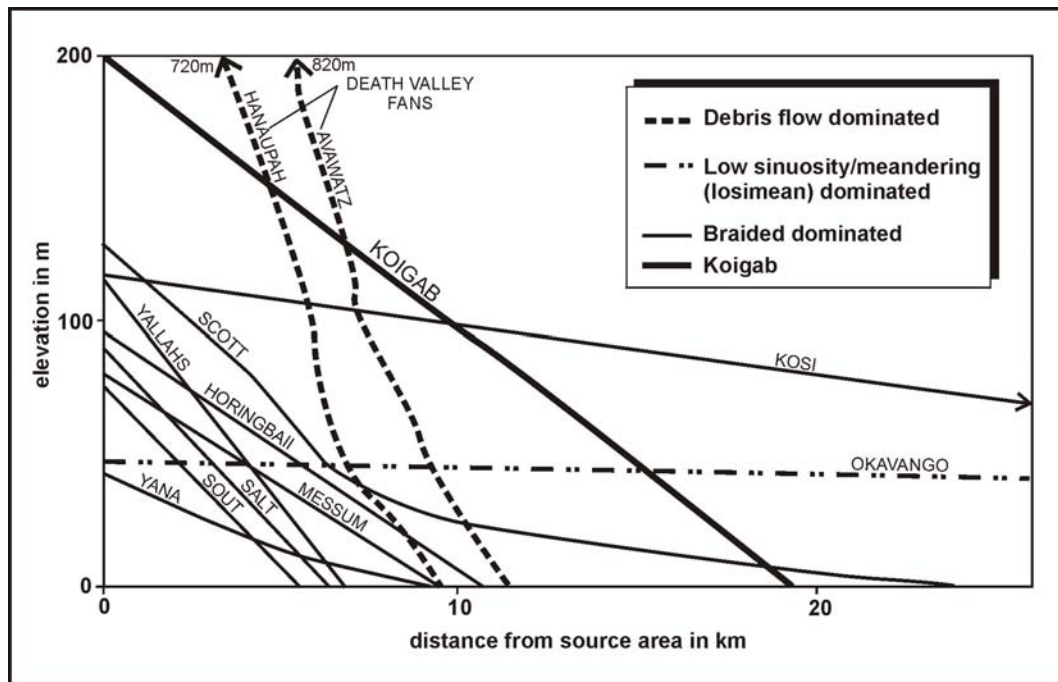


Fig. 4.30: Classification of the Koigab Fan within the subaerial fan classes of the fan classification scheme of STANISTREET & MCCARTHY (1993).



In terms of gradient the Koigab Fan is rather steep (1:89) in contrast (Figs. 4.31, 4.32) to other braided river dominated fans such as the Kosi (1:5000 GOHAIN & PARKASH, 1990), and Alaskan fan systems (typically 1:150 (proximal) to 1:300 (distal), BOOTHROYD & NUMMEDAL, 1978) and shows profiles closer to debris flow dominated fans (BLAIR & MCPHERSON, 1994a). Likewise the four other Skeleton Coast fans show slope gradients from 1:63 to 1:108 (Fig. 26).

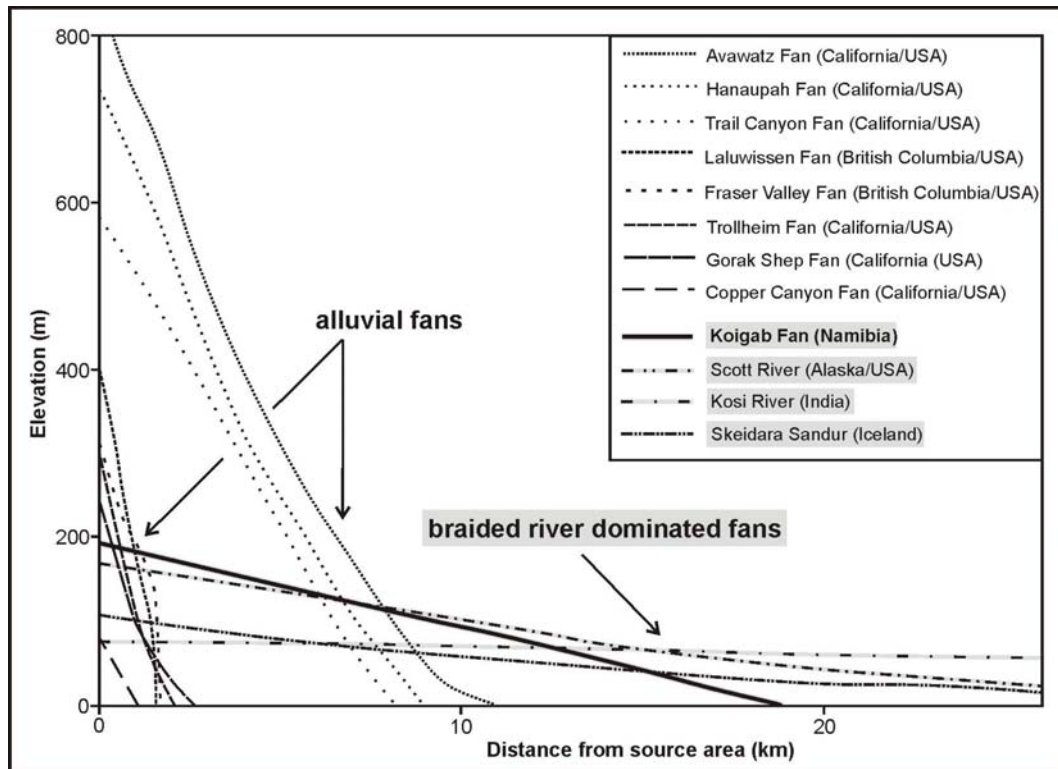


**Fig. 4.31:** Comparative gradients of various fan types (compiled after BOOTHROYD & ASHLEY, 1975; STANISTREET & MCCARTHY, 1993; WESCOTT, 1990).

In terms solely of geometry, size and depositional setting the Koigab Fan is close to fans and fan-delta systems as described from the Arctic and sub-Arctic (BOOTHROYD & ASHLEY, 1975, BOOTHROYD & NUMMEDAL, 1978). In terms of depositional style, slope (Figs. 4.29 - 4.32), climatic setting and fan surface, however, the contrast could not be less. The Arctic fans are proglacial, fed by perennial river systems associated with ice melt, whereas the Koigab Fan is fed by an ephemeral river providing both sediment and water discharge in short energetic bursts. This may to some extent explain differences in fan gradient between the two types of fans.

In contrast with other fans described in the literature, the Koigab Fan and the four other Skeleton Coast fans show no evidence for subdivision into upper, middle and lower fan. This is also confirmed by the fluvial style in the river bedform, which appears not to change considerably in style between apex and fan toe.

The Koigab Fan and its subordinates are thus of vital importance in bridging a gap in both size and gradient between high gradient small fans and lower gradient fans and megafans.



**Fig. 4.32:** Gradients of 'typical' alluvial fans after MCPHERSON et al. (1987) compared with gradients from the Koigab Fan and other braided river dominated fans.

#### 4.7 Koigab Fan: significance for Precambrian and Early Palaeozoic fans

In terms of climate, unlike other braided river dominated alluvial fan examples, the Koigab Fan is deposited in a hyper-arid setting, it is only precipitation in the mountainous catchment that allowed its present style of development. This negates concepts of only debris-flow dominated fans developing in arid to semi-arid climates. Like the Okavango Fan, the Koigab Fan provides an important caveat in too easily utilising fan-types as climatic indicators in ancient sequences. Fan types depend as much on catchment conditions to decide their depositional characteristics as the conditions that pertain in their depositional area. Other subaerial braided fan systems developed in low-latitude tropical locations, for example the subaerial portion of the Yallahs Fan-delta of Jamaica, (BURKE, 1967; WESCOTT & ETHRIDGE, 1980; WESCOTT, 1990) are heavily vegetated, even to the extent of a tropical rain forest. In contrast, the arid tropical-latitude setting of the Koigab Fan ensures the smallest degree of vegetation. The latter is restricted to vegetation associated with aeolian bedforms, exemplified by shrub coppices, for which moisture is

provided by the famous perennial coastal mists and fogs associated with the Skeleton Coast (WARD, 1989). The lower delta plain of the Yallahs Fan, which is covered by marshes, swamps and open ponds, is characterised by muddy sands and organic-rich mud deposits. The Koigab Fan by contrast bears little vegetation and lesser chemical weathering ensures a much lower provision of clay-grade material.

Difficulties are encountered in finding modern examples of braided river dominated fans that can exactly analogue ancient fan sequences. This problem becomes even larger when dealing with fluvial sequences and fan systems, which are older than the Silurian/Devonian, times before plants initially colonised the land (RUST, 1978). On one hand proglacial alluvial fans represent a rather specialised set of circumstances that, while providing a picture of how perennial rivers may operate on a fan surface, represent a set of conditions uncommonly encountered during earths history with the exception of the Permo-Carboniferous, Late Ordovician, Neoproterozoic and possibly Palaeoproterozoic ice ages. By contrast, modern non-glacial braided river dominated fans are commonly highly vegetated (e.g. subaerial portions of Yallahs Fan-delta, WESTCOTT & ETHRIDGE, 1980), and are often heavily affected by human occupation (e.g. Kosi Fan) and agricultural activity (e.g. Colorado Fan).

The Koigab Fan therefore offers an unusual opportunity to view a fan surface and system that allows the perception of how Precambrian and Early Palaeozoic fans might have appeared and acted.

#### **4.8 Conclusions**

The unique climatic and hydrological setting of the Koigab Fan with its hyper-aridity, permanently strong southwesterly onshore winds, longlasting interflood periods and flood events operating at high intensity but low frequency, favours fluvio-aeolian interaction on its surface. Aeolian processes operate throughout the year and cause deflation and the development of lag deposits. Fluvial processes provide abundant sand during and after flood events, which are followed by enhanced aeolian winnowing of sand out of dry channelways onto and over the fan surface. Heavy mineral assemblages within fluvial deposits and grain size analysis from aeolian sand samples have been tested as a tool to demonstrate the amount of aeolian material input into the river system and the amount of fluvial material output of the river system.

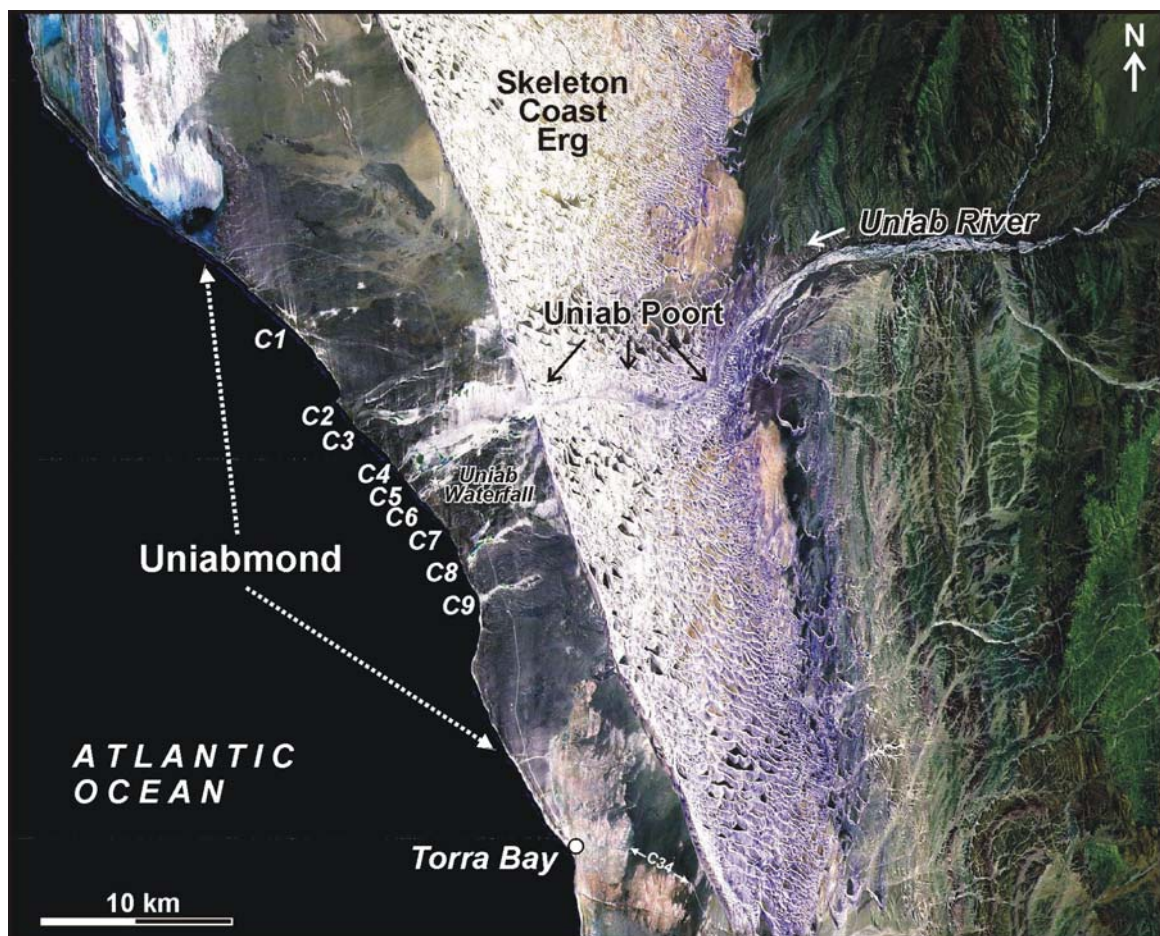
The Koigab Fan extends the knowledge of the variability of the braided fluviially dominated fan class. In terms of form, magnitude and characteristics it represents an important intermediate both within that class and within the range of worldwide subaerial fans as a whole. In terms of the latter, it and nearby fans in Namibia provide an important bridge between ultrahigh and ultralow gradient fan systems.

In addition, as the Koigab Fan lacks significant surface vegetation it can act as a model for certain Precambrian and Early Palaeozoic fan depositional systems deposited prior to the evolution and widespread occurrence of land plants.

## 5 The Cenozoic succession in the Uniabmond area

### 5.1 The Uniab River system and the Uniabmond area

The Uniab River is an ephemeral braiding river system, which originates in the Grootberg-Palmwag area, NW Namibia. On its way to the Atlantic Ocean the river impinges on the Skeleton Coast Erg 25 km east of the coastline. The Uniab River passes through the erg during floods by using a semi-permanent break-through corridor, the Uniab Poort, and enters the coastal plain about 6,5 km east of the Atlantic coastline (Fig. 5.1).



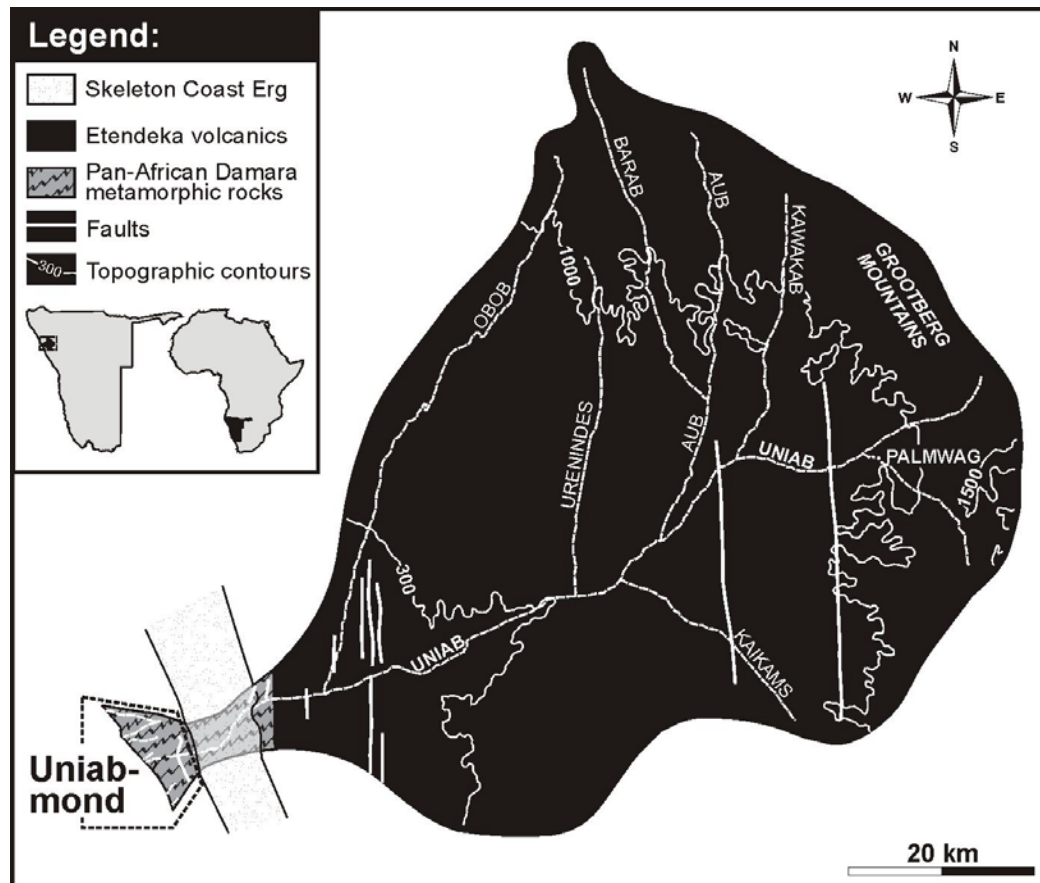
**Fig. 5.1:** Landsat TM-5 scene 181-074 (30.03.1995; 7-4-1 RGB) giving an overview of the lower reaches and the mouth area of the Uniab River.

The Uniabmond area is named after the mouth area of the Uniab River between the western margin of the Skeleton Coast Erg and the coastline (Fig. 5.1). It has a size of approximately 45 km<sup>2</sup> and is characterized by a prominent 18 km long and up to 35 m high seacliff which is dissected by nine main incised valleys (channel C1- channel C9, see Fig. 5.1) and a number of smaller ones (SCHEEPERS & RUST, 1999; KRAPF, 2000). Only the three central channels (C4-6) are active during modern day runoff.



### 5.1.1 Catchment and source area characteristics

The Uniab River is the southernmost dune-dammed ephemeral river of the Skeleton Coast. With a length of 110 km it drains a 4.500 km<sup>2</sup> catchment area (Fig. 5.2) of which the elevation ranges from 0-1635 m (JACOBSON et al., 1995). The maximum E-W extent of the catchment area is about 100 km, from N-S about 75 km. The catchment morphology is characterised by rolling hills and table mountains varying in heights between 400-1.635 m asl. (JACOBSON et al., 1995).



**Fig. 5.2:** Overview of the Uniab River catchment area (modified after: MILLER, 1988; JACOBSON et al., 1995) and its geology.

Like the Koigab River, the catchment of the Uniab River does not make a break into the Great Escarpment but is limited to the east by the Grootberg Mountains (Fig. 5.2). They form part of the Etendeka Plateau which is built up by Early Cretaceous Etendeka flood basalts and interbedded quartz latites (MILLER, 1988; see also Chapter 2). The exposures of the Etendeka volcanics end in the area where the Uniab River hits the Skeleton Coast Erg. There, a coastal escarpment has developed in the Etendeka rocks. In the area between the Skeleton Coast Erg and the Uniab Waterfall isolated outcrops of Damara metamorphic basement rocks are exposed. The basement rocks consists of schists and migmatitic

gneisses of the Damara Group (STANISTREET & CHARLESWORTH, 2001). The schists are composed of quartz, biotite and garnet. The schist and migmatites are intruded by and interlayered with syn- and post-tectonic pegmatites. The schists and pegmatites dip gently to SW (ZELLER, 2000) and are unconformably overlain by various Cenozoic sediments.

Extensive parts of the catchment area, especially east of the Skeleton Coast Erg, were affected by post-breakup uplift of the newly developed continental margin of Namibia during Early and Late Cretaceous times. This resulted in  $\pm$  coast-parallel trending normal and listric normal faults and favoured considerable river incision.

### **5.1.2 Climate and flood characteristics**

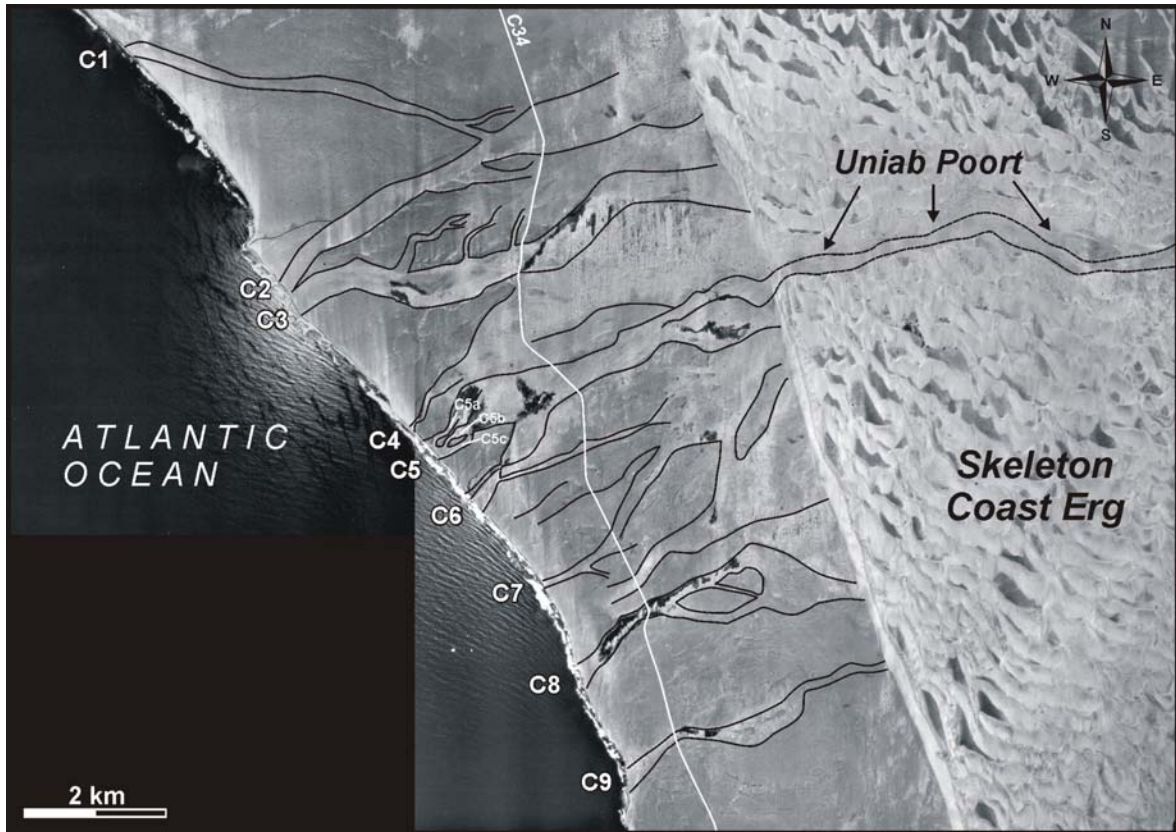
Annual rainfall in the catchment area varies between 0-125 mm with only 2.3 % of it receiving over 100 mm/a (JACOBSON et al., 1995). In comparison to other rivers of the Skeleton Coast, the Uniab River has developed nowadays a semi-permanent break-through corridor through the Skeleton Coast Erg, which is also clearly visible on remote sensing data from the last 47 years. Observations from the Nature Conservation staff at Möwe Bay shows that in the last 10 years the Uniab River experienced river flooding nearly every year with major flood events during 1995 and 2000.

Observations during and shortly after flood events by SCHEEPERS & RUST (1999) and own observations during fieldwork in 2000 show that the depth of flow in the main channel of the Uniab River between W of the erg and the Uniab Waterfall is generally less than 40 cm. Thereby the river is flowing over a width of a few hundred meters. The peak stage of a flood lasts rarely more than a few hours and the entire flood event rarely last longer than a few days. A couple of big boulders of sizes up to 4 m in diameter indicates that the Uniab River has experienced much bigger flood events of unknown magnitudes compared to today's ones, where it was able to transport these huge blocks during main mode. BLÜMEL et al. (2000) and SVENDSEN et al. (in press) interpret the transportation of these boulders as the catastrophic outburst of floods resulting from dune-damming and –collapse.

## **5.2 The lithostratigraphic framework of the Uniabmond area**

The Uniabmond area exposes a thick Cenozoic sedimentary successions in which nine major channels (C1-C9) and several smaller ones have been incised to variable degrees (Fig. 5.3) resulting in relatively good exposures of this succession. The position of five abandoned channels, identified directly at the western margin of the Skeleton Coast Erg,

indicates that the main channel of the Uniab River has changed its position in former times. The modern day break through channel splits up to three presently active channels C4-C6 2,5 km before reaching the ocean. The incised channels are accompanied by a vast number of terraces. Apart from the channels themselves they are the most conspicuous morphological features in the Uniabmond area. These terraces occur as single, paired and complex terrace cups.



**Fig. 5.3:** Aerial photograph composite of the Uniabmond area showing the incised channels C1 to C9 and the modern day break-through corridor of the Uniab River. Also visible is the position of the five abandoned channels at the western margin of the erg indicating former shifting of the Uniab River.

In this study a new stratigraphic framework has been worked out for the Cenozoic deposits in the Uniabmond area. The sedimentary succession subdivides into three major unconformity-bounded units for which the terms “Red Canyon Formation“, “Whitecliff Formation” and “Uniabmond Formation” are introduced here.

The following chapters describe the Cenozoic succession of the Uniabmond area in closer detail and also discuss possible correlation with comparable Cenozoic sediments of southwestern Africa, e.g. the Kuiseb River area (Central Namibia) and the Sperrgebiet (S-Namibia).

Fig. 5.4 gives an overview of the geology of the Uniabmond area and shows the distribution of the investigated Cenozoic sediments.

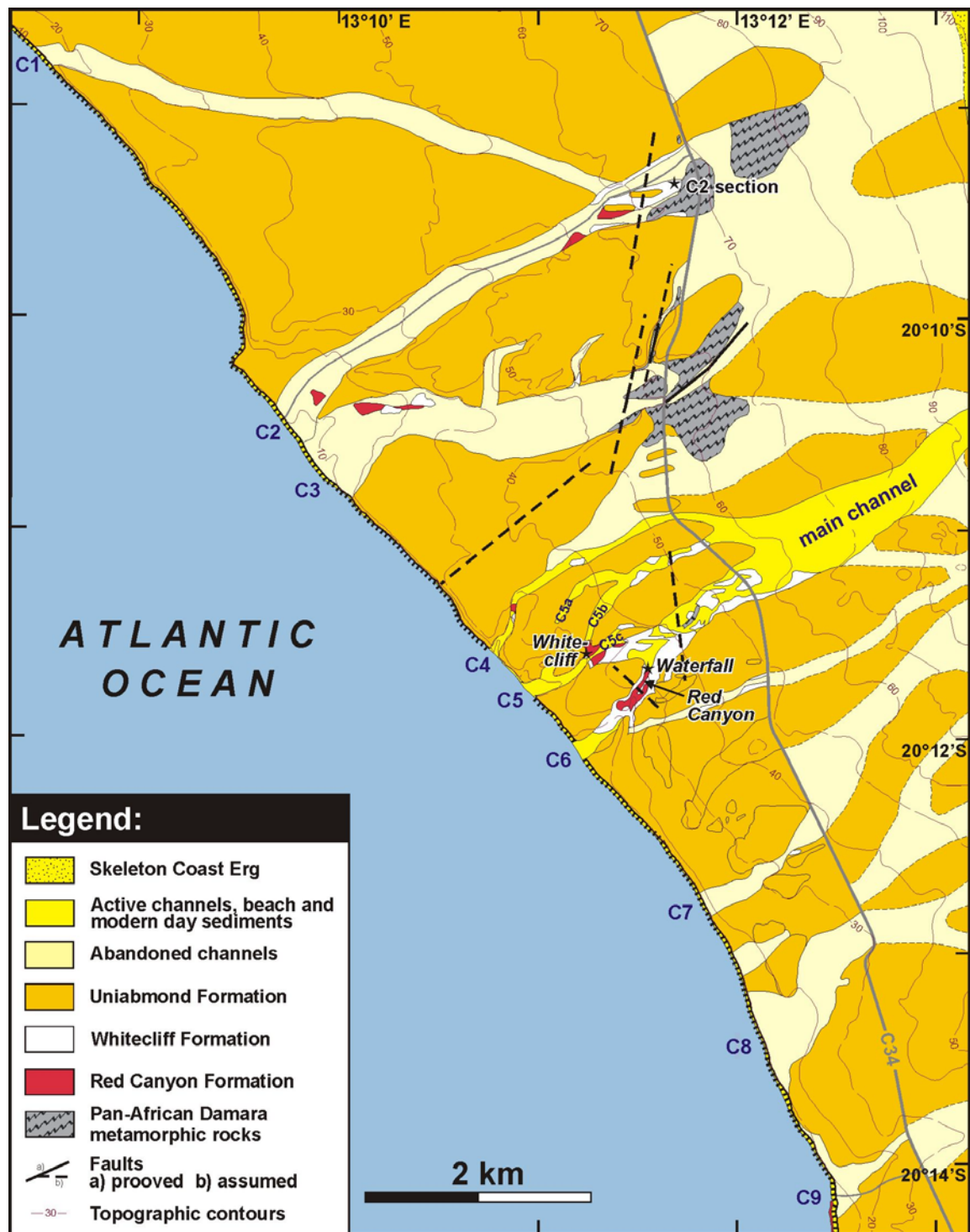


Fig. 5.4: Geological map of the Uniabmond area (compiled and modified from: ZELLER, 2000).

### 5.3. Red Canyon Formation

The oldest Cenozoic sediments exposed in the Uniabmond area are deposits of the Red Canyon Formation representing a lithostratigraphic unit which consists predominantly of reddish terrestrial, mainly fluvial sediments showing an overall upward fining trend from dominantly coarse-grained, feldspar-rich conglomerates and sandstones to mainly fine-grained clay-rich silt- and sandstones. These weakly consolidated sediments overlie Pan-African Damara metamorphic rocks with a major unconformity and are themselves unconformably overlain by sediments of the Whitecliff Fm. (see Chapter 5.4).

The term 'Red Canyon Formation' was chosen because of spectacular outcrops in the walls of the Uniab Canyon (Fig. 5.4) located in channel C6 about 1 km E of the Atlantic coastline. The Red Canyon is also the type locality for the lower stratigraphic subunit of the Red Canyon Fm., the "Waterfall Member". The type locality for the upper lithostratigraphical subunit, the Bone Area Member, is situated within channel C5. Additional, smaller outcrops have been newly discovered in C3 and C2 (Fig. 5.4). During extreme low tides further exposures can be found occasionally at the beach seaward of the channel mouths of C2, C3 and C9 (Figs. 5.7 C+D).

The succession has been previously described by EITEL et al. (1999a), ZELLER (2000), SVENDSEN (2000) and KRAPF et al. (2002). EITEL et al. (1999a) described reddish loamy sediments with a thickness of about 10 m from the present main discharge channel (C5) of the Uniab River. They termed these deposits 'Uniab-Loam' and interpreted them as a deposit of reworked, intensively weathered soil. ZELLER (2000) and SVENDSEN (2000) however showed that outcrops of the Red Canyon Fm. are much more widespread than previously recognized. According to ZELLER (2000) the Red Canyon Fm. has a preserved thickness of about 60 m.

Following EITEL et al. (1999a), ZELLER (2000) termed the sedimentary succession 'Uniab Loam Formation'. Grain-size distribution and composition of the sediments actually suits the term 'loam', however, the application of this term should be restricted to soils (GARY et al., 1972; SCHEFFER, 2002). The Red Canyon Fm. represents an unconformity-bounded sedimentary succession and therefore, although soily material and soil horizons are present within this formation, a non-genetic stratigraphic nomenclature should be applied. Based on its type locality, the succession will be termed Red Canyon Formation and is subdivided into a lower Waterfall Member and an upper Bone-Area Member.



### 5.3.1 Waterfall Member

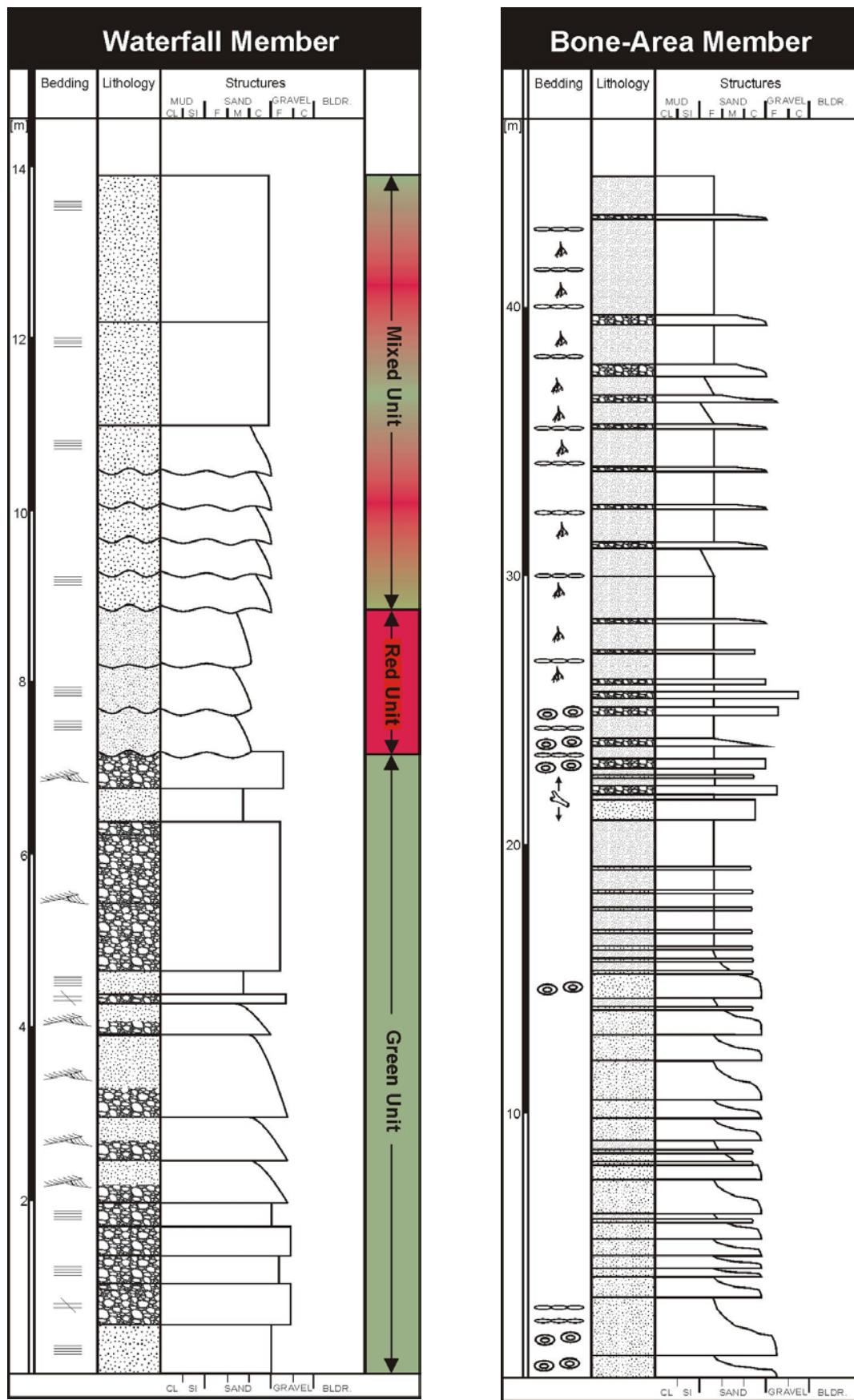
The Waterfall Mb. (Fig. 5.5) represents the lower part of the Red Canyon Formation. No exposures of its basal contact to the underlying Damara metamorphic rocks have been discovered so far. The Waterfall Mb. consists predominantly of conglomeratic and sandy sediments in contrast to the argillaceous sediments of the overlying Bone-Area Member. However, the contact between the two members is not exposed.

The sediments of the Waterfall Mb. are well accessible in the walls of the Red Canyon in C6 from the waterfall to the seaward end of the canyon. Three different subunits of the Waterfall Mb. have been recognized by SVENDSEN (2000) and were given the field terms Green, Red and Mixed Unit (Fig. 5.6 A).

The basal Green Unit, up to 7 m thick, consists of massive, poorly sorted, coarse-grained sandstones and conglomerates which fine gradually upward into trough cross-bedded, better sorted, medium- to coarse-grained sandstones. Crude bedding structures indicate channel forms with a high width/depth ratio (<50). Clasts are dominantly composed of intensively weathered, subangular to subrounded basalts and quartz latites most probably derived from erosion of the Etendeka Group. Minor components are granite, mica schist and feldspar clasts (the latter up to 7 cm in diameter), which are derived from the underlying Damara metamorphic rocks. The fluvial sediments show a greenish colour due to bleaching by groundwater.

The Green Unit is overlain by the Red Unit, up to 2 m thick, showing the red colour typical for most parts of the Red Canyon Formation (Fig. 5.6 B). The Red Unit consists of moderately to well sorted, medium-grained sandstones and some conglomeratic channel fills with well developed erosional bases.

The up to 5 m thick Mixed Unit represents the uppermost part of the Waterfall Member (Fig. 5.6 C). The boundary to the underlying Mixed Unit is marked by a local unconformity. The Mixed Unit shows similarities with both of the formerly described units. It consists of a series of massive, poorly sorted, coarse-grained sandstones and minor conglomerates, which fine upward into medium to well sorted, medium- to coarse-grained sandstones displaying well established channel forms. The Mixed Unit is overlain in the area of the Red Canyon with a major unconformity by sediments of the Whitecliff Fm. (see chapter 5.3.2).



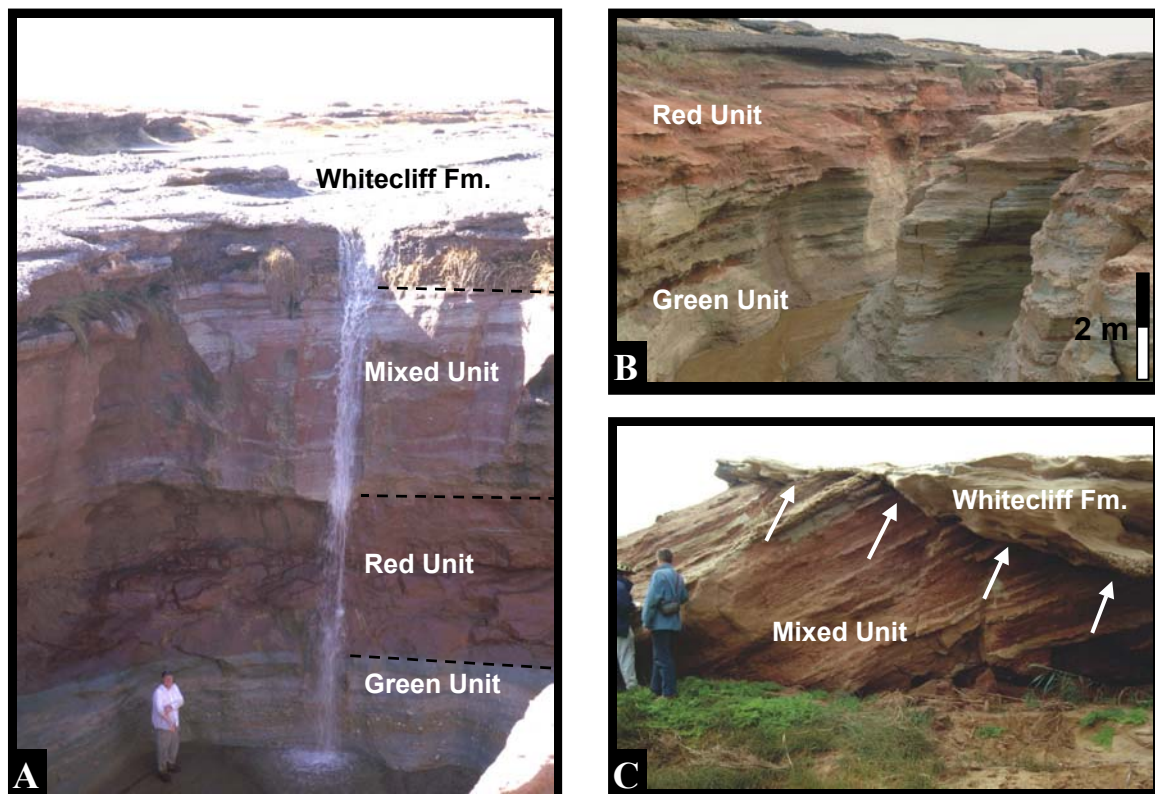
**Fig. 5.5:** Sedimentary logs of the Waterfall and Bone-Area-Member of the Red Canyon Fm. (compiled from: ZELLER, 2000; SVENDSEN, 2000; note the different scale of the profiles!). See Appendix I for explanation of symbols.

### 5.3.2 Bone-Area Member

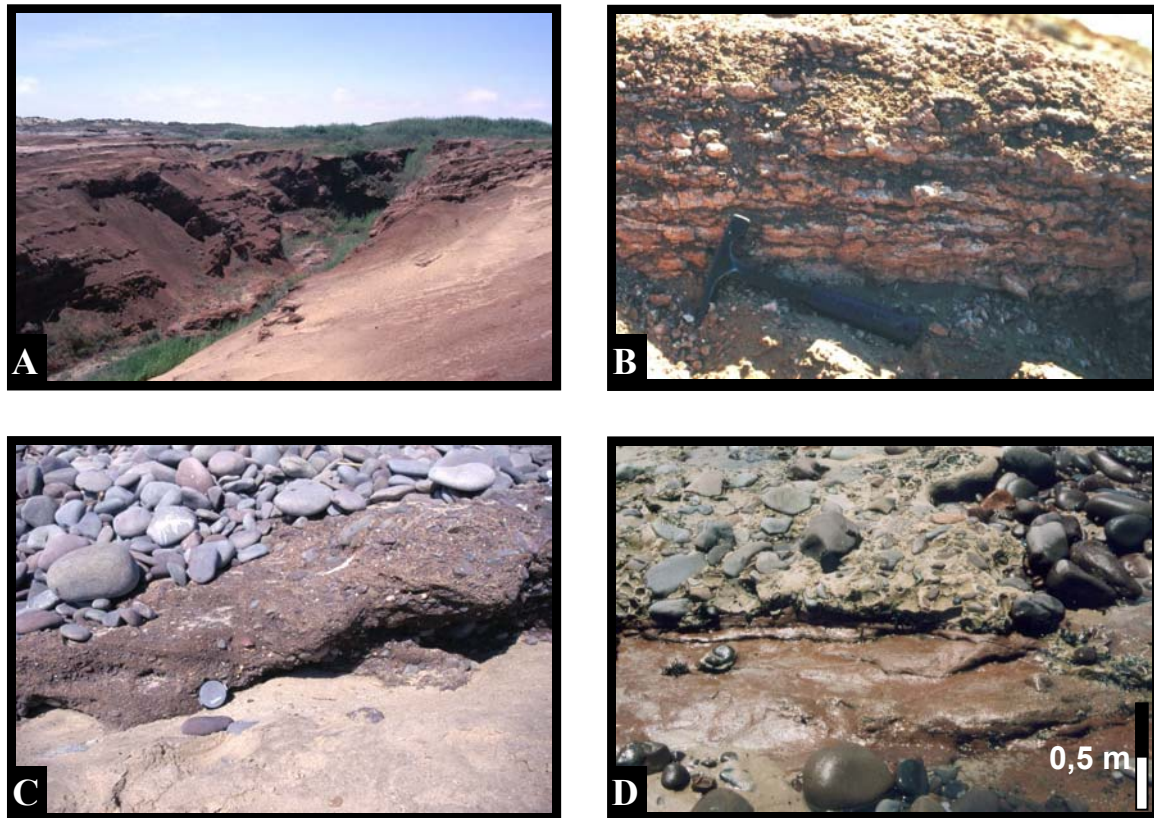
The type locality for the upper part of the Red Canyon Fm., the Bone-Area Member, is situated in channel C5. The contact to the underlying Waterfall Member is not exposed.

The up to 46 m thick succession (see Figs. 5.5, 5.7 A) comprises three different interbedded facies: 1) laterally extensive massive or horizontal to low-angle, cross-bedded, coarse-grained sandstones and conglomerates, 2) massive to weakly horizontal-bedded, fine-grained sand- and siltstones with rhizocreations, wood and bone fragments and 3) thin whitish calcareous, caliche-rich sand- and siltstone horizons, which weather out as solid beds (Fig. 5.7 B). Based on their geometry and bedding features, these sediments are interpreted as sheet flood deposits. The thin caliche horizons are interpreted as pedogenetic features developed under semi-arid climatic conditions.

In the Bone-Area Mb. an upwardly increasing abundance of caliche horizons and a decrease of coarse-grained sandstones and conglomerate interbeds has been observed. Therefore it might be suspected that aridity increased during deposition of the Bone Area Mb. causing only rare flooding but long periods of non-deposition and pedogenic overprinting.



**Fig. 5.6:** **A:** Outcrop of the Waterfall Mb. directly at the Waterfall in C6; view is towards E; person for scale. **B:** Outcrop of the Waterfall Mb. about 300 m WSW of picture A; sediments of the Mixed Unit are not preserved; view towards E. **C:** Tilted sediments of the Mixed Unit at the exit of the Red Canyon in C6; arrows indicate unconformity between Red Canyon Fm. and Whitecliff Fm.; view towards ESE; person for scale.



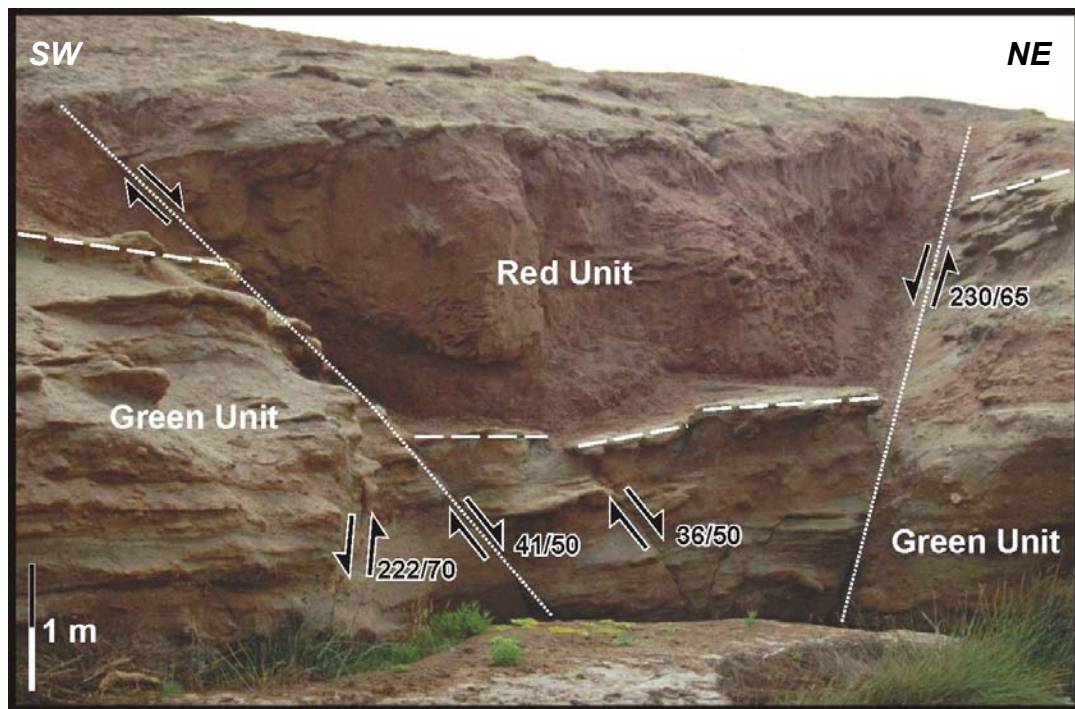
**Fig. 5.7** **A:** Type locality of the Bone-Area Mb. in C5; view towards ENE. The outcrop in the left part of the photograph has a height of about 20 m. **B:** Interbedded caliche horizons in the upper Bone-Area Mb. in channel C5c; hammer for scale. **C/D:** Newly discovered outcrops of the Red Canyon Fm. with C showing the outcrop at the beach directly S of the channel mouth of C3 (photo cap for scale) and D showing an outcrop directly in front of the channel mouth of C9. In D the fine-grained sandstone of the Red Canyon Fm. is unconformably overlain by conglomerates of the Whitecliff Formation.

### 5.3.3 Tectonic features

The deposits of the Red Canyon Fm. are markedly affected by tectonic activity recorded by faulting, tilting and jointing. The restricted coast parallel outcrops of the Red Canyon Fm. between 1.5 km east of the present day coastline and the foreshore suggests that the extent of the Red Canyon Fm. towards the E is limited by a coast parallel fault, which has a similar NNW-SSE oriented strike like the small faults shown in the geological map (Fig. 5.4).

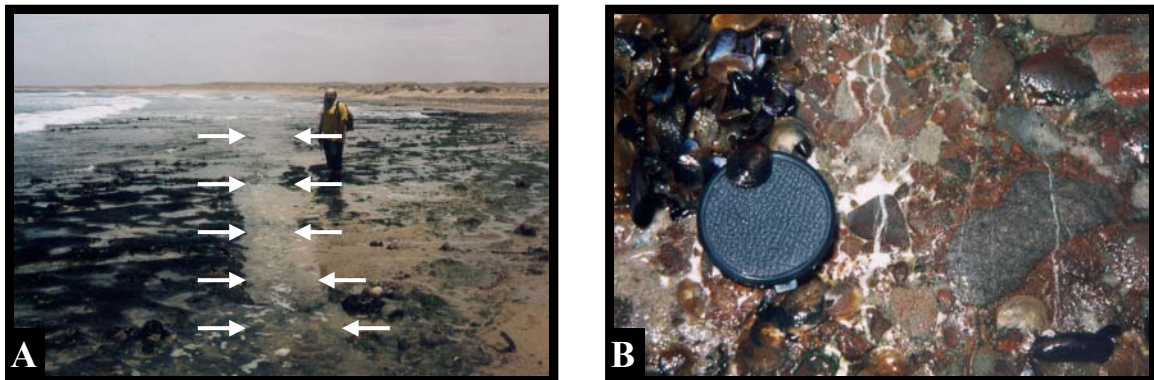
At the western end of the Red Canyon a small graben structure is exposed within in the sediments of the Red Canyon Fm. and displaces the Red Unit against the Green Unit (Fig. 5.8). This structure runs in about  $41^\circ$  direction and has a size of about 6 x 5 m. Some 20 cm thick arkosic layers of the Green Unit indicate vertical displacements of up to 3,5 m. The sediments of the Whitecliff Fm. overly this structure undisplaced and with an angular conformity. Therefore, a pre-Whitecliff age (see below) for the tectonic activity can be concluded in this case.





**Fig. 5.8:** The graben structure at the western margin of the Red Canyon in C6 showing the displacement of the Green and Red Unit (view towards NNE).

In another, only temporarily accessible outcrop of the foreshore area seaward of the channel mouth C9 sediments of the Red Canyon Fm. dip towards SSE. There, N-S striking quartz veins penetrate single clasts of the conglomeratic sediments (Figs. 5.9 A+B).



**Fig. 5.9:** **A:** Exposures of the Red Canyon Fm. seaward of channel mouth C9 during extreme low tides. A nearly N-S striking lineament is visible; view towards NNE; person for scale. **B:** Quartz-filled cracks and veins through single clasts of conglomerates from the Red Canyon Fm. are visible; same locality as in A; photo cap for scale.

### 5.3.4 Interpretation and age estimates

SVENDSEN (2000) interpreted the overall upward fining trend within the succession of the Red Canyon Fm. as a change from alluvial fan and braided river sediments to deposits of a meandering river and finally deposits of a huge floodplain area controlled by a rise in base



level. Alternatively the vertical development in the sedimentary facies might be also explained by a fan model, whereby the coarse-grained basal parts represent deposits of the proximal inner fan area which gradually change as the result of a base level rise into finer-grained deposits of the middle fan area with deposits of the distal outer fan/floodplain area finally forming the top of the succession (MIALL, 1977; READING, 1996). However, the limited exposure, extent and preservation of the Red Canyon Fm. sediments impede a more precise interpretation.

The occurrence of strongly weathered clasts of Etendeka basalts and quartz latites in all stratigraphic units of the Red Canyon Formation implies a late Early Cretaceous maximum age. A recently discovered fossil bovid bone from the Bone Area Mb., however, strongly suggests a post-Upper Cretaceous age for the upper part of the Red Canyon Fm. [pers. comm. B. Rubidge, 2002].

Some additional information to improve the age estimation for the Red Canyon Formation was collected in the Sperrgebiet area, S-Namibia, during an IAS conference field trip in 2002. In a borrow pit 15 km north-northwest of the Chameis Gate (for locality see WARD et al., 2002) pedogenic silcretes, developed in lag deposits, overlie a mottled red soil, which developed on deeply weathered and kaolinised basement rocks (WARD et al., 2002). The silcrete is interpreted to relate to the Chalcedon-Tafelberg Fm. (Pomona/Tafelberg Silcrete Fm.) which is placed close to the K-T-boundary (PARTRIDGE & MAUD, 1989; PETHER et al., 2000). This age estimate is corroborated by offshore well data from the adjacent Namibian shelf where a hard and resistant horizon was drilled at the K-T-boundary by SHELL [pers. comm. J. Ward, 2002]. Therefore, the red soil underneath the silcrete is most probably of Latest Cretaceous age. It is very likely that such a red soil developed in wide areas in southern Africa at the end of the Cretaceous under tropical humid conditions. This soil represents a highly potential source material for the sediments of the Red Canyon Formation.

Other reddish sediments are reported from southern Namibia and are represented by the Tsondab and Rooilepel Sandstones for which a Middle Neogene age is supposed (PETHER et al., 2000; pers. comm. J. Ward, 2002). A considerable part of both sandstones is represented by an aeolian facies indicating deposition under semi-arid to arid climatic conditions (WARD, 1987). In contrast, the sediments of the Red Canyon Fm. display characteristics of deposition from humid- to semi-arid conditions. Therefore, it seems likely that they have formed earlier than the Tsondab/Rooilepel Sandstones, maybe during the Paleogene.

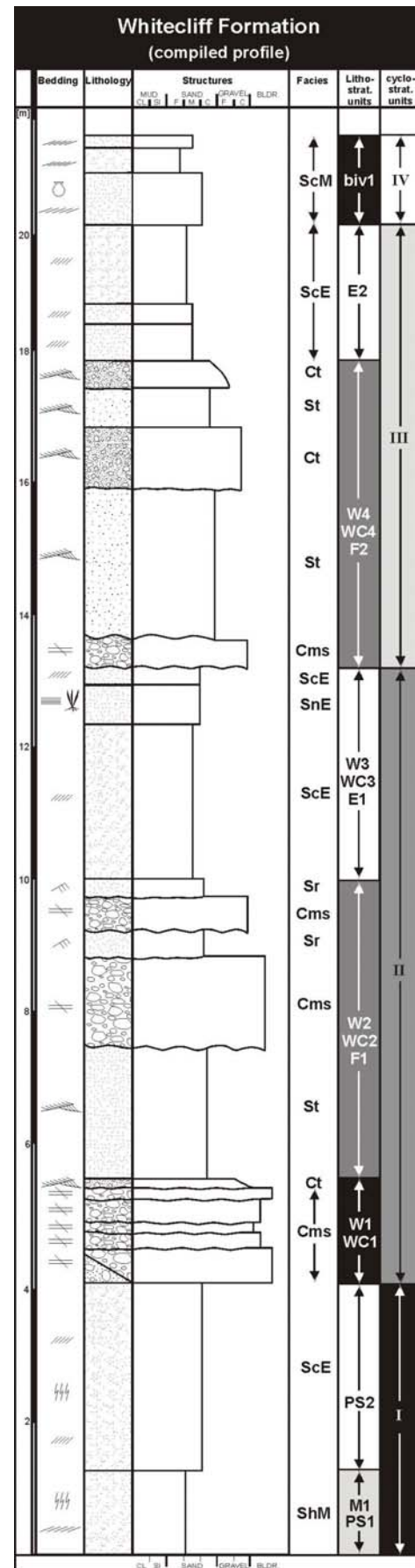
### 5.4 Whitecliff Formation

The Whitecliff Formation represents a lithostratigraphic unit consisting of light coloured indurated, carbonate-cemented sandstones and conglomerates, which overlie both the sediments of the Red Canyon Fm. and the Pan-African Damara metamorphic rocks with a major unconformity. Overlain is the Whitecliff Fm. by younger sediments of the Uniabmond Fm. (see Chapter 5.5). The term 'Whitecliff Fm.' was introduced by ZELLER (2000). He named the light coloured deposits of the Whitecliff Fm. after a locality in channel C5c, where sediments of this formation, deposited on an ancient seacliff, are well exposed. Important outcrops are located in channels C2, C5c and C6. However, small isolated outcrops of the Whitecliff Fm. can be found all over the whole Uniabmond area (see Fig. 5.4).

The Whitecliff Fm. has a maximum cumulative thickness of about 23,5 m (Fig. 5.10) and displays a wide variety of continental and marine facies (ZELLER, 2000; KRAPF et al., 2002). The deposits are strongly cemented by carbonate with CaCO<sub>3</sub>-contents ranging between 15,6 and 39,5 vol. % (see Tab. 5.1). Due to carbonate-cementation the sediments show a relatively high resistance against erosion.

The succession was previously described by RUST (1987), VAN ZYL & SCHEEPERS (1991, 1992), HÜSER et al., (1997), EITEL et al. (1999a, b) and ZELLER (2000).

RUST (1987) reported of calcified sediments from most ephemeral rivers at the Skeleton Coast, which he summarized in the Ogams



**Fig. 5.10:** Compiled profile of the Whitecliff Formation

Formation. Ogams is a locality at the Sechumib River in the northern part of the Skeleton Coast, about 35 km east of the Atlantic coast and about 220 km north of the Uniabmond area. Since correlation of deposits in the Uniabmond area with deposits of the Ogams area is not at all established, the use of the term 'Ogams Formation' in the Uniabmond area seems inappropriate.

VAN ZYL & SCHEEPERS (1991, 1992) interpreted the deposits of the Whitecliff Fm. as equivalents of the well-lithified conglomerates and sandstones of the Early to Middle Pleistocene Oswater Conglomerate Formation originally described by WARD (1987, 1988) from the Kuiseb Valley. They termed them Oswater-equivalent sediments (VAN ZYL & SCHEEPERS (1991, 1992), however, their correlation was only based on purely lithological similarities.

HÜSER et al. (1997) and EITEL et al. (1999a, b) describe the investigated deposits of the Whitecliff Fm. as strongly carbonate-cemented fluvial sandstones and conglomerates and aeolian sandstones with a thickness of up to 4 m. HÜSER et al. (1997) interpreted them as the basal calcified part of the unconsolidated Uniab conglomerate ('Uniabkonglomerat' after HÜSER et al., 1997). EITEL et al. (1999a) termed these deposits 'basal conglomerate' (Basiskonglomerat after Eitel et al., 1999a, see their Fig. 3) and distinguished between the solidified 'basal conglomerate' and the overlying non-lithified 'Uniab conglomerate' ('Uniabmond Fm.' after KRAPF et al., 2002; see also Chapter 2 & 5.5). Both authors did not recognize the stratigraphic relationships between these two units in detail and incorporated the sediments to a single depositional unit. However, because of the erosional unconformity between the two depositional sequences and their different diagenetic solidification, a separation into two individual formations is justified (ZELLER, 2000; KRAPF et al., 2002).

A first detailed description of the distribution and the variable lithofacies of the Whitecliff Fm. was then given by ZELLER (2000), who introduced the term 'White Cliff Formation'. He distinguished between an 'older' Uniab and a 'younger' White Cliff Formation. Both formations are characterized by calcified sediments. The Uniab Fm. comprises fluvial conglomerates and interbedded aeolian sandstones, whereas the White Cliff Fm. sensu ZELLER (2000) consists of coastal, fluvial and aeolian sediments. The age relationship between both formations was deduced from the observation that consolidated, mainly aeolian sandstones - interpreted by ZELLER (2000) as Uniab Fm. - occur as large clasts within the White Cliff Formation. On the other hand it has been observed during fieldwork that semi-consolidated fluvial and aeolian sand deposits were eroded and transported during flood events and then re-deposited as large intraformational clasts. In addition, own

mapping and logging has shown that facies successions of the Uniab and White Cliff Fm. correlate with one another and thus represent lateral equivalents. Therefore, ZELLER's (2000) Uniab and White Cliff Fm. is merged into one formation, termed 'Whitecliff Fm.' (KRAPF et al., 2002).

To further the understanding of stratigraphic relationships between different facies successions of the Whitecliff Fm. several cross sections and profiles were logged in the major outcrop areas of the Whitecliff Fm. in channels C2 and C6.

#### **5.4.1 Facies of the Whitecliff Formation**

The Whitecliff Fm. displays a wide variety of continental and marine facies, all of which are characterized by an intensive carbonate cementation (Tab. 5.1). If not indicated otherwise, the description of the different facies originates from outcrops in channel C6 in between the waterfall and the coast (cf. Fig. 5.4 & Fig. 5.14). Each facies has been given a facies code (cf. Tab. 5.2).

##### **5.4.1.1 Fluvial facies**

###### **Massive conglomerates (Cms)**

Massive conglomerates are dominantly poorly-sorted and matrix-supported with some clast-supported patches (Fig. 5.13 A). Only in few places a crude planar bedding is visible. These conglomerates are mainly composed of subrounded to rounded quartz latite and minor basalt clasts derived from the Etendeka Group with maximum clast sizes of 13 to 23 cm. They have only slightly erosional base contacts and usually form sheet-like units with a thickness of 30 to 75 cm and lobate to semi-tabular geometries. Individual units are vertically and laterally amalgamated and form stacked conglomeratic successions.

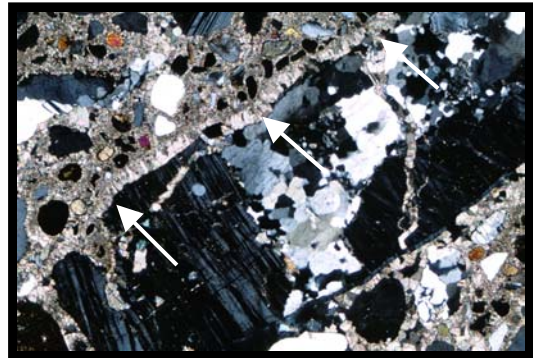
The arenaceous matrix content averages 5-15 vol. %. The matrix consists mainly of angular to subangular volcanic and minor well-rounded quartz grains (75 %) with aeolian grain characteristics, microcline grains (10 %) and very well rounded dark brown, iron-oxide coated quartz grains (5 %). Accessory constituents are lithics of Damaran metamorphic rocks and Etendeka volcanics as well as small grains of sub- to well-rounded clinopyroxenes, subrounded orthoamphiboles, subangular rutiles, muscovite, garnet and oligoclase (ZELLER, 2000). Matrix content may reach 40 %. The matrix is highly carbonate cemented and only few grain-contacts have been observed in thin sections. Columnar

calcite is situated around single grains and nearly no porosity has been determined in thin sections (Fig. 5.11).

Due to the paucity of sedimentary structures, the lack of grading and their sheet-like appearance these sediments are interpreted as the result of high density debris flows.

### **Feldspar-rich conglomerates of facies (Cms)**

Within facies Cms very immature and poorly sorted conglomerates consisting of 20-30 Vol. % of angular and only slightly weathered pinkish to orange feldspar from Damara metamorphic rocks and of 70-80 % of subrounded to rounded Etendeka quartz latite and minor basalt clasts occur. This relatively high percentage of basement components is very unique within the Whitecliff Formation and occurs only in deposits of facies Cms in channel C2 about 150 m west of the main access road to Terrace Bay. The basement clasts derived directly from the underlying crystalline basement rocks and represent locally reworked debris. The conglomerate is matrix-supported with coarse-grained arenaceous matrix mainly composed of angular to subangular volcanic and well-rounded aeolian reworked quartz grains. Like in facies Ct, columnar calcite is developed around single grains (Fig. 5.11). In most outcrops these conglomerates appear massive, only at few localities a weakly developed planar-bedding is visible. At one locality low-angle cross-bedding and thin (2 cm) upward-fining units have been observed (ZELLER, 2000). The feldspar-rich, matrix-supported conglomerate facies is interpreted to represent mass flows with variable viscosities causing changes in sediment facies.



**Fig. 5.11:** Columnar calcite (indicated by arrows) fringing a quartz-feldspar clast in a sample of the feldspar-rich conglomerate of facies Cms in C2. Width of thin section is 1 cm.

### **Trough cross-bedded conglomerates (Ct)**

Trough cross-bedded, medium sorted conglomerates consist of subrounded to well rounded Etendeka derived quartz latite and minor basalt clasts with maximum clast sizes of 4-15 cm. The composition of the matrix and the matrix content is equivalent to that of the Cms facies (see above). Clast imbrication has been observed in several places close to channelized base contacts.



These sediments are interpreted to represent channel fills of a braided river under regular flow regime.

### **Trough cross-bedded sandstones (TS)**

Trough cross-bedded, medium to very coarse-grained, poorly sorted pebbly sandstones represent the most common facies of the Whitecliff Formation. Single troughs are about 2 m wide and 0,05 to 0,1 m high. The majority of lithic clasts within the sandy matrix have grain sizes between 1 and 5 cm. The lithic clasts are mainly composed of subrounded Etendeka quartz latites and subordinately, subangular basalts of the same derivation. Conspicuous components of these sandstones are cobble- to boulder-sized (up to 1 m in diameter), subangular to subrounded, intraformational clasts derived from fluvial (facies TS) as well as aeolian sandstone facies (facies AS). Soft-sediment deformation features can be observed in sandstones where such intraformational clasts are embedded (Fig. 5.13 B). The medium to very coarse-grained arenaceous matrix consists mainly of angular to subrounded quartz grains, about 10 to 20 % of which are well rounded and probably of aeolian origin.

The described lithological characteristics and the bedding indicate deposition in the lower flow regime in a major channel (MIALL, 1978).

### **Ripple cross-laminated sandstones (Sr)**

Ripple cross-laminated, medium- to coarse-grained sandstones with lithic grains and heavy mineral laminae have only been observed in channel C6 in an outcrop area near the waterfall. These sandstones have thicknesses between 30 and 50 cm. Palaeocurrent directions towards WSW are deduced from linguoid ripple data and are comparable to modern-day discharge directions. The ripple-cross laminated sandstone facies has weakly developed erosional bases and is interpreted to record waning flow conditions in an overall fluvial environment.

### **Horizontal-bedded to low-angle cross-bedded sandstones (Sh)**

Horizontal-bedded to low-angle cross-bedded, medium to well sorted, medium to coarse-grained sandstones make up fining-upward units up to 10 cm thick. They show non-erosional basal contacts and draping of obstacles is common. Frequently subangular metamorphic basement and subrounded quartz latitic Etendeka clasts of an average grain

size of 0,5-1 cm occur in the basal parts of these units. In some places there are associated massive conglomerates, aeolian sediments and caliche horizons. Furthermore, the facies is underlain by up to 50 cm thick massive, moderately sorted, medium-grained sandstones with a few subangular Etendeka lithics up to 4 mm in size. These sediments reflect planar bed flow in the lower and upper flow regime (MIALL, 1978).

#### 5.4.1.2 Aeolian facies

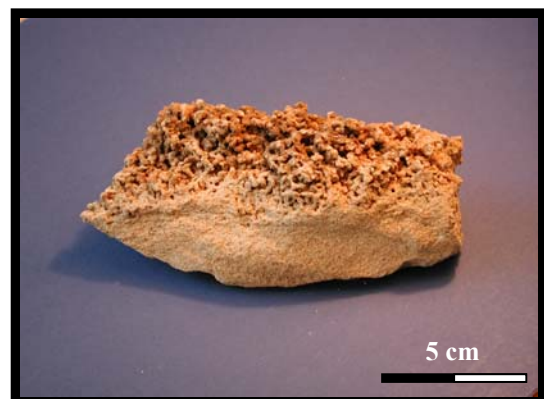
##### Large-scale cross-bedded sandstones (ScE)

Large-scale cross-bedded, fine- to coarse-grained, well sorted mature sandstones are intercalated in fluvial deposits or conformably overlie them (Fig. 5.13 C). They are mainly composed of subrounded to well-rounded quartz grains. Grains of sub- to well-rounded garnet and very well-rounded magnetite are also common. In some outcrops heavy mineral lamination was detected. Subrounded to rounded Etendeka and basement lithics, feldspar and iron-coated quartz grains occur only accessory. Bedding sets are 0,1 to 2,20 m in thickness and are characterized by steep planar foresets. In several places the sediments show signs of bioturbation.

These deposits are interpreted as aeolian sandstones and are regarded as analogues of today's lee sand deposits, sandramps and coastal barchan dunes. The dip directions of the foresets vary between NW and NNE indicating southeasterly to south-southwesterly palaeowind directions, which slightly differ from the modern-day wind regime (see Chapter 2).

##### Nodular sandstones (SnE)

Medium to well sorted, medium- to coarse-grained nodular sandstones with single Etendeka clasts up to 3 cm diameter were found intercalated in the ScE facies in C6 near the Waterfall (see Fig. 5.4). Sandstones with only few nodules allow identification of small-scale trough cross- and plane-bedding. Bed thickness varies from 10 to 30 cm depending on the topography of the underlying sediment. The majority of these sandstones are



**Fig. 5.12:** Sample of nodular sandstone of facies SnE from Waterfall section in C6 (see Chapter 5.4.2.1). Nodular structures start abruptly in the underlying sediment causing disintegration of primary sedimentary structures.

so rich in nodules, that no sedimentary structures can be detected.

In some stratigraphic levels growth of nodular structures starts abruptly in the underlying sediment causing disintegration of primary sedimentary structures (Fig. 5.12). The nodules show spherical to ellipsoidal shapes between 2 and 5 mm (Fig. 5.13 D). They are interpreted as rhizcretions resulting from growth of the grass species *Stipagrostis* (Poaceae) in interdune settings. *Stipagrostis* is known to grow on coastal and inland dunes as well as on loose sand sheet accumulations (YEATON, 1990; DANIN, 1996; BORNKAMM et al., 1999). They are adapted to sand accretion by having vertical aerial stems and the ability to produce nodal roots when covered (DANIN, 1996). The roots of *Stipagrostis* stabilize the loose shifting sand and a calcareous arenosol develops (PFISTERER et al., 1996).

Facies SnE shows aeolian grain characteristics, the observed sedimentary structures, however, are more typical for fluvial sediments. SVENDSEN et al. (in press) describe an analogue facies from modern sediments of the Uniab Poort area. They explain such a similarity between the two facies by fluvial reworking of aeolian sand in shallow-braided river channels flooding into interdune settings.

#### 5.4.1.3 Marine facies

##### **Bivalve-bearing sandstones (ScM)**

This facies consists of medium-scale cross-bedded, very well sorted, medium- to coarse-grained sandstones which contain well preserved shells of the bivalve *Aulacomya* (since Miocene, family: Mytilacea; COX et al., 1969). Most shells are disarticulate (see Fig. 5.13 G), but a few are still in an articulate condition. The sediments onlap onto a small palaeo-seacliff in C6 about 500m inland from the present coastline (see Figs. 5.25, 5.28). Directly at the palaeo-seacliff the layers are steeply inclined towards W to SW with a dip angle of about 35°. The foresets are progressively less inclined with increasing seaward distance from the palaeo-seacliff (see Chapter 5.4.2.6 and Fig. 5.19). Grain size analysis (see Tab. 5.2) of samples from the ScM facies show that the sediments are negatively skewed, which is regarded as characteristic for a beach environment (TUCKER, 1988).

Thin section inspections of these sandstones reveal green, very well rounded grains with an ellipsoidal to spherical shape. These grains do not show internal structures and under crossed nichols they display a green colour and appear isotropic. The pellet-like grains consist obviously of a green clay mineral or a clay mineral mixture, which is characteristic for the marine glaucony, celadonite or verdine facies (after ODIN, 1988). The well

developed sorting of the sandstone, the negative skewness, the steep dip of the foresets, the presence of abundant disarticulated bivalve shells, and the occurrence of glauconite components point to a beach environment for the deposition of these sandstones. Therefore, the sediments are interpreted as marine beach sediments deposited in a high energy beach environment.

### **Bioturbated sandstones (ShM)**

Planar cross-bedded, well sorted, fine- to medium-grained sandstones onlap the large paleo-seacliff in C5c located 700 m inland from the coast (see Fig. 5.19). Elsewhere the sediments are associated with facies ScE and ScM. These sediments display a conspicuous bluish-grey colour, which results from the presence of abundant opaque heavy mineral layers. Also characteristic for this facies is the occurrence of numerous vertical and horizontal burrows (Fig. 5.13 E+F). The burrows have a length between 2 to 50 cm and are less than 1 cm in diameter. No internal structures have been observed. The sandstones are composed of subangular to rounded quartz grains (80%), very well rounded magnetite grains (10 %) and well rounded Etendeka lithics (10%). Accessories comprise grains of angular to subangular feldspar, clinopyroxenes, amphiboles and garnet. Some of the quartz grains are very well rounded and are most probably of aeolian origin. In thin sections the same green pellet-like mineral grains as described from facies ScM have been recognized, which also points to a marine origin of these deposits (Fig. 5.13H).

The planar cross-beds are dipping seaward towards SSW with steep angles of 30° to 35°. In places spectacularly steep dip angles of 40°, 55° and 64° were measured.

The intensive bioturbation, the occurrence of glauconite-pellets, the high concentration of heavy mineral laminae, grain size parameters as well as the good sorting and rounding strongly indicate a marine, high energy beach/foreshore depositional environment for these sediments.

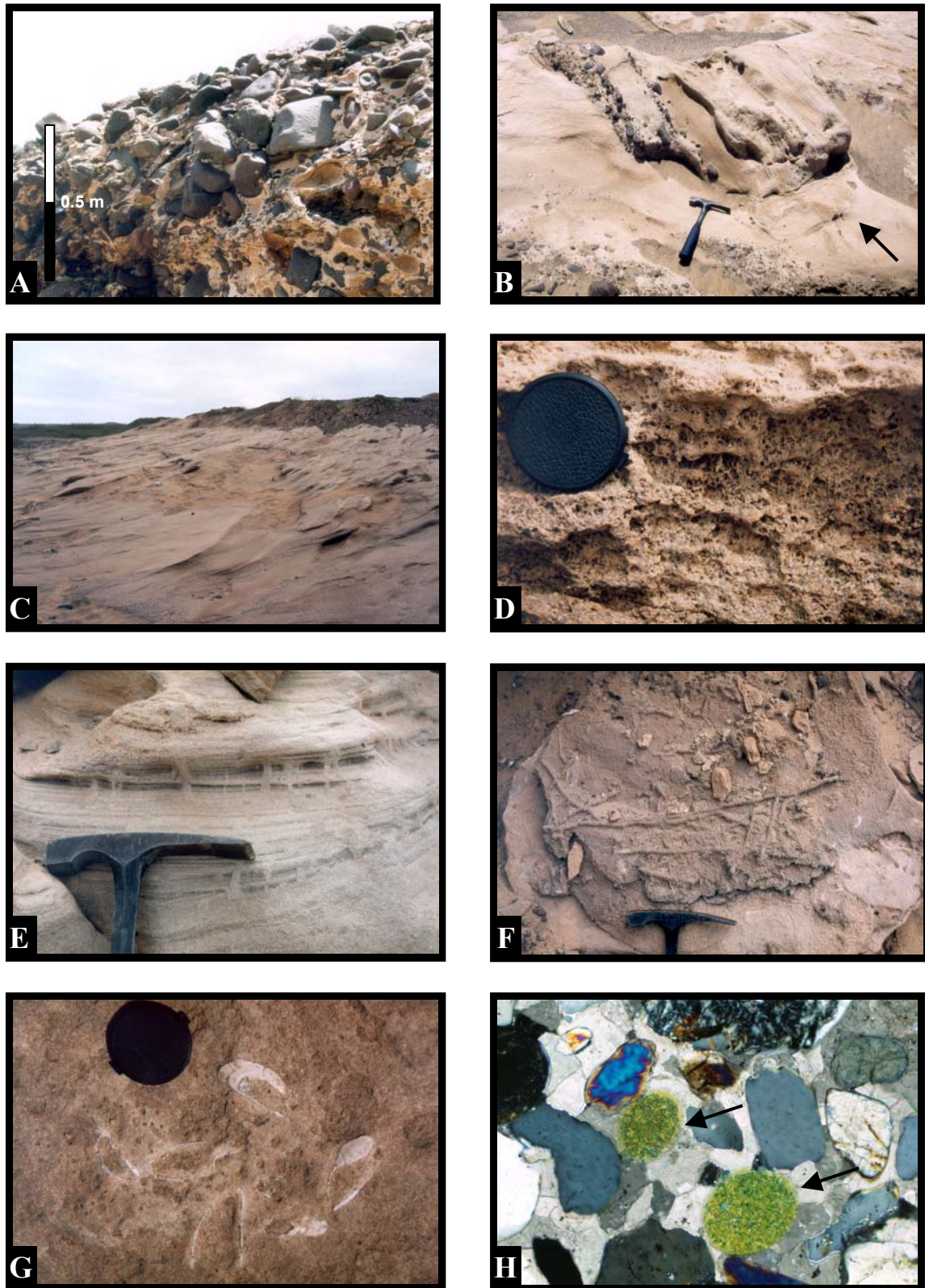
| Sample | Facies | Median | Mean | Standard Deviation | Skewness | Kurtosis | Silt- & Clay-Content in % | CaCO <sub>3</sub> -Content in % |
|--------|--------|--------|------|--------------------|----------|----------|---------------------------|---------------------------------|
| WC-1   | Cms    | 0,15   | 0,53 | 1,27               | 0,47     | 0,81     | 0,43                      | 36,1                            |
| F1     | St     | 1,89   | 1,93 | 0,56               | 0,09     | 0,73     | 0,87                      | 29,9                            |
| F2     | St     | 1,69   | 1,77 | 0,72               | 0,08     | 0,99     | 0,33                      | 25,9                            |
| biv-4  | St     | 1,74   | 1,82 | 0,58               | 0,19     | 1,02     | 0,06                      | 15,8                            |
| biv-3  | St     | 1,56   | 1,35 | 0,68               | -0,01    | 1,38     | 0,06                      | 21,2                            |
| WC-2   | ScE    | 2,47   | 2,37 | 0,65               | -0,15    | 1,24     | 1,23                      | 28,5                            |
| E1     | ScE    | 1,47   | 1,47 | 0,36               | -0,06    | 0,92     | 1,35                      | 37,2                            |
| E2-1   | ScE    | 1,00   | 1,07 | 0,87               | 0,11     | 1,01     | 0,51                      | 31,8                            |
| E2-2   | ScE    | 1,51   | 1,49 | 0,53               | -0,03    | 1,21     | 0,31                      | 35,4                            |
| WCF    | ShM    | 2,84   | 2,87 | 0,74               | -0,02    | 0,89     | 0,43                      | 39,0                            |
| biv-1  | ScM    | 2,47   | 2,40 | 0,44               | -0,23    | 1,3      | 1,46                      | 33,4                            |
| biv-2  | ScM    | 2,47   | 2,35 | 0,49               | -0,30    | 1,24     | 1,19                      | 34,1                            |

**Tab. 5.1:** Summary of grain size parameters, silt- & clay- and CaCO<sub>3</sub>-contents from various facies of the Whitecliff Formation.

| Facies Code | Lithofacies   | Sedimentary Structures                        | Geometry   | Basal Contact  | Fossils                 | Interpretation                         |
|-------------|---------------|---|------------|----------------|-------------------------|--|
| Cms         | conglomerates | massive, rarely horizontal-bedding            | sheet      | sharp, erosive | ---                     | debris flows                           |
| Ct          | conglomerates | through cross-bedding                         | lenticular | erosive        | ---                     | channel fills                          |
| St          | sandstones    | trough cross-bedding                          | lenticular | erosive        | ---                     | dunes (lower flow regime)              |
| Sr          | sandstones    | ripple cross-lamination                       | sheet      | gradational    | ---                     | ripples (lower flow regime)            |
| Sh          | sandstones    | horizontal-bedding to low-angle cross-bedding | sheet      | rarely erosive | ---                     | planar bed flow                        |
| ScE         | sandstones    | large-scale cross-bedding                     | blanket    | sharp          | trace fossils           | aeolian dunes, sand sheets, sand ramps |
| SnE         | sandstones    | nodules                                       | sheet      | gradational    | trace fossils           | interdune deposits                     |
| ScM         | sandstones    | horizontal-bedding                            | blanket    | gradational    | bivalves, trace fossils | beach deposits                         |
| ShM         | sandstones    | horizontal-bedding, bioturbation              | blanket    | sharp          | trace fossils           | foreshore deposits                     |

**Tab. 5.2:** Overview of facies type characteristics in the Whitecliff Formation.

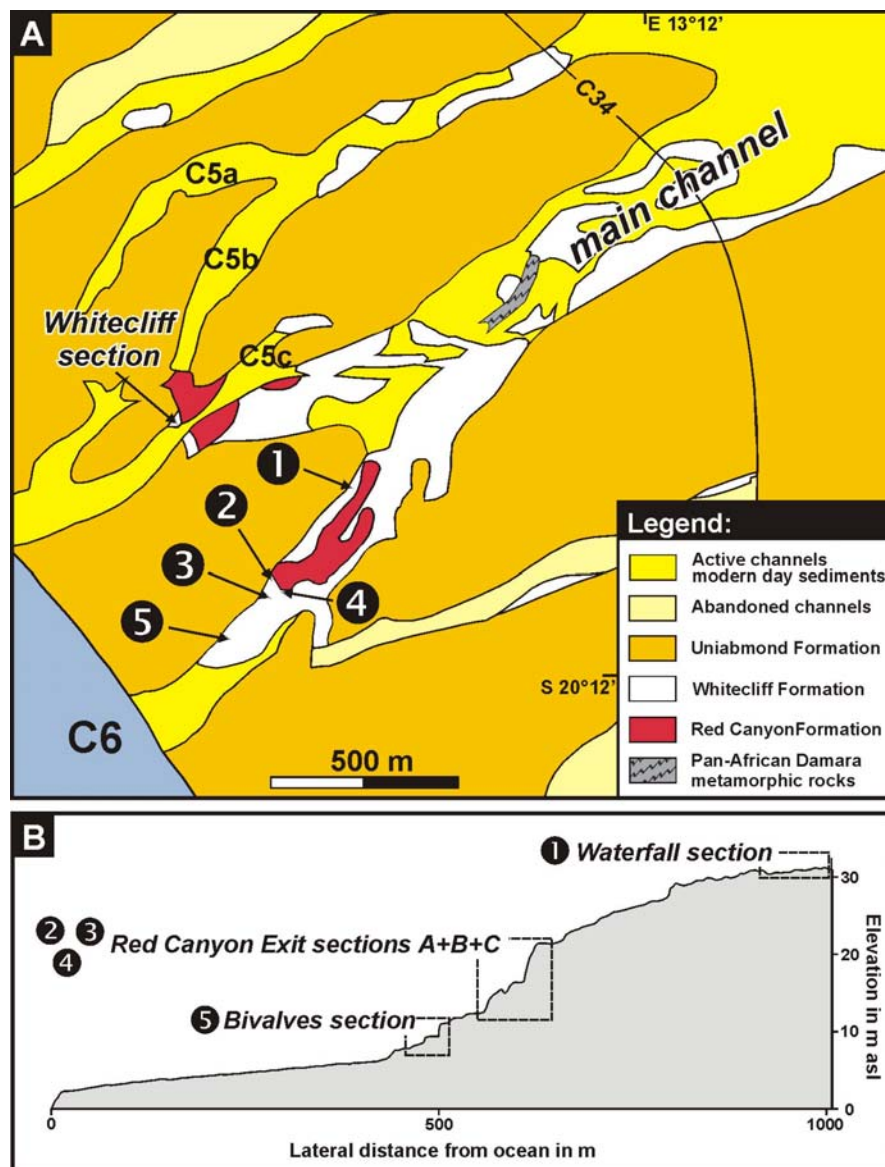




**Fig. 5.13:** The different facies of the Whitecliff Formation. **A:** Facies Cms in C2 about 350 m west of the main road; note varying matrix contents. **B:** Intraformational clast of facies St in fluvial sandstones of the same facies; arrow indicates location of soft sediment deformation features. **C:** Typical outcrop of facies ScE in C5 south of Red Canyon Exit section B (see Chapter 5.4.2.3); dune foresets indicate palaeo-wind directions towards N comparable to the modern day wind regime. **D:** Nodules in sandstones of facies SnE interpreted as rhizocretions of *Stipagrostis* grass species. **E/F:** Examples of bioturbation in marine sandstones of facies ShM from the Whitecliff locality in channel C5c. **G:** Disarticulate shells of *Aulacomya* in marine sandstones of facies ScM in C6. **H:** Thin-section of a sample from facies ScM in C6; pellet-like, very well-rounded green mineral grains (indicated by arrows) are composed of glauconite-related clay minerals.

### 5.4.2 Investigated sections and outcrops of the Whitecliff Formation

For the investigation of the Whitecliff Fm. five sections and seven sedimentary logs were mapped in channels C2, C6 and C5c. The exposed sedimentary sections were divided into several lithostratigraphical subunits resulting in a lithostratigraphical correlation, which will be presented in Chapter 5.4.3.



**Fig. 5.14:** Figures showing the localities of the investigated sections of the Whitecliff Fm. indicated in **A:** on geological map and in **B:** on topographic cross-profile of channel C6.

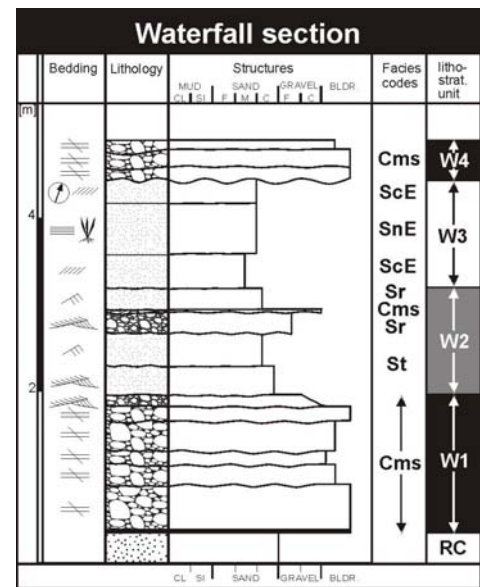
#### 5.4.2.1 Waterfall and C2 section

The sediments of the Waterfall and the C2 section represent the basal part of the Whitecliff Formation. In the Waterfall section (S 20°11.699', E 13°11.501') four lithostratigraphical units have been mapped, termed W1 to W4 (Fig. 5.15).

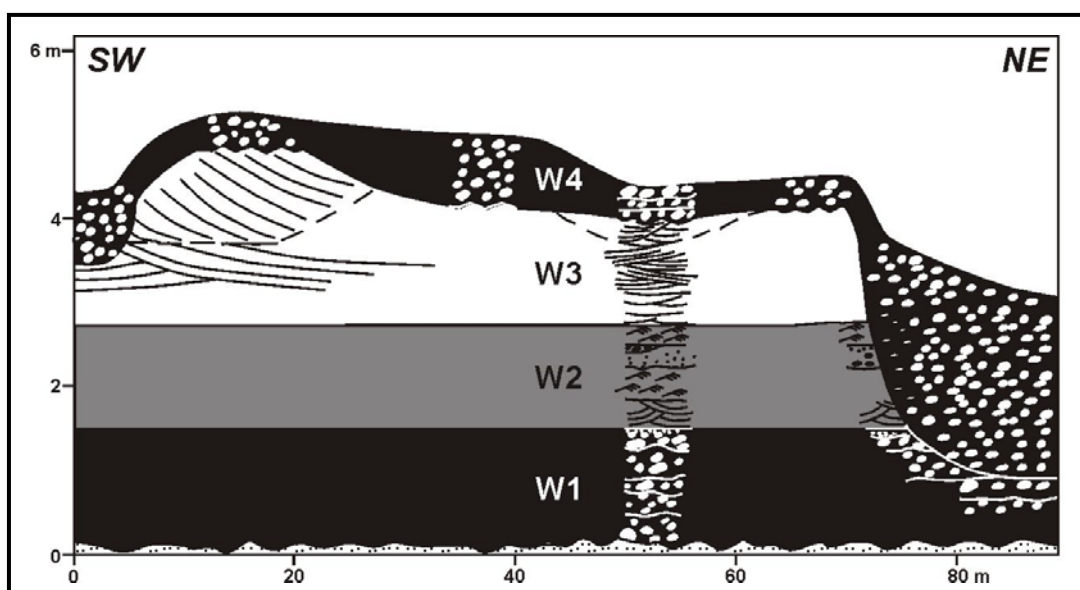


W1 represents a succession of up to seven conglomeratic channels of facies Cms which overlies the Red Canyon Fm. unconformably and protects the latter from erosion. Reworking of sediments of the Red Canyon Fm. can be deduced from a red colouration of the finer grained matrix of overlying conglomerates of unit W1. Unit W1, which reach a thickness of up to 1,50 m, is overlain by unit W2 showing a facies association of St and Sr. This facies association represents a decrease in flow velocity represented by a change from trough cross-bedded to ripple cross-laminated sandstones. They are overlain conformably by unit W3 consisting of up to 1,20 m thick large-scale cross-

bedded sandstones of facies ScE and nodular sandstones of facies SnE. The uppermost preserved unit (W4) in the Waterfall section comprises a series of single sheet-like massive conglomeratic channels (facies Cms) resulting from extensive flood events showing strong erosional potential and marked incision into the underlying sediments (Figs. 5.14 & 5.29 B). This situation was also observed in section C2 (see below). There, unit WC4 overlies aeolian deposits and incises into the underlying sediments. In addition, the conglomerates of these two units belong to the same facies and show similar lithological and structural attributes. Therefore, a correlation between unit W4 and WC4 seems reasonable.



**Fig. 5.15:** Sedimentary log of the Waterfall section. See Fig. 5.14 for location and Appendix 1 for explanation of symbols.

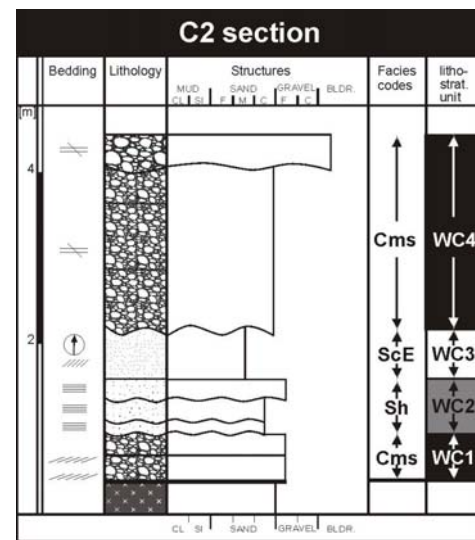


**Fig. 5.16:** Cross section of the investigated sediments of the Whitecliff Fm. in the Waterfall section showing the erosional character of unit W4.

Calcified conglomeratic remnants, most probably belonging to the Whitecliff Fm., are attached to the walls of the Red Canyon which are composed of sediments of the Red Canyon Formation. This shows, that incision formed a palaeo-channel at the same locality as the present day Red Canyon.

The Whitecliff Fm. outcrop in C2 (see Fig. 5.4) is situated about 150 W of the main road (S 20°09.493', E 13°11.684'). The whole C2 section was divided into four lithostratigraphical units, termed WC1, WC2, WC3 and WC4 (Figs. 5.17, 5.29 A).

The basal part of the succession (WC1) comprises very immature and unsorted low-angle cross-bedded conglomerates of facies Cms which are erosively overlain by plane-bedded coarse-grained sandstones of facies Sh. Large-scale cross-bedded aeolian sandstones of facies ScE (WC2) conformably overlie these fluvial deposits. In the uppermost part of the succession massive conglomerates of facies Cms (WC3) are preserved, which strongly eroded into the underlying sediments. The succession is up to 4.20 m thick. The C2 section represents a good example of the relationship between the deposited sediments and



**Fig. 5.17:** Sedimentary log of the C2 section. See Fig. 5.14 for location and Appendix 1 for explanation of symbols.

the underlying bedrock geology (see Chapter 5.4.1.1, facies Cms). The sediments of facies FC and Sh are the first sedimentary strata-record in C2. They were deposited in a palaeo-channel which developed probably after the deposition of the Red Canyon Fm. and prior to the deposition of the Whitecliff Formation. During this time a palaeo-channel, which is incised about 2 m into the underlying bedrock, developed and represents a precursor of the modern channel C2. The base of this palaeo-channel is filled by fluvial sediments of facies Cms and Sh. The relatively high feldspar content (10-20 %) in facies Cms, which is not found in other sediments elsewhere in the Uniabmond area, is related to the underlying Damaran metamorphic rocks (see Chapter 5.4.1.1). These fluvial sediments were covered by sandramps which developed in the lee of a gravel terrace of the palaeo-channel. The sedimentation of facies ScE was followed by extensive floods resulting in the deposition of sheet-like massive conglomerates of facies Cms. In places, they deeply incised into the underlying sediments.

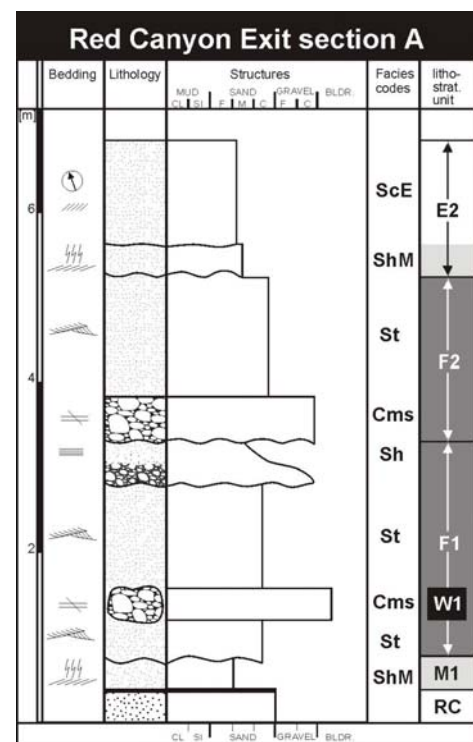
The Whitecliff sediments in C2 are interpreted as deposited under arid to hyper-arid climatic conditions, comparable to the modern day environment in the Uniabmond area. This is also reflected by recent sandramps at this locality, which show the same lithological and structural characteristics like the fossil sandramps of facies AD. Consistent aeolian foreset dip directions towards N show that the palaeo-wind directions were similar to the present-day one (see Chapter 1.2.2).

#### 5.4.2.2 Red Canyon Exit section A

Located at the lower end of the Red Canyon, the Red Canyon Exit section A (S 20°11.699', E 13°11.501') comprises a succession of five lithostratigraphical subunits, termed M1, W1, F1, F2 and E2 (Figs. 5.18 & 5.19).

The sediments are attached to a steep slope developed in the sediments of the Red Canyon Formation. The sediments of the Red Canyon Fm. are unconformably overlain mainly by fluvial and aeolian deposits. At a single locality a small wedge of marine bioturbated sediments (facies ShM) is preserved at the base of the succession (see Fig. 5.29 C). The low-angle cross-bedded, very well sorted, medium- to coarse-grained sandstones contain flat Etendeka beach cobbles with sizes up to 15 cm and represent unit M1. They are erosively overlain by trough cross-bedded fluvial sandstones of facies St (unit F1). Embedded within these deposits are three huge 'floating' blocks, consisting of massive to plane bedded conglomerates of facies Cms and with dimensions of up to 5 m x 1,20 m (Figs. 5.20, 5.29 C). They obviously represent

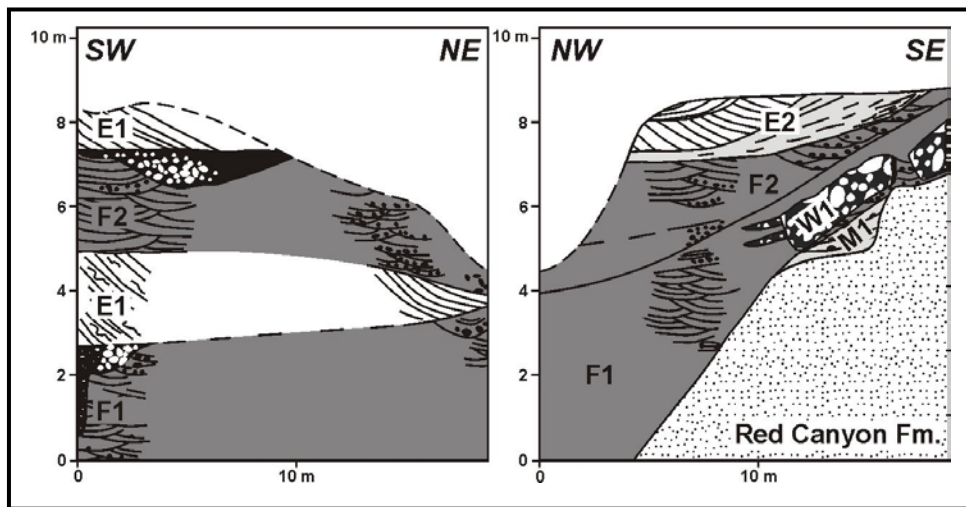
eroded blocks of unit W1 (described in the Waterfall section above), derived from a place further upstream. The orientation of these blocks have been measured as 148/15, 138/15 and 162/28. This is consistent with bedding surface measurements in pebbly sandstones of facies St located directly at the opposite cliff wall (see Red Canyon Exit section C). They also show southerly transport directions. This points to a palaeo-topographical feature



**Fig. 5.18:** Sedimentary log of the Red Canyon Exit section A. See Fig. 5.14 for location and Appendix 1 for explanation of symbols.

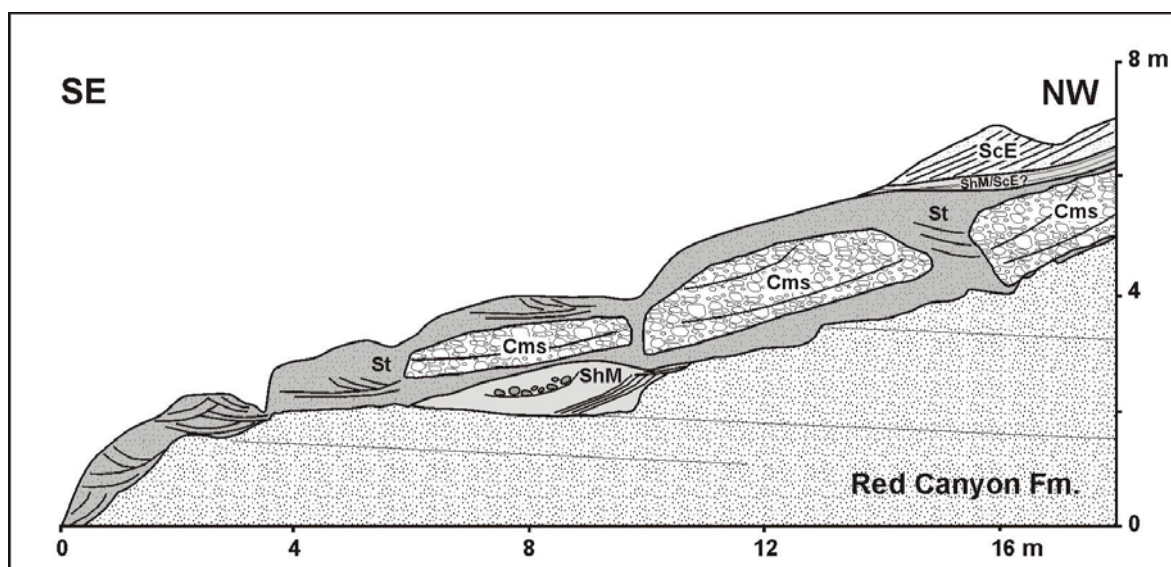


within the ancient river channel and could be interpreted as a former knickpoint in the river gradient or a small waterfall.



**Fig. 5.19:** Cross section of the investigated sediments of the Whitecliff Fm. in Red Canyon Exit sections A & B showing the overall geometry of the different units.

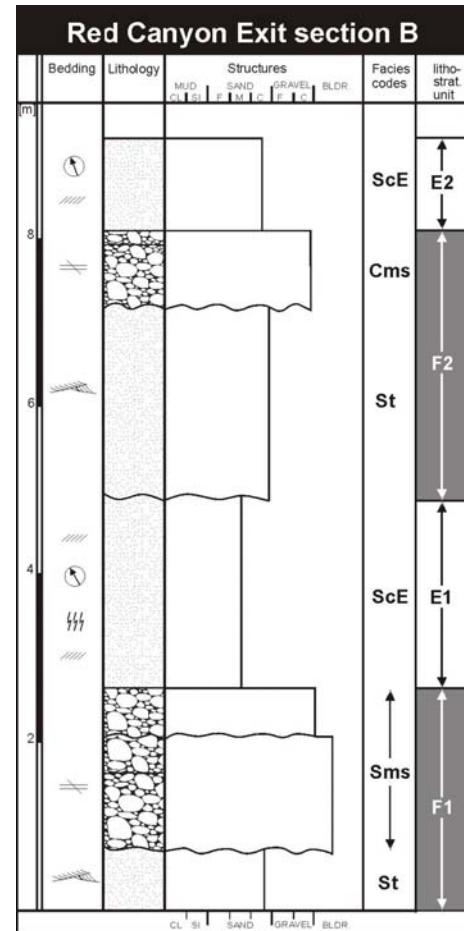
Unit F1 is erosively overlain by fluvial deposits of unit F2 consisting of sediments of facies Cms and St. The uppermost unit E2 consists in its basal parts of planar cross-bedded, well sorted, medium-grained sandstones, which show some signs of bioturbation and some heavy mineral laminae. These sandstones show similarities with facies ShM as well as with facies ScE. In the upper part of the unit E2 large-scale cross-bedded sandstones of facies ScE are preserved with foresets indicating a palaeo-wind direction towards NNW.



**Fig. 5.20:** Detailed cross section of Red Canyon Exit section A in C6. Sediments of the Whitecliff Fm. overlie the palaeo-seacliff developed in sediments of the Red Canyon Formation. Conglomerates of facies Cms are embedded ('floating blocks') in sandstones of facies St. The top of the succession is formed by dunes of facies ScE (see also photo in Fig. 5.29 C).

### 5.4.2.3 Red Canyon Exit sections B

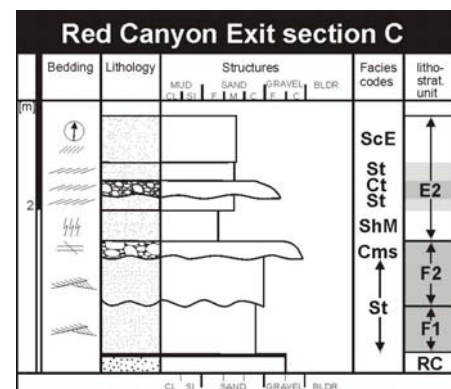
Red Canyon Exit section B (S 20°11.813', E 13°11.357') is situated on the right bank of the present-day discharge channel of C6 about 30 m downstream (west) of section A. The four lithostratigraphical units F1, E1, F2 and E2 have been determined (Fig. 5.21). In comparison to section A the contact to the underlying formation is not directly exposed at the Red Canyon cliff section B but in a small outcrop 50 m west of section B where sediments of the Red Canyon Fm. underlay the Whitecliff Formation. The basal part of section B is composed of trough cross-bedded sandstones of facies St which are erosively overlain by conglomerates of facies Cms and Ct. These deposits are grouped into unit F1. Unit F1 is conformably overlain by dune deposits of facies ScE which show some bioturbation in the middle part. These aeolian sediments of unit E1 are erosively overlain by trough cross-bedded sandstones and massive conglomerates of facies St and C1s of unit F2. In some places conglomerates of unit F2 incised into the underlying units of F1 and E1. The uppermost part of section B (unit E2) is composed of large-scale cross-bedded aeolian sandstones of facies ScE. In Red Canyon Exit section B two fluvio-aeolian cycles are preserved.



**Fig. 5.21:** Sedimentary log of the Red Canyon Exit section B. See Fig. 5.14 for location and Appendix 1 for explanation of symbols.

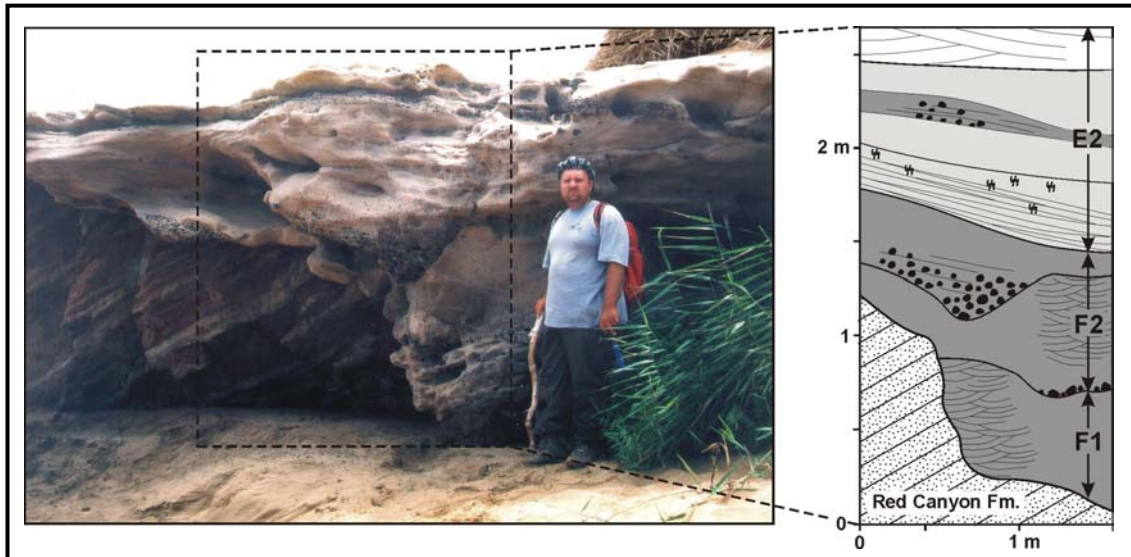
### 5.4.2.4 Red Canyon Exit section C

The Red Canyon Exit section C (S 20°11.880', E 13°11.420) is located directly opposite to section A. The succession unconformably overlies the Red Canyon Fm. and is divided into three lithostratigraphical units termed F1, F2 and E2 (Figs. 5.22 & 5.23). Unit F1 is represented by sandstones of facies St, which are erosively overlain by unit F2



**Fig. 5.22:** Sedimentary log of the Red Canyon Exit section A. See Fig. 5.14 for location and Appendix 1 for explanation of symbols.

consisting of sandstones and conglomerates of facies Cms and St (Fig. 5.22). Bedding surfaces at the base of unit F1 have been measured and yielded data of 165/45 to 195/15 indicating southerly transport directions. Like in section A unit F2 is directly overlain by sediments that either belong to facies ShM or ScE and followed by a thin conglomeratic layer. At the top of unit E2 aeolian sediments of facies ScE are exposed.

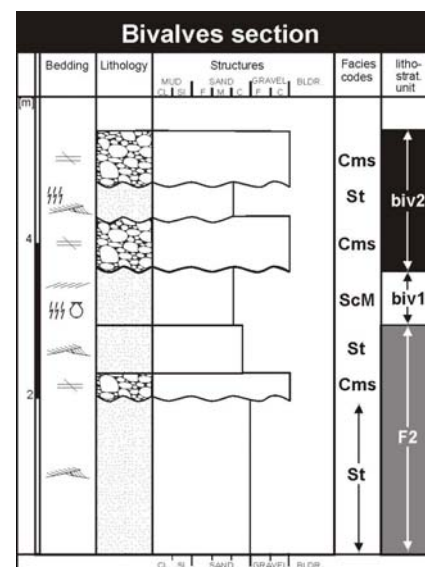


**Fig. 5.23:** The outcrop photograph shows the locality of the Red Canyon Exit section C in C6. View is towards ESE. The tilted sediments of the Red Canyon Fm. are overlain by a succession of fluvial and aeolian deposits.

#### 5.4.2.5 Bivalves section

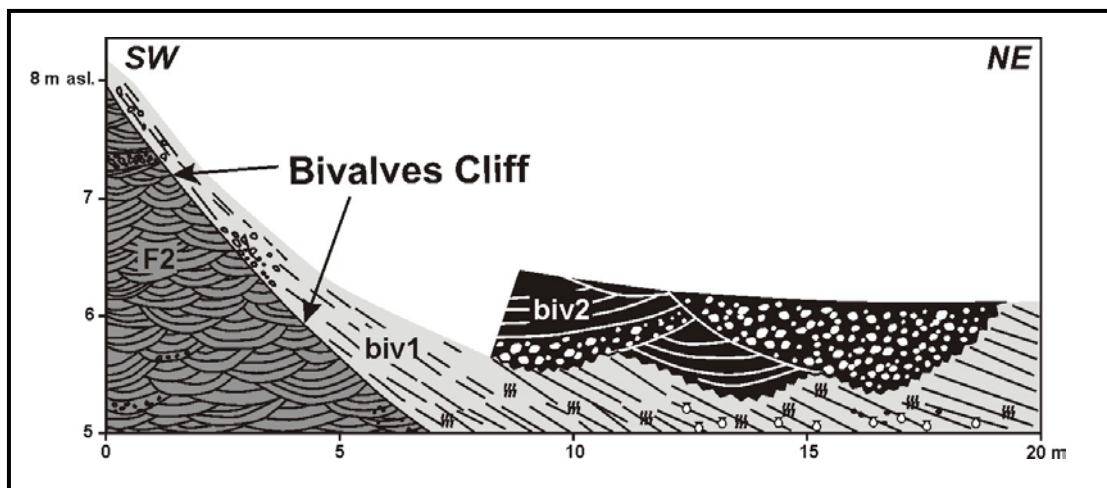
The Bivalves section (S 20°11.19', E 13°11.370') is situated about 500 m east of the present coastline in C6. This section was divided into three lithostratigraphical units termed F2, biv1 and biv2 (Fig. 5.24). The Bivalves section is the type locality of facies ScM.

In sediments of facies St, which represent unit F2, an up to 3 m high palaeo-seacliff has been developed about 480 m east of the present coastline. Surveying the top of this palaeo-seacliff with a level-meter has shown, that it is situated 8,20 m above the present sea level. This palaeo-seacliff, which is named Bivalves Cliff (see Fig. 5.27) has a broad V-shaped outline, striking NNE-SSW north of the runlet and NW-SE



**Fig. 5.24:** Sedimentary log of the Bivalves section. See Fig. 5.14 for location and Appendix 1 for explanation of symbols.

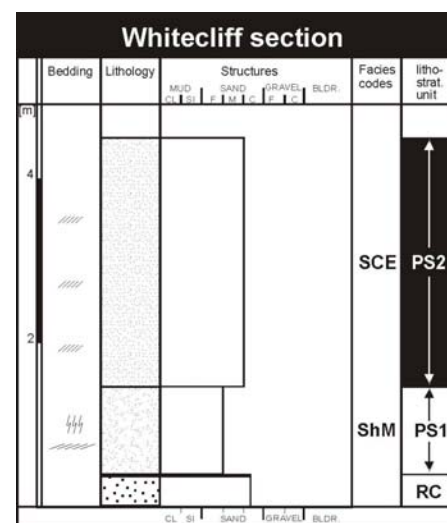
south of it. Beach sediments of facies ScM containing well preserved shells of the bivalve *Aulacomya* onlap this palaeo-seacliff. This bivalve is known since the Miocene (COX et al., 1969). The layers, which were directly deposited at the palaeo-seacliff are steeply inclined towards W to SW with a dip angle of 35° and become progressively less inclined (3°-5°) with increasing distance from it. These marine sediments are erosively overlain by fluvial conglomerates and sandstones of facies Cms and St representing unit biv2. As the sediments of unit biv2 shows the same lithology as other fluvial Whitecliff deposits, they were first interpreted as part of the Whitecliff Formation. However, two artefacts of probably Neolithic and Middle Stone Age [pers. com. J. Kempf, 2001] have been found in sandstones of unit biv2 indicating a much younger age as postulated for the other deposits of the Whitecliff Fm. (see Chapter 5.4.3 and 5.4.4).



**Fig. 5.25:** Cross section of the investigated sediments of the Whitecliff Fm. in the Bivalves section showing unit biv 1 attached to the palaeo-seacliff.

#### 5.4.2.6 Whitecliff section in C5c

A spectacular palaeo-seacliff, termed the Whitecliff, can be found in channel C5c (Figs. 5.14 & 5.27). It is located 700 m inland from the coastline and its base is about 10 m above the present day sea level. This fossil seacliff is oriented NW-SE and is eroded in its central part by the present-day river channel in C5c. Therefore, only remnants of it can be found on either side of the channel. The outcrops on the right bank are best preserved. The fossil seacliff has developed in the Bone Area Mb. of the Red Canyon

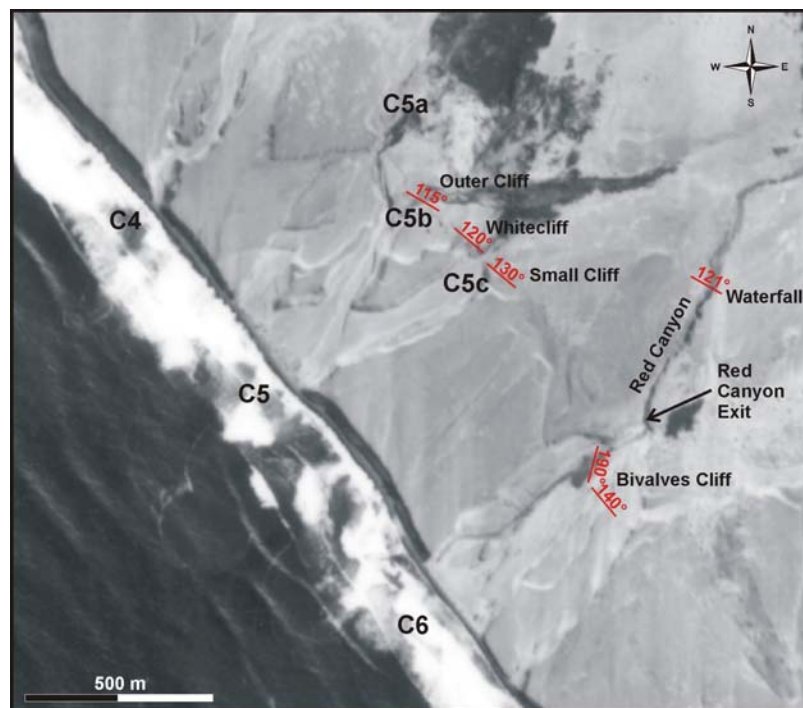


**Fig. 5.26:** Sedimentary log of the Whitecliff section. See Fig. 5.14 for location and Appendix 1 for explanation of symbols.



Fm. and has a height of 15 m above the modern day river channel. The palaeo-seacliff is termed 'Whitecliff' (after ZELLER, 2000) and represents the type locality of facies ShM. It is draped by up to 1.20 m thick planar cross-bedded, well sorted, fine- to medium-grained, heavily bioturbated sandstones of facies ShM which represents unit PS1 (Fig. 5.26). This unit is conformably overlain by unit PS2 and consists of large-scale cross-bedded aeolian sandstones of facies ScE. These dune deposits show also signs of bioturbation. The non-uniform dip directions of the foresets of the aeolian sediments indicate varying wind directions, which are typical for a coastal dune environment (ILLENBERGER & RUST, 1988; GOLDSMITH, 1978).

This seacliff is also exposed on the southern sidewall of C5c and can be traced 50 m further to the southeast (Small Cliff, Fig. 5.27). To the north a continuation of this palaeo-seacliff is exposed in the so called Outer Cliff in channel C5b (Fig. 5.27).



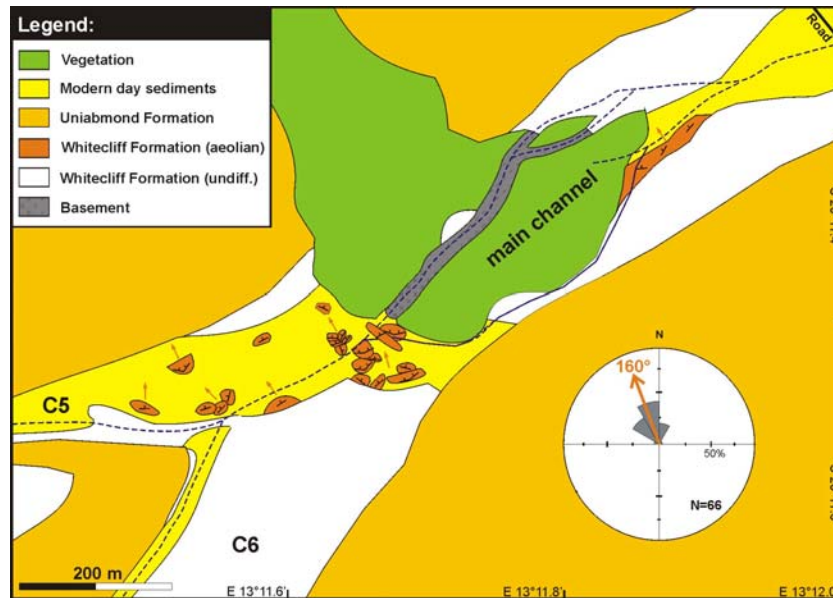
**Fig. 5.27:** Aerial photograph of the main part of the Uniabmond area showing the occurrence and directions of outcrops of the different palaeo-seacliffs.

#### 5.4.2.7 Palaeo-dunefield in the main channel

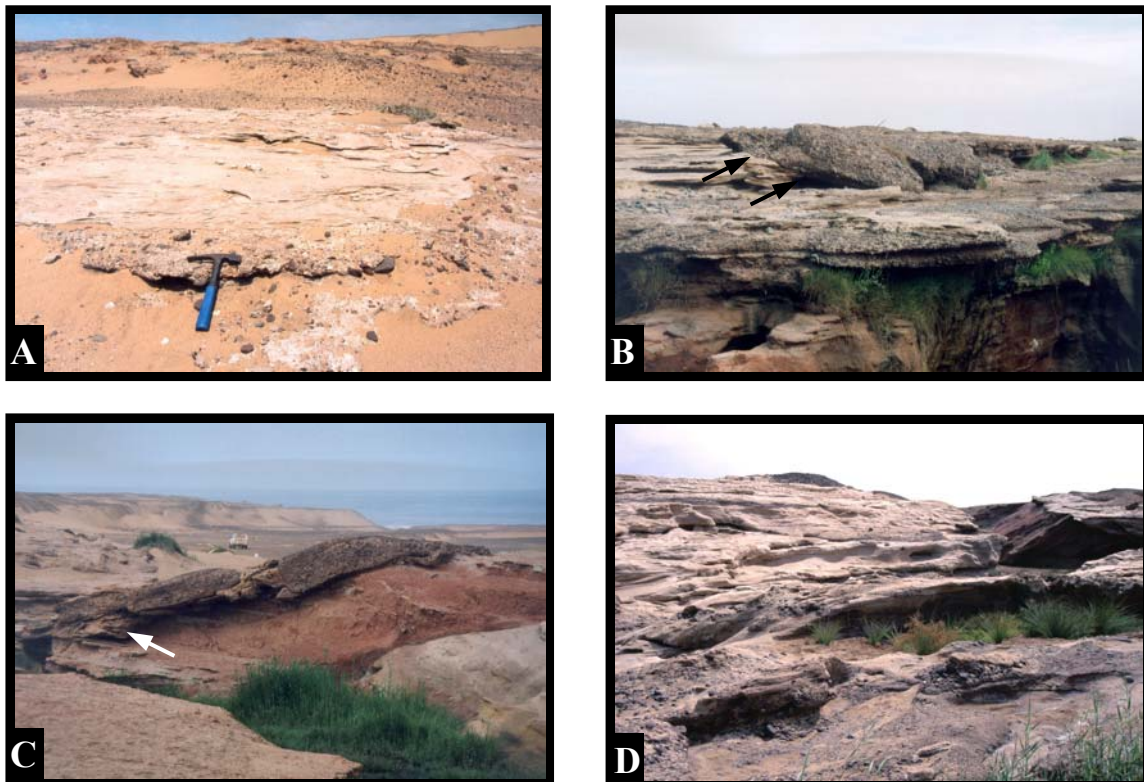
Approximately 50 to 150 m east of the area where the main channel splits into C5 and C6 outcrops of a wide palaeo-dunefield being part of the Whitecliff Fm. have been found (see Fig. 5.28). These outcrops represent an example of ancient aeolian deposits comparable to modern day ones in the Uniab River channels. The fossil sandramps were deposited in the lee of the cutbanks of a palaeo-channel, incised into fluvial sediments of the Whitecliff Formation. Northward, in downwind direction, a barchan dunefield has been established.



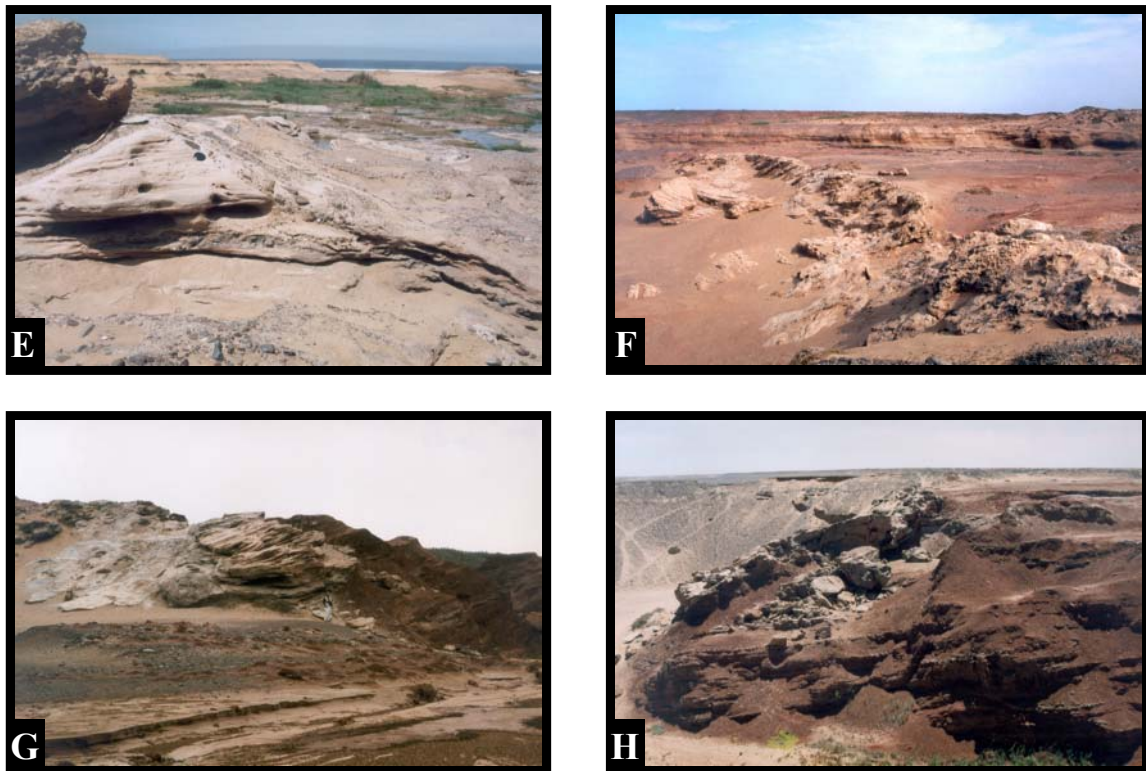
The dip directions of the foresets indicate wind directions from SSW to SE whereas the modern day wind regime is dominated by winds from S to SSW (see Chapter 1.2.2). Again, the slightly varying dip directions of the foresets are typical for a coastal dune environment (ILLENBERGER & RUST, 1988; GOLDSMITH, 1978). Furthermore, topographic funnelling caused by the morphology of incised channels may have effected the local wind regime.



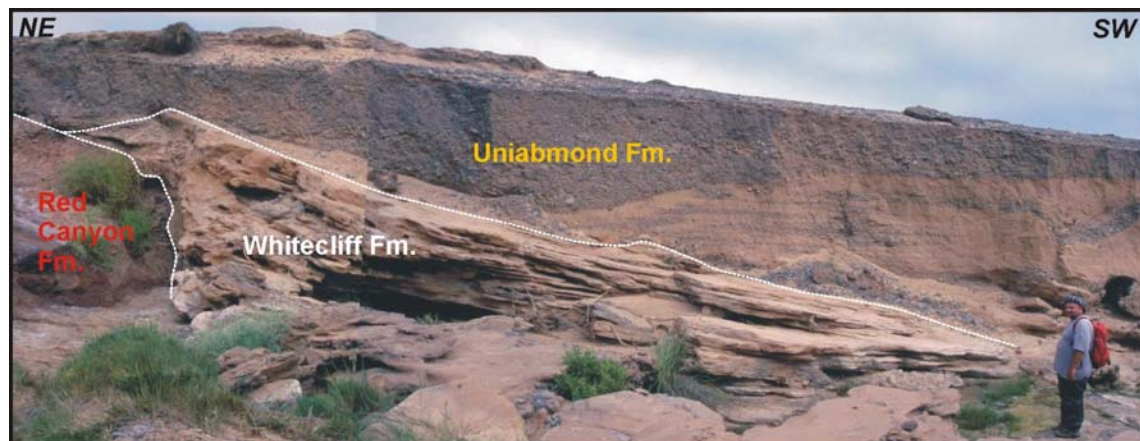
**Figure 5.28:** Simplified geological map of the main channel (after: ZELLER, 2000). The barchans and sandramp deposits of the palaeo-dunefield in the main channel are coloured in black and major orientations of foresets are indicated by arrows.



**Fig. 5.29 A- D:** Explanation see following page.



**Fig. 5.29** **A:** Outcrop of C2 section about 200 m W of main road in channel C2; photo shows the type locality of the feldspar-rich conglomerate (facies Cms) of unit WC1, which overlies the metamorphic basement rocks with a major unconformity; view towards SSE. **B:** Overview of the eastern part of the Waterfall section; the Red Canyon Fm. is overlain by sheet-like conglomerates of unit W1; unit W4 eroded deeply into the underlying units (indicated by arrows); view towards NE. **C:** 'Floating blocks' in Red Canyon Exit section A (see schematic sketch Fig. 5.22); arrow indicating small wedge of marine sediments of unit M1; view towards WSW. **D:** Overview of the Whitecliff Fm. in Red Canyon section B; view towards ENE. **E:** Bivalves Cliff developed in fluvial sandstones of unit F2; steeply inclined marine sediments of unit biv1 onlap the palaeo-seacliff; view towards SW. **F:** Outcrop of the Small Cliff about 50 m SSW of the Whitecliff in C5c; heavily bioturbated aeolian sandstones draping this palaeo-seacliff developed in sediments of the Bone area Mb. of the Red Canyon Fm.; view towards NNW. **G:** The Whitecliff on the right bank of C5c; steeply inclined bluish-grey intensively bioturbated marine sandstones of facies ShM overlaying the palaeo-seacliff developed in sediments of the Bone Area Mb.; the marine sediments are conformably overlain by bioturbated aeolian sandstones; in the foreground of the photo the modern day discharge channel of C5c is visible; view towards ENE. **H:** The NW-SE striking Whitecliff in channel C5c; the sediments of the Bone Area Mb. dip towards NW with an dip angle between 15-28°; in places, where the sediments of the Bone Area Mb. were eroded, up to 5 m thick blocks of the overlying Whitecliff sediments broke off; view towards NNE.



**Fig. 5.30:** Outer Cliff locality, where the palaeo-seacliff developed in sediments of the Red Canyon Fm. are draped by marine and aeolian deposits of the Whitecliff Fm.; both formations are overlain by fluvial sediments of the Uniabmond Fm.; person for scale.



### 5.4.3 A combined litho- and cyclo-stratigraphic correlation approach for the deposits of the Whitecliff Formation

Based on the interpretation of measured sections and facies analysis a correlation of the various depositional successions of the Whitecliff Fm. will be presented here for the first time. In addition to the correlation of lithological units (Fig. 5.31) also the development within a depositional sequence, expressed as four sedimentary cycles (Fig. 5.32), can be used for correlation purposes. These cycles are represented by marine-aeolian, fluvial-aeolian and marine-fluvial cycles. Beside fluvio-aeolian deposits also marine deposits form parts of the sedimentary successions.

At the base of Red Canyon Exit section A a small wedge of marine bioturbated sediments (facies ShM) is preserved. These sediments of unit M1 overlie the Red Canyon Fm. with a major unconformity. In the Whitecliff section in C5c marine and aeolian deposits are attached to the palaeo-seacliff whereas fluvial sediments of the Whitecliff Fm. can only be found east of it. Both marine units are located approximately at the same height above present day sea level and the same distance from the modern day coastline. Therefore, it is suggested that both marine units are equivalents and form the basal part of the first sedimentary cycle (I) of the Whitecliff Fm. represented by beach to foreshore sediments overlain by coastal dune deposits. The latter ones are only preserved in C5c whereas in C6 (Red Canyon Exit section A) they are eroded by the overlaying fluvial sediments of the following cycle.

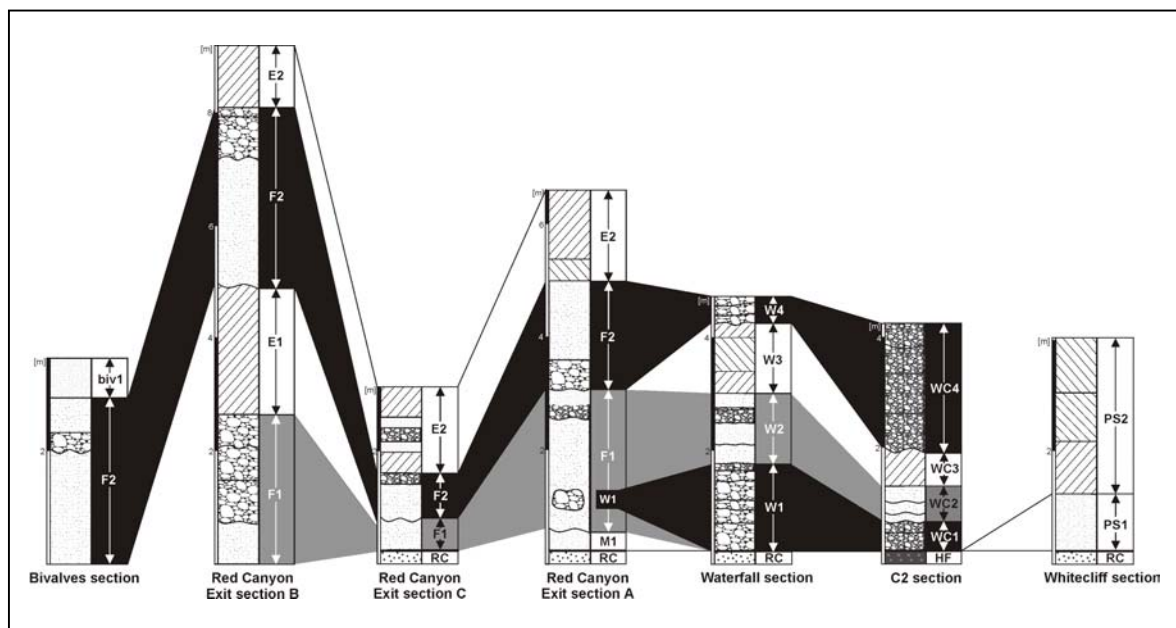


Fig. 5.31: Litho-stratigraphic correlation of the studied Whitecliff Formation sections.

This fluvio-aeolian cycle II is completely preserved in the Waterfall section in C6. There, coarse conglomerates of unit W1 overlie unconformably Red Canyon Fm. sediments. Unit W1 grades into more sandy fluvial deposits of unit W2 and are followed by aeolian and nodular sandstones of unit W3 completing cycle II. A comparable sedimentary cycle has been observed in section C2 (Fig. 5.17) where feldspar-rich conglomerates of unit WC1 overlie unconformably Damaran metamorphic rocks. Similar to the Waterfall section the conglomerates grade into sandy fluvial deposits of unit WC2, which are followed by sandramp deposits of aeolian origin (unit WC3). In Red Canyon Exit section A this fluvio-aeolian cycle II shows a different appearance. There, sandy fluvial deposits of unit F1 overlie unconformably sediments of the Red Canyon Fm. and the marine unit M1 of the Whitecliff Formation. Unit F1 contains three huge 'floating' conglomeratic blocks obviously representing eroded blocks of unit W1 (see Chapter 5.4.2.2). In Red Canyon Exit section C the basal part of cycle II is represented entirely by sandy fluvial deposits of unit F1. In Red Canyon Exit section B unit F1 contains in its upper part also conglomeratic layers. There, unit F1 is followed by aeolian deposits forming the top of cycle II.

Cycle III again represents a fluvial-aeolian depositional sequence. The base of this cycle shows a pronounced erosional character with strong incision into the underlying deposits of cycle II (see Figs. 5.15 & 5.16, Waterfall section) forming a marked palaeotopography. Fluvial deposits (unit F2) of cycle III are preserved in all measured sections (see Fig. 5.33). Like in cycle II the top of this cycle is represented by aeolian sediments (unit E2). In all Red Canyon Exit sections these aeolian sediments form the top of the preserved sedimentary succession of the Whitecliff Formation. East of the Waterfall section, 300 m further inland, aeolian sediments of the palaeo-dunefield in the main channel described in Chapter 5.4.2.7 are equivalents of unit E2. Unit E2 can also be traced coastward to the outcrop area of the Bivalves section but only towards the left channel bank of C6.

Unit F2 is traceable as a continuous outcrop from the Red Canyon Exit sections to the Bivalves section, where 480 m east of the present coastline an up to 3 m high palaeo-seacliff has been developed in unit F2 8,20 m above present day sea level (see Chapter 5.4.2.5 and Fig. 5.29 E). Marine sediments (unit biv1) of the Bivalves section unconformably onlap this palaeo-topographic feature (see Chapter 5.4.2.8) forming the base of cycle IV. These marine sediments are the uppermost preserved deposits of the Whitecliff Fm. in the Uniabmond area.

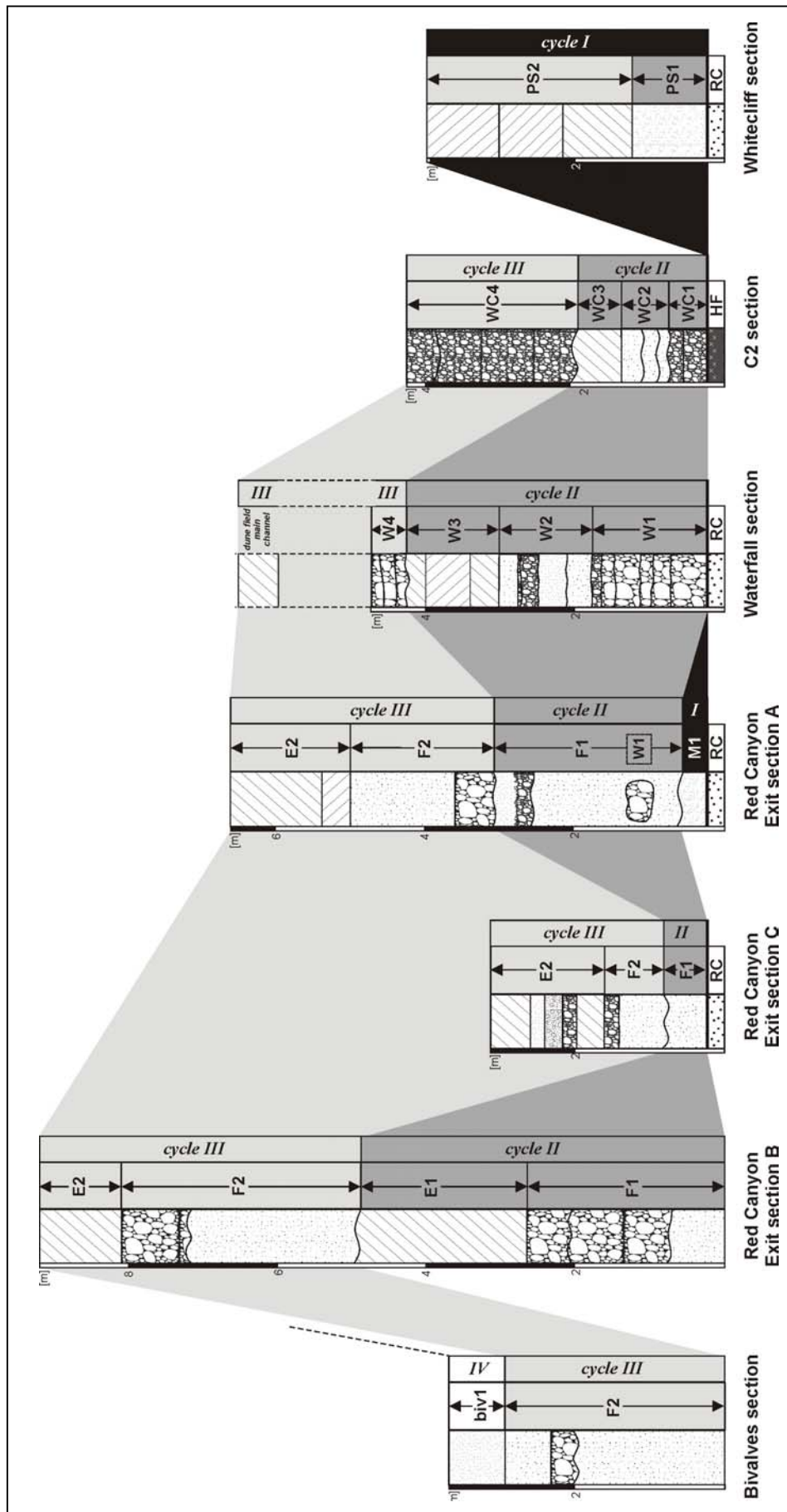


Fig. 5.32: Cyclo-stratigraphical correlation of the deposits of the Whitecliff Formation



#### 5.4.4 Age estimate for the Whitecliff Formation

So far only few age constraints are available for the deposits of the Whitecliff Formation. VAN ZYL & SCHEEPERS (1991) interpreted the sediments of the Whitecliff Fm. as equivalents of the Oswater Conglomerate Fm. (after WARD, 1987) from the Kuiseb River area for which an Early to Middle Pleistocene age has been suggested by WARD (1987). HÜSER et al. (1997) postulated a Pliocene age for the Whitecliff Fm. deposits. Both authors based their age estimations on climatic and morphostratigraphic considerations due to absence of suitable datable material.

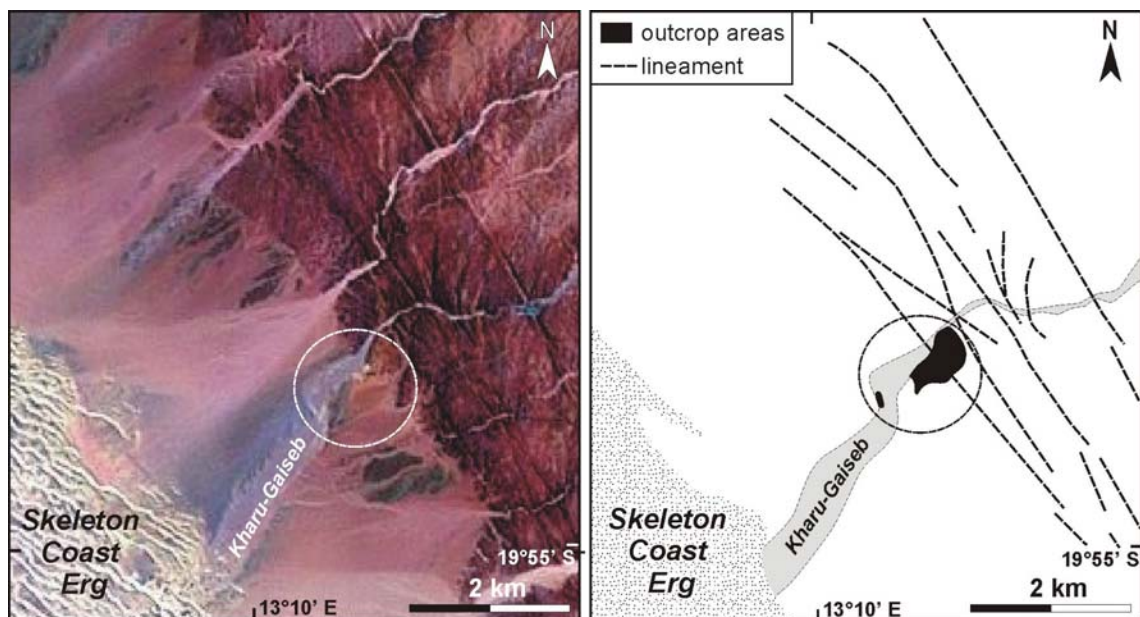
PICKFORD & SENUT (1999, Tab. IV-2) described the genetic relationships between ages and altitudes of palaeo-beach niveaus from south-western Africa. Late Pliocene beach complexes are associated with altitudes of around 30 m asl., whereas Pleistocene ones have altitudes of up to 8 m asl.. This is almost identical with the present day topographic heights of the two palaeo-seacliffs in the Uniabmond area. For the top of the so-called 'White Cliff' in channel C5c a height of about 25 m asl. was levelled out and the top of the so-called 'Bivalves Cliff' in channel C6 lies at 8,20 m asl.. Based on these analogue heights, the above mentioned ages seem transferable to the Whitecliff Fm. deposits in the Uniabmond area. Therefore, a Late Pliocene to Early Pleistocene age for the basal parts of the Whitecliff Fm. (cycle I) and a Middle Pleistocene age for the uppermost part (cycle 4) is postulated. Since raised beaches along the western coast of Southern Africa may not only reflect changes in sea-level but also the influence of post-breakup uplift, the age estimate has to be considered with caution (PICKFORD & SENUT, 1999; PARTRIDGE & MAUD, 2000; TYSON & PARTRIDGE, 2000). However, in comparison to the Eastcoast of southern Africa (uplift up to 1150 m; MAUD & BOTHA, 2000) uplift at the western coast is reported as being much lower (less than 30 m at Port Nolloth; MAUD & BOTHA, 2000). As there are no indications of pronounced local uplift in the Uniabmond area, the marine terraces and sea-cliffs are interpreted to be a result of predominantly sea-level changes.

Shells of the bivalve *Aulacomya* are so far the only body fossil finds in the whole sedimentary succession of the Whitecliff Fm. (unit biv1, Chapter 5.4.2.5). As *Aulacomya* occurs since the Miocene it can be concluded that the deposits of the Whitecliff Fm. are Miocene in age or younger. A better age estimate could be obtained from ESR (Electron-Spin-Resonance) dating on quartz grains and calcareous shell material (LAURENT et al., 1998; WODA, 2000) which is planned in future projects.

### 5.4.5 Red-beds and calcified sediments in the lower Kharu-Gaiseb River – equivalents of the Red Canyon and Whitecliff Formation?

About 1,5 km east of the Skeleton Coast Erg whitish to light red calcified and reddish sediments have been encountered within and next to the Kharu-Gaiseb River (see Fig. 5.33). These sediments overlie and truncate Palaeo-Proterozoic (Vaalian) basement rocks with a major unconformity (Fig. 5.34 A) and show a thickness of more than 25 m.

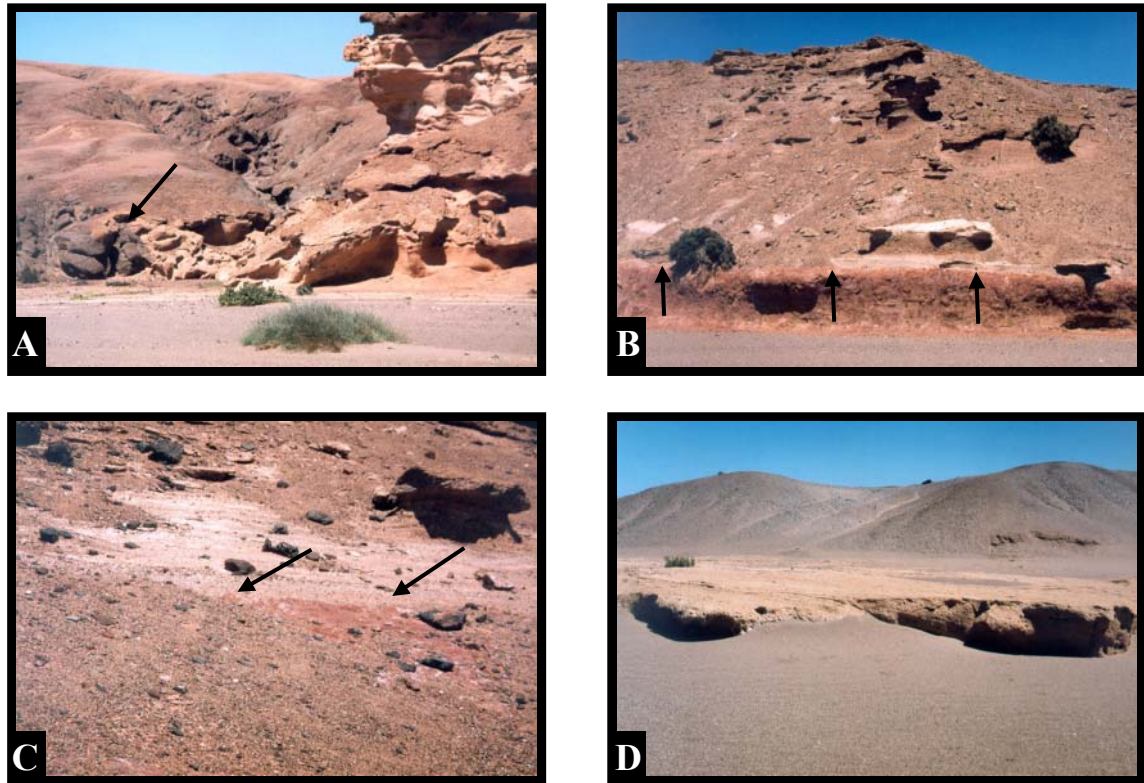
The lowermost part of the succession is composed of red, poorly sorted, massive coarse-grained sandstones with rootlets comparable to those in the Red Canyon Fm. (Fig. 5.34 B). Isolated deeply weathered Etendeka clasts occur within the sandstones, indicating a syn- to post-Etendeka age. These sediments are unconformably overlain by whitish to light red carbonate-cemented sandstones and conglomerates showing similarities with the fluvial parts of the Whitecliff Formation (Fig. 5.34 B, C). Further downstream a small exposure of calcified aeolian dune deposits show similarities with aeolian sediments of the Whitecliff Fm. (Fig. 5.34 D). Regarding clast and matrix composition the sediments differ from those of the Uniabmond area in their higher content of basement clasts. It is suggested that the deposits exposed at the Kharu-Gaiseb are comparable to the sediments of the Red Canyon and the Whitecliff Fm. in the Uniabmond area.



**Fig. 5.33:** Locality map of the outcrop area (circle) of the red-beds in the lower Kharu-Gaiseb River (left: Landsat TM-5 subset 181-074, 7-5-3, 30.03.1995; right: simplified structural interpretation map with lineaments as dotted black lines)

WARD & MARTIN (1987) also reported of a rudaceous terrestrial conglomerate, exposed only a few kilometres upstream from the present termination of the Kharu-Gaiseb River at

the eastern margin of the Skeleton Coast Erg about 20 km NE of Terrace Bay. They termed these sediments 'Kharu-Gaiseb Conglomerate' and described it as a clast-supported, almost unsorted conglomerate of about 500 m thickness. These deposits should not be mixed up with the above described sediments.



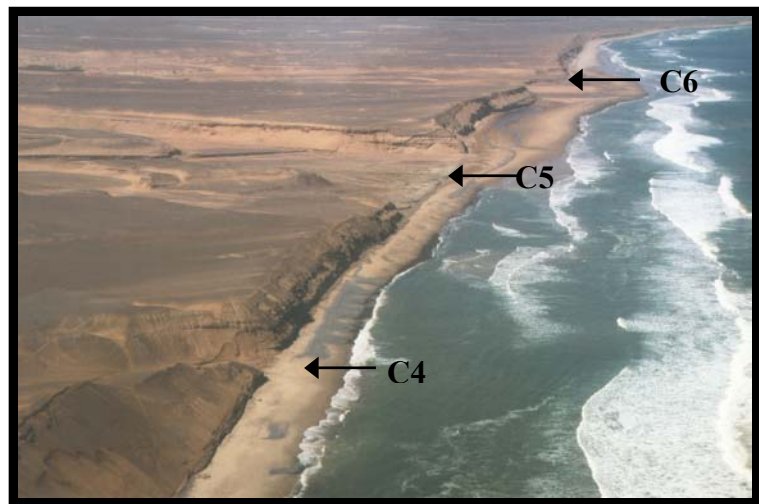
**Fig. 5.34:** **A:** Carbonate-cemented white to light red sediments truncating and overlying Palaeo-Proterozoic basement rocks; arrow indicates contact between basement rocks and overlying sediments. **B/C:** Contact between red (possible Red Canyon Fm. equivalent) to carbonate-cemented (possible Whitecliff Fm. equivalent) sediments indicated by arrows. **D:** Carbonate-cemented dune deposits exposed in the modern day river channel of the Kharu-Gaiseb (south-westernmost outcrop indicated in Fig. 5.33).

### 5.5 Uniabmond Formation

The Uniabmond Formation represents a unit of semi- to unconsolidated sediments, which overlie the Whitecliff Fm. with a major unconformity. This lithostratigraphic unit is composed of gravels, sands and muds. The term ‘Uniabmond Formation’ was introduced by ZELLER (2000) and is named after its occurrence in the Uniabmond area.

The up to 35 m thick succession of the Uniabmond Fm. displays a wide variety of continental and marine facies and are characterized by drastic vertical and lateral facies changes. Many of the facies are comparable to those of the Whitecliff Formation. The difference between these two formations is their contrasting degree of cementation. The Whitecliff Fm. is intensively carbonate-cemented, whereas the sediments of the Uniabmond Fm. are much less carbonate-cemented.

The major outcrops of the Uniabmond Fm. are situated along an 18 km long impressive seacliff which rises continuously from south of Torra Bay to its central part, where the river mouths of the three main channels (C4, C5, C6; Fig. 5.35) are located, and then declines gradually to the north until it merges with the beach about 19 km south of

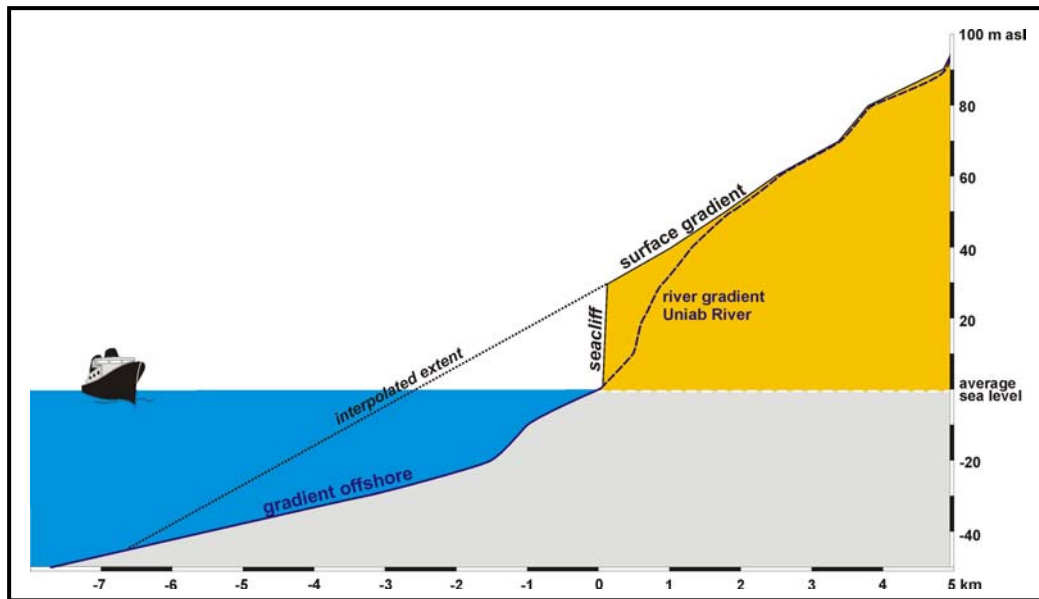


**Fig. 5.35:** Oblique view towards S showing the outcrop area of the Uniabmond Fm. between channels C4 and C6. All three channels are active during major floods. Distance between channels C4 and C5 is about 500 m.

Terrace Bay. This also represents approximately the N-S extent of the Uniabmond Formation. Towards the E its sediments can be traced along the modern day Uniab River far upstream beyond the Skeleton Coast Erg. Towards the W outcrops are terminated by the Atlantic Ocean. In addition, the outcrops at the seacliff and also the sidewalls of the incised channels provide good exposures.

Major parts of the Uniabmond Fm. build up the Uniab Fan (see Chapter 5.5.4) whose deposits extend farther west of the present day coastline into areas below sea level (SCHEEPERS & RUST, 1999; KRAPP et al., 2002). Interpolation of the surface gradient shows that the whole sedimentary body could have had an extent of 6 to 7 km offshore the present coastline (see Fig. 5.36). Further inland, sediments of the Uniabmond Fm. form the modern day land surface in most parts of the Uniabmond area most of which represents terrace and deflation surfaces.





**Fig. 5.36:** Diagram showing the interpolation of the surface gradient estimating its original seaward extent (compiled from Topographic map 1:50.000, sheet 2013AA Uniabmond and SAN 103, 1:150.000, Hydrographic Office, South African Navy).

The Uniabmond Fm. was previously described by WARD (1987), VAN ZYL & SCHEEPERS (1991, 1992), HÜSER et al. (1997), SCHEEPERS & RUST (1999), BLÜMEL et al. (2000), KRAPF (2000), ZELLER (2000) and KRAPF et al. (2002).

WARD (1987) reported cross-bedded coastal dune sands, mud lenses, sands and gravels from the lower and middle parts of the Uniab seacliff and correlated these deposits with the Awa-gamteb Muds in the Kuiseb River, Central Namib Desert. There, the Awa-gamteb Muds comprise unconsolidated fine-grained deposits consisting of clay, silt and intercalated sand layers and are interpreted to represent distal, coastal equivalents of the Homeb Silt Fm. (WARD, 1987). For the Awa-gamteb Muds a Late Pleistocene age is estimated based on lithostratigraphic correlation and artefact findings (WARD, 1987). Uncemented gravels from the uppermost part of the Uniab seacliff-succession were correlated by WARD (1987) with the Gobabeb Gravel Formation, which is supposed to be of Late-End Pleistocene age. HÜSER et al. (1997) termed the deposits of the Uniabmond Fm. 'Uniabkonglomerat' and BLÜMEL et al. (2000) described them as layers of coarse-grained basalt clasts, which are interbedded with cross-bedded sandy layers of varying thickness. Intercalated aeolian sands and muddy layers with sand-filled desiccation cracks occur. BLÜMEL et al. (2000) postulate an semi-arid to arid climate during the deposition of the 'Uniabkonglomerat'. SCHEEPERS & RUST (1999) were the first who giving a detailed description of the un- to semi-consolidated sediments of the Uniabmond area. They did not name the deposits and referred to them as 'unconsolidated alluvial gravel fan deposits'



(SCHEEPERS & RUST, 1999). The deposits were described as unconsolidated sands and pebble- to boulder-sized gravels, with interbeds of erosively based lenses, lenticular, massive to faintly bedded pebble beds with rare cobbles, and mud-cracked silt layers forming thin blanket-like drapes. The lateral persistence of single bed sets varies from a few meters up to 150 m and the thickness varies between a few cm and 4 m. The sediments show typical coarsening-up and fining-up cycles and a complex interfingering between gravels and sands. SCHEEPERS & RUST (1999) interpreted these sediments as deposits of an alluvial gravel fan, whereas the modern day fan was regarded as an erosional remnant of a previous larger one (see Fig. 5.36). This larger fan may have been largely removed by marine erosion (SCHEEPERS & RUST, 1999).

### **5.5.1 Facies of the Uniabmond Formation**

The Uniabmond Fm. displays a wide variety of fluvial, aeolian and marine facies. The description of the various facies derives from outcrop-logging along the seacliff (mainly between channel C2 and C7) and from logging of the sidewalls of the incised valleys of channel C4, C5 and C6.

#### **5.5.1.1 Fluvial facies**

##### **Massive, matrix-supported gravels (GmS)**

This facies consists of massive, matrix-supported, very poorly sorted, granule to boulder-sized gravels which are mainly composed of subangular to well-rounded clasts of quartz latites and minor subangular to subrounded basalt and basement clasts. Also subangular to well-rounded “soft” clasts of reworked Uniabmond Fm. sediments are common. They are composed of up to metre-sized mud and sand clasts and boulders. The matrix of facies GmS consists of poorly sorted, medium- to coarse-grained sand. In places the matrix content decreases and the gravels develop more clast-supported fabrics but still remain very poorly sorted.

The thickness of such deposits varies from 0,5 up to 2 m and lower contacts show sharp but non-erosional bases (see Fig. 5.37 A).

Due to the lack of bedding and the very poor sorting these gravels are interpreted as deposits of cohesive debris-flows marking the peak of a catastrophic flooding event. However, this facies is only exceptionally preserved in the Uniabmond Fm. because such

deposits are easily winnowed and reworked during decreasing flood intensity when more regular flow conditions prevail in the channels.

### **Massive clast-supported gravels (Gm)**

This facies consists of massive to very crudely bedded, clast-supported, poorly sorted gravels with pronounced erosional bases. Components are predominantly subangular to rounded cobble-sized Etendeka quartz latite clasts. Maximum clast size can reach up to 60 cm in diameter. Minor components are subrounded to rounded Etendeka basalt clasts, subangular to subrounded basement clasts and some reworked clasts of the Whitecliff and Red Canyon Formations. Single coarse-grained, poorly sorted thin sand lenses are interbedded in the gravels at a few places. These gravels often fill conspicuous, deeply incised, U-shaped (gutter/gully-like) channels with a very low width/depth ratio (w/d-ratio: 3,35; see Fig. 5.37 B). The lateral extent of such incised channels varies between 1 to 20 m rectangular to flow with 0,3 and 3,5 m incision. In places, this facies also appears at bases of large channels, sometimes with large flutes, filled with very coarse gravels. There, they grade upwards into crudely plane-bedded gravels (facies Gh) and alternating layers of gravels and sand (facies GS) forming an overall fining upward sequence with several meters thickness (Fig. 5.37 C). This facies is quite frequently encountered at exposures along the seacliff introduced above. Due to the above described characteristics lithofacies Gm can be interpreted as longitudinal gravel bar deposits.

### **Large-scale cross-bedded gravels (Glc)**

At one outcrop between the channel mouths of C4 and C5 large-scale cross-bedded gravels have been observed at the base of the seacliff. There, large, clearly discernible planar foresets, confined to one single layer, have been modeled out by the action of breaking waves (Fig. 5.37 D). The foresets are dipping towards SSE with angles of about 30° (160/30, 155/25, 165/32, 140/30). The tabular cross-bedded gravel deposit has a thickness of c. 2 m and individual foresets have a length of about 3 m. The pebble- to boulder-sized gravels are poorly to moderately sorted and are composed of subangular to subrounded quartz latites and minor Etendeka basalt and basement clasts with maximum clast sizes of about 75 cm. The cross-bedded gravels are gradually overlain by massive (facies Gm) or plane-bedded gravels (facies Gh), which in turn grade upward into alternating sand and gravel layers of facies GS (Fig. 5.37 E).

Since this facies is composed of one single foreset layer these large foresets are interpreted as lateral accretion surfaces oriented parallel to the flow direction. As mentioned above this facies type was only observed at one locality.

### **Horizontal-bedded gravels (Gh)**

Horizontal-bedded, clast-supported, granule- to boulder-sized, poorly to moderately sorted gravels form a very common facies of the Uniabmond Fm. (Fig. 5.37 F). The gravels show a similar composition to facies Gms and are dominated by sub-rounded to rounded Etendeka quartz latite clasts, up to 40 cm in diameter. Minor components are sub-rounded to rounded Etendeka basalts and sub-angular to sub-rounded basement clasts. Reworked mud clasts and clasts of the Whitecliff and Red Canyon Fms. are rather rare. The gravel sets, sometimes intercalated with thin medium- to coarse-grained sandy layers, show tabular to slightly trough-shaped geometries with well defined erosional bases. Thickness of this facies varies between 0,2 to 4,5 m. In comparison to facies Gm, the channels, in which these gravels have been deposited, show markedly higher width/depth ratios. They can reach lateral extents up to about 100 m with 0,1 - 2 m incision (Fig. 5.37 G). These sediments are interpreted as deposits of wide shallow channels of a braided fluvial system.

### **Gravel-sand alternations (GS)**

Layers of horizontal- to low-angle cross-bedded gravel-sand alternations are a frequently observed facies of the Uniabmond Formation. Each of these alternations represents a fining-upward cycle starting with clast-supported, granule- to cobble-sized gravels grading upward into weakly horizontal bedded, poorly to moderately sorted, medium- to coarse-grained sands (Fig. 5.37 H). The gravels are mainly composed of sub-angular to rounded Etendeka quartz latites with a maximum clast size of 25 cm. Minor components are sub-rounded to rounded Etendeka basalts, sub-angular to subrounded basement clasts and rarely reworked clasts of the Whitecliff and Red Canyon Formations. The matrix is composed of medium- to coarse grained sand. The arenaceous parts of the alternations are mainly composed of angular to rounded quartz grains. Accessory constituents are lithic fragments of Etendeka volcanics and basement rocks as well as heavy mineral grains and rare shell fragments.

The succession varies in thickness between 10 and 90 cm and can be traced laterally for several tens of meters along the outcrops exposed in the seacliff. These alternations form the infills of not very well confined channels with a very high width/depth ratio and are interpreted to represent multi-storey stacked channels. The tabular architecture and the lack

of pronounced erosion surfaces within this facies shows the pronounced aggradational character of these sediments.

This facies interfingers laterally with massive to weakly plane-laminated sands (facies Sm) as well as plane-bedded, clast-supported gravels of facies Gh.

#### **Low-angle trough cross-bedded gravels (Gt)**

This facies is build up by low-angle trough cross-bedded, moderately sorted gravels forming laterally amalgamated shallow channel deposits (Fig. 5.37 I). These gravels are composed of sub- to well-rounded quartz latites and minor Etendeka basalt clasts with maximum clast sizes varying between 2-10 cm. Individual channel fills show widths of a few meters and depths of less than 50 cm. The thickness of these gravels reach rarely more than 1,5 m. Such deposits have been observed only in a few outcrops of the Uniabmond Formation. It is suggested that these channel fills have been deposited in small gullies that formed either during minor discharge events (e.g. local rainfalls) or during the waning stages of a flood event.

#### **Medium-scale cross-bedded sands and gravels (GSc)**

The characteristic feature of this facies are medium-scale, steeply inclined tabular cross-beds with planar forsets. Compositionally this facies is formed by poorly to moderately sorted, coarse-grained sands and granule- to cobble-sized gravels. The clast composition is comparable to other described facies mainly composed of Etendeka quartz latites. This facies has only been observed at a few places at the seacliff. Fig. 5.37 J shows this facies as part of a channel fill with an asymmetrical architecture. At one channel margin a pronounced cutbank is preserved and the channel fill at this side is gravel-dominated and shows steeply inclined cross-beds. Within the channel this facies grades laterally into more sandy gravels with decreasingly inclined cross-beds. Finally it grades into plane-bedded sands and gravels of facies Gh and GS. The thickness of the sediments of this facies is about 1 m and their lateral extent about 4 m.

Due to the above described characteristic facies GSc most probably represents lateral accretion surfaces.

#### **Surge-like sands and gravels (GSh)**

Horizontal bedded, moderately sorted, coarse-grained sands and granule- to pebble-sized gravels with convex upward bedforms onlap and drape the underlying morphology. Fig. 5.37 K shows the type-example of this facies which was only observed at a single locality

in the seacliff between C7 and C8. The surge-like appearance of this facies points to deposition under upper flow regime conditions.

### **Massive sands (Sm)**

This facies is composed of massive, moderately to well sorted, medium-grained sands. Several meter thick sand successions, laterally traceable for several tens of meters, can be internally subdivided by bounding surfaces in structureless beds of 0.5 to a few meters thickness (Fig. 5.37 N). The base of individual beds is slightly undulating but not markedly erosive (see Figs. 5.37 N+P). Abundant cm-sized mud pebbles are more or less irregularly distributed within these sands strongly emphasizing the structureless fabric of these sediments (Fig. 5.37 O). In some places this facies grades upward over a transitional facies with diffuse lamination into parallel-laminated sands (Fig. 5.37 N). Again, this facies is quite frequently observed in the Uniabmond Formation.

The absence of cross-bedding and other sedimentary structures in the sands between bounding surfaces point to 'en-masse' deposition of individual units. Grain size analyses show a narrow range for grain-size means and standard deviations indicating a well sorted, medium-grained, lithological homogeneous source for these sediments (see Tab.5.3). Therefore, it is suggested that these sediments originate from cohesive, sandy debris flows (JONES & BLAKEY, 1997), mass wasting (LOOPE et al., 1995), or sediment-gravity flows (BENAN & KOCUREK, 2000). They represent reworked aeolian dune sands deposited as mass flows or hyperconcentrated flows (SVENDSEN et al., in press). In comparison to aeolian dune sands, which normally have an average silt/clay content of about 0.1 to 0.2 wt % in the Skeleton Coast area, these sediments show a slightly higher average silt/clay-content of about 0.75 wt % (see Tab. 5.3). Such mud-enrichment is a very important factor for generating mass or hyperconcentrated flows because the presence of clay between the sand grains reduces shear strengths within the flow. Another important factor is the clay type, which is smectite in the case of the Uniabmond Formation. Smectite is abundantly available in the Uniab catchment due to weathering of the basaltic and andesitic lavas and significantly increases the strength of a flow (SVENDSEN et al., in press).

### **Horizontally-bedded sands (Sh)**

This facies is quite common in the Uniabmond Fm. and is composed of horizontal-bedded, moderately to well sorted, medium- to coarse-grained sands (Fig. 5.37 L). In some places also low-angle cross-bedding is developed (Fig. 5.37 M). Gentle undulation with low-angle

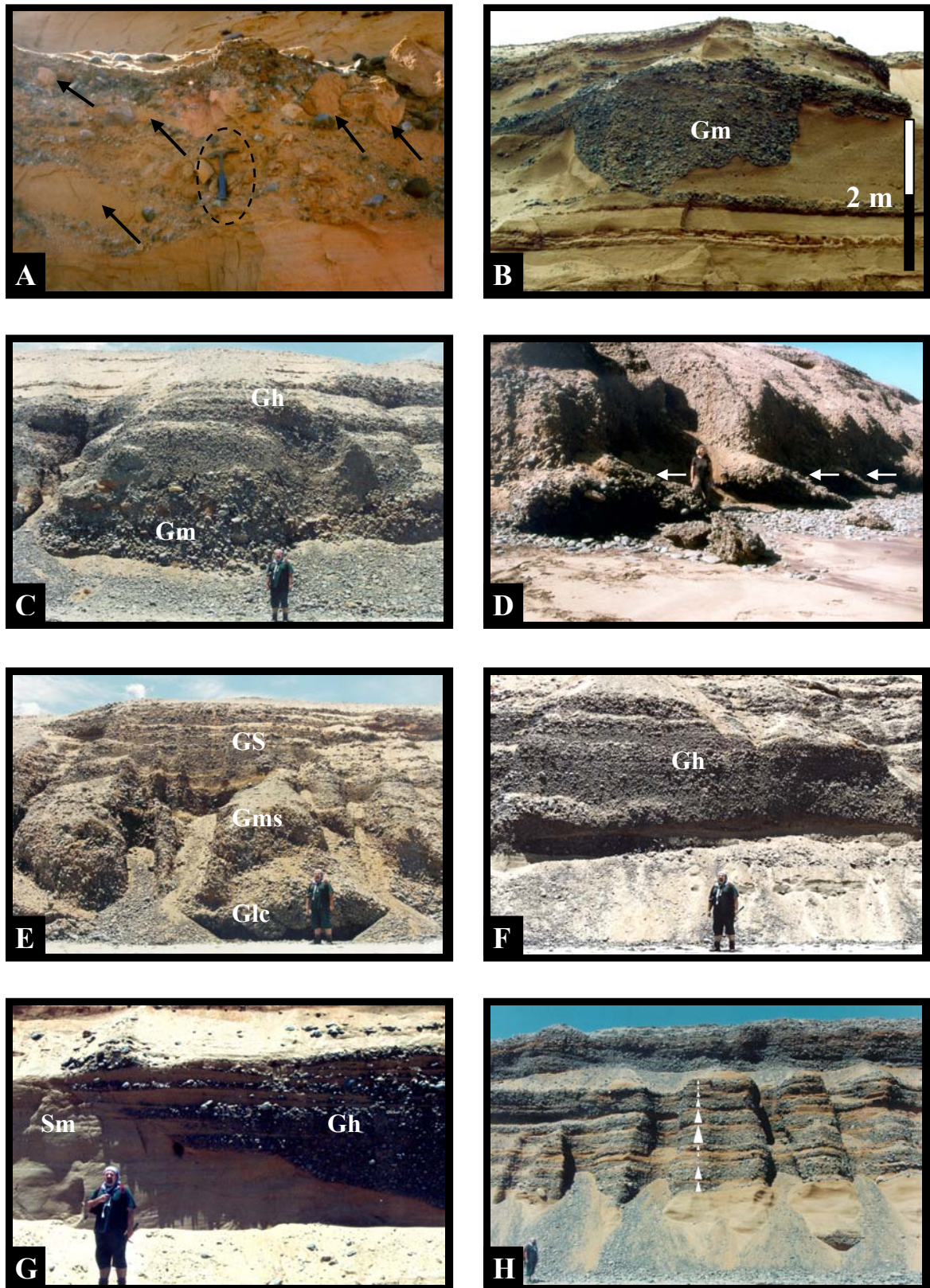


truncation of heavy mineral laminae are frequently observed. Single beds, often representing large scale troughs with a wavy base, vary in thickness between 1 and 10 cm. This facies forms successions of up to several meters thickness. Within these sand dominated successions often cm to dm thick, isolated, lens-like gravel layers occur, whereby the origin of the clasts can be intra- or extrabasinal. Extrabasinal clasts are mainly composed of Etendeka quartz latites whereas intrabasinal clasts are made up of reworked blocks and flakes of muds. Small carbonate nodules, 0,5-1,5 cm in size, are widely distributed within this facies. In addition, also calcified rootlets are frequently observed. Horizontal bedding, sorting and grain size of these sands point to a deposition in the upper flow regime. Therefore, facies Sh can be interpreted as the product of upper stage plane bed transport.

### **Laminated muds (Fm)**

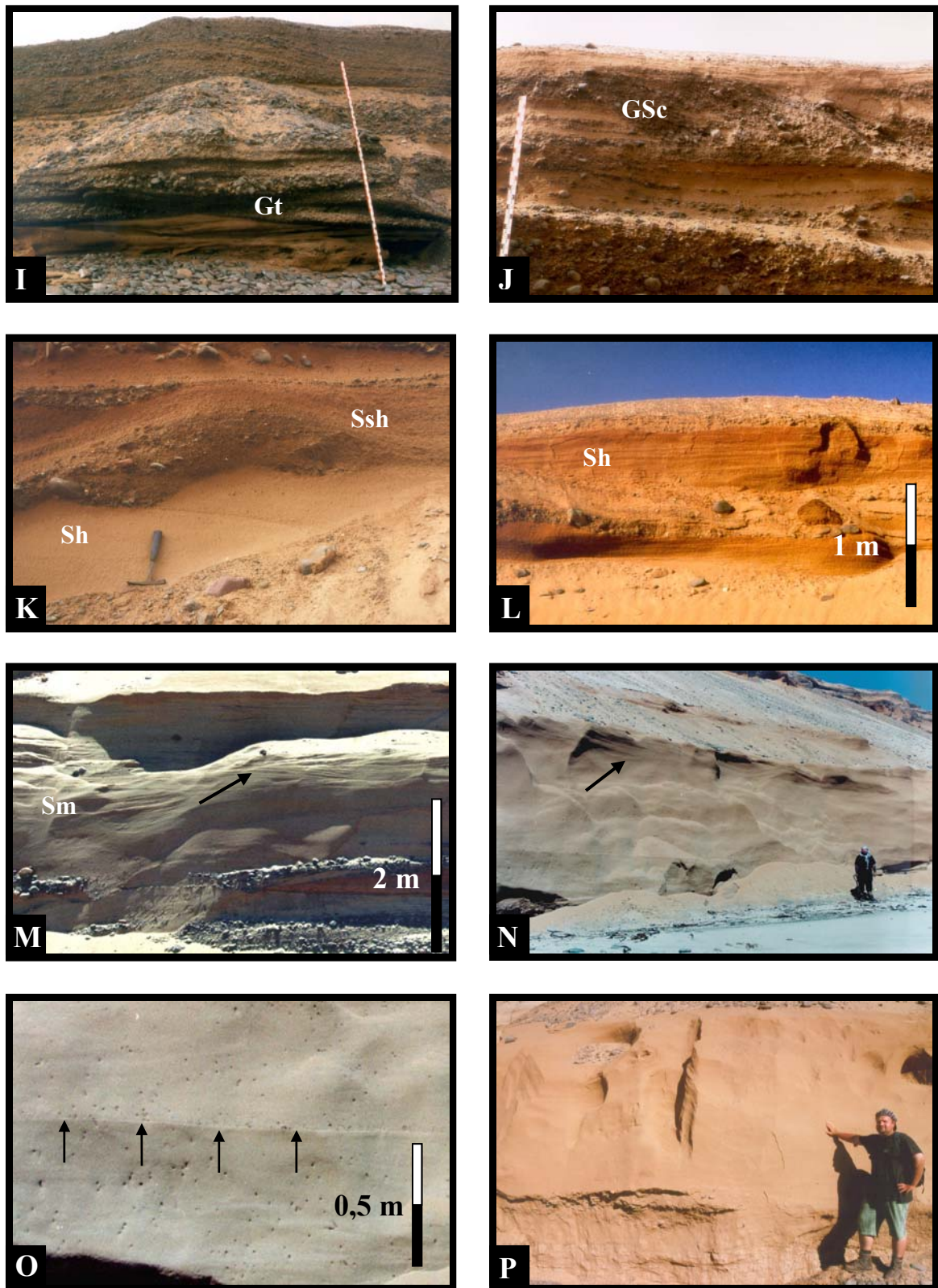
Light to dark brown beds of stacked, massive to fine laminated silt and clay layers each up to 50 cm thick form a considerable part of the sedimentary succession of the Uniab seacliff at one locality between channel mouth C3 and C4 (Fig. 5.37 Q). There, they form a mud-dominated succession of about 6 m cumulative thickness. Furthermore, isolated mud layers are irregularly intercalated and preserved in the outcrop area of the Uniabmond Formation (Fig. 5.37 R). These sediments display sharp bases draping underlying sediment morphologies. The mud beds vary in thickness between 5 and 50 cm and are laterally traceable for several tens of meters. They show frequently desiccation cracks, which are mainly filled with fine- to medium-grained, well sorted sand (Fig. 5.37 S) composed mainly of well-rounded quartz grains and heavy minerals (garnet and magnetite) showing aeolian grain characteristics. In places, some of them are also filled with clast-supported gravels (Fig. 5.37 T). Due to desiccation the mud layers are often bent up showing tepee-like structures (Fig. 5.37 U). Mud curls often occur and are preserved by overlying aeolian sand that is abundantly deposited after flood events (LÖFFLER & PORADA, 1998). Other thin isolated mud layers up to 20 cm thick are overlying cross-bedded sandstones of facies ScE with a sharp basal contact (Fig. 5.37 V). They drape the underlying topographies and pinch out against larger dune forms. These muds are also laminated.

The initially described thick stacked mud succession is interpreted to represent deposits of a frequently flooded pond in an overbank setting. The isolated mud layers within fluvial sediments represent intra-channel waning flow suspension fallout deposits.

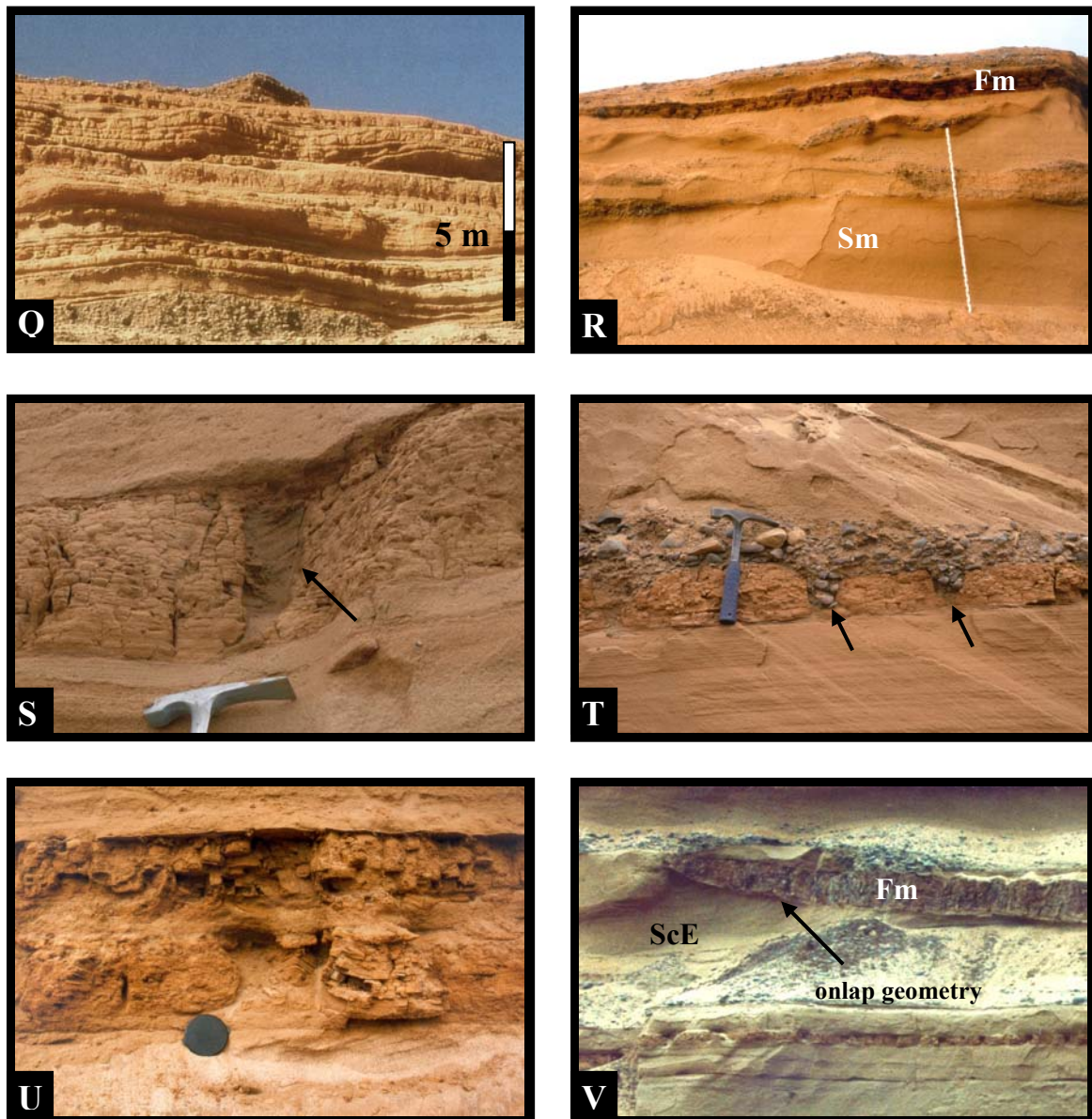


**Fig. 5.37 A-H:** Photographs showing the different facies of the Uniabmond Formation. **A:** Typical appearance of facies Gms with up to boulder-sized intraclasts (indicated by arrows) of reworked Uniabmond Fm. sediments. **B:** Photograph showing facies Gm filling a deeply incised, U-shaped channel. **C:** Common upward transition from facies Gm into facies Gh. **D:** Single layer of large foresets (indicated by white arrows) of facies Glc dipping towards SSE. **E:** Facies association Glc-Gms-GS. **F:** Plane-bedded gravel layers of facies Gh are quite common in the Uniab Formation. **G:** Photograph showing lateral transition of facies Gh into facies Sm. **H:** Typical appearance of facies GS showing multiple fining-upward cycles.





**Fig. 5.37 I-P:** Photographs showing the different facies of the Uniabmond Formation. **I:** Facies Gt is characterized by low-angle trough cross-beds which are exposed in the seacliff between C7 and C8. **J:** Planar foresets of facies GSc. **K:** Photo showing surge-like deposits of facies GSh onlapping and draping the underlying morphology. **L+M:** Horizontal to low-angle cross-bedded sands of facies SH. Arrow in M indicates low-angle rejuvenation surfaces. **N:** Massive sand deposits of facies Sm grades over a transitional facies with diffuse lamination into laminated sands (arrow). **O:** Detailed view of picture 5.36 N showing an internal bounding surface (arrows) and irregularly distributed cm-sized holes representing former mud pebbles which are removed by weathering. **P:** Photograph of facies Sm showing the lack of structures of these sands.



**Fig. 5.37 Q-V:** Photographs showing the different facies of the Uniabmond Formation. **Q:** Succession of stacked silt and mud layers of facies Fm representing deposits of a frequently flooded pond. **R:** Photo showing a single, isolated, dark brown mud layer of facies Fm in a seacliff outcrop between C7 and C8. **S:** Desiccation cracks filled with cross-bedded aeolian sands. **T:** Desiccation cracks in facies Fm filled with clast-supported gravels. **U:** Due to desiccation the mud layers are often bent up showing a tepee-like structure (lens cap for scale). **V:** Onlap geometry of a single mud layer draping the lower part of an aeolian dune avalanche face.

### 5.5.1.2 Aeolian facies

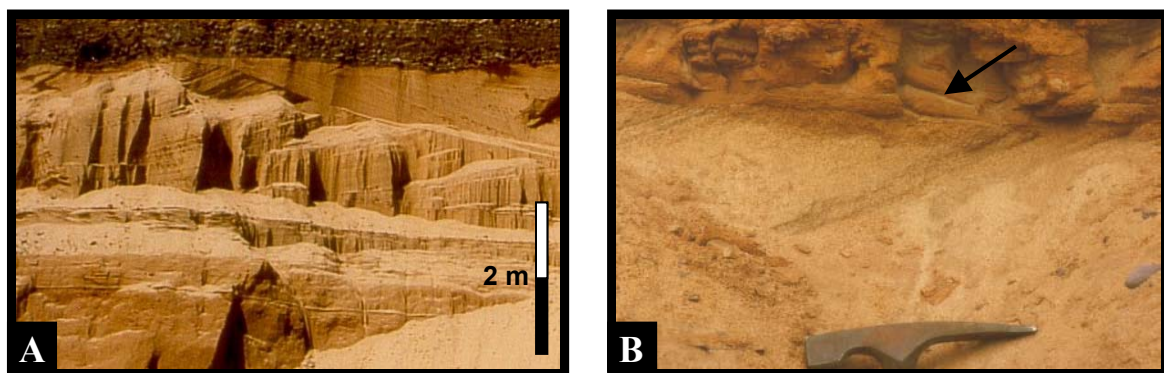
#### Large-scale cross-bedded sands (ScE)

Large-scale cross-bedded, fine- to coarse-grained, well sorted, mature quartz sands are commonly found in the upper third of the Uniab seacliff exposures and along the sidewalls of channel C4 and C5. They have a thickness of up to 4 m. The aeolian succession shows tabular to bowl-shaped, steeply inclined foresets. Abundant internal subhorizontal bounded surfaces can be observed (Fig. 5.38 A), which is very characteristic for aeolian dunes.



Alternating layers are composed of thin heavy mineral-rich laminae and thicker, medium- to coarse-grained sand layers with a high percentage of lithic grains that are mainly composed of quartz latites of the Etendeka Group. In some places the medium- to coarse-grained sand layers show reverse grain-size grading. This reflects avalanche face accretion by grain flow (FRYBERGER, 1993). However, normal graded coarse-grained layers recording a decrease in wind velocity are also common. The sands are texturally and compositionally mature and consist mainly of well-rounded quartz grains. Semi-angular shell fragments with sizes up to 2 mm are quite common. Slump structures caused by sand grain avalanches are rare but have been observed in one outcrop on the northern cutbank of channel C4 about 150 m east of the beach. Multi-polar dip-directions of the foresets indicate dune forms with curve crests or compound dune morphologies with local deviations from the overall wind regime characteristic for a coastal dune settings (cf. GOLDSMITH, 1978; ILLENBEGER & RUST, 1988). This documents a well established dunefield with continuous sand supply. At some localities the basal parts of these predominantly light-coloured sediments show an intensive orange coloration, which indicates an incipient soil development due to a rise in groundwater table.

Large-scale cross bedding, the high textural and compositional maturity, the wide range of foreset dip directions, the occurrence of coarse-grained ‘caviar’ layers and particularly the near absence of clay point to a coastal barchanoid dune origin for these sediments. Coastal dune development is favoured where sufficient sand supply and dominant strong onshore winds are present (REINECK & SINGH, 1986).



**Fig. 5.38:** **A:** Examples of facies AS exposed in the southern bank of the channel mouth of C5. **B:** Detailed photograph of facies AS overlain by muds of facies IM. Note the rolled up desiccated mud flakes (arrow).

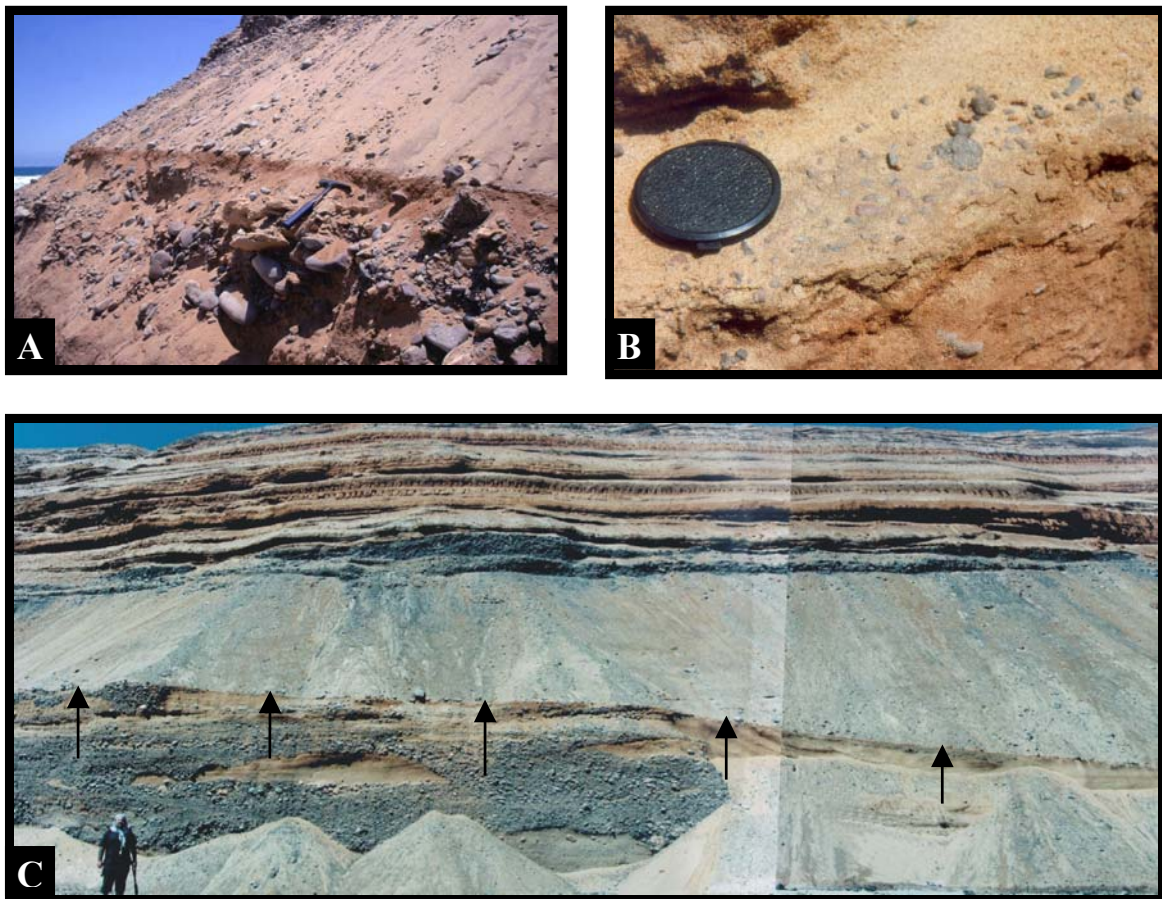
Furthermore, thin layers within the Uniabmond Fm. show the same lithological and compositional characteristics as facies ScE. In contrast to facies ScE the foresets are more closely spaced and show a more uniform dip direction. Thicknesses rarely reach more than 70 cm. Often they are closely associated with abandoned channel muds (facies Fm) where



they also fill desiccation cracks (see Fig. 5.38 B). In a few places these aeolian sands overlie a deflation surface (see below).

### Deflation surfaces and palaeo-soils

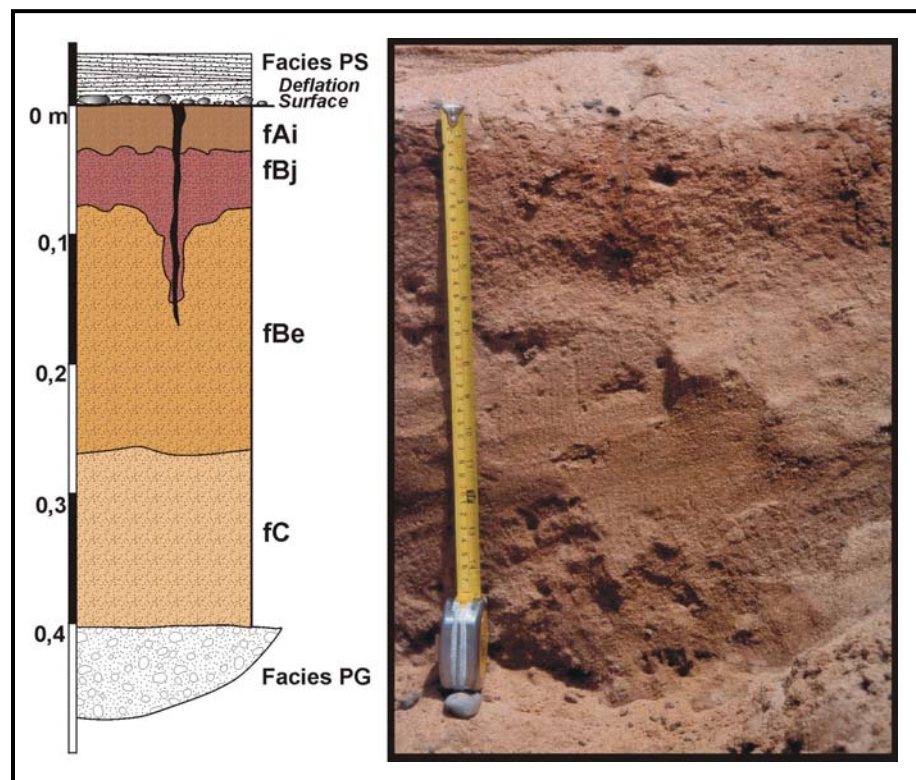
At the base of facies Slc but also at the base of various fluvial facies a conspicuous, thin, often resistant, brownish horizon is traceable in some parts of the seaciff over distances between 20 and 300 m (Fig. 5.39 A+C). Closer inspection reveals that on the planar to slightly inclined top of such a horizon a sharp-based single clast layer has developed (Fig. 5.39 B). The thickness of such a single clast layer corresponds to the average clasts diameter (~1.5 cm). The platy-shaped clasts are mainly composed of angular to subangular Etendeka quartz latites (Fig. 5.39 B). Within these layers clasts and sandgrains are often coated and cemented by limonite.



**Fig. 5.39:** **A:** Example of a deflation surface underlain by a palaeo-soil on the northern bank of channel C4 about 50 m east of the beach (hammer for scale). **B:** Plan view of the excavated deflation surface of Fig. 5.38 A showing the clast rich top (lens cap for scale). **C:** Showing the lateral persistence of a major deflation surface. Note the surface palaeo-topography representing an older land surface.

Directly below this single clast layer often a brownish, about 3 cm thick, fine-grained sandy horizon has developed showing typical indications of an initial fAi-soil horizon containing about 10% loam and is low in organic components. It grades downward into a reddish, 6-10 cm thick, rubified, fersialitic weathered, medium- to coarse-grained layer which can be interpreted as a fBj-horizon. The quartz grains are slightly weathered and in some places coated by iron-oxide. Below this horizon a light brownish, up to 20 cm thick, groundwater bleached, elluvial fBe horizon has developed. Finally, a poor to moderately sorted, medium-grained regic sand represents the fC horizon. The whole described succession represents a palaeo-soil, which can be classified after the FAO as a fossil rhodichromic arenosol (FAO, 1988). A representative profile of such a palaeo-soil has been logged in detail in an outcrop on the northern cutbank of channel C4 about 70 m east of the beach (see Fig. 5.40). Due to a higher clay content and the cementation by limonite and carbonate such palaeo-soils show higher resistance in comparison with the under- and overlying sediments.

**Fig. 5.40:** Detailed profile of the palaeo-soil on the northern bank of channel C4 about 50 m east of the present beach-line. Explanation of soil-codes see text.



Combined with the observation that such horizons are sometimes overlain by aeolian sediments, associated single clasts layers are interpreted as deflation surfaces, which developed by the removal of the fine-grained fraction through aeolian winnowing. The incipient soil development below the deflation surfaces suggests that they represent surfaces of a long time of non-deposition and non-erosion with sediment bypass as the

main acting process. Such features are interpreted as palaeo-land surfaces and single deflation surfaces, which can be traced along the seacliff over long distances thus forming important time markers within the stratigraphic framework (Fig. 5.39 C).

### **5.5.1.3 Marine facies**

Outcrops of marine deposits are rare and were observed exclusively in the lowermost parts of the seacliff. Most of them are only temporarily exposed due to changing beach morphology, erosive activity of breakers and scree cover. Small outcrops have been found between channel mouth C4 and C5 (Fig. 5.41 A) and between channel mouth C5 and C6. The marine deposits are all overlain by a major erosion surface, which often cuts below the base of the present seacliff.

#### **Bioturbated horizontal-bedded sands (ShM)**

Horizontal-bedded, moderately to well sorted, medium- to fine-grained bioturbated sands can be found in the lowermost part of the seacliff between C4 and C5. Lamination is formed by abundant opaque heavy mineral layers and is often disturbed by bioturbation. Characteristic for this facies is the occurrence of vertical to sub-vertical burrows with diameters between 1.5 and 3.5 cm and lengths between 15 and 25 cm. The burrows are concentrated in a layer, about 30-40 cm thick, and are filled with heavy mineral rich (mainly garnet and magnetite) medium- to fine-grained sand (Fig. 5.41 B). Because of the poor consolidation of the sediment, no observations could be made on the inner and outer wall structure of the burrows. The burrows point to a domichnium of crustaceans, typical for a high energy marine environment (cf. CRIMES, 1975).

Layers of horizontally orientated beach cobbles mainly consisting of Etendeka quartz latites of sizes up to 27 cm are interbedded with these sands.

Bedding and bioturbation indicate a marine origin of these sediments in an upper shoreface environment (cf. READING & COLLINSON, 1996; REINECK & SINGH, 1986).

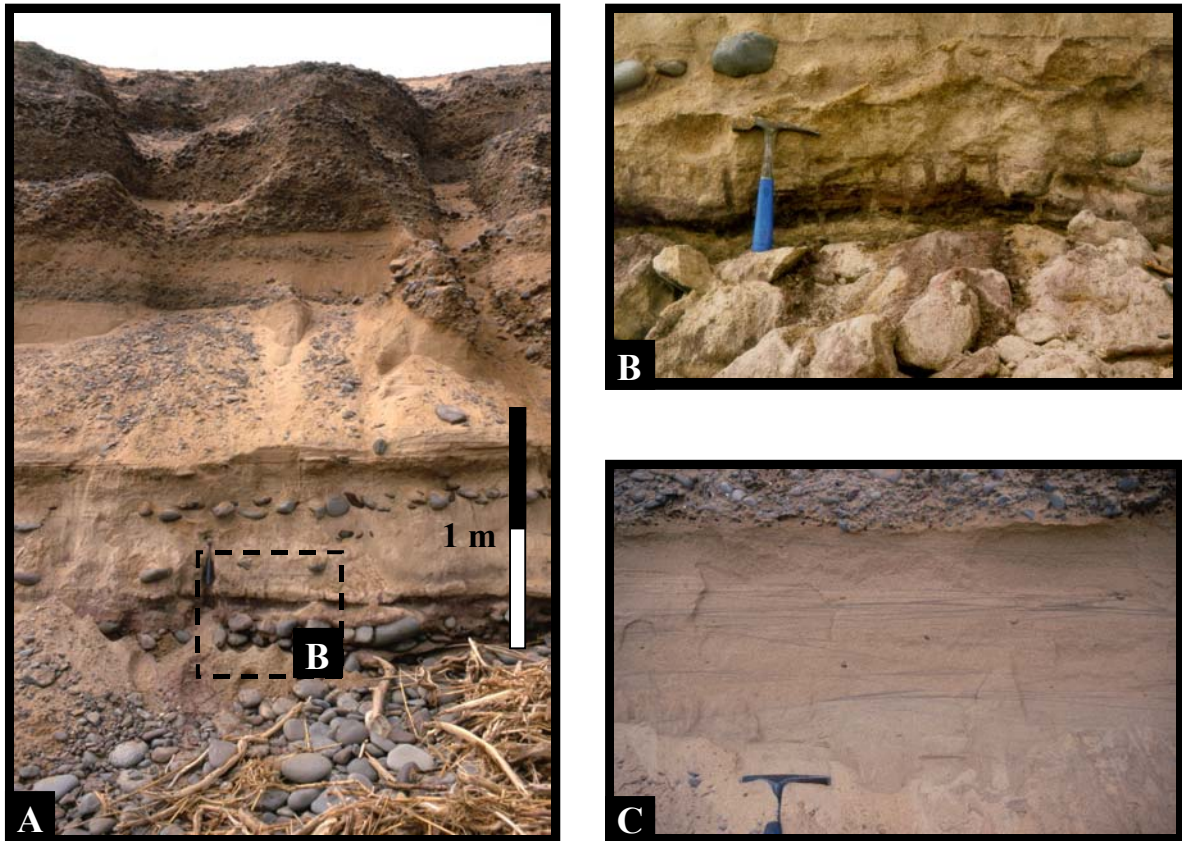
#### **Cross-bedded sands (ScM)**

This facies is composed of well sorted, medium- to fine-grained sands. Cross-bedding is formed by dark, flat and wavy heavy mineral laminae composed of magnetite and garnet,



and forming low-angle cross-beds within the sand. Sand beds between the laminae are 1-10 cm thick (Fig. 5.41 C).

These sediments are interpreted as a succession of amalgamated, tongue-shaped sand sheets resulting from swash and backwash movement on a wave-dominated beach. Analogues of these sediments can be found all along the modern day beach. Therefore, these sediments are interpreted as beach deposits.



**Fig. 5.41:** Outcrop of the marine facies at the seacliff between channel C4 and C5. **A:** Appearance of the outcrop in April 2000. Note the layer of horizontally oriented beach cobbles. Frame indicating position of Fig. 5.40 B. **B:** Detailed photograph of facies ShM showing the vertical to sub-vertical burrows which are filled with reddish heavy mineral enriched (mainly garnet and magnetite) medium- to fine-grained sand. **C:** Photo of facies ScM (hammer for scale) showing a succession of amalgamated, tongue-shaped sand sheets.

| Sample    | Facies | Median | Mean | Standard Deviation | Skewness | Kurtosis | Silt/Clay-Content |
|-----------|--------|--------|------|--------------------|----------|----------|-------------------|
| UK2,0 hc1 | Sm     | 1,43   | 1,39 | 0,73               | -0,10    | 1,25     | 1,03              |
| UK2,0 hc2 | "      | 1,40   | 1,36 | 0,71               | -0,03    | 1,22     | 0,98              |
| UK2,0 hc3 | "      | 1,40   | 1,32 | 0,74               | -0,10    | 1,09     | 0,97              |
| UK2,0 hc4 | "      | 1,43   | 1,37 | 0,76               | -0,10    | 1,18     | 0,94              |
| U3 RB 1   | "      | 1,56   | 1,58 | 0,61               | 0,04     | 1,13     | 0,89              |
| U3 RB2    | "      | 1,74   | 1,81 | 0,58               | 0,14     | 0,98     | 0,99              |
| U3 RB 3   | "      | 1,69   | 1,79 | 0,57               | 0,22     | 0,95     | 0,88              |
| U3 RB5    | "      | 2,06   | 1,96 | 0,70               | -0,18    | 0,87     | 0,15              |
| U3 RB 6   | "      | 1,84   | 1,81 | 0,74               | -0,10    | 0,85     | 0,14              |
| U3 RB 7   | "      | 2,00   | 1,95 | 0,68               | -0,10    | 0,85     | 0,16              |
| U3 RB 10  | "      | 1,64   | 1,74 | 0,59               | 0,21     | 0,99     | 1,43              |
| UKC4-1c1  | "      | 1,69   | 1,69 | 0,89               | 0,00     | 0,86     | 0,95              |
| UKC4-1c2  | "      | 1,89   | 1,88 | 0,74               | -0,01    | 0,87     | 0,62              |
| UKC4-1c3  | "      | 1,64   | 1,65 | 0,90               | -0,01    | 0,82     | 0,24              |
| UKC4-1c4  | "      | 2,32   | 2,10 | 0,60               | -0,41    | 0,73     | 0,13              |
| U5-1      | "      | 1,43   | 1,36 | 0,71               | -0,10    | 1,08     | 0,69              |
| U5-2      | "      | 1,47   | 1,43 | 0,59               | -0,60    | 1,19     | 0,67              |
| U5-3      | "      | 1,56   | 1,53 | 0,55               | -0,03    | 1,22     | 0,85              |
| U5-4      | "      | 1,51   | 1,52 | 0,42               | 0,09     | 0,91     | 0,75              |
| U5-5      | ScE    | 1,40   | 1,32 | 0,57               | -0,20    | 1,05     | 0,05              |
| U5-6      | "      | 1,60   | 1,66 | 0,44               | 0,20     | 1,16     | 0,29              |
| U5-7      | "      | 1,51   | 1,50 | 0,57               | -0,01    | 1,22     | 1,17              |
| U5-8      | "      | 1,18   | 1,27 | 0,86               | 0,17     | 0,82     | 0,27              |
| U5-9      | "      | 2,23   | 2,22 | 0,48               | -0,29    | 1,08     | 0,04              |
| U5-10     | "      | 2,47   | 2,40 | 0,39               | -0,23    | 1,20     | 0,10              |
| U5-11     | "      | 2,47   | 2,44 | 0,27               | -0,07    | 0,81     | 0,05              |
| U5-12     | "      | 2,47   | 2,40 | 0,39               | -0,24    | 1,09     | 0,05              |
| U5-13     | "      | 1,94   | 1,97 | 0,53               | 0,02     | 0,77     | 0,05              |
| UKC4-1a1  | "      | 1,40   | 1,40 | 0,79               | 0,02     | 0,88     | 0,05              |
| UKC4-1a2  | "      | 1,47   | 1,51 | 0,90               | 0,03     | 0,69     | 0,03              |
| U3 RB 4   | "      | 1,64   | 1,73 | 0,59               | 0,13     | 0,94     | 0,04              |
| U3 RB 9   | "      | 2,12   | 1,95 | 0,76               | -0,30    | 0,92     | 0,05              |
| U3 RB 11  | "      | 0,79   | 0,85 | 0,65               | 0,11     | 0,90     | 0,11              |
| UMT-1     | ShM    | 1,79   | 1,83 | 0,59               | 0,12     | 0,87     | 0,41              |
| UMT-2     | "      | 1,84   | 1,86 | 0,64               | 0,03     | 0,86     | 0,27              |
| UMT-3     | "      | 1,84   | 1,87 | 0,60               | 0,09     | 0,82     | 0,48              |
| UMT-6     | "      | 1,84   | 1,88 | 0,60               | 0,10     | 0,82     | 0,37              |
| UMT-7     | ScM    | 1,60   | 1,66 | 0,56               | 0,13     | 1,04     | 0,36              |

**Tab. 5.3:** Summary of grain size parameters calculated according to FOLK & WARD (1957) and silt- & clay-content from samples of different facies of the Uniabmond Formation.



| <b>Facies Code</b> | <b>Lithofacies</b> | <b>Sedimentary Structures</b>  | <b>Geometry</b> | <b>Basal Contact</b>          | <b>Interpretation</b>         |
|--------------------|--------------------|--------------------------------|-----------------|-------------------------------|-------------------------------|
| Gms                | gravels            | massive, matrix-supported      | sheet           | sharp, erosive                | debris flows                  |
| Gm                 | gravels            | massive to crudely bedding     | channel         | erosive                       | channel fills                 |
| Glc                | gravels            | large-scale cross-bedding      | sheet           | sharp, erosive                | lateral accretion surfaces    |
| Gh                 | gravels            | horizontal-bedding             | sheet           | rarely erosive                | channel fills                 |
| GS                 | gravel-sand        | horizontal-bedding             | sheet           | rarely erosive                | multi-storey stacked channels |
| Gt                 | gravels            | low-angle trough cross-bedding | channel         | erosive                       | channel fills                 |
| GSc                | gravels            | medium-scale cross-bedding     | sheet           | erosive                       | lateral accretion surfaces    |
| GSh                | gravels and sands  | horizontal-bedding             | blanket         | gradational                   | surges                        |
| Sh                 | sands              | horizontal-bedding             | sheet           | gradational                   |                               |
| Sm                 | sands              | massive                        | sheet           | gradational to rarely erosive | hyperconcentrated flows       |
| Fm                 | muds               | lamination                     | blanket         | sharp                         | overbank flood deposits       |
| ScE                | sands              | large-scale cross-bedding      | sheet           | sharp                         | dunes                         |
| ShM                | sands              | horizontal-bedding             | sheet           | sharp                         | upper shoreface deposits      |
| ScM                | sands              | cross-bedding                  | sheet           | gradational                   | beach deposits                |

**Tab. 5.4:** Overview of the different facies of the Uniabmond Fm.

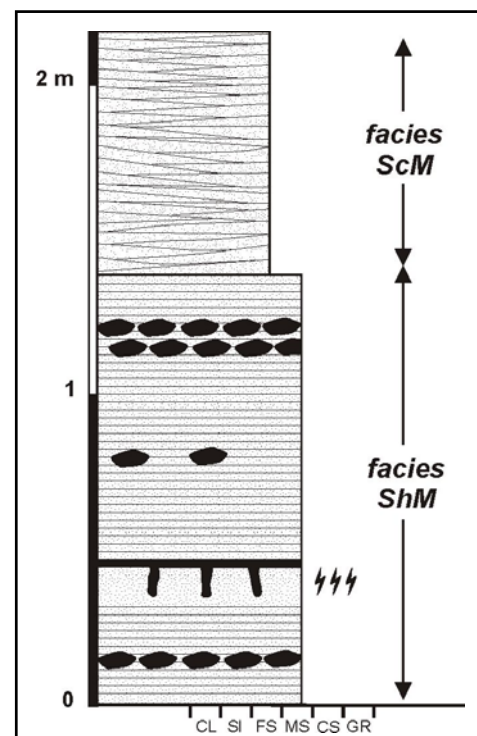
### 5.5.2 Stratigraphic subdivision of the Uniabmond Formation

Tracing and detailed mapping of prominent erosion surfaces within the seacliff exposures of the Uniabmond Fm. resulted in the subdivision of the succession into four units (Unit 1-4, see Fig. 5.43 A and Appendix V-VII). The individual units are characterized by their facies associations, their lateral and vertical facies changes, their internal architecture and the geometry of their bounding surfaces. Mapping was done in the field on photographs which were taken as a continuous picture-series along the exposures of the Uniab seacliff. In addition, three sections were logged from cutwall directly adjacent to the seacliff in the mouth area of the three main channels C4, C5 and C6.

The sediments of Unit 1 have a marine, nearshore origin whereas the overlying units were deposited in an arid continental environment. The characteristic features of Units 2 & 3 are marked incision and cyclic arrangement of their sediments as well as pronounced vertical and lateral facies changes. Unit 4 represents a relatively thin, sheet-like, conglomeratic deposit with dominantly tabular internal geometries.

#### 5.5.2.1 Unit 1

Unit 1 is the lowermost exposed unit of the Uniabmond Formation. These marine deposits have only been found in three small outcrops at the base of the seacliff between C4 and C5 and between C5 and C6. Because of changing beach topography and morphology along the highly energetic coastline and changing scree cover these outcrops are only temporarily exposed. Between channels C4 and C5 (20°11,5'S, 13°10,7'E) about 2 m of marine deposits are cropping out, which display a succession of plane- to cross-bedded sands (Fig. 5.42). The plane-bedded sands (facies ShM) are bioturbated in places and contain locally single beach cobble layers. An upper shoreface origin for these deposits is suggested (see Chapter 5.5.1.3). The cross-bedded sands (facies ScM) are



**Fig. 5.42:** Sedimentary log of Unit 1 in the outcrop between C4 & C5. See Appendix 1 for explanation of symbols.

interpreted as deposits of the swash and backwash zone of a wave-dominated beach (see also Fig. 5.41 A). This succession is erosively overlain and incised by fluvial sediments of

Units 2 & 3. Due to this incision only a few deposits of Unit 1 are exposed above the modern day beach at the base of the seacliff. Within the sedimentary succession of Unit 1 a regressive trend from deeper, less energetic to shallower, higher energetic marine deposits can be recognized.

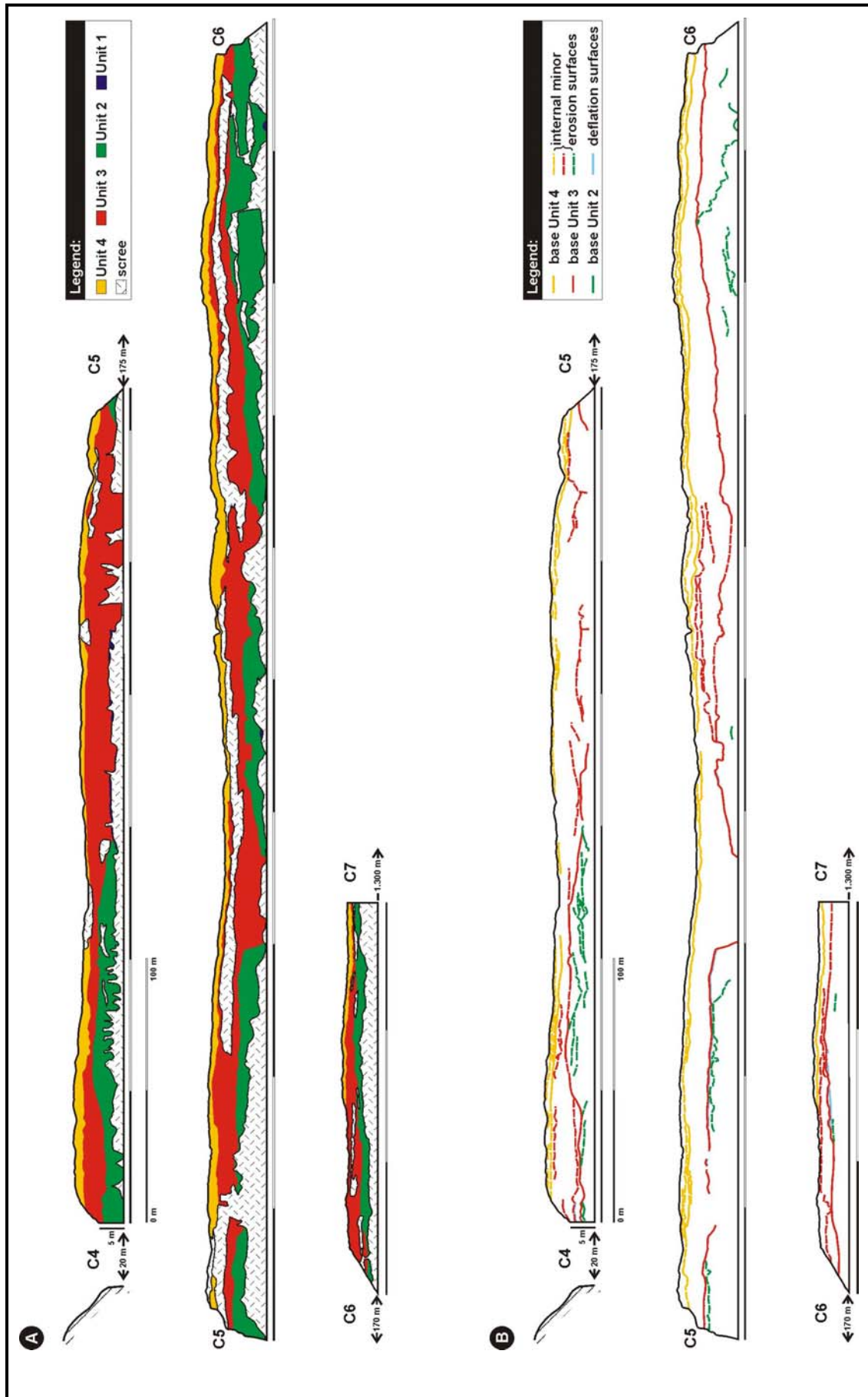
The uppermost preserved beach sediments indicate the position of a palaeo-beach at an elevation of at least 4-5 m above present day sea level. A 4-5 m beach level can be found in many places along the southwestern African coastline (PETHER et al., 2000). This level could well represent the sea level highstand of the last Interglacial during Isotope Stage 5e (BLUM & TÖRNQVIST, 2000). Therefore, it is suggested that in the Uniabmond area this stage is also preserved in and represented by Unit 1.

### 5.5.2.2 Unit 2 & 3

Units 2 & 3 show comparable facies associations as well as vertical facies developments (cycles) and are therefore described together. Each unit comprises a single cycle, which is composed of a fining-upward succession of fluvial sediments topped by aeolian deposits. An idealized cycle is illustrated in Fig. 5.44. Due to lateral facies changes and erosion by the overlying unit parts of the idealized cycle may not be present or preserved in individual sections.

The base of each cycle is formed by a major erosion surface, which cuts into the underlying sediments. In the case of Unit 2 the major part of its erosional base runs below the bottom edge of the seacliff and it can only be traced at a few places where the marine sediments of Unit 1 are exposed (see Figs. 5.43 A+B). In contrast, the erosional base of Unit 3 is traceable along the whole mapped seacliff section between channels C4 and C7. Furthermore, it is also traceable further to the N up to channel C2. At two localities Unit 3 cuts deeply into the underlying sediments displaying an incised valley geometry (see Figs. 5.43 A+B). Between channels C4 and C5 such an incised valley has a width of about 70-80 m and cuts at least 6 m into the underlying units, whereas between channels C5 and C6 a smaller incised valley has a width of about 30 m and again a minimum depth of 6 m (see Fig. 5.43 A).

A fully developed, idealized depositional cycle is illustrated in Fig. 5.44. Such a cycle starts with massive or large-scale cross-bedded gravels of facies Gm and Glc, which fill



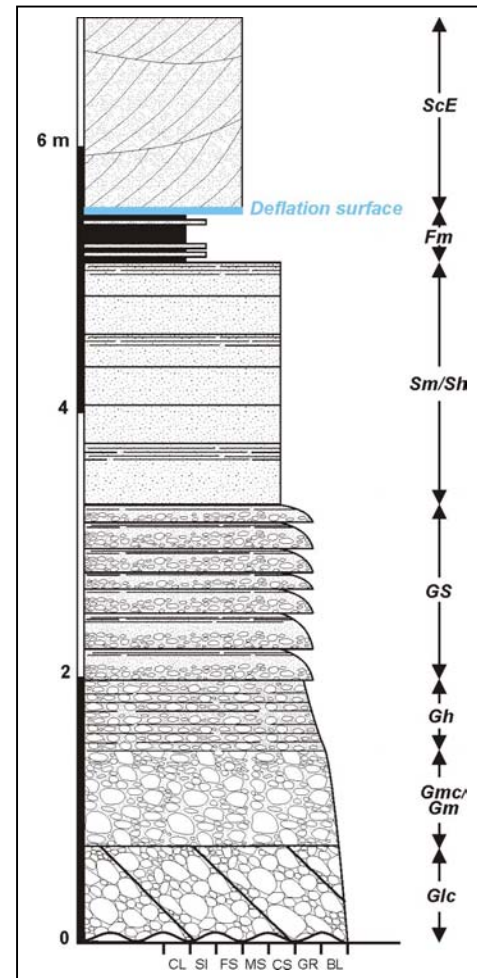
**Fig. 5.43** **A:** Schematic cross-sections showing the architecture of the Uniabmond Fm. exposed in the seacliff between channel C4 and C7. **B:** Cross-sections showing the mapped surfaces of Units 1-4.

deeply incised valleys. These deposits grade over plane-bedded gravels of facies Gh into a succession of gravel-sand couplets (facies GS) representing multi-storey stacked channel deposits (see Chapter 5.5.2.1). Each couplet represents a small scale fining-upward cycle reflecting the existence of a lower order cyclicity, which is superimposed by the higher order cyclicity forming Units 2 & 3. They are in turn overlain by plane-bedded to massive sands of facies Sh and Sm. In the upper part of the fluvial succession laminated muds are intercalated with or overlie these sandy deposits. At the top of the fluvial sediments a laterally traceable deflation surface associated with incipient soil formation is frequently developed (see Chapter 5.5.2.2). The top of the cycle is formed by aeolian sediments, which overlie the deflation surface or are intercalated within muddy deposits.

As mentioned above, a fully developed cycle is rather exceptional. For example, the basal coarse-

grained gravels filling the central lower part of the incised valleys are only exposed in Unit 3, whereas the lowermost exposed part of Unit 2 represents already the upper part of the gravel succession. The central part of the cycle is well developed in both units. The thickness of the muddy succession is laterally highly variable. In the mapped part of the seacliff only thin mud layers can be found, whereas 200 m NNE of channel mouth C4 an up to 6 m thick mud succession is exposed (see Fig. 5.45). Aeolian deposits occur only very localised at the top of Unit 2 and attain there only thicknesses of a few dm. In contrast, the aeolian sands at the top of Unit 3 occur more widespread and their preserved thickness can reach up to 2,50 m (see Fig. 5.46). The reason for this is that Unit 4 has not markedly incised into the underlying Unit 3 and form more a sheet-like cover. In contrast, the base of Unit 3 has a pronounced erosive character removing considerable parts of the upper section of Unit 2.

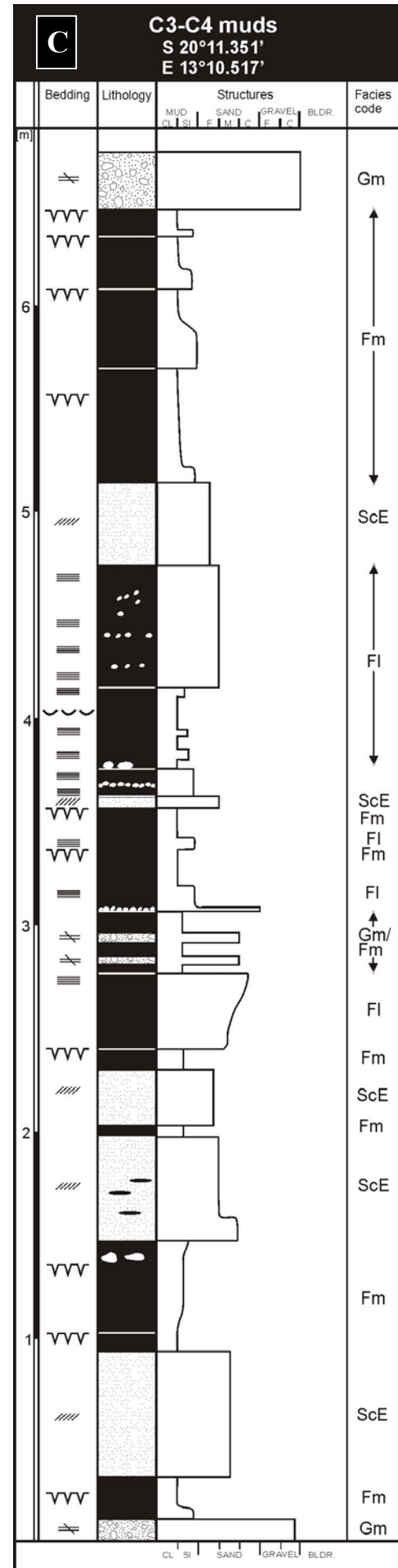
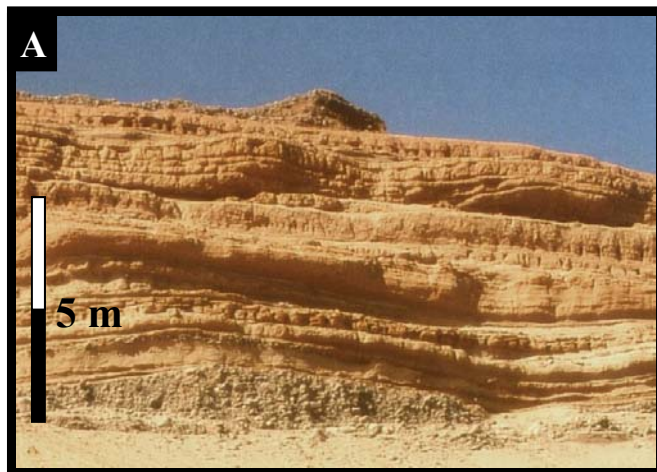
Units 2 & 3 document phases of major incision with the formation of incised valleys followed by depositional phases, in which not only the incised valleys were filled but also a new sedimentary unit was deposited over the whole seacliff area. In the central part of



**Fig. 5.44:** Idealized depositional cycle of Unit 2 & 3.



such incised valleys the thickness of the valley fills is greatest and its facies are dominated by coarse-grained gravel deposits. Towards the marginal parts of such a valley thicknesses and grain sizes of the deposits decrease. Therefore, the thickness of one cycle is highly variable and ranges mainly from about 2 to 6 m and attains a thickness of up to 12 m within the incised valleys. The internal architecture of Unit 2 & 3 is characterized by multiple, trough-shaped channel fills with pronounced erosive bases, which can be interpreted as large-scale scour and fill structures.



**Fig. 5.45 A:** Photograph illustrating the thick mud and silt accumulations in the seaciff between channel C3 and C4; view towards ENE. **B:** Detailed photograph of a ca. 40 cm thick succession composed of clay, silt and sand from the outcrop shown in Fig. 5.44 A. Also desiccation cracks filled with aeolian sand are visible in the lowermost part of the photo (arrow). **C:** Sedimentary log of the mud and silt accumulations shown in Fig. 5.44 A; see Appendix 1 for explanation of symbols.

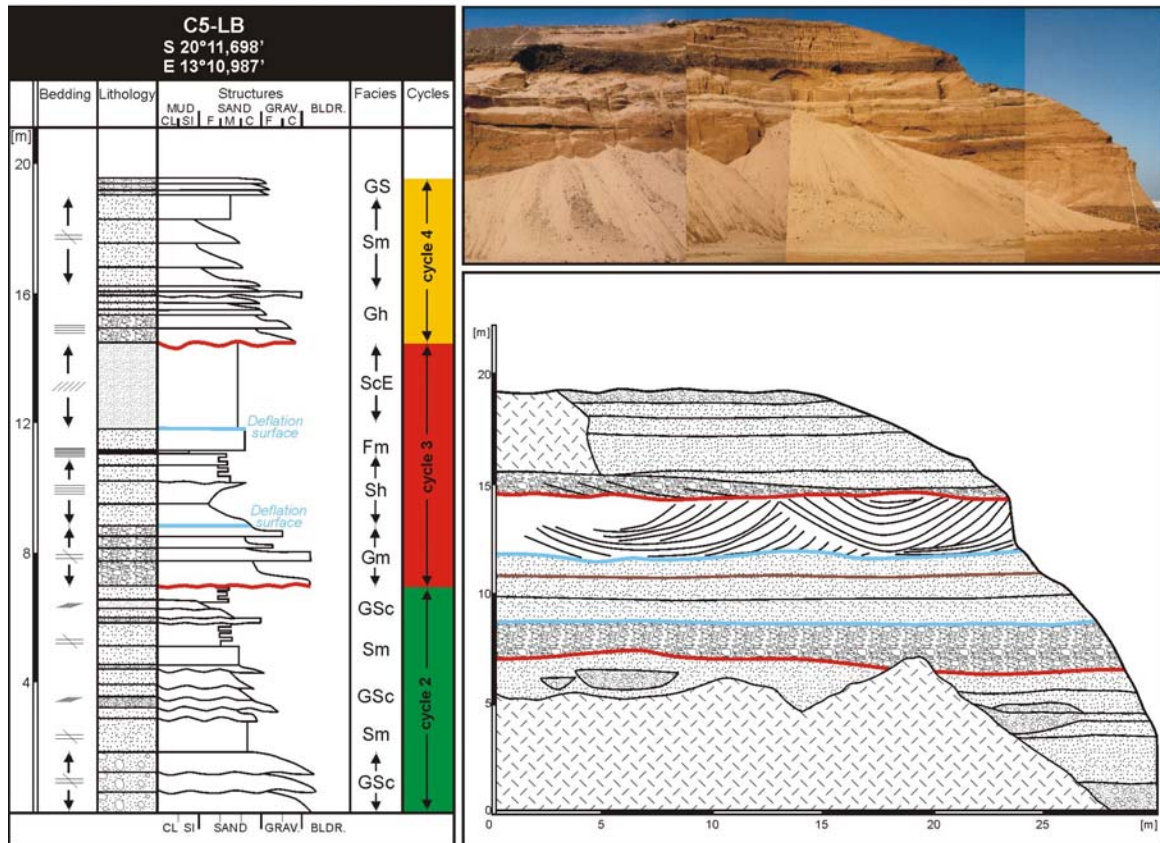


Fig. 5.46: Photomosaic, sedimentary log and cross-section of an outcrop of the Uniabmond Fm. in the southern sidewall of channel mouth C5. See Appendix 1 for explanation of symbols.

### 5.5.2.3 Unit 4

The deposits of Unit 4 built up the uppermost part of the Uniab seacliff and also the uppermost part of the Uniabmond Formation. The base of Unit 4 forms also a major unconformity, however, in contrast to Units 2 & 3 it does not incise markedly into the underlying deposits and the sediments form a more sheet-like cover. Unit 4 is dominated by plane-bedded gravels and gravel-sand intercalations (facies Gh & GS, see Fig. 5.47) and has an average thickness between 2-5 m. Within Unit 4 another erosive surface has been traced higher up in the section, which also shows a tabular geometry (see Fig. 5.43 B). The overall tabular internal geometry of Unit 4 is also expressed by the difficulty to recognize individual channels within this unit.

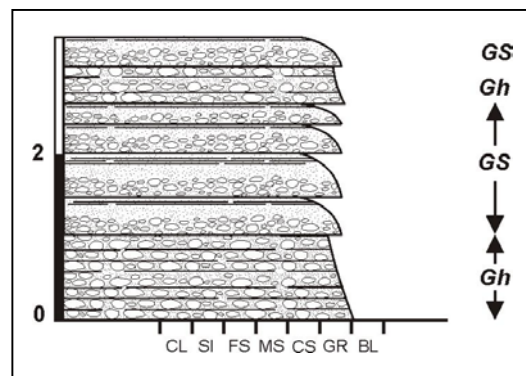
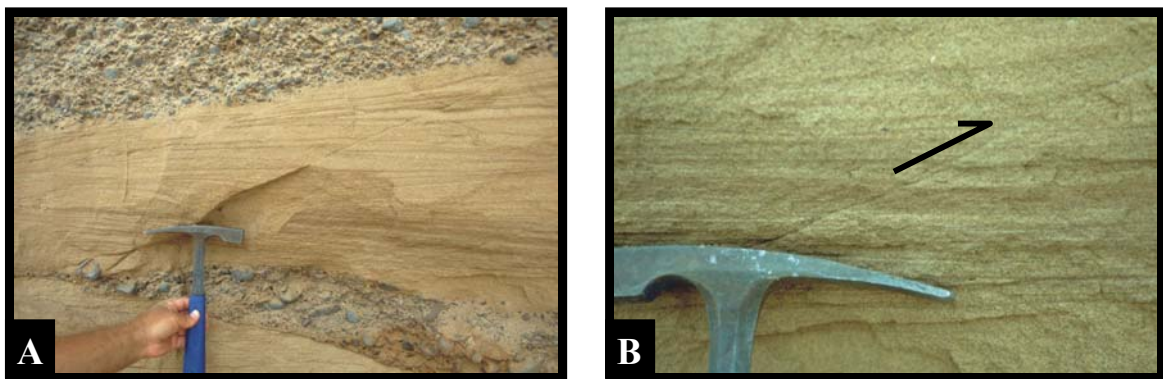


Fig. 5.47: Idealized depositional cycle of Unit 4.

### 5.5.3 Tectonic structures

Only at one locality in the seacliff about 50 m north of channel mouth C5 small tectonic structures have been observed within Unit 3. In these outcrops a series of small thrusts are visible. Measurements indicate a consistent NW-ward dip direction of the thrust surfaces with dip angles of 20-28°. These structures have been observed in a channel deposit of facies Sh about 30 cm thick, which is over and underlain by gravels of facies Gm. The offset of single marker layers of facies Sh is only a few mm to 1,5 cm and continuous into the underlying gravels of facies Gm (see Fig. 5.48). These structures are the only signs of brittle tectonics observed in the Uniabmond Formation. Therefore, regional tectonic forces are unlikely to have caused these faults. It is believed that these small-scale thrusts are rather associated with evasion movements due to sedimentary loading.



**Fig. 5.48** A: Small thrusts in the seacliff exposure of Unit 3 about 50 m north of channel mouth C5. B: Detailed photograph of A showing offsets of individual laminae.

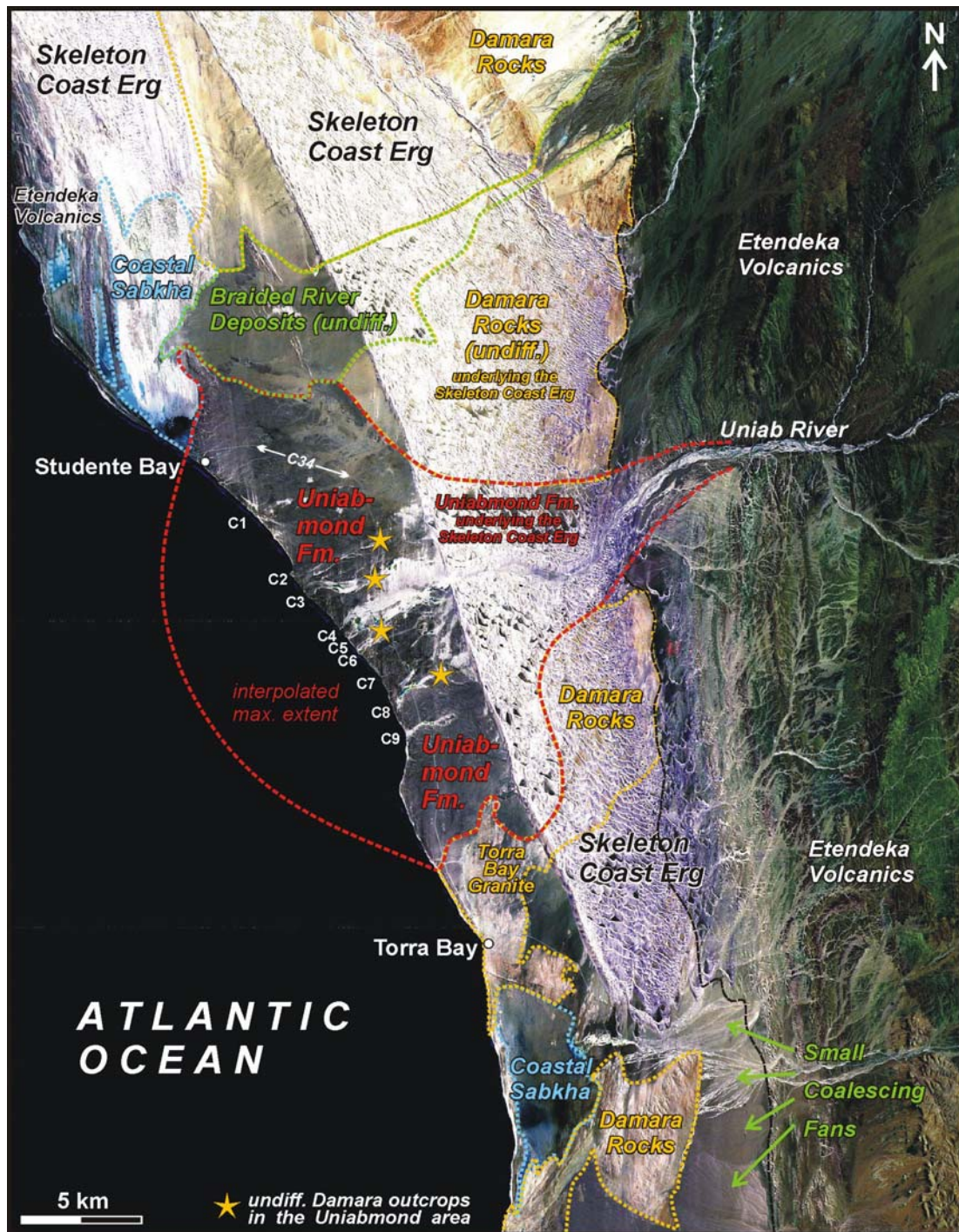
### 5.5.4 A fan model for the continental deposits of the Uniabmond Formation

In Chapter 5.5.3 it has been shown that the Uniabmond Fm. is composed of four sedimentary units with a maximum exposed thickness of about 35 m. Only the basal deposits have a marine origin, whereas the major part of the sequence is dominated by braided fluvial deposits with aeolian intercalations.

The distribution of the Uniabmond Fm. is shown in Fig. 5.49. Its extent was mapped on a Landsat TM-5 image using both field data and spectral information. To the W the outcrops are limited by the Atlantic Ocean. A coastal sabkha forms the northwestern limit. Further inland it partly coalesces with fluvial deposits of a neighbouring ephemeral river which is today inactive due to damming by the Skeleton Coast Erg. In the NE and SE the Uniabmond Fm. is bounded by Damaran crystalline rocks. These boundaries are mainly concealed under dunes of the Skeleton Coast Erg but can be traced reasonably well in the satellite image of Fig. 5.49 by the spectral information of the interdune areas. Yellow-

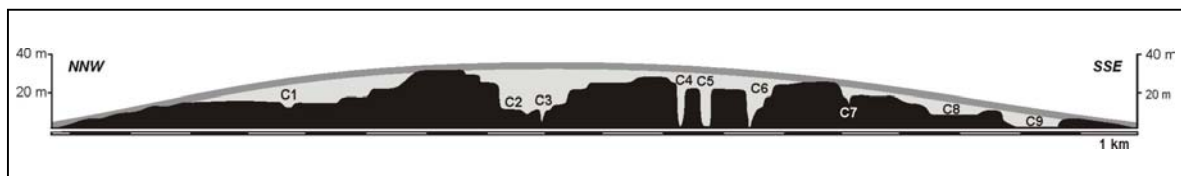


brown colours indicate areas underlain by Damaran rocks, dark greenish colours indicate areas underlain by gravels of dominantly volcanic composition. The eastern boundary is build up by volcanics of the Etendeka Plateau whose western margin forms in this area a pronounced coastal escarpment. In the SSW the deposits of the Uniabmond Fm. are bounded by outcrops of the Damaran Torra Bay Granite building up small hills, coppice and ridges of up to 5 m high. As a result, the extent and distribution of the Uniabmond Fm. outlines in plan view a roughly triangular, delta-shaped area.



**Fig. 5.49:** Landsat TM-5 scene 181-074 (30.03.1995; 7-4-1, R-G-B) illustrating the outline of the distribution of the Uniabmond Formation.

In Chapter 5.1 - Fig. 5.4 it was shown that the projection of the present day land surface of the Uniabmond area beyond the seacliff allows the estimation of the original seaward extent of the Uniabmond Formation. If this area is added to the land exposures the resulting shape is clearly that of a fan (see Fig. 5.49). Furthermore, a coast parallel section over the whole Uniabmond area reveals the former convex shape of the sedimentary body formed by the Uniabmond Fm. now dissected by numerous incised valleys (see Fig. 5.50). All these observations strongly implicate that the braided fluvial/continental deposits of the Uniabmond Fm. built up a compound fan recording multiple cycles of erosion and deposition. Therefore, the term 'Uniab Fan' will be used in the following for further descriptions.



**Fig. 5.50:** Coast-parallel topographic section over the Uniab seacliff showing the convex shape of the former fan surface.

The Uniab Fan lies at the northern margin of an area in which numerous other fans can be observed today. This area stretches from few km north of the Huab River up to few km north of the Uniab River. For example, the Koigab Fan, described in Chapter 4, represents one of the larger fans in this area, whereas the Salt and Sout Fans (see also Chapter 4) are examples of smaller ones. In the satellite image of Fig. 5.49 also several smaller, coalescing fans are visible in the lower left part of the picture. All these fans originate at and are aligned along the western margin of the Etendeka Plateau. The reason for the abundance of fans within this area is that here the Etendeka volcanics form a pronounced coastal escarpment, whereas N and S of this area outcrops of Damaran crystalline rocks form a more gentle topography.

When leaving the Etendeka Plateau the floods of the modern day Uniab River are partly blocked by the dunes of the Skeleton Coast Erg and are strongly channelized during river break through within the dunefield and also on their way to the Atlantic Ocean where they are guided through the incised channels C4, C5 and C6 during run-off. This shows that during the development of the Uniab Fan no major dunefield can have existed in this area, which would have prevented the development of a fan. However, the aeolian component within the Uniabmond Fm. (aeolian and fluvially reworked dune sand) proofs the aridity of



the depositional environment. Therefore, the Uniab Fan has to be a pre-Skeleton Coast Erg feature which has been modified and is nowadays inactive.

As shown in Chapter 5.5.2 the major erosional surfaces at the base of Unit 2 and 3 of the Uniabmond Fm. display incised valley morphologies. Also the present day morphology of the Uniabmond area is characterized by deep, canyon-like incised valleys accompanied by multiple, unpaired, erosional terraces. Therefore, one might tend to classify the Uniabmond Fm. as an incised valley fill. In this case the Uniabmond Fm. should represent the infill of a linear depression cut into the underlying, pre-Cenozoic 'hard-rock' basement, resp. within Etendeka volcanics or/and Damaran crystalline rocks. To verify this, the 3-D topography of the basement surface has to be known. In the study area this interface is unfortunately largely covered and concealed. Indeed, the coastal strip along the seacliff is characterized by a lack of basement outcrops. North of the seacliff volcanics of the Etendeka Group are exposed at the coast whereas south of it Damaran rocks crop out at sea level. However, several outcrops of Damaran gneisses and mica schists 1,5 to 4 km inland in the central part of the Uniabmond area (see yellow stars in Fig. 5.49) at elevations similar to the basement outcrops bordering the Uniabmond Fm. in the N and S do not support an incised valley topography of the basement surface. The absence of basement outcrops along the seacliff could be explained by a near coastal, approximately coast-parallel, NW-SE trending, slightly crescentic, listric fault with a downthrow to the west, a maximum offset in the centre of the Uniabmond area and decreasing offset towards N and S. Such a fault is not directly exposed in the Uniabmond area, but is inferred based on the spatial relationship between the Red Canyon Fm. and Damara outcrops within the Uniabmond area, i.e. that outcrops of the Red Canyon Fm. are only preserved W of the westernmost basement outcrops (see also ZELLER, 2000). Furthermore, such faults are very common features along the Atlantic continental margin in the Skeleton Coast area (see Chapter 2). They are related to continental rifting and opening of the Atlantic Ocean and can be well studied e.g. in the coastal area between the Huab and the Koigab River (see MILLER, 1988). Comprisingly it can be concluded that there is no striking evidence that the Uniabmond Fm. was deposited in an incised valley. In fact, the floor of the Uniab Fan is formed widely by a rock peneplain which is interpreted by some authors as a marine cut platform of Tertiary age (SCHEEPERS & RUST, 1999).

Therefore, the discussion above consolidates the fan-model - based on morphological characteristics - for the continental deposits of the Uniabmond Formation. The question if the Uniab Fan represented a fan-delta in the past is difficult to answer since the fan toe was largely removed by abrasion during sea level rise after the Late Glacial Maximum. During

deposition of the continental deposits of the Uniabmond Fm. the sea level was lower than today (BLUM & TÖRNQUIST, 2000) but it is not known if the sediment delivery and the progradation of the fan was high enough to reach palaeo-sea level. Today, in the case of the Koigab Fan, only a small sector of this fan interacts directly with the Atlantic Ocean whereas the smaller Sout Fan debouches into a coastal sabkha (see Chapter 4.4 & 4.5).

A fan-model for the Uniab Fan was also proposed by SCHEEPERS & RUST (1999). They termed it an 'unusual alluvial fan' because of the very low regional radial gradient (0.5-0.7°). This terminology can not be supported because the Uniab Fan does not represent an alluvial fan but a braided river dominated fan and resembles in this respect the Koigab Fan. For braided river dominated fans a low radial gradient is not unusual (KRAPP et al., in press). Furthermore, SCHEEPERS & RUST (1999, p. 290) wrote: "The hyper-arid Uniab River fan is controlled by two main forces: (1) the dunefield barrier across the main channel; and (2) the change in sea-level during the Late Quaternary." That the development of the Uniab Fan is most probably controlled by sea level changes is reflected in the internal fan architecture but it is believed that the dunefield barrier rather terminated the build-up of the fan than controlled it. SCHEEPERS & RUST (1999) also attribute the formation of the incised channels to sea level rise since the LGM (Flandrian Transgression). In their model marine erosion of the lower fan generated a steeper channel gradient leading to pronounced incision. Alternatively, channel incision on the fan surface could have also taken place already during peak of sea level fall within the period of the LGM. Marine erosion of the fan front during the following sea level rise indeed caused a gradient steepening but only active channels were able to adjust to the new base/sea level whereas less active or abandoned channels were not able to cope with gradient steepening and as a result are nowadays characterized by hanging mouths.

Therefore, the Uniab Fan is understood in this study as a sedimentary body which was built up by the continental sediments of the Uniabmond Formation. The incised channels in the modern day Uniabmond area form together with the regressive seacliff and the deflation surfaces a part of the erosional features that have degraded and modified the original fan and fan surface after deposition of the Uniabmond Fm. (see Chapter 5.6.2).

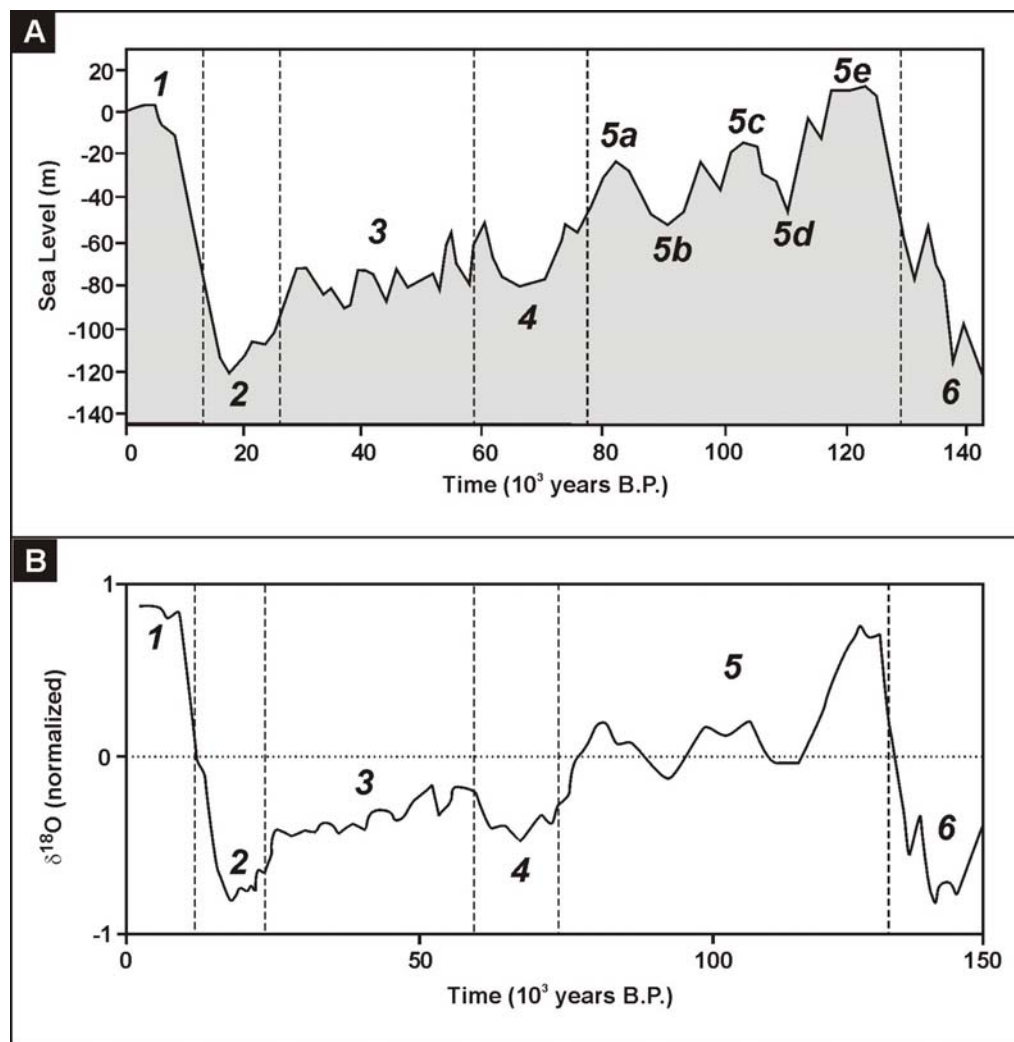
### 5.5.5 Age constraints for the Uniabmond Formation

SCHEEPERS & RUST (1999) reported a preliminary TL-age of 175 Ka for a sample from the base of the seacliff. However, this study has shown that between channels C4 and C6 sediments of Unit 1, 2 and 3 are cropping out at the base of the seacliff (Fig. 5.43 A+B) and consequently deposits exposed there do not necessarily represent the oldest ones. Since no details are given for sample localities it is not known from which stratigraphic unit the dated sample originates. In addition, no information is available if dating was done on marine, fluvial or aeolian sediments.

The stratigraphic investigations of this study have shown that marine deposits represent the oldest exposed part of the Uniabmond Fm. and at the top of this unit (Unit1) beach sediments are elevated 4-5 m above present day sea level. Along the Namibian coastline several other localities are known where marine beach deposits are elevated to comparable heights (cf. DAVIES, 1959; STOCKEN, 1962; BESLER et al., 1994; PICKFORD & SENUT, 1999; KEMPF, 2000; PETHER et al., 2000; WARD et al., 2002). The 4-6 m palaeo-strandline is called 'B-Beach' in the southern Sperrgebiet (PETHER et al., 2000; WARD et al., 2002) and is attributed to the sea level highstand during the Eemian (isotope stage 5 e, 120–130 Ka BP; BLUM & TÖRNQVIST, 2000; see Fig. 5.51 A). Because of the comparable topographic position of the beach sediments of Unit 1 an Eemian age is also suggested for them and this provides a lower age limit for the Uniabmond Formation. Thus the 175 Ka TL-age from SCHEEPERS & RUST (1999) seems to be too old and should be checked by further age datings and improved by OSL-datings.

Another sample taken from the top of the seacliff yielded a preliminary TL-age of about 18 Ka (SCHEEPERS & RUST, 1999). Again no details about the locality and the sediment type of this sample are given. From the results of the seacliff mapping in this study it seems highly probable that the sample is derived/were taken from Unit 4 of the Uniabmond Formation which forms the top of the seacliff. As argued in Chapter 5.5.4 it is believed that incision into the fan surface occurred after deposition of Unit 4. However, contrary to SCHEEPERS & RUST's (1999) point of view it is suggested here that the incised channels of the Uniabmond area were mainly formed as a result of a pronounced sea level fall caused by climatic deterioration leading to the extensive Weichsel glaciation (LGM; isotope stage 2) and not during subsequent sea level rise (Flandrian transgression). Therefore, Unit 4 pre-dates the channel incision. Furthermore, the development of the Skeleton Coast Erg is also related to the LGM (BARNARD, 1988). The dunes of the erg overlie the uppermost deposits of the Uniabmond Fm. with a major unconformity and therefore post-dates Unit 4. However, the exact timing of the sea level fall and rise during isotope stage 2 is not very

well constrained but is estimated to have taken place between 25 and 15 Ka according to the adjustment of stacked  $\delta^{18}\text{O}$  records to a time scale applying an orbital tuning approach (BRADLEY, 1999; see also Fig. 5.51 B). The older part of isotope stage 2 comprising the period of pronounced sea level fall ranges from approximately 25-18 Ka, which most probably represents an upper age limit for Unit 4 and consequently for the Uniabmond Formation.



**Fig. 5.51 A:** Eustatic sea-level curve with oxygen isotope stages (boundaries shown by dashed lines) compiled from BLUM & TÖRNQUIST (2000). **B:** SPECMAP composite chronology from stacked  $\delta^{18}\text{O}$  records with oxygen isotope stages (boundaries shown by dashed lines) compiled from BRADLEY (1999).

In summary it is proposed that the deposition of the Uniabmond Fm. occurred within a time frame lasting from isotope stage 5e to early isotope stage 2, which represents an overall regressive period in which the fan build-up and progradation could have taken place. The three major unconformities within the Uniabmond Fm. are most probably related to sea level low stands within this period. Such sea level low stands are inferred

from  $\delta^{18}\text{O}$  lows/minima represented by isotope stage 5d, 5c and 4 (BRADELY, 1999). The verification of the age model proposed in this study could be achieved by detailed dating of the single units of the Uniabmond Fm. using OSL-dating techniques.

### **5.6 Skeleton Coast Erg and Uniab Poort deposits**

About 6.5 km east of the coast dunes of the Skeleton Coast Erg overlie the Uniabmond Formation. There, the erg has a width of about 8 km and the barchanoid to compound dunes attain a thickness of about 20 m. The development of the Skeleton Coast Erg is correlated with the sea level lowstand during the Last Glacial Maximum (BARNARD, 1989). Adjacent to the Uniab River break-through corridor, called the Uniab Poort, the interdune areas are characterized by up to several meter thick successions of muddy deposits interfingering with sandy deposits (see Chapter 6.3). The muds represent the suspension load of interdune floodponds whereas the sandy deposits represent aeolian dunes as well as hyperconcentrated flow deposits (intra erg mass flows after SVENDSEN, et al., in press). These deposits seem to represent a phase of higher frequent river flooding and dune break-through causing intensive interdune flooding. So far no age datings are available for these deposits. However, they might correlate with silt deposits encountered in other ephemeral rivers along the Namibian coast, e.g. the Hoarusib Clay Castles, the Khowarib silt terraces and the Homeb silts (EITEL et al., 2002; BOURKE et al., in press). They represent deposits of the most humid period since the LGM, which started approximately at 9-8 Ka (EITEL et al., 2002).

### **5.7 Modern day sediments**

The modern day landscape of the Uniabmond area is characterized by deeply incised valleys, accompanying terraces, vast deflation surfaces, aeolian sandramps, shrub coppices, small dunes, and few vegetated spots. Due to the semi-arid climatic conditions in the catchment and the hyper-aridity in the mouth area the Uniab River experiences only floods of short durations flowing through the main channels (C4-C6). Fluvial sedimentation only takes place within the channels (Fig. 5.52 A), in the lower overbank areas, and on the adjacent shelf in front of the active channel mouths. For example, a small sedimentary prism in front of channel mouth C6 can be seen in Fig. 5.52 B. The modern day fluvial deposits are predominately coarse- to medium-grained sands, which contain a high percentage of reworked aeolian sand derived from the Skeleton Coast Erg, from sandramps



(Fig. 5.52 C) and small shrub coppice fields (Fig. 5.52 D). Conglomeratic deposits are rather exceptional. Beside deposition of silt and mud in depressions, the overbank areas are widely covered with plant fragments and tree-trunks indicating flood high-stands.



**Fig. 5.52:** **A:** Braided stream network at the base of an active Uniab River channel about 300 m W of the main road after April 2000 flood. View towards SSW. **B:** Oblique view towards S showing the sedimentary prism in front of C6 deposited during April 2000 flood. **C:** Fluvial reworking of aeolian sand: erosion in the basal part of a sandramp in the main channel C5 about one week after April 2000 flood. **D:** Shrub coppice field covering vast parts of the valley floor of channel C 5. View towards SSW. Single shrubs are about 50 cm high.

Modern day deposits are of insignificant thickness in the Uniabmond area and have only a low preservation potential due to modifications by subsequent floods, deflation and marine reworking. Therefore, sedimentary processes are more resulting in sediment redistribution and bypass rather than accumulation.

### 5.8 Summary and conclusions

For the first time a detailed and comprehensive lithostratigraphic subdivision has been established for the Cenozoic sediments in the Uniabmond area. As a result, the whole succession was divided into three formations, namely the Red Canyon, Whitecliff, and Uniabmond Fms., which are bounded by major unconformities representing considerable

time gaps within the succession. Due to comparison with other Cenozoic sequences along the southwestern African coastal strip it is possible to place the Cenozoic sedimentary succession of the Uniabmond area into a broader southern African regional stratigraphic context. This correlation also provides a timeframe in which these sediments have been deposited (see Tab. 5.5).

| Stratigraphic units  | Age indicators  | Stratigraphic correlation   | References   | Age  |
|--|---|---|--|--|
| post-Uniabmond Fm.   |   | + 2 m A-Beach<br>Skeleton Coast Erg   | PETHER et al., 2000<br>BARNHARD, 1988  | Holocene<br>LGM  |
| Uniabmond Fm.<br>Unit 1  | + 4 m beach deposits of Unit 1  | + 4 m palaeo-strand-line, B-Beach<br>+ 4-6 m<br>+ 6 m                                   | PETHER et al., 2000<br>BESLER et al., 1994<br>TANKARD, 1976                                  | Late Pleistocene<br>Eemian   |
| Whitecliff Fm.<br>upper Whitecliff Fm.<br>lower Whitecliff Fm. | + 8 m palaeo-seacliff 'Bivalves Cliff'<br>+ 25 m palaeo-seacliff 'Whitecliff' | Oswater Conglomerate<br>+ 6-8 m palaeo-strandline, C-Beach<br>+ 30-12 m marine deposits | WARD, 1987; VAN ZYL & SCHEEPERS (1991, 1992)<br>PETHER et al., 2000<br>PETHER et al., 2000   | Early to Middle Pleistocene<br>Middle Pleistocene<br>Pliocene – Earliest Pleistocene |
| Red Canyon Fm.   | Etendeka clasts/<br>bovid bone  | pre-Tsondab/<br>Rooilepel Sandstone<br><i>and</i><br>post-Chalcedon-Tafelberg Fm.       | PETHER et al., 2000<br>pers. comm. WARD, 2002<br>PARTRIDGE & MAUD, 1989; PETHER et al., 2000 | Palaeogene?  |

**Tab. 5.5:** Correlation scheme and age estimates for the Cenozoic succession in the Uniabmond area.

The Red Canyon Formation, which is subdivided into the Waterfall and the Bone-Area Member, consists of reddish sediments deposited in alluvial fan and braided river to floodplain palaeoenvironments. In comparison to the alluvial and braided fluvial dominated deposits of the Waterfall Mb. the sediments of the Bone-Area Mb. represent fine-grained floodplain deposits with crevasse conglomerates, caliche horizons rhizcretions, rootlets and bone fragments. A marked increase in caliche horizons and decrease in conglomerates towards the upper part of the Red Canyon Fm. indicates aridification of the depositional environment with time. The deposits of the Red Canyon Fm. are markedly affected by tectonic activity resulting in faulting and jointing. The

occurrence of strongly weathered clasts of Etendeka basalts and quartzites in all stratigraphic units implies a post-Early Cretaceous Etendeka age for the whole succession. A recently discovered fossil bovid bone clearly indicates a post-Upper Cretaceous age of the Bone-Area Member. According to palaeoclimatic indications based on sedimentological observations a Paleogene age is inferred.

The Whitecliff Formation displays a variety of continental and marine facies comprising fluvial sandstones and conglomerates, aeolian dunes and beach deposits, which are all entirely calcified. They provide good possibilities to examine ancient fluvio-aeolian-marine interaction and spectacular, steep onlap relationships towards older sediments preserved in fossil seacliffs. Litho- and cyclo-stratigraphic correlations of various exposures of Whitecliff Fm. deposits resulted in the alignment of four cycles. Cycle I is composed of a marine-aeolian succession preserved as a palaeo-seacliff 25 m asl.. Cycle I is followed by the fluvio-aeolian successions of Cycle II and III, which are topped by marine deposits documenting a palaeo-beach at about +8 m asl.. These palaeo-seacliffs allow an age estimation by correlation with similar elevated beaches in the southern Sperrgebiet (see Tab. 5.5). For the lower Whitecliff Fm. a Pliocene to Earliest Pleistocene age and for the upper part of the Whitecliff Fm. a Middle Pleistocene age is proposed.

The Uniabmond Formation provides for southwestern Africa a unique insight into the depositional history during the last Pleistocene glacial cycle ranging from about 125 to 18 Ka. Today's recent seacliff exposures provide an excellent section through the whole formation. Four sedimentary units were identified that are suspected as the result of sea level changes during the Late Pleistocene. In the basal parts of the seacliff marine beach sediments represent Unit 1. The top of the beach sands are elevated +4 m asl. and are correlated with the Eemian B-Beach (see Tab. 5.5). Units 2 & 3 each consist of a fluvio-aeolian succession. The base of Units 2 & 3 are characterised by marked incision displaying incised valley geometries. The uppermost Unit 4 forms a more sheet-like cover of fluvial gravels and shows an overall tabular internal geometry. Further inland the Uniabmond Fm. is overlain by the dunes of the Skeleton Coast Erg, whose development is related to the LGM and post-dates the upper part of the Uniabmond Formation. The continental deposits of the Uniabmond Fm. build up the Uniab Fan, which is nowadays degraded and characterised by deeply incised valleys, deflation surfaces, aeolian sandramps, shrub coppices, small dunes, and few vegetated spots.

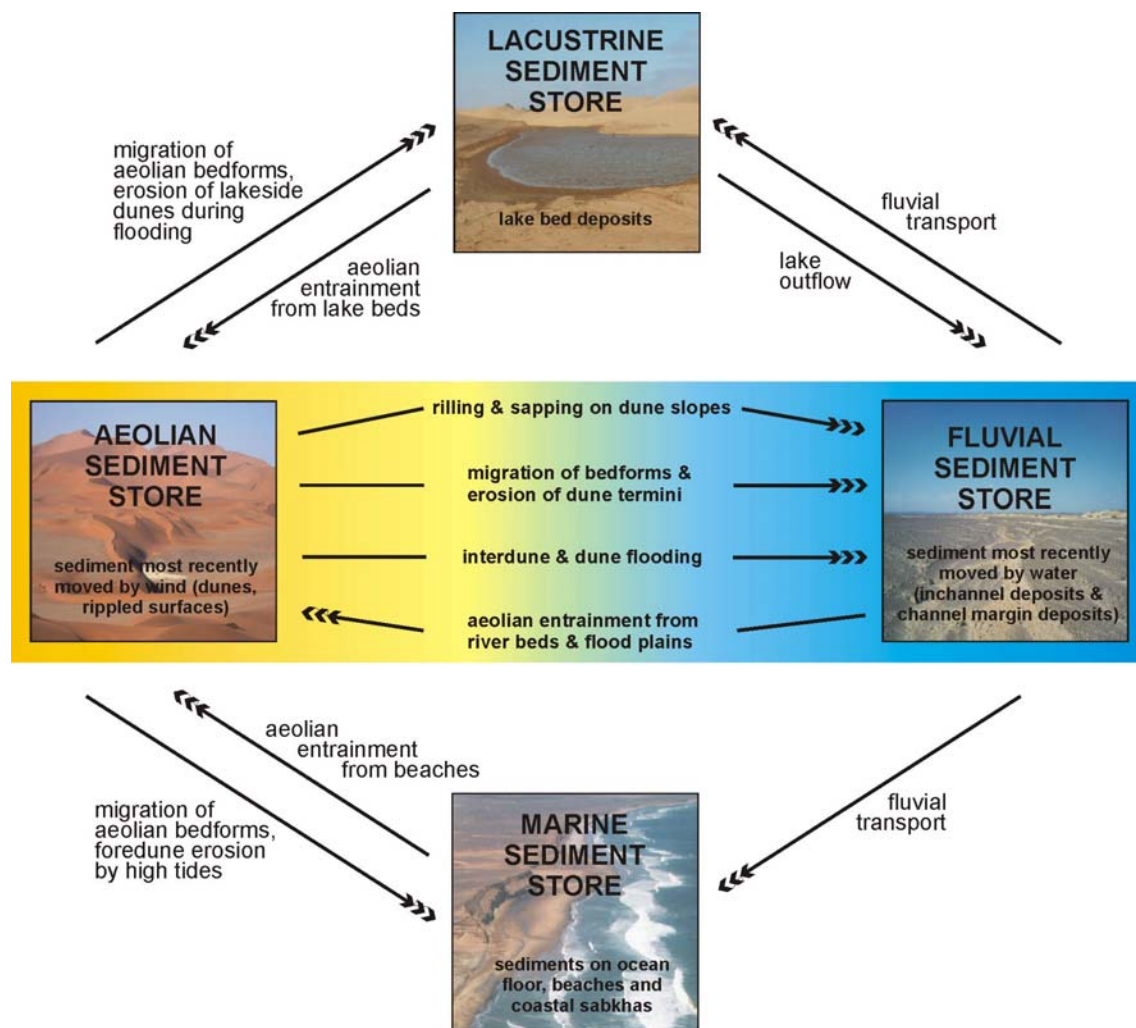
The ancient landscape deduced from the sedimentary record of the Whitecliff and Uniabmond Fm. mirrors quite well the present day landscape indicating quite similar

climatic conditions. Erosion and deposition were mainly controlled by sea-level changes during the Pleistocene.

## 6 A comparison of fluvio-aeolian interaction between ephemeral rivers and the Skeleton Coast Erg

According to BULLARD & LIVINGSTONE (2002) fluvio-aeolian interaction can be described as the transfer of sediment from the fluvial sediment store to the aeolian sediment store and vice versa (Fig. 6.1). The interactions between the two systems have not only important implications for the geomorphology of the landscape (KRAPP et al., 2000; BULLARD & LIVINGSTONE, 2002), but also for the sediments preserved in such an environment (WARD, 1988; LANGFORD, 1989; LANGFORD & CHAN, 1989; NORTH & PROSSER, 1993; STANISTREET & STOLLHOFEN, 2002; KRAPP et al., 2003).

The variable signatures of fluvio-aeolian interactions in the sedimentary record are exceptionally important for the understanding of fluvio-aeolian facies models, particularly for the interpretation of ancient sedimentary sequences from desert environments (LANGFORD & CHAN, 1989; NORTH & PROSSER, 1993).



**Fig. 6.1:** The linkage between the four main sediments stores for sand-sized material in drylands (modified after BULLARD & LIVINGSTONE, 2002)

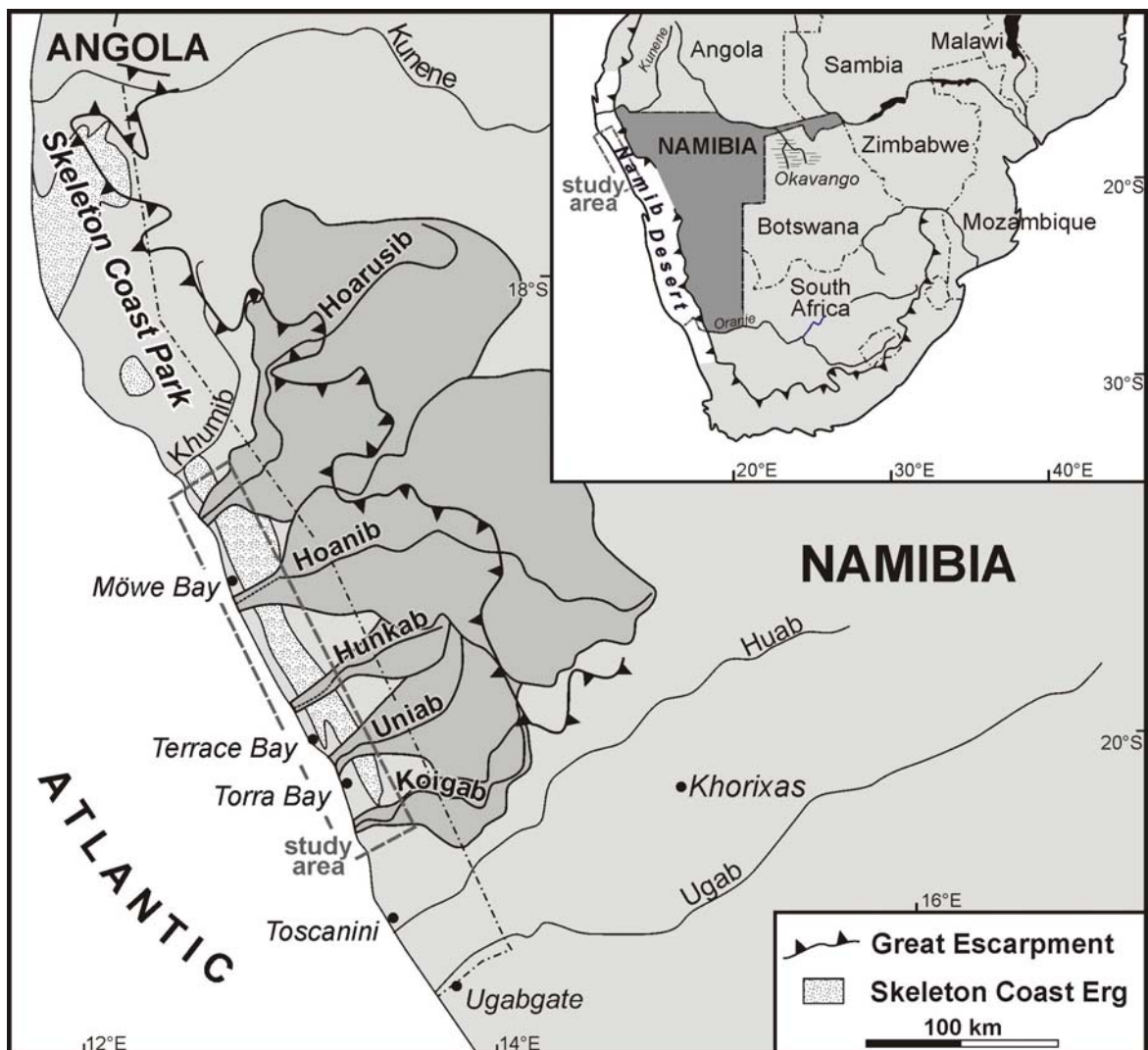


In the hyper-arid, vegetation-free environment of the Skeleton Coast with its ephemeral flash flood river systems and the Skeleton Coast Erg, effects of fluvio-aeolian interaction can be well observed and documented. The Skeleton Coast rivers display a spectrum of interactions but because of their remote location little has been published concerning their characteristics.



**Fig. 6.2:** Landsat TM-5 overview scene 181-074 (7-4-1, R-G-B) of the investigated area in the Skeleton Coast National Park/NW Namibia, taken on August, 22<sup>nd</sup>, 1984. Dominant in the Skeleton Coast Erg are simple and locally compound, barchanoid and transverse dunes which are arranged in a 6 to 20 km wide belt that parallels the Atlantic coastline 2 to 5 km inland. The main wind direction is from south-southwest.

The drainage pattern of the Skeleton Coast of Namibia comprises seven major and several smaller ephemeral rivers which flow sub-parallel west-southwestward towards the Atlantic Ocean (Figs. 6.2 & 6.3). Their main catchment areas are about 100 to 300 km further inland and are situated in areas with relatively high mean rainfall of 150 to 500 mm per year (JACOBSEN et al., 1995), most of which falls in late summer between January and March. On their routes to the hyper-arid coastal area, the rivers pass through a steep climatic gradient where rainfall declines to an average of less than 50 mm per year with a rainfall variability of 72%. All year strong onshore south to southwesterly winds dominate the coastal regime (LANCASTER, 1982; BARNARD, 1989), whereas the 'Bergwind' from easterly directions blows only for periods of several days between April and July (see Chapter 1.3).



**Fig. 6.3:** Location map of the study area in NW Namibia illustrating the arrangement and the catchment areas of the five investigated WSW flowing ephemeral rivers and the coast-parallel Skeleton Coast Erg.

Within the coastal plain of the NW Namibian margin between Torra Bay (20°20'S) and the Hoarusib River (19°S) lies the 2000 km<sup>2</sup> large Skeleton Coast Erg (Fig. 6.1), forming part of the northern Namib Sand Sea (SEELY, 1978). It consists of simple and locally compound, barchanoid and transverse dunes which are 20-50 m high (LANCASTER, 1982). The Landsat images in Fig. 6.2 shows that they are arranged in a 165 km long and 6 to 20 km wide dune belt that parallels the Atlantic coastline 2 to 5 km inland. The erg is not yet dated but a Late Pleistocene age has been suggested by BARNARD (1989) and SCHEEPERS & RUST (1999), based on the assumption that the erg post-dates the Last Glacial Maximum.

The regional climate of the Skeleton Coast area is strongly influenced by the cool northward-flowing Benguela Current and its associated cold-water upwelling systems off the Namibian coastline, causing low humidity of southerly winds. Additional impact on the regional climate comes from the subtropical south Atlantic anticyclone and particularly from monsoonal influences from the northeast which are associated with disturbances of the intertropical convergence zone (VAN ZINDEREN BAKKER, 1984). The latter effect may initiate heavy thunderstorms with torrential rainfall in the river catchments causing flood events. Minor river flows are usually dammed by the dune barrier running perpendicularly to the river courses that extend towards the Atlantic Ocean. Since 1934 only eight significant regional flood events have been recorded in which many of the Skeleton Coast rivers reached the Atlantic Ocean (floods 1934, 1950, 1963 & 1984: SHANNON et al., 1986; floods 1988, 1995, 1997, 2000: J. Patterson, 2000 pers. comm., STANISTREET & STOLLHOFEN, 2002, own observations 2000). It might be assumed that these flood events were a result of a South Atlantic equivalent of the Pacific El Niño/ENSO, but SHANNON et al. (1986) concluded from the combined analyses of temperature, salinity, sea level, wind, rainfall and NOAA satellite data that only the flood events of 1963 and 1984 were caused by true El Niño-type conditions.

The river systems and their interaction with the erg are classified using a combination of Landsat TM-5 and Landsat 7 data, aerial photographs, CORONA satellite photographs and field data.

## **6.1 Varieties of ephemeral rivers and aeolian interaction**

Five ephemeral rivers (from South to North: Koigab, Uniab, Hunkab, Hoanib and Hoarusib) were chosen for the purposes of the study (Figs. 6.2 & 6.3). These rivers are spread along a coast-parallel distance of about 220 km. They were selected for their variety of interactions with the Skeleton Coast Erg (Figs. 6.2 & 6.3). The southernmost river, the Koigab River, plays an important role providing sand for the southern end of the erg (see also Chapter 4.3.3). North of the Koigab a chain of low basement hills, 40-50 m high and 4-5 km wide, provide a localized trap for sand deflated off the fan surface through flow separation. This trap feeds sand into the downwind edge of the erg, representing a major sand input area (LANCASTER, 1982). In contrast, the Hoarusib flows sufficiently often to prevent a northward migration of the erg. Therefore, the Hoarusib forms the northern boundary of the erg by flushing aeolian sand into the Atlantic Ocean, in a manner akin to the effects of the Kuiseb River as the northern boundary of the southern Namib Sand Sea (see Chapter 6.6; WARD, 1987).

Between these two, the remaining rivers provide a spectrum of types of interaction with the dunes of the erg. The five rivers will be described in turn from south to north in order to illustrate these variations.

## **6.2 Koigab and the southern margin of the Skeleton Coast Erg**

### **6.2.1 Koigab River and Koigab Fan**

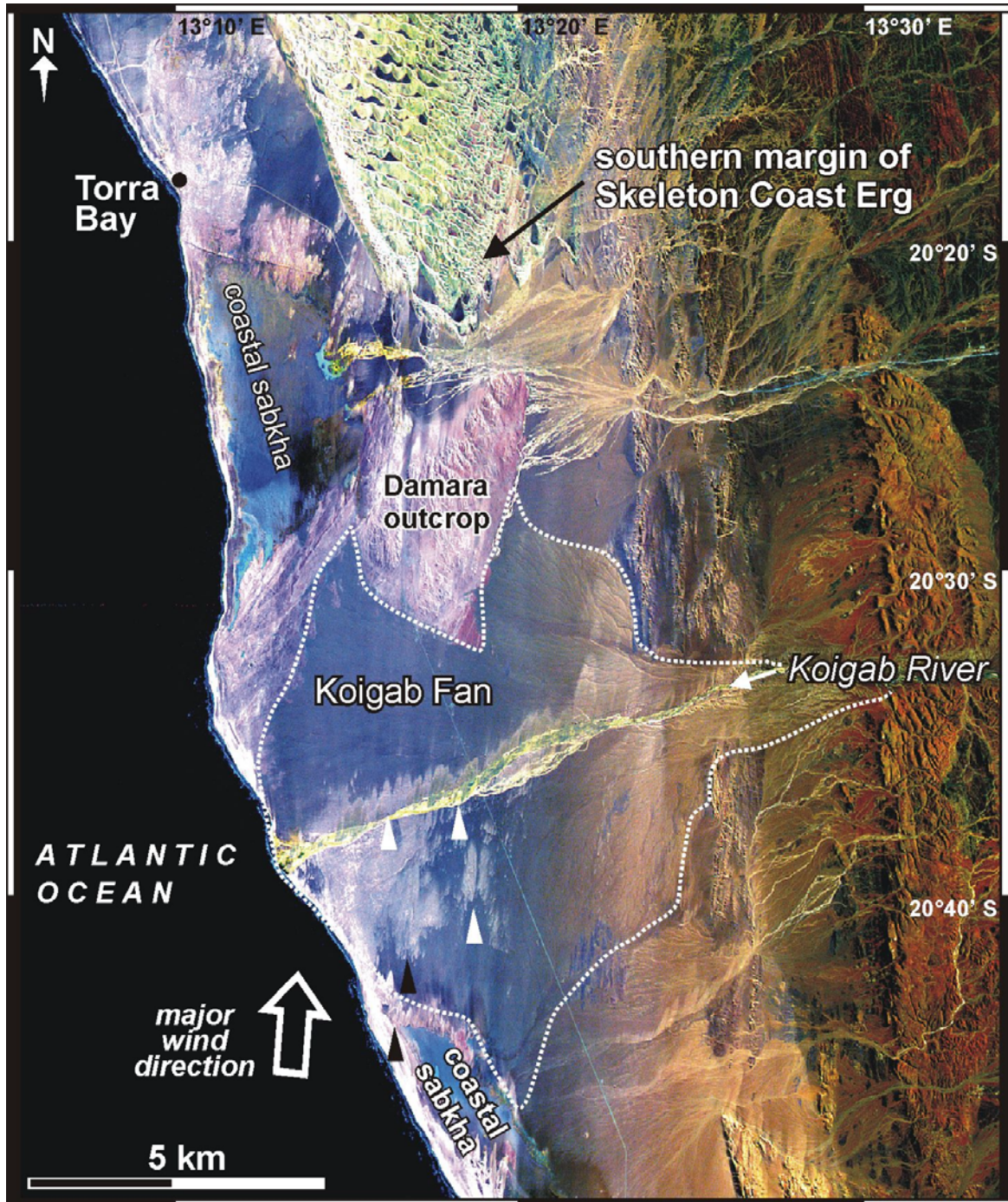
The Koigab River is situated 15 km south of the Skeleton Coast Erg (Figs. 6.2 & 6.3). With a length of 130 km and a catchment area of about 2,400 km<sup>2</sup>, of which only 2% receives a mean annual rainfall >100 mm, this river is one of the smallest of the Skeleton Coast ephemeral rivers (JACOBSEN et al., 1995).

The modern Koigab River (Fig. 6.4) provides the active channel system of the braided river dominated Koigab Fan (see also Chapter 4), covering an area of about 135 km<sup>2</sup> (VAN ZYL & SCHEEPERS, 1993) and extending over about 15 km from the Sugar Loaf Hill towards the Atlantic coastline. The Koigab Fan consists mainly of semi- to unconsolidated sand and gravel with an estimated midfan thickness of at least 30 m. Its existence is due to the special source area provided by the Etendeka Plateau comprising a thick sequence of Early Cretaceous flood basalts and interleaved quartz latites.

The modern fan surface is modified by both fluvial and aeolian processes. The majority of the gentle sloping (gradient ~1:90) braided river dominated fan (KRAPF et al., 2001, in



press) appears as a vast deflation surface on which lithic pebbles are concentrated by wind removal of fines. Within the deflation surface, however, the morphology of long abandoned (southern half of fan) and more recently abandoned (northern half of fan) radial channels can still be discerned.



**Fig. 6.4:** Landsat TM-5 image 181-074 (30.03.1995; 7-4-1, R-G-B) of the Koigab Fan. The active channel (Koigab River) bisects the fan and incises into the fan surface, the least at the coast and the most at the fan apex. Sandy material is winnowed by the strong onshore southerly wind from the beach and the Koigab River onto and over the fan surface. The winnowed material is deposited in the lee side of the Damara outcrop and added to the Skeleton Coast Erg. Figure also shows the network of long abandoned (southern half of fan) and more recently abandoned channels (northern half of fan) on the fan surface.



The presently active Koigab channel bisects the fan along its central axis. It is incised into the fan surface the least at the coast and the most at the fan apex. The channel extends headwards into the Etendeka Plateau to generate pronounced channel incision of about 24 m at Koigab Canyon Poort, 20 km east of the coast.

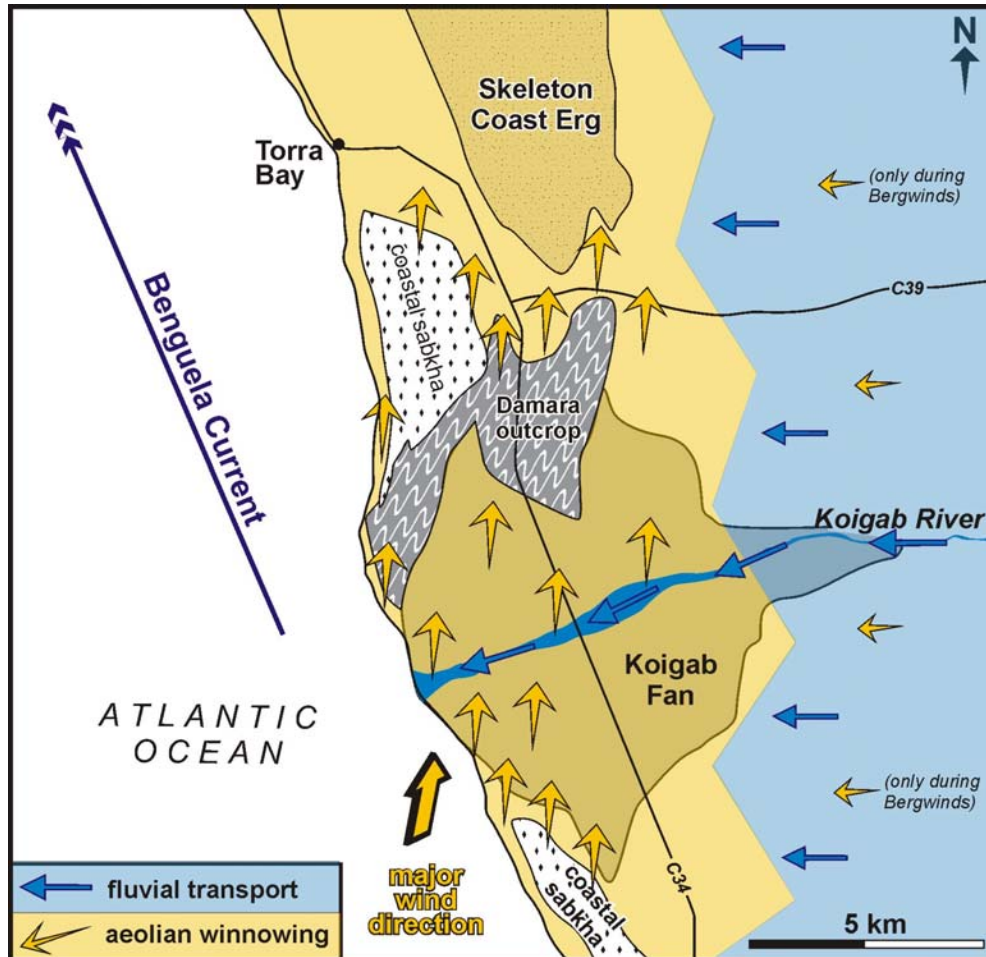


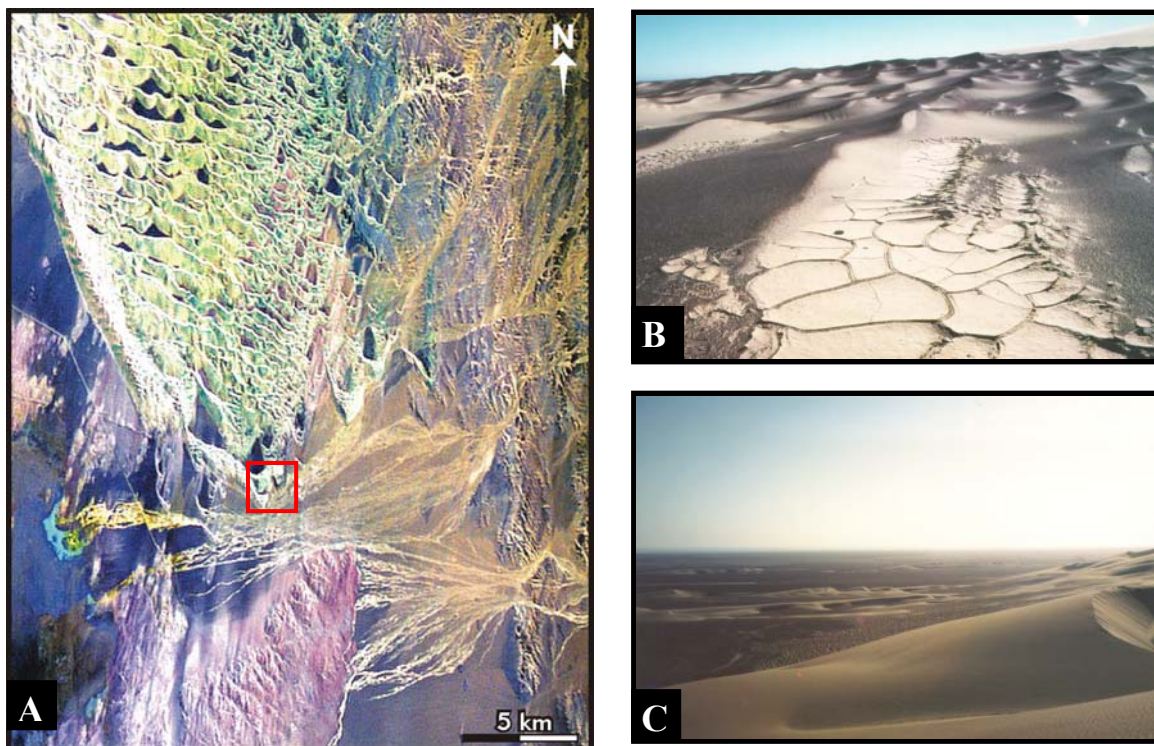
Fig. 6.5: Figure demonstrating the modification of the Koigab Fan by fluvial and aeolian activity.

The area of the Koigab Fan farther downstream provides considerable information concerning sources for sediment input into the nearby Skeleton Coast Erg. The modern river system is dominated by channelized flow in numerous shallow braided river channels. Volcanic clasts and grains from the Etendeka volcanics brought into the system by the river and quartz grains are blown onto the fan from the beach near the southern margin of the fan (Fig. 6.5). The resulting deposits serve as an important source of aeolian sand added to the erg through the action of the predominant south-southwesterly onshore winds. The dominant sedimentary process in the drainage area is aeolian winnowing of fluvial sands during long-lasting inter-flood intervals. Small shrub coppice dunes fixed by bushes of *Salsola spp.* and sand ramps cover the fan surface. Coarse-grained sand, rich in

volcaniclastic components, accumulates behind obstacles, in front of the downwind channel cutwalls and within shallow abandoned channel depressions, locally forming zones of large wind ripples. Many shrub coppice dunes and barchans are developed in intra- and inter-channel areas. Sand provenance has been determined from heavy mineral assemblages and the microscopical and chemical characteristics of heavy minerals discriminative of Etendeka and basement source rocks (SCHLICKER, 2000b; KRAPF et al., 2000; see also Chapter 4.3.3).

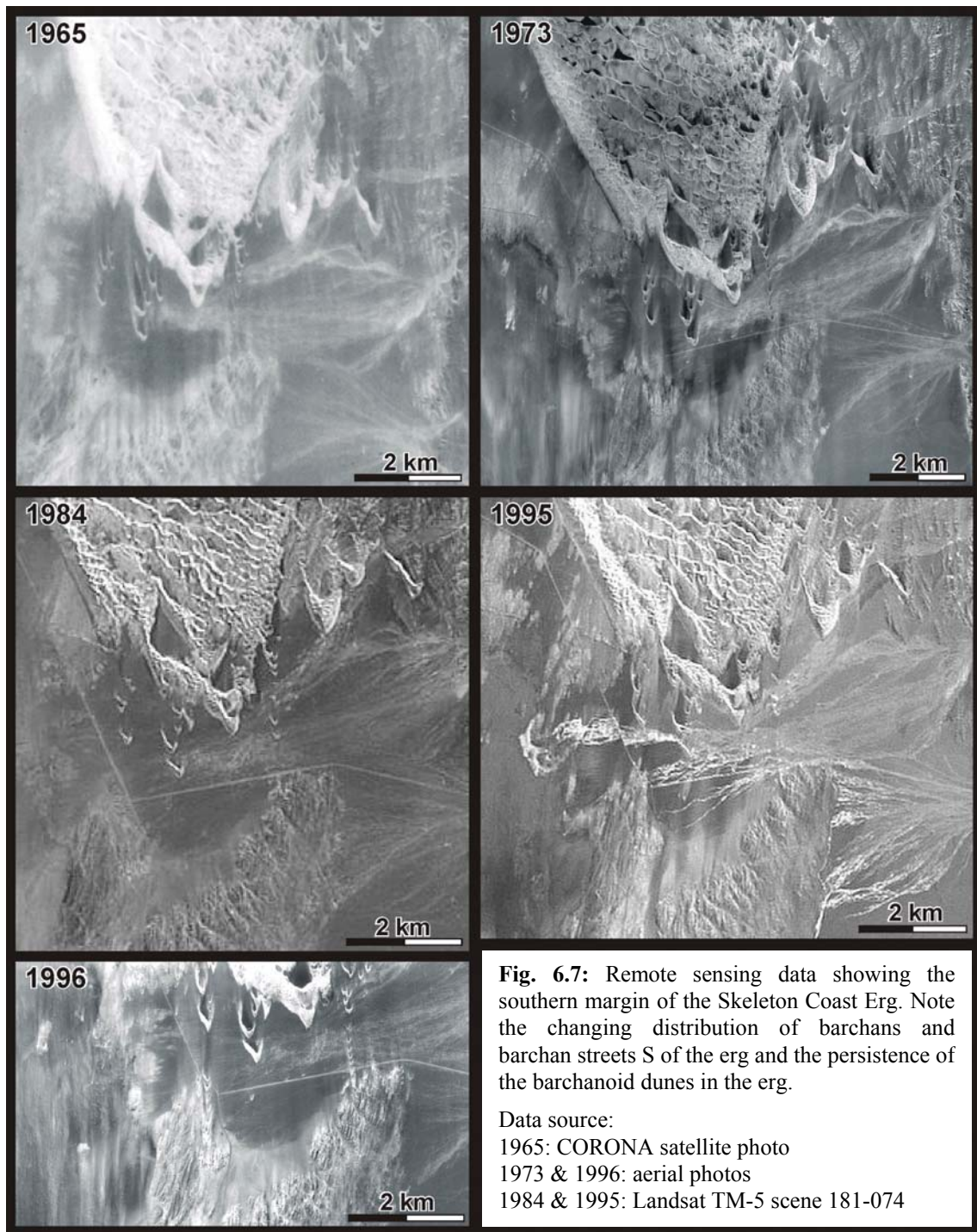
### 6.2.2 Southern margin of the Skeleton Coast Erg

Barchans and barchan trains are quite frequent farther north, towards the southern sand input area of the Skeleton Coast Erg (Fig. 6.6 C). There, isolated barchans and barchan trains can be identified, that migrate into the erg (LANCASTER, 1982), particularly during dry periods following floods. Major floods such as those in late March/early April 1995 flushed the barchans (Fig. 6.6 A & B) and rejuvenated the channel network on the fan (Fig. 6.7, 1995), generating new areas for aeolian reworking and deflation in the aftermath of the flooding (Fig. 6.7, 1996).



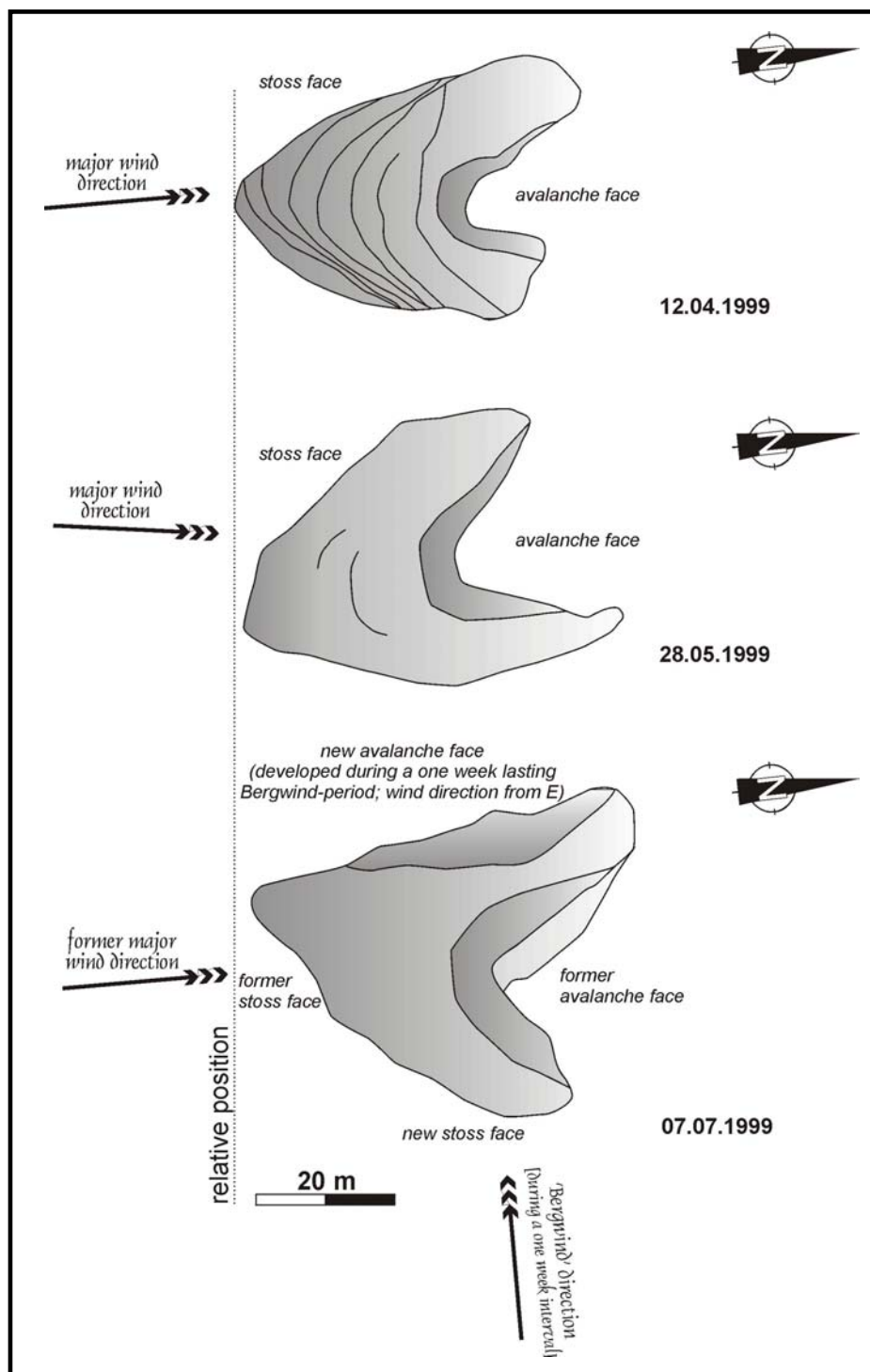
**Fig. 6.6:** **A:** Landsat TM-5 scene 181-074 (30.03.1995; 7-4-1 RGB) showing the southern margin of the Skeleton Coast Erg one month after the big flood of February, 1995. The barchan trains are washed away by smaller ephemeral streams issuing from the adjacent Sugar Loaf Hill. Box indicating position of Fig. 6.6 B. The water was partly dammed behind the barchans forming small flood ponds. Mud deposits drape the stoss face of the barchans (**B**) and can be found up to 5 m above the surrounding deflationary coastal plain. **C:** View towards W of the southern margin of the erg in June, 1999.



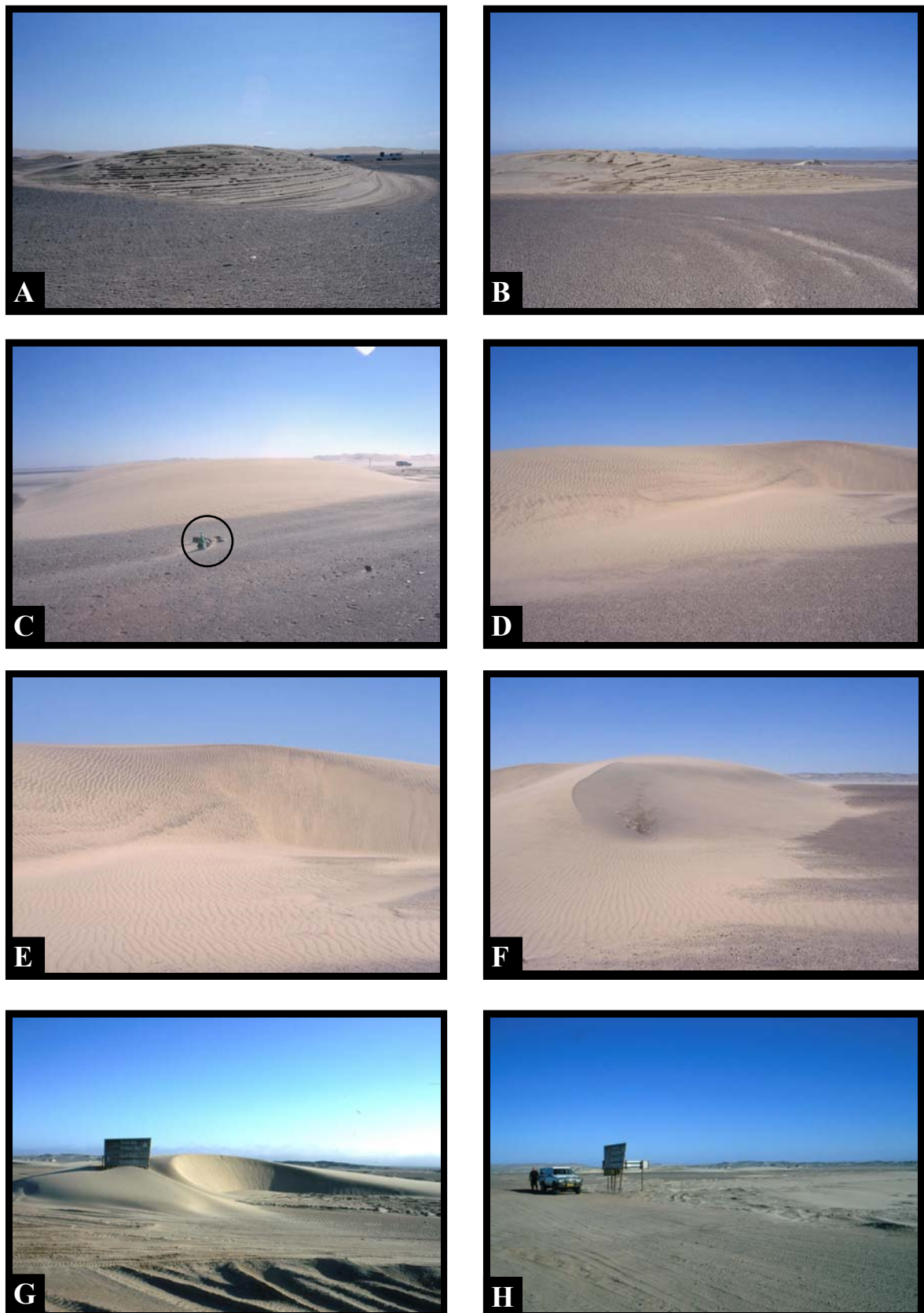


During field work in 1999 one barchan was mapped in detail three times during a three months period using a plane table. This documents the dynamic shape change of such aeolian landforms at the southern margin of the Skeleton Coast Erg during short time periods. The surveyed barchan was situated during the observation period directly west of the T-junction of the two main roads (C34/C39) of the Skeleton Coast Park (S 20°23'27", E 13°17'57") about 15 km S of Torra Bay. Figs. 6.8 and 6.9 show the changes of the barchan morphology. During the survey period the barchan has moved about 3,80 m northward. In

the first week of July 1999 the Skeleton Coast experienced one week of strong, dry and hot 'Bergwinds'. During this time the previous stoss and avalanche face was strongly modified and new ones developed aligned to the easterly winds. As these easterly winds operate only for a couple of days these modifications are short time features. Several days after the 'Bergwind' ceased, the original barchan shape with orientation of the slip face towards NNE reformed. Furthermore, the outline of the barchan increased.



**Fig. 6.8:** Sketches of the investigated barchan (S 20°23'27", E 13°17'57") showing the morphological changes and its movements during a three months period.

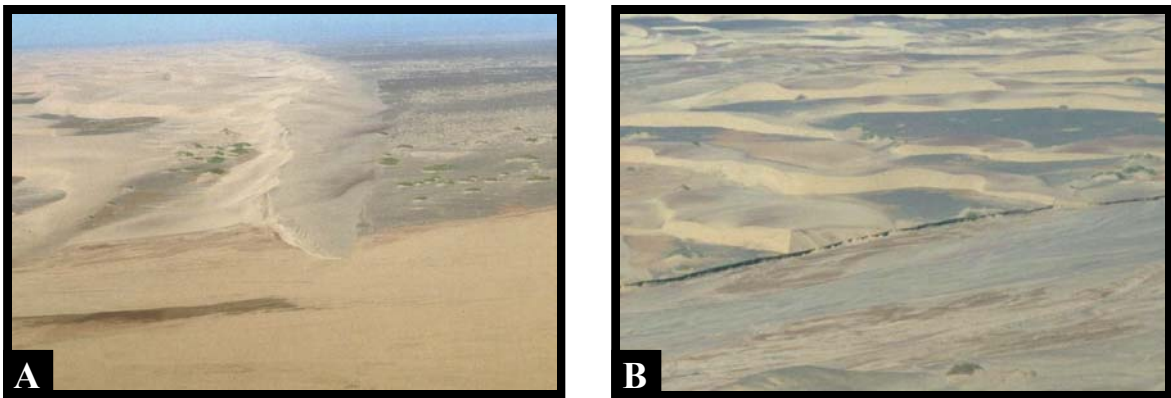


**Fig. 6.9:** A+B: Photo showing the investigated barchan at 12.04.1999 (A: view towards ENE; B: towards W). C-F: Appearance of the barchan three month later on 07.07.1999 during 'Bergwind'. C: The modified former stoss face, view towards ENE; circle indicates marked position of barchan foot at first measurement in April 1999. D+E: Showing the modified former avalanche face; view towards SSW. F: Illustrating the newly developed avalanche face on the western side of the barchan. G: Position of the barchan in 2000 ca. 25 m away from position in A. H: After having passed the traffic sign the barchan was removed by bulldozers in April 2002.



### 6.3 Uniab

The Uniab River is about 110 km long and drains a 4.500 km<sup>2</sup> catchment area with only 2,3% of the area receiving mean annual rainfall of >100 mm (JACOBSEN, et al. 1995). It is located about 20 km north of the southern erg margin. The limited dune belt width (about 7 km) and average dune heights of less than 30 m, are not a substantial barrier to river flow. The sharp western margin of the dune belt is formed by a pronounced dune wall with a large slip face to the east (Fig. 6.10 A). Dune forms, heights and crest to crest spacings are not uniformly developed across the belt as a whole. The largest crescentic dunes, often compound in form, are up to 30 m high and spaced at average intervals of greater than 200 m and are found along the western and central part of the erg (LANCASTER, 1982). Towards the east, in contrast, barchanoid dunes dominate and dune heights decrease to an average of less than 15 m (LANCASTER, 1982). The dunes are superimposed on the coastal plain deflation surface which is well exposed in many interdune areas (Fig. 6.10 B).

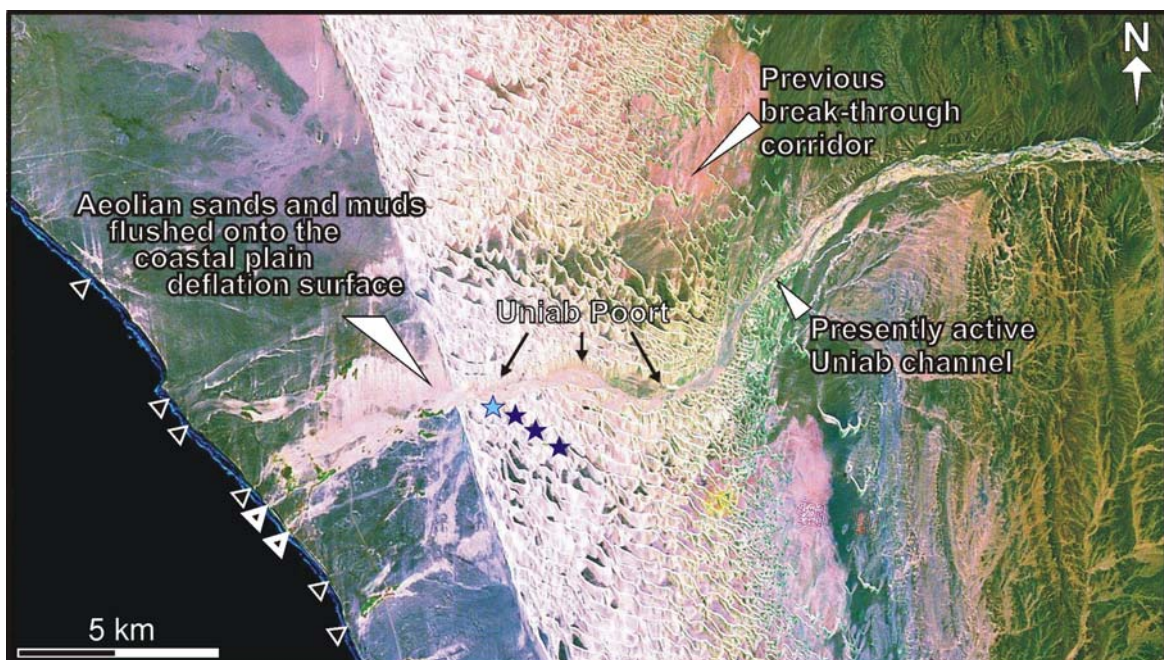


**Fig. 6.10:** **A:** The pronounced dunewall at the western margin of the Skeleton Coast Erg which is disturbed by the break through corridor of the Uniab River. **B:** Showing the corridor of the Uniab River through the Skeleton Coast Erg two weeks after the flood in April, 2000. The barchanoid to crescentic dunes are superimposed onto the deflation surface, which is exposed in the interdune areas (darker colour).

Considerable down-cutting of the river into the erg is reflected by a broad corridor through the erg where fluvial processes dominate (Fig. 6.10 B). Healing of aeolian dune forms requires considerable time after each flood event. Aerial photographs and satellite images covering the last 35 years reveal the continuity of the river bed through the erg. The trace of the river course is always obvious, even during periods when no flood runs downstream for many years. Such inter-flood periods can have considerable duration, only in early April 1995 did the Uniab River break through the dunes which had blocked its path to the sea for 13 years since 1982 (JACOBSEN et al., 1995). Since then, minor floods in March 1997 and in April 2000 flushed the river course and prevented healing of the dune belt.

Even 2 years after the 1995 flood, the 1997 flood found only dune forms in the river channel which were less than 2 m high.

Fig. 6.11 shows the area where the Uniab crossed the erg during early April 1995. The presently active channel route is clearly indicated by aeolian sand and mud flushed out of the dune barrier and distributed over the adjacent coastal plain deflation surface. The satellite image also shows, however, an earlier major breakthrough corridor of the Uniab about 2 km to the north and the channel followed by the Uniab to enter that corridor. The width of this former breakthrough corridor varies from 800 m in the west to 2700 m in the east. This indicates enhanced healing of the corridor on the western erg margin where the prevailing SSW onshore wind has greatest effect. A remnant patch of sand and mud flushed onto the coastal plain is clearly visible at the mouth of the earlier breakthrough corridor (arrows in Fig. 6.11). To the south of the presently active Uniab channel other previous break-through corridors have been buried by dune migration. Excavated interdunal mud-draped floodponds (Fig. 6.12) originally filled from adjacent river channels (cf. STANISTREET & STOLLHOFEN, 2002) mark areas, where such earlier break-through corridors existed (BLÜMEL et al., 2000; SVENDSEN et al., in press).



**Fig. 6.11:** Landsat TM-5 image 181-074 (30.03.1995; 7-4-1 RGB) of the Uniab River, showing the presently active channel (centre of image) and an ancient flood corridor through which the Uniab has passed through the erg. Small arrows in the coastal area west of the erg mark active (bold) and abandoned channels. Light blue star locates recent flooding of an interdune area during April 2000 flood (see Fig. 6.8) and dark blue stars locate paleo-interdune pond deposits.

Characteristic sediments resulting from previous flood events comprise not only normal stream flow and interdunal flood pond deposits (Fig. 6.13 A-C) but also intra erg mass flows (SVENDSEN et al., in press) and isolated very large boulders (SCHEEPERS & RUST, 1999) up to 5 m in diameter (Fig. 6.12).



Degraded terrace remnants of thin interbedded mud and sand units that sit

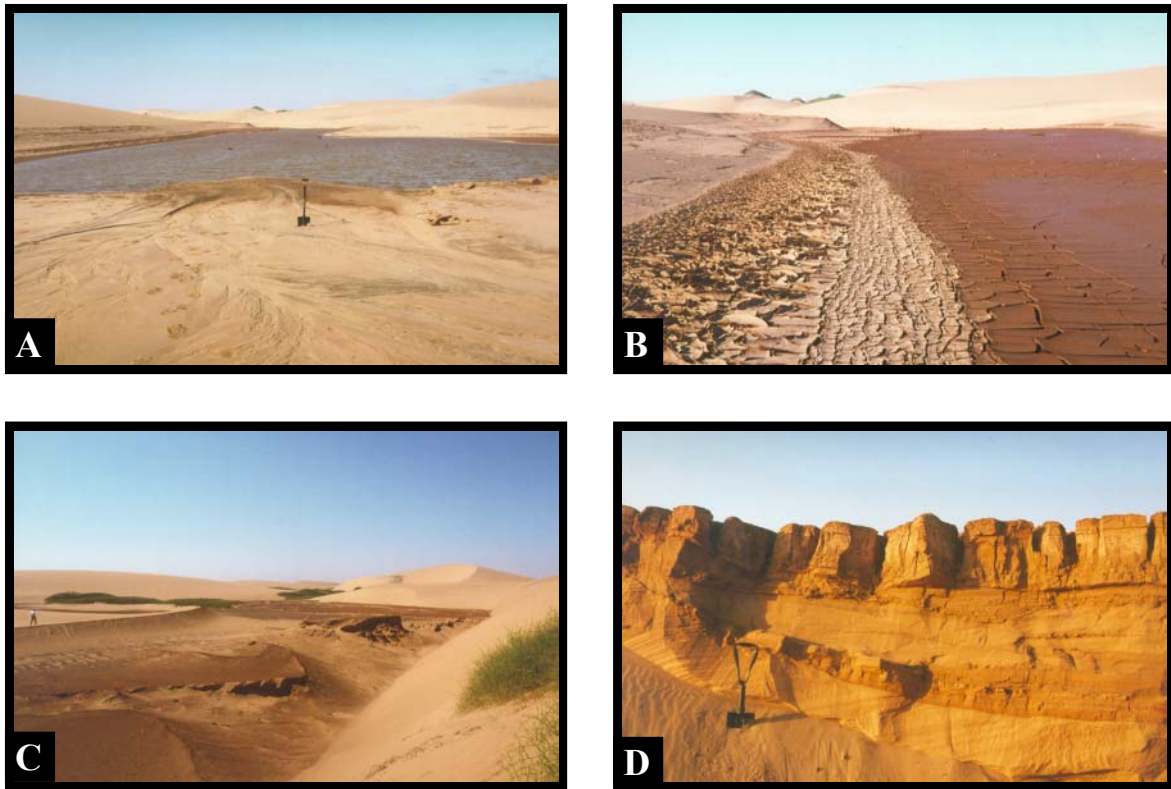
**Fig. 6.12:** An isolated granite boulder about 1.5 km W of the erg on a terrace 1.5 m above the present day Uniab River river bed.

on rocky deflation surfaces are widespread immediately east of the area where the river enters the erg. They are interpreted to have resulted from suspension-fallout in a dune-dammed flood basin when the dune barrier prevented the river from crossing the erg.

Uniab Poort terms the area where the Uniab River breaks through the Skeleton Coast Erg (see Fig. 5.1). In the interdune areas along the Uniab break-through corridor several outcrops of fluvial and aeolian sediments were exposed in freshly exposed cutwalls of the modern day break-through corridor after the flood event in April, 2000. Detail studies of these sediments were undertaken in cooperation with J. Svendsen (Univ. Arhus) during jointed fieldwork in April 2000 (Fig. 5.13 D). These studies show that the sediments exposed in the Uniab Poort comprises a wide variety of fluvial and aeolian facies from which the intra-erg mass flow deposits are of major importance (SVENDSEN et al., in press). SVENDSEN et al. (in press) introduced this term for moderate to well sorted medium-grained deposits which are characterized by the absence of sedimentary structures and the lack of erosional capacity. They reach thicknesses between 0,2 and 3,0 m and have a lateral extent between 40 to 60 m. The intra erg mass flows - using the criteria defined by BEVERAGE & CULBERTSON (1964) - can also be classified as hyperconcentrated flow deposits and are lithologically and texturally comparable to facies Sm of the Uniabmond Formation. The presence of smectite as the dominant clay mineral proved to be of crucial importance in formation of such mass deposits (PIERSON & COSTA, 1987; SVENDSEN et al., in press). This clay mineral form by weathering of basalts, which built up vast parts of the Uniab River catchment. Only 3 Vol. % clay matrix is necessary to initiate hyperconcentrated flows, whereas < 13 Vol. % clay matrix are necessary if the dominating clay mineral is kaolinite or illite (PIERSON & COSTA, 1987). This is the reason for the



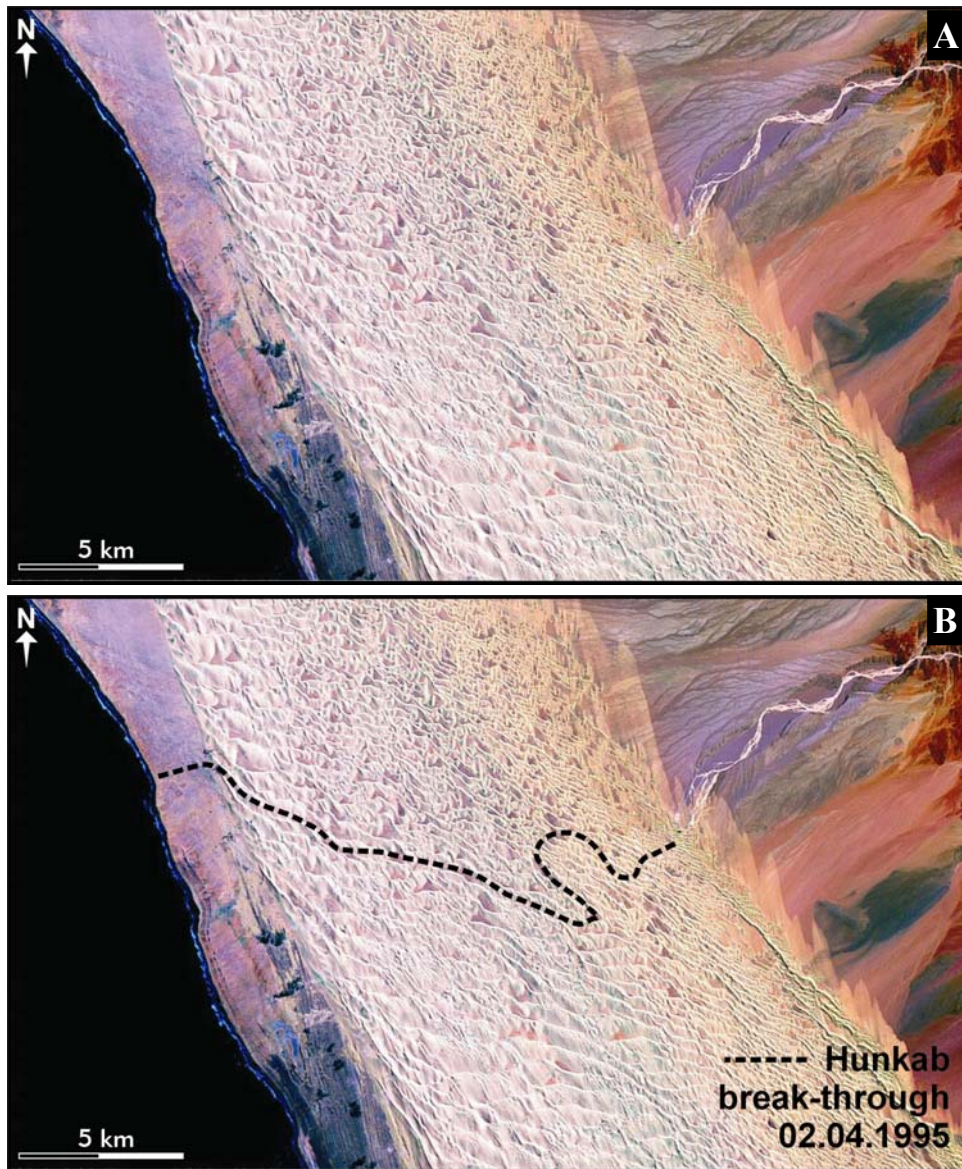
augmented occurrence of hyperconcentrated flow deposits in the lower reaches of the Uniab River.



**Fig. 6.13:** **A:** Flooded interdune area (indicated by light blue star in Fig. 6.7) during April 2000 flood. **B:** Same area two weeks later. **C:** Stacked muddy interdune flood pond deposits preserved in a channel-centred flood halo south of the presently active Uniab channel (location marked in Fig. 6.7 with dark blue stars). The lowermost mud layer is 12 m above the base of the presently active Uniab channel and registers a period of pronounced dune damming and elevated base level. Such mud layers record dune field flooding and the vertical stacking reveals that the river system did not breach the dune dam at those times. **D:** Outcrop of interdune-pond deposits draping aeolian dunes preserved in the cutwalls of the modern day break-through corridor of the Uniab River.

#### 6.4 Hunkab

The Hunkab River has a much shorter river course (90 km) with a very small catchment ( $\sim 700 \text{ km}^2$ ) receiving mean annual rainfall below 100 mm. For long periods the river course was blocked by the about 15 km-wide accreted erg, comprising mainly large, 30-50 m high, compound crescentic dunes. The satellite image taken in late March 1995 (Fig. 6.14 A) reveals no permanent river course traceable through the erg and no substantial flood reservoir developed east of the dune belt. However, as with the Uniab, degraded terrace remnants of thin ( $< 1 \text{ m}$ ) but originally widespread interbedded mud and sand horizons are obvious immediately east of the river entry into the erg cf. (BLÜMEL et al., 2000; their Fig. 6, p. 47).

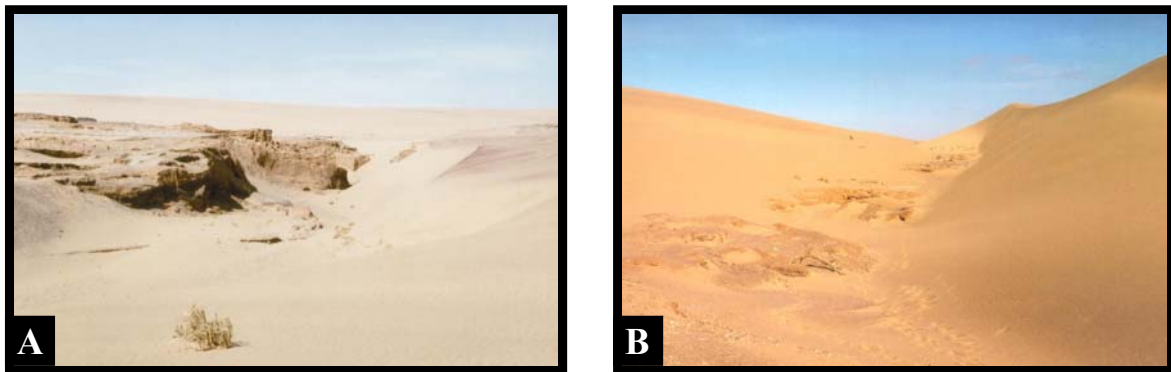


**Fig. 6.14:** **A:** Landsat TM-5 image 181-074 (30.03.1995; 7-4-1 RGB) of the Hunkab River. No permanent river course is traceable through the erg. **B:** Same satellite image, break-through corridor of April, 2000 flood is added. The water was guided along the avalanche faces of the transversal dunes during break-through.

Break-through of the Hunkab River is only recorded twice in the 20<sup>th</sup> century, in April 1995 (JACOBSEN et al., 1995) and in March 2000 (own observations). The major flood in 1995 (Fig. 6.14 B) came through on the night of the 2<sup>nd</sup>/3<sup>rd</sup> April and by the morning of the 3<sup>rd</sup> April the flood had completely abated (WARD et al., 1997). On the seaward side of the dunes, the river cut a new canyon, some 10 to 15 m deep with interbedded fluvio-aeolian deposits exposed at the base of the cut walls recording previously successful dune breaks (WARD et al., 1997). Satellite images and aerial photograph interpretation provide the information that shortly after breakthrough the newly initiated river valley was soon re-occupied by aeolian sand dunes. During and following the break-through large amounts of



sand, silt and huge blocks (>10 m) of semi-consolidated dune sands (JACOBSEN et al., 1995; their Fig. 2, p. 118) were transported and deposited west of the erg. The canyon through which the river issued from the erg at its western side was still recognizable prior to the minor April 2000 floods, 5 years after the initial breakthrough (Fig. 6.15A). Healing of the dune barrier is also more effective towards the western margin, where large dunes had re-occupied most of the Hunkab channel only 1 year after the April 2000 flood.

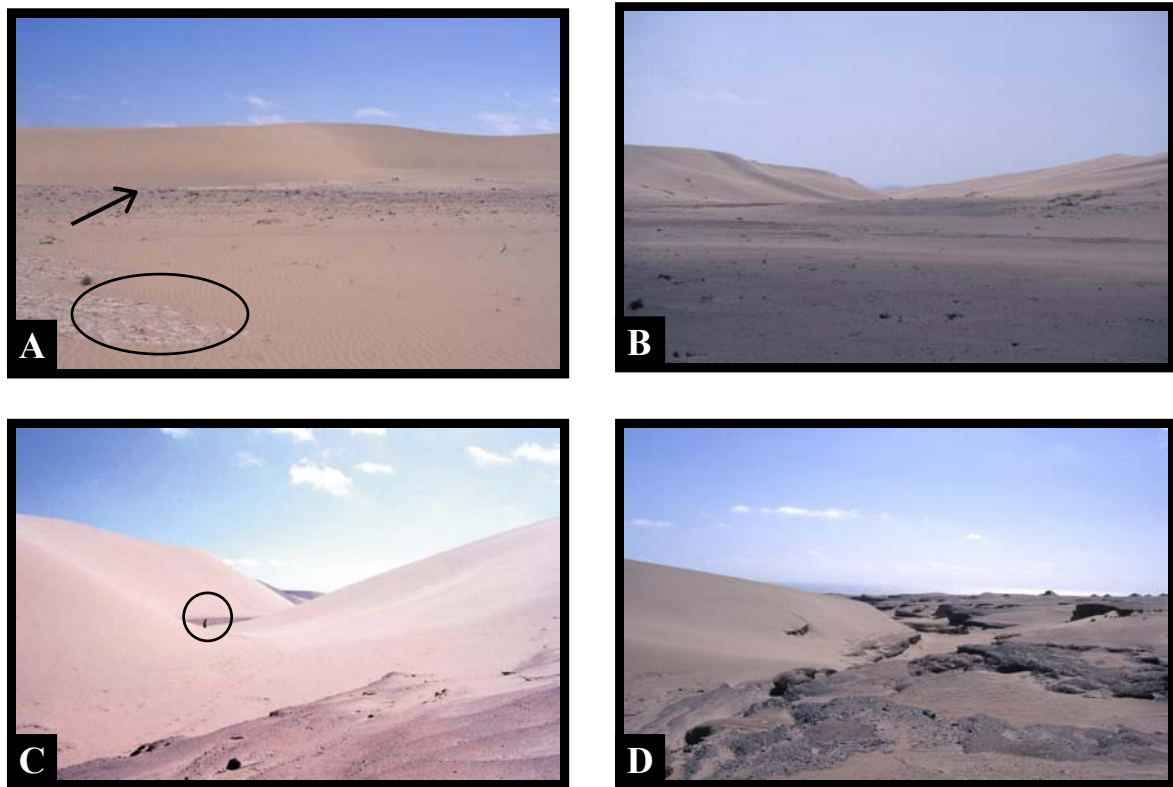


**Fig. 6.15:** **A:** Photo showing the Hunkab river bed west of the margin of the Skeleton Coast Erg five years after the flood of 1995 (view towards E). **B:** The pronounced dunewall at the western margin of the erg reestablished only a few month after the big flood of 1995 and the river bed of the Hunkab was covered by dunes (view towards ESE).

Less successful attempts of the river to breach the dune barrier are recorded near the eastern margin of the erg. There, thick (>3m) sandy hyperconcentrated flood flow deposits are overlain by multiple desiccation-cracked mudlayers which settled out from suspension during waning flood conditions. Finally, aeolian sand sheet deposits form an elongate tongue-shaped sediment body, penetrating deeply into the heart of the erg (BLÜMEL et al., 2000; their Fig. 8, p. 49). It has been suggested, that these sediments were deposited when an earlier Hunkab flood failed to break completely through the dune barrier with the flood dying away only 1 km away from the western border of the dune belt. Due to efficient dune damming, river transport capacities dramatically dropped and the river released most of its load *en masse*, draping and partly infilling its own previously cut flooding corridor through the dune belt (BLÜMEL et al., 2000). The thin but widespread waning-flood mudlayers are important as they are resistant to wind as well as other types of erosion. Sandy fluvial deposits, which are not protected by overlying mud layers are winnowed and quickly eroded by southerly winds funnelled sub-parallel to the eastern margin of the erg. The 1995 flood benefited from the pre-existing impermeable mud seals generated by failed break-through attempts. From comparison to the Hoanib River (STANISTREET & STOLLHOFEN, 2002) it can be speculated that the mud layers largely prevented flood water

from seeping into the permeable aeolian sands and that the resulting build-up of water successfully allowed the 1995 flood to pass through the entire dune belt.

During field work in 2001 an excursion to the Hunkab River east of the Skeleton Coast Erg was undertaken. As the Hunkab broke through the erg in 2000 an attempt was made to passage the break through corridor of the previous flood.



**Fig. 6.16:** **A:** Flood pond with mud deposits (circle) and plenty driftwood (arrow) of the Hunkab River at the eastern margin of the erg. Hunkab break-through channel in the central part of the erg one year after April 2000 flood. **B:** Visible channel of former break through in central part of the erg. **C:** Narrowed passage of former break through channel by moving dunes (person for scale, see circle). **D:** Incised Hunkab River valley at western margin of Skeleton Coast Erg.

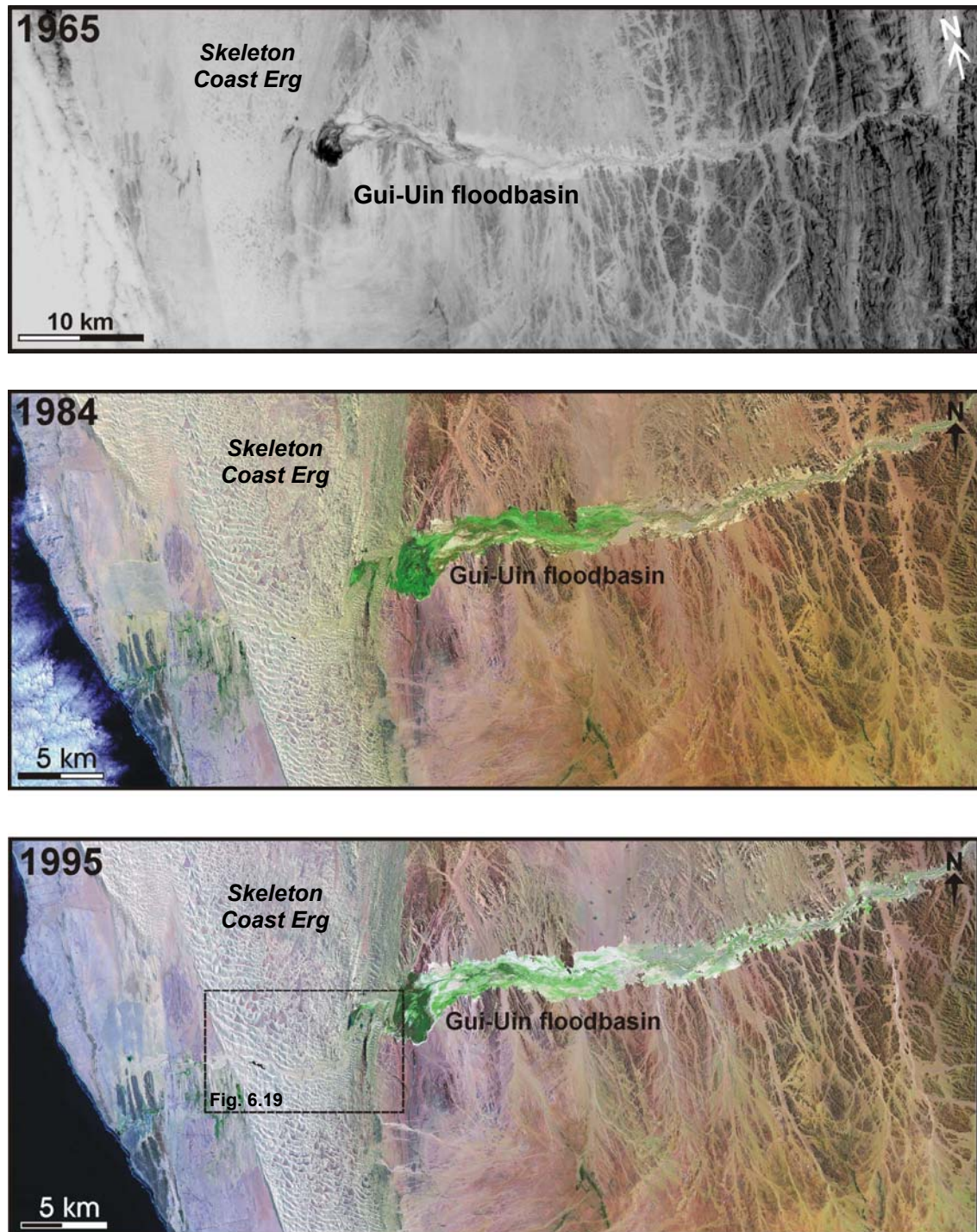
At the eastern margin of the erg a labyrinth of blind valleys ending in dune-encircled dried-up flood ponds made it extremely difficult to locate the main break through channel (Fig. 6.16 A). In these ponds driftwood was deposited up to 2.20 m above the dune foets indicating flood highstands (Fig. 6.16 A, arrow). Heading to the W the passage through the up to 150 m wide channel was still passable one year after the flood (Fig. 6.16 B). Some parts of this corridor narrowed and were partly covered by moving dunes (Fig. 6.16C). At the western margin of the dunefield the Hunkab River has incised into previous deposits forming a waterfall-like morphology with deep scours and potholes (Fig. 6.16 D). The

prominent western dunewall forming the western margin of the Skeleton Coast Erg already started to recover and refill the break through corridor there.

### 6.5 Hoanib

The Hoanib is the second largest ephemeral river interacting with the Skeleton Coast Erg. The river extends over a length of 270 km, draining a 17.200 km<sup>2</sup> catchment area of which 72% receives average rainfall of >100 mm/a and 12% >300 mm/a (JACOBSEN et al., 1995). The 20 km wide erg comprises transverse dunes up to 50 m in height and efficiently blocks the river, which, therefore, formed the extensive 15 by 4 km Gui-Uin floodbasin (Fig. 6.17) east of the dune barrier (STOLLHOFEN & STANISTREET, 1997; STANISTREET & STOLLHOFEN, 2002).

Figs. 6.17 A & B illustrate some effects of the 1984 and 1995 floods. The active Hoanib channel is clearly displayed through the erg and widespread overbank deposition of mud in the upstream area of the Gui-Uin floodbasin indicates the pronounced damming effect of the dune barrier. Thick accumulations of mud layers are developed in the floodbasin and a lush vegetation of tamarisk and other bushes can be found (Fig. 6.18). Only exceptional rainfalls provide water discharges high enough to break through the dune belt. During the last 64 years, such floods occurred on a nine years average (STOLLHOFEN et al., 1999). Since 1984 the Hoanib broke through the dunes and reached the Atlantic only three times in 1995, 1997 and 2000 (STANISTREET & STOLLHOFEN, 2002). In late February 1995 high discharge floods initially built up a lake behind the dune barrier for several days until the water-level within the extensive flood reservoir basin was high enough to overtop the dune lowpoints. The morphology of the transversal dunes then guided the river through the erg and provided access for passive lateral flooding into interdunal areas. There, floodwater clays infiltrated into the sediments of the interdunal areas and settled to form impermeable seals, on top of which perched several floodponds, particularly south of the active river course (STANISTREET & STOLLHOFEN, 2002). Measured floodponds were >1 km in length (Fig. 6.19) and were seen to exist for considerable periods of >3 years (Patterson 2000, pers. comm). Subsequent floods in 1997 and 2000 refilled these ponds, benefiting from the pre-existing impervious seals (STANISTREET & STOLLHOFEN, 2002).



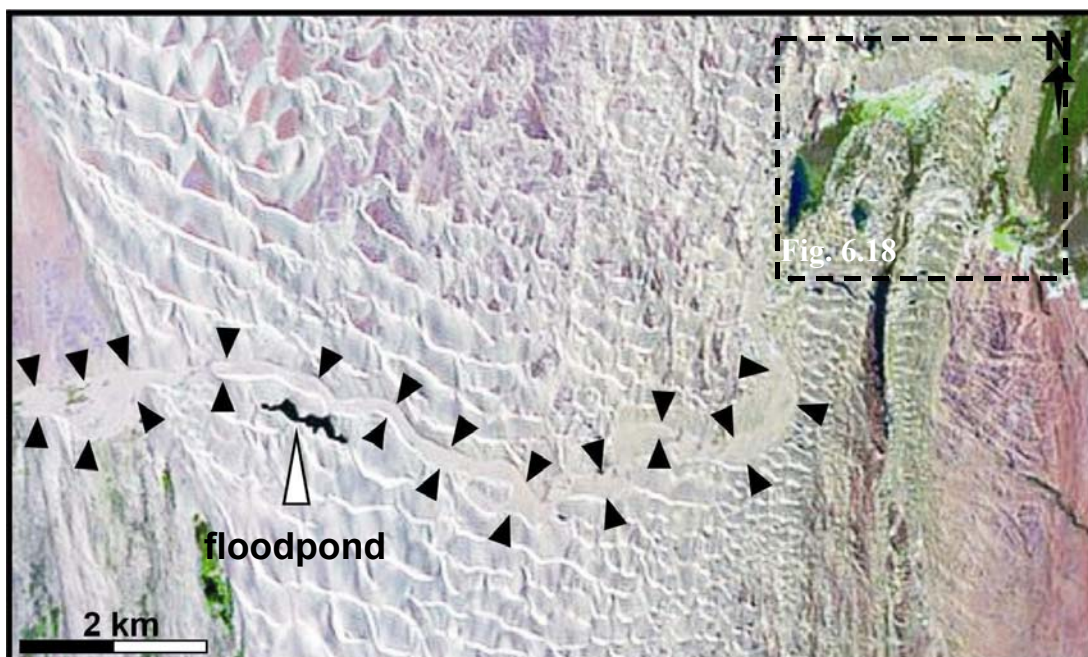
**Fig. 6.17:** Comparative images of the Hoanib River. **A:** Two years after the big flood of 1963 (CORONA satellite picture 1965). **B:** After flooding in 1984 (Landsat TM-5 scene 22.08.1984; 7-4-1, R-G-B). **C:** After flooding in 1995 (Landsat TM-5 scene 30.03.1995; 7-4-1, R-G-B). Flushing of sand and mud beyond the river banks records the width of the flooded halo to both sides of the main channel way. Pronounced damming effects of the Skeleton Coast Erg are revealed by the presence of the Gui-Uin floodbasin with thick mud accumulations and development of lush vegetation (green colours in sat images) [box marks position of Fig. 6.18].





**Fig. 6.18:** Aerial photo (15.04.1997; H. Stollhofen) illustrating the anatomy, extent and lush vegetation of the Gui-Uin floodbasin (view toward ESE).

After a flood, aeolian activity soon affects the system. In the aftermath of the floods in 1995, 1997 and 2000 most of the low relief, flat-topped sandy fluvial bars were eroded by the wind leaving behind only isolated deflation lag gravels, wood debris, and mud layers. Aeolian dunes migrated slowly into the southern edge of the channel. Only a few weeks after the river became dry, the channel beds were already covered by low aeolian bedforms and barchanoid ripples. However, complete healing of the dune belt has been hindered by the frequency of the recent floods which have repeatedly flushed the river passage once the initial obstacle to their entry into the erg was removed.

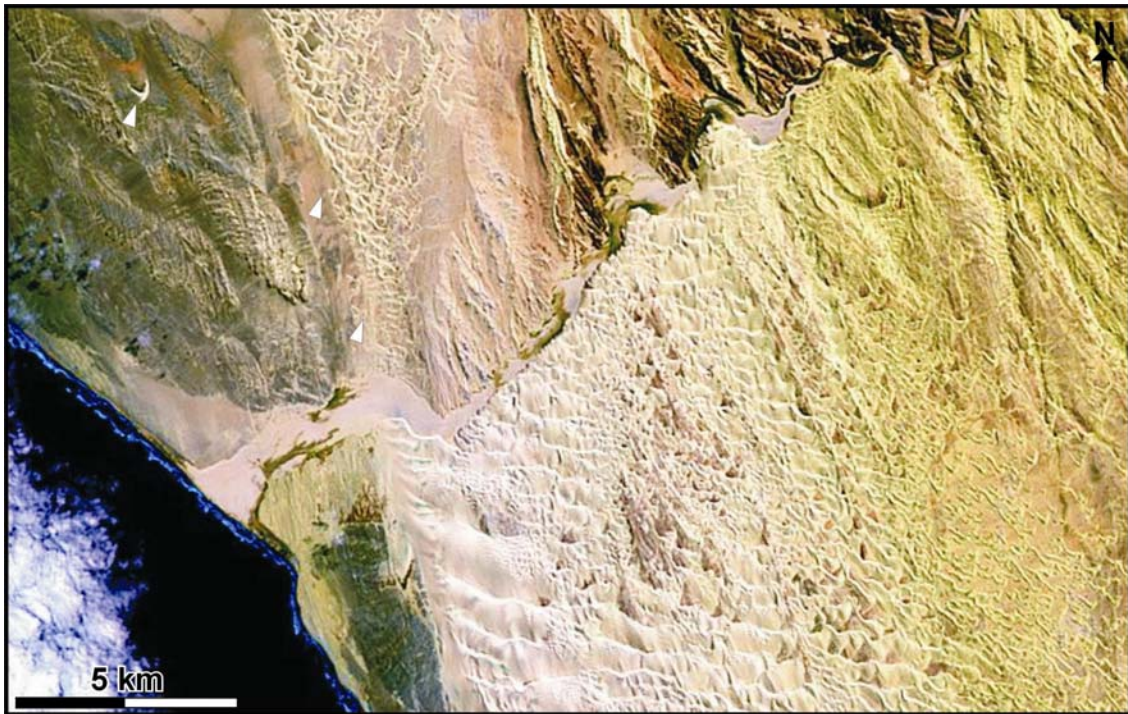


**Fig. 6.19:** Landsat TM-5 image 181-074 (30.03.1995; 7-4-1 RGB) of the break-through corridor of the Hoanib River after the big flood event of February, 1995. A <1 km long floodpond at the western margin of the Skeleton Coast Erg is indicated by the white arrow.



## 6.6 Hoarusib

The Hoarusib River is the second biggest of the larger ephemeral rivers affecting the Skeleton Coast Erg. The river is about 300 km long and is fed by a 15,100 km<sup>2</sup> catchment area of which 40% receives >100 mm and 8% >300 mm average annual rainfall (JACOBSEN et al., 1995). In contrast to the rivers discussed above, the Hoarusib flows quite regularly, reaching the sea almost every year because of its proximity to the intertropical convergence zone.



**Fig. 6.20:** Landsat TM-5 image 181-074 (22.08.1984; 7-4-1, R-G-B) illustrating how effectively the Hoarusib river valley reduces aeolian sand transport towards the north. The valley is less incised westwards and floods are less frequent, allowing aeolian sand to cross the river in small amounts (see arrows) within the coastal regions.

The Hoarusib supports large wetlands and a riparian forest along its banks (JACOBSEN et al., 1995). The upstream parts of the river valley are deeply incised and river flows are so frequent and of such high discharge that they are sufficient to almost terminate the northward advance of windblown sand (Fig. 6.20). This scenario was previously described from the Kuiseb River in the southern Namib (WARD, 1987; WARD & SWART, 1997). Like the Kuiseb, the Hoarusib allows aeolian sand to cross in its coastal region, where the valley is less incised and floods are not as frequent. There, a 1-2 km wide train of individual and linked barchans crosses the valley (white arrows in Fig. 6.20) and continues 25 km farther north to the Khumib River where aeolian transport is terminated (LANCASTER, 1982). An additional similarity to the southern Namib Sand Sea is that after its crossing of the Kuiseb

River near the coast around Walvis Bay, the Namib aeolian system is similarly terminated by the Swakop River near Swakopmund.

## **6.7 The river systems and their settings compared**

### **6.7.1 Similarities**

The Skeleton Coast rivers share significant similarities with regard to the processes of dune barrier breakthrough, but there are also important differences. The constants amongst the river systems are:

- the climatic setting
- the wind regime
- the river style

#### **6.7.1.1 Climatic setting**

The lower reaches and mouth areas of the investigated rivers are all situated in the hyper-arid setting of the Skeleton Coast with annual rainfall averaging less than 50 mm. Rainfall events in this setting are rare and quite spotted. Therefore, rainfalls in the lower reaches of the rivers rarely causes river flooding. Flooding is caused by rainfalls in the upper reaches of the river catchments, where annual precipitation increases up to 500 mm (JACOBSON et al., 1995). Rain is falling during the summer rainy season between December and April and river run off predominantly takes places during this period. But only exceptional rainfalls in the catchments causes big flood events like the one in February 1995. These rainfalls are associated with disturbances of the intertropical convergence zone and occur only in intervals of a couple of years (SHANNON et al., 1986; STOLLHOFEN et al., 1997).

#### **6.7.1.2 Wind regime**

The wind regime in the whole study area is dominated by the strong south-southwesterly onshore winds that control dune forms and aeolian sand transport (LANCASTER, 1982; see Chapters 1.3 & 4.3.3). LANCASTER (1982) show, that 98 % of the annual sand flow is from this direction. Wind from easterly direction, the Bergwind, which last only for short-periods of a couple of days, blow silt and mud out of the dried river beds and transport them over more than 100 km westwards on the Atlantic Ocean (see Chapter 1, Fig. 1.5).

### 6.7.1.3 River style

All described rivers in the study area are of ephemeral braided nature. Furthermore, the rivers have an overall west-southwestward flow direction and have to pass on their way to the Atlantic Ocean the Skeleton Coast Erg, which is orientated perpendicular to the river flow.

### 6.7.2 Differences

Differences become apparent when individual segments of the coast-parallel erg and the individual characteristics of the river systems are contrasted.

#### 6.7.2.1 Skeleton Coast Erg anatomy

The Skeleton Coast Erg is characterized by changes both parallel and perpendicular to its NNW-SSE strike in:

- dune belt width
- dune height
- dune spacing
- dune form
- interdune elevation

These are important control parameters of fluvio-aeolian interaction because the potential and type of ephemeral river break throughs depend on the damming efficiency of the dune barrier (LANGFORD, 1989; STANISTREET & STOLLHOFEN, 2002; KRAPF et al., 2003).

In the southern part of the erg barchanoid dunes, superimposed on the coastal deflation surface dominate whereas northeast of Terrace Bay and Möwebay (cf. Fig. 6.2) an aggraded erg with large compound transverse dunes up to 50 m high is developed (LANCASTER, 1982). In the same direction, the width of the dune belt widens discontinuously from about 7 km at the Uniab in the south to more than 22 km where it meets the Hoarusib in the north (Fig. 6.21).

Sections across the dune belt also reveal an apparent asymmetry: Along the eastern downwind margin of the erg, where sand supply is less, simple crescentic or barchan dunes, 3-10 m high with an average dune spacing of 150 m, are common (LANCASTER, 1982). In contrast, towards the western windward side of the erg where sand supply is

greater, large transverse and compound crescentic dunes, 30-50 m high, are developed. In places these are coalescing to form a 20-80 m high prominent longitudinal "dune wall" (LANCASTER, 1982; KRAPP et al., 2002) which separates the erg towards the west from the coastal plain (Fig. 6.21).



**Fig. 6.21:** Schematic sketch illustrating the anatomy of the Skeleton Coast Erg. At the western margin of the erg a 20-80 m high prominent longitudinal "dune wall" has formed, separating the dune field from the coastal plain.

Mean grain size of dune sands (1.7-2.2 phi) varies through the erg and shows no consistent fining trend from south to north but from southwest to northeast accompanied by an improvement of sorting trends in the same direction (LANCASTER, 1982). This pattern reflects the degree of the obliquity of the erg to the direction of sand supply and the availability of multiple source regions for aeolian sand throughout its length, each



providing new, relatively coarse and only moderately sorted “juvenile” as well as aeolian recycled fluvial detritus (LANCASTER, 1982).

In general, wind transport and fluvial transport are broadly perpendicular to each other. However, funneling of southwesterly winds by deeply incised river valleys such as those of the Hoanib and Hoarusib valleys in the northern part of the erg allow eastward directed aeolian transport with deposition of low aeolian bedforms as far as 50 km upstream of the main erg.

### 6.7.2.2 The catchment areas of the investigated ephemeral rivers

The most obvious variability between the rivers in the southern and northern part of the study area are due to:

- the size of the river catchment areas
- the amount and frequency of rainfall in their catchment areas
- the rock types exposed in their catchment areas
- their depositional architecture
- and their gradients in longitudinal profiles.

|   | Koigab             | Uniab              | Hunkab                    | Hoanib                                 | Hoarusib                               |
|---|--------------------|--------------------|---------------------------|--|--|
| Catchment area in km <sup>2</sup>                             | 2.400              | 4.500              | 700                       | 17.200                                 | 15.100                                 |
| River length in km  | 130                | 110                | 65                        | 270                                    | 300                                    |
| Elevation range in m  | 0-1571             | 0-1625             | 0-1220                    | 0-1821                                 | 0-1964                                 |
| Precipitation range in mm/a                                   | 0-100              | 0-125              | 0-50                      | 0-325                                  | 0-325                                  |
| River gradient over last 20 km in %                           | 0.98               | 1.18               | 1.68                      | 0.93                                   | 0.55                                   |
| Catchment area in % receiving rainfalls <100 mm               | 2 %                | 2.3 %              | <i>no data</i>            | 72 %                                   | 40 %                                   |
| Floodbasin  | ---                | ---                | ---                       | ✓                                      | ---                                    |
| Interdune flooding  | ---                | ✓                  | ✓                         | ✓                                      | ---                                    |
| Dominating duneform in the area of fluvio-aeolian intercation | ---                | barchanoid         | barchanoid to transversal | transversal                            | transversal                            |
| Persistent riverbed through erg                               | ✓                  | ✓                  | ---                       | ---                                    | ✓                                      |
| Exposed rock types in the catchment area                      | Etendeka volcanics | Etendeka volcanics | Etendeka volcanics        | Pre-Damara & Damaran metamorphic rocks | Pre-Damara & Damaran metamorphic rocks |

**Tab. 6.1:** Compiled overview of the characteristics of the investigated ephemeral rivers (composed after: JACOBSON et al., 1995; LANCASTER, 1982; MILLER, 1988).

#### **6.7.2.2.1 The size of the catchment areas**

The larger the catchment area, the more rainfall can be caught and the possibility of river run off and river flood increases. With 15.100 km<sup>2</sup> (Hoarusib) and 17.200 km<sup>2</sup> (Hoanib) the northern ephemeral rivers are fed from much larger catchments areas (JACOBSON et al., 1995). In contrast, the southern rivers have relatively restricted catchment areas (Hunkab: 700 km<sup>2</sup>; Uniab: 4.500 km<sup>2</sup>; Koigab: 2.400 km<sup>2</sup>; JACOBSON et al., 1995). Therefore, the rivers in the northern part of the study area flow more frequently and experience higher flood pulses than the southern ones.

#### **6.7.2.2.2 Precipitation in the catchment areas**

The northern catchments (Hoarusib & Hoanib) receive much higher average annual rainfall (Tab. 6.1) and exceptional rainfall events causing floods are also favoured because of their proximity to the intertropical convergence zone. In addition, larger areas of these catchment areas receive rainfalls over 100 mm/a (Hoarusib: 40 %; Hoanib: 72 %) and even smaller parts receive rainfalls over 300 mm/a (Hoarusib: 8 %; Hoanib 12 %) (JACOBSON et al., 1995).

The combined effects of catchment size and rainfall availability are expressed by relatively short infrequent ephemeral flows in the south but higher discharge and more frequent flows in the north. As a consequence of more frequent river flows, thick mud accumulations associated with abundant vegetation characterize the Gui-Uin flood-reservoir basin of the Hoanib. In the case of the Uniab and Hunkab Rivers, less frequent river flows do not support thick mud accumulations in dune-dammed floodbasins and resulting thin mud drapes can be destroyed by wind erosion.

#### **6.7.2.2.3 The geology in the catchment areas**

The Koigab, Uniab and Hunkab catchments in the south are dominated by Cretaceous Etendeka volcanic rocks (basalts and quartz latites; Fig. 6.22). In contrast thereto the catchment areas of the Hoanib and Hoarusib are characterized by various Late Proterozoic to Early Palaeozoic basement rocks (granites, pelitic and psammitic schists, marbles, limestones, diamictites and iron formations; STANISTREET & CHARLESWORTH, 2001; Fig. 6.22). Weathering of basement rocks provides dominantly illites with minor amounts of kaolinite (EITEL et al., 1999b), but basalts in the southern catchments tend to form smectites as main weathering products (SVENDSEN et al., in press). This difference in clay

mineralogy is of crucial importance for the yield strength of sediment-water mixtures with high sediment concentrations. Yield strength increases considerably if the main clay is smectite rather than illite or kaolinite, so that a flow with 10% illite or kaolinite will have the same strength as a flow with only 2% smectite (TRASK, 1959; PIERSON & SCOTT, 1985). Consequently, hyperconcentrated flows will be favoured in rivers which are fed by basalt-dominated catchments such as the Uniab (SVENDSEN et al., in press).

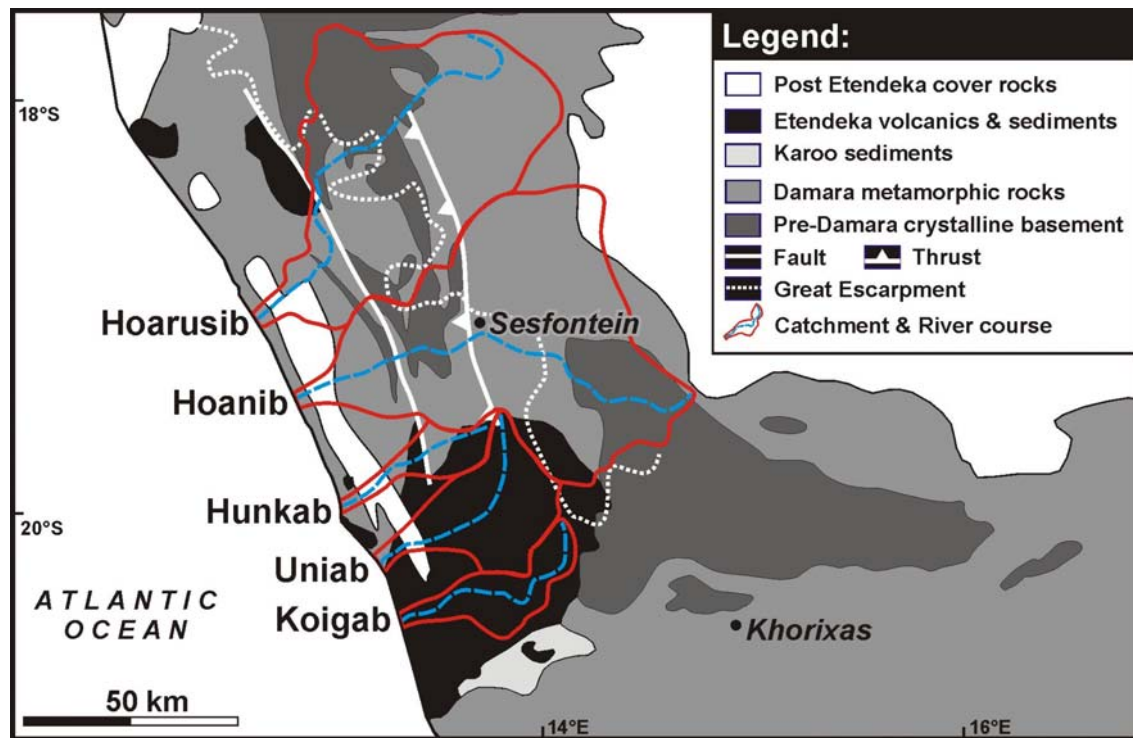


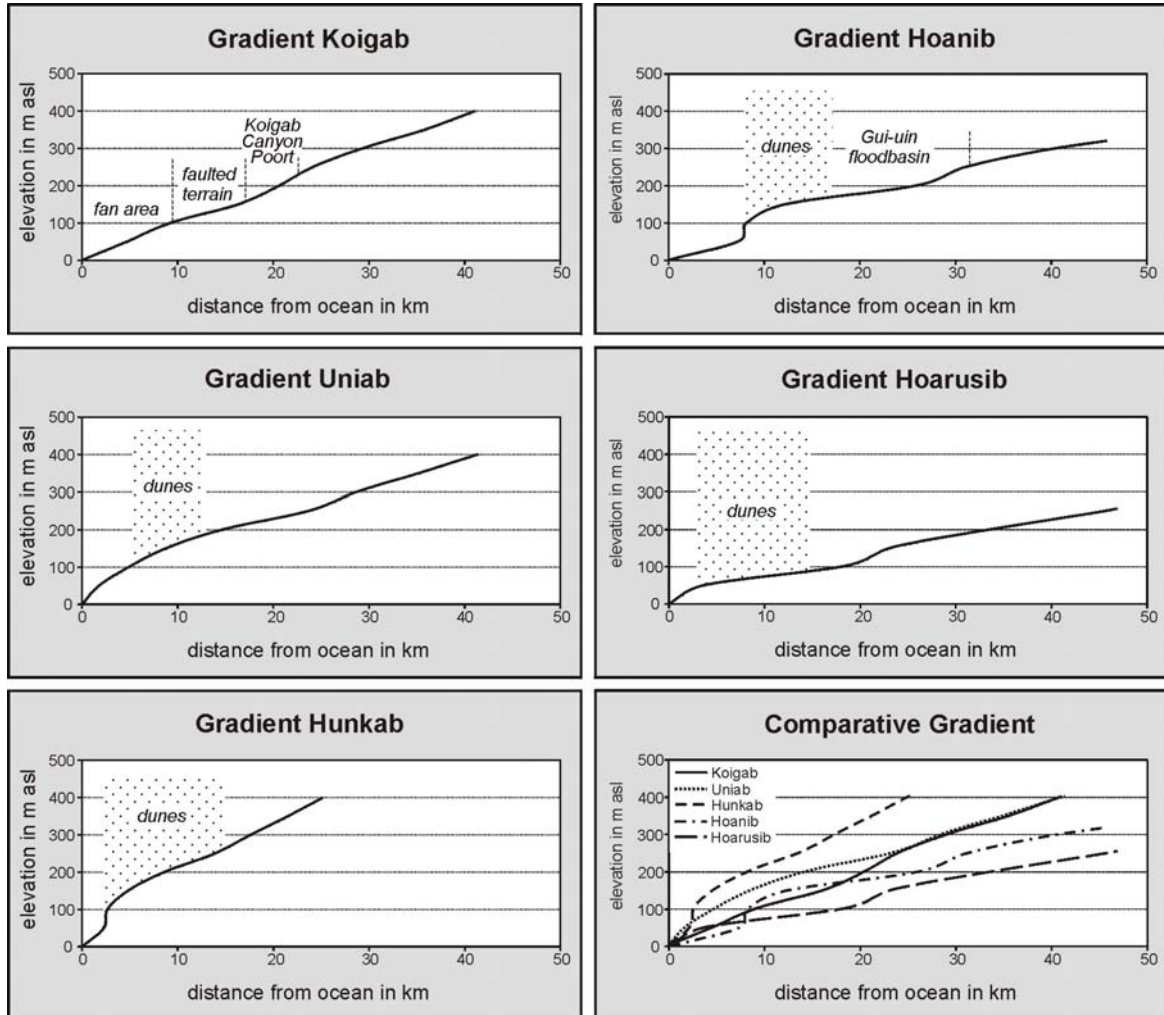
Fig. 6.22: Geological overview of the river catchment areas (compiled after Miller, 1988).

A further difference is related to the contrasting sediment loads of the rivers. Dominated by gravels, the Uniab has a mixed sandy/gravelly river bed and the rivers farther north have largely sand dominated loads. Due to their dominantly sandy grain size and the higher sensitivity of sandy fluvial bar forms to wind erosion northern river deposits consequently have a lower preservation potential than the gravel-dominated fluvial deposits in the south.

#### 6.7.2.2.4 Depositional architecture and longitudinal river gradients

Additional differences among the Skeleton Coast rivers are expressed by their depositional architecture and their grades in longitudinal profiles. The southernmost river system, the Koigab River, provides the active channel network of the shallowly sloping braided fluvial Koigab Fan. The latter is the largest active fan system formed by the Skeleton Coast rivers,

issuing from a branch of the Ambrosiusberg fault zone. The Uniab River channel system severely dissects a clastic bajada-shaped like wedge. Both, river dissection and surf erosion along a prominent sea cliff, modify the original depositional geometry of the Uniabmond area, whereas the original shape of the Koigab Fan is still preserved.



**Fig. 6.23:** The river gradients of the investigated ephemeral rivers compared. Note the effects of dune barriers and faults.

The Hunkab, Hoanib and Hoarusib Rivers are not aggrading but incising. Longitudinal profiles of Koigab, Uniab and Hoarusib (Fig. 6.23) show relatively gentle river grades with no significant steps whereas Hunkab and Hoanib profiles include clear steps in the coastal areas, coinciding with the western margin of the erg. This suggests that in the latter two cases no equilibrium has been established between river grades in the coastal region and sea-level through the dune belt because of the scarcity of dune breakthroughs. In sharp contrast, the unimpeded course of the Koigab results in a gradual grade to the marine base-level. The frequency with which the Koigab reaches the Atlantic Ocean is expressed by the



development of a small sedimentary prism deposited on the adjacent shelf in front of the active Koigab mouth.

## 6.8 Conclusions

The damming of river flow by aeolian landforms has been previously recognized as one of several principal types of fluvial-aeolian interaction (e.g. LANGFORD, 1989; TELLER et al., 1990; LOOPE et al., 1995; WARD et al., 1997; RUST, 1999). This study of the Skeleton Coast ephemeral river systems is complementary in terms of considering variability of parameters within the fluvio-aeolian systems and the resulting differences in the effectiveness of aeolian damming.

The potential of river flooding increases towards the north of the Skeleton Coast Erg because the northern river catchments are larger and receive higher rainfall due to their proximity to the intertropical convergence zone. However, the potential for damming of river flow increases in the same direction because of: (1) the increasing dune belt width and heights; (2) the increasing aggradation of the erg; (3) the change from low barchanoid dune forms in the south to large composite transverse dunes in the north; and (4) the increasing dune spacing favouring individual flood reservoirs. Whereas traverses across the southern part of the erg (e.g. of the Uniab) show a considerable asymmetry with low barchans in the east but a high dune wall in the west, cross-sections of the northern erg (e.g. at the Hoanib) are more uniform. As a consequence, the northern rivers are effectively dammed at the eastern margin of the dune barrier, causing Gui-Uin type flood basins. These flood reservoirs can cause a delay of several days between rainfall in the catchment and dune breakthrough, because the floodwaters need to dam up to the height of a dune belt lowpoint. Southern rivers such as the Uniab are dammed within the erg as the most pronounced barrier is provided by the dunewall at the western border of the dune belt. Such settings may in turn be recorded by stacked and widespread floodpond mud layers (cf. Fig. 6) interbedded with thin aeolian sand sheets. The stacking of mud layers results from repeated rising of the water table within flooded interdune depressions before or without dune break through. In contrast, interdune depressions associated with Hoanib-type river systems which dam flood waters outside the erg, receive mud only during river break-through. Once there has been a successful dune break, the threshold for rivers to enter the dune belt is significantly reduced and even minor floods can flush the river course and prevent healing of the dune barrier.

Grain size and nature of fluvial deposits resulting from dune collapses vary significantly along the dune belt because of contrasting rock types and weathering products provided by the river catchments (SVENDSEN et al., in press). In areas of fluvio-aeolian interaction selective wind removal of sandy and not gravelly fluvial deposits causes over-representation of the latter in the resulting sequences. This means that in the analysis of ancient equivalent sequences there can be an overinterpretation towards the gravelly end of the spectrum of fluvial types.

## 7 References

- Abdullatif, O.M.** (1989) Channel-fill and sheet-flood facies sequences in the ephemeral terminal River Gash, Kassala, Sudan. *Sedimentary Geology*, **63**, 171-184.
- Abel, H.** (1959) Beiträge zur Morphologie der Großen Randstufe im südwestlichen Afrika. *Deutsche Geographische Blätter*, **48**, 130-268.
- Ahrendt, H., Behr, H.J., Clauer, N., Hunziker, J.C., Porada, H. and Weber, K. (1983)** The Northern Branch. Depositional development and timing of the structural and metamorphic evolution within the framework of the Damara Orogen. In: *Intra-continental fold belts; case studies in the Variscan belt of Europe and the Damara Belt in Namibia* (Eds H. Martin and F.W. Eder), pp. 723-743. Springer-Verlag, Berlin.
- Barnard, W.S.** (1989) Die sandseë van die Namib en hul verbreiding. *South African Geographer*, **16(1/2)**, 14-38.
- Bascomb, C.L.** (1974) Physical and chemical analysis of <2 mm samples. In: *Soil survey methods* (Eds B.W. Avery and C.L. Bascomb), *Technical Monograph*, **6**, 14-41.
- Benan, C.A.A. and Kocurek, G.A.** (2000) Catastrophic flooding of an aeolian dune field: Jurassic Entrada and Todilto Formations, Ghost Ranch, New Mexico, USA. *Sedimentology*, **47**, 1069-1080.
- Besler, H., Blümel, W.D., Heine, K., Hüser, K., Leser, H. and Rust, U.** (1994) Geomorphogenese und Paläoklima Namibias. Eine Problemskizze. *Die Erde*, **125**, 139-165.
- Beverage, J.P. and Culbertson, J.K.** (1964) Hyperconcentrations of suspended sediment. *Journal of Hydraulics Division, Proceedings of the American Society of Civil Engineers*, **90**, 117-128.
- Blair, T.C. and McPherson, J.G.** (1992) The Trollheim alluvial fan and facies model revisited. *Geological Society of America Bulletin*, **104**, 762-769.
- Blair, T.C. and McPherson, J.G.** (1994a) Alluvial fans and their natural distinction from rivers based on morphology, hydraulic processes, sedimentary processes, and facies assemblages. *Journal of Sedimentary Research*, **A64/3**, 450-489.
- Blair, T.C. and McPherson, J.G.** (1994b) Alluvial fan processes and forms. In: *Geomorphology of Desert Environments* (Eds A.D. Abrahams and A.J. Parson), pp. 354-402. Chapman & Hall, London.
- Blum, M.D. and Törnqvist, T.E.** (2000) Fluvial responses to climate and sea-level change. *Sedimentology*, **47**, 2-38.

- Blümel, W.D., Hüser, K. and Eitel, B.** (2000) Uniab-Schwemmfächer und Skelettküsten-Erg: Zusammenspiel von äolischer und fluvialer Dynamik in der nördlichen Namib. *Regensburger Geographische Schriften*, **33**, 37-55.
- Boothroyd, J.C. and Ashley, G.M.** (1975) Process, bar morphology and sedimentary structures on braided outwash fans, North-eastern Gulf of Alaska. In: *Glaciofluvial and glaciolacustrine sedimentation* (Eds A.V. Jopling and B.C. McDonald), *SEPM Spec. Publ.*, **23**, 193-222.
- Boothroyd, J.C. and Nummedal, D.** (1978) Proglacial braided outwash: a model for humid alluvial fan deposits. In: *Fluvial sedimentology* (Ed. A.D. Miall), *Mem. Can. Soc. Petrol. Geol.*, **5**, 641-668.
- Bornkamm, R., Darius, F. and Prasse, R.** (1999) On the life cycle of *Stipagrostis scoparia* hillocks. *Journal of Arid Environments*, **42**, 177-186.
- Bourke, M.C., Child, A. and Stokes, S.** (in press) Optical age estimates for hyper-arid fluvial silts at Homeb, Namibia. *Quaternary Science Reviews*.
- Bradley, R.S.** (1999) Paeoclimatology. Reconstructing Climates of the Quaternary. In: *International Geophysics Series Vol. 64* (Eds R. Dmowska and J.R. Holton), 613 pp., Harcourt Academic Press, San Diego.
- Brown, R.W., Gallagher, K., Gleadow, A.J.W. and Summerfield, M.A.** (2000) Morpho-tectonic evolution of the South Atlantic margins of Africa and South America. In: *Geomorphology and Global Tectonics* (Ed M.A. Summerfield), pp. 255-281. Wiley & Sons, Chichester.
- Brunotte, E. and Spönemann, J.** (1997): Die kontinentale Randabdachung Nordwest-namibias: eine morphotektonische Untersuchung. *Petermanns Geographische Mitteilungen*, **141**, 3-15.
- Bull, W.B.** (1963) Alluvial-fan deposits in western Fresno County, California. *Journal of Geology*, **71**, 243-251.
- Bull, W.B.** (1968) Alluvial fans. *Journal of Geologic Education*, **16**, 101-106.
- Bull, W.B.** (1977) The alluvial fan environment. *Progress in Physical Geography*, **1**, 222-270.
- Bullard, J. E. and Livingstone I.** (2002) Interactions between aeolian and fluvial systems in dryland environments. *Area*, **34.1**, 8-16.
- Burke, K.** (1967) The Yallahs Basin: a sedimentary basin southeast of Kingston Jamaica. *Mar. Geol.*, **5**, 45-60.
- Chamley, H.** (1990) *Sedimentology*. Springer, Berlin, 285 pp.

- Clemson, J., Cartwright, J. and Booth, J.** (1997): Structural segmentation and the influence of basement structure on the Namibian passive margin. *J. Geol. Soc. London*, **154**, 477-482.
- Cockburn, H.A.P., Brown, R.W., Summerfield, M.A. and Seidl, M.A.** (2000) Quantifying passive margin denudation and landscape development using a combined fission-track thermochronology and cosmogenic isotope analysis approach. *Earth planet. Sci. Lett.*, **179**, 429-435.
- Cooke, R., Warren, A. and Goudie, A.** (1993) *Desert Geomorphology*. University College London, London, 526 pp.
- Craven, P. and Marais, C.** (1998) *Namib Flora*. Gamsberg Macmillan Publishers Ltd., Windhoek, 128 pp.
- Crimes, T.P.** (1975) The stratigraphical significance of trace fossils. In: *The study of trace fossils; a synthesis of principals, problems, and procedures in ichnology* (Ed. R.W. Frey), pp. 109-130, Springer-Verlag, New York.
- Cox, L.R., Newell, N.D., Branson, C.C., Casey, R., Chavan, A., Coogan, A.H., Dechaseaux, C., Fleming, C.A., Haas, F., Hertlein, L.G., Keen, A.M., LaRoque, A., McAlester, A.L., Perkins, B.F., Puri, H.S., Smith, L.A., Soot-Ryen, T., Stenzel, B., Turner, R.D. and Weir, J.** (1969) Mollusca 6. Bivalvia. In: *Treatise on Invertebrate Paleontology, Part N* (ed. R.C. Moore), 1224 pp; Geol. Soc. Am. & Univ. Kansas Press, Boulder.
- Daly, M.C., Chorowicz, J. and Fairhead, J.D.** (1989) Rift basin evolution in Africa: the influence of reactivated steep basement shear zones. In: Inversion tectonics (Eds M.A. Cooper and G.D. Williams), *Spec. Publ. Geol. Soc. London*, **33**, 309-334.
- Danin, A.** (1996): Adaptations of *Stipagrostis* species to desert dunes. *Journal of Arid Environment*, **34**, 297-311.
- Davies, O.** (1959) Pleistocene raised beaches in South-West Africa. *Proc. Ass. Afr. Geol. Surv.*, 20<sup>th</sup> Int. Geol. Congr., Mexico City, 347-350.
- de Wit, M.C.J., Marshall, T.R. and Partridge, T.C.** (2000) Fluvial deposits and drainage evolution. In: *The Cenozoic of Southern Africa* (Eds T.C. Partridge and R.R. Maud), pp. 55-72, Oxford University Press, Oxford.
- Dingle, R.V.** (1992/93) Structural and sedimentary development of the continental margin off southwestern Africa. *Communs. geol. Surv. Namibia*, **8**, 35-43.
- Eckhardt, F.D. and Schemenauer, R.S.** (1998) Fog water chemistry in the Namib Desert, Namibia. *Atmospheric Environment*, **32 (14/15)**, 2595-2599.



- Eitel, B., Blümel, W.D. and Hüser, K.** (1999a) Der Uniab-Lehm: Relikt feuchttropischer Tertiärklimate in der Nördlichen Namib (Skelettküste/Namibia). *Die Erde*, **130**, 17-27.
- Eitel, B., Blümel, W.D. and Hüser, K.** (1999b) River silt terraces at the eastern margin of the Namib Desert (NW Namibia): Genesis and palaeoclimatic evidence. *Zentralblatt für Geologie und Paläontologie*, **5/6**, 243-254.
- Eitel, B., Blümel, W.D. and Hüser, K.** (2002) Environmental transitions between 22 ka and 8 ka in monsoonally influenced Namibia – A preliminary chronology. *Z. Geomorph. N.F.*, **126**, 31-57.
- FAO** (1988) *Soil map of the world, Vol. I: Revised Legend*. FAO, Rome, 119 pp.
- Fryberger, S.G.** (1993) A review of aeolian bounding surfaces, with examples from the Permian Minnelusa Formation, USA. In: *Characterization of fluvial and aeolian reservoirs* (Eds C.P. North and D.J. Prosser), *Geol. Soc. London Spec. Publ.*, **71**, 1-6.
- Folk, R.L. and Ward, W.C.** (1957) Brazos River Bar: A study of the significance of grain size parameters. *Journal of Sedimentary Petrology*, **27**, 3-26.
- Galloway, W.E. and Hobday, D.K.** (1996) *Terrigenous clastic depositional systems. – Application to fossil fuel and groundwater resources*. Springer, Berlin, 489 pp.
- Gary, M., McAfee R. Jr. and Wolf, C.L.** (1972) *Glossary of Geology*. American Geological Institute, Washington, 805 pp.
- Gloppen, T.G. and Steel, R.J.** (1981) The deposits, internal structure and geometry in six alluvial fan-fan delta bodies (Devonian-Norway); a study in the significance of bedding sequence in conglomerates. In: *Recent and ancient nonmarine depositional environments; models for exploration* (Eds F.G. Ehtridge and R.M. Flores), *SEPM Spec. Publ.*, **31**, 49-69.
- Gohain, K. and Parkash, B.** (1990) Morphology of the Kosi megafan. In: *Alluvial Fans – A Field Approach* (Eds A.H. Rachocki and M. Church), pp. 151-178. John Wiley & Sons, Chichester.
- Goldsmith, V.** (1978) Coastal dunes. In: *Coastal Sedimentary Environments* (Ed. R.A. Jr. Davies), pp. 171-235, Springer, New York.
- Goudie, A.** (1972) Climate, weathering, crust formation, dunes, and fluvial features of the Central Namib Desert, near Gobabeb, South West Africa. *Madoqua*, **1 (54-62)**, 15-31.
- Goudie, A., Viles, H.A. and Parker A.G.** (1997) Monitoring of rapid salt weathering in the central Namib Desert using limestone blocks. *Journal of Arid Environments*, **37**, 15-31.

- Hartnady, C.J.H. and Partridge, T.C.** (1995) Neotectonic uplift in southern Africa: a brief review and geodynamic conjecture. In: *Extended Abstracts. Centennial Geocongress, Johannesburg (RSA)*, 456-459.
- Harvey, J.M. and Wells, S.G.** (1994) Late Pleistocene and Holocene changes in hillslope sediment supply to alluvial fan systems: Zzyzx, California. In: *Environmental change in drylands* (Eds A.C. Millington and K. Pye), pp. 66-84, Chichester, New York.
- Hawkesworth, C.J., Gallagher, K., Kelley, S., Mantovani, M., Peate, D.W., Regelous, M. and Rogers, N.W.** (1992) Paraná magnetism and the opening of the South Atlantic. In: *Magnetism and the causes of continental break-up* (Eds B.C. Storey, T. Alabaster and R.J. Pankhurst), *Spec. Publ. geol. Soc. London*, **68**, 221-240.
- Hoffmann, K.-H.** (1983) Lithostratigraphy and facies of the Swakop Group of the southern Damara Belt, SWA/Namibia. In: *Evolution of the Damara Orogene* (Ed. R.McG. Miller), *Spec. Publ. Geol. Surv. S. Afr.*, **11**, 43-63.
- Hüser, K.** (1989) Die Südafrikanische Randstufe. Grundsätzliche Probleme ihrer geomorpologischen Entwicklung. *Z. Geomorph. N.F.*, **74**, 95-110.
- Hüser, K., Blümel, W.D. and Eitel, B.** (1997) Geomorphologische Untersuchungen an Rivierterrassen im Mündungsbereich des Uniab (Skelettküste/NW-Namibia). *Zbl. Geol. Paläont. Teil 1*, **12**, 1-21.
- Holzförster, F.** (2002) Sedimentology, stratigraphy and synsedimentary tectonics of the Karoo Supergroup, N-Namibia. *Beringeria*, **30**, 144 pp.
- Hooke, R. LeB.** (1967) Processes on arid-region alluvial fans. *Journal of Geology*, **75**, 438-460.
- Illenberger, W.K. and Rust, I.C.** (1988) A sand budget for the Alexandria coastal dunefield, South Africa. *Sedimentology*, **35**, 513-521.
- Jacob, J. R.** (2001) Incision and aggradation in the Orange River valley, southwestern Africa. In: *Program and abstracts. 7<sup>th</sup> International Conference on Fluvial Sedimentology, Lincoln, Nebraska (USA)* (Eds J.A. Mason, R.F.Jr. Diffendal and R.M. Joeckel), p. 138.
- Jacobson, P.J., Jacobson, K.M. and Seely, M.K.** (1995) *Ephemeral rivers and their catchments: sustaining people and development in western Namibia*. Desert Research Foundation of Namibia, Windhoek, 160 pp.
- Jones, L.S. and Blakey, R.C.** (1997) Aeolian-fluvial interaction in the Page Sandstone (Middle Jurassic) in south-central Utah, USA – a case study of erg-margin processes. *Sedimentary Geology*, **109**, 181-198.

- Jury, M.R.** (1996) Regional teleconnection pattern associated with summer rainfall over South Africa, Namibia and Zimbabwe. *International Journal of Climatology*, **16(2)**, 135-153.
- Kelly, S.B. and Olsen, H.** (1993) Terminal fans – a review with reference to Devonian examples. *Sedimentary Geology*, **85**, 339-374.
- Kempf, J.** (2000) Klimageomorphologische Studien in Zentral-Namibia: Ein Beitrag zur Morpho-, Pedo- und Ökogenese. Unpubl. PhD thesis, Univ. Würzburg, 562 pp.
- King, L. C.** (1951) South African scenery; a textbook of Geomorphology, ed. 2. Oliver and Boyd, Edinburgh, 379 pp.
- Klein, J.A.** (1980) Pleistocene to recent faulting in the area west of Omaruru (SWA/Namibia). *Geol. Surv. Namibia, Regional Geology Series, Open File report, RG 4*, 1-26.
- Korn, H. and Martin, H.** (1957) The Pleistocene in South-West-Africa. In: *Proceedings of the Third Pan-African Congress on Prehistory, Livingstone*, 14-22.
- Krapf, C.B.E.** (2000) Depositional system at the Uniab seacliff - Skeleton Coast, Namibia. In: *Abstract IGCP 413 Meeting: Linkages between fluvial, lacustrine and aeolian systems, Desert Study Centre Zzyzx, California* (Ed. N. Lancaster), p. 10.
- Krapf, C.B.E., Stanistreet, I.G. and Stollhofen, H.** (2001) The low-latitude ephemeral unvegetated Koigab braided fluvial fan, Skeleton Coast, Namibia. – Abstract 7<sup>th</sup> Internat. Conf. on Fluvial Sedimentology, Lincoln, Nebraska, USA.
- Krapf, C.B.E., Stanistreet, I.G. and Stollhofen, H.** (in press): Morphology and fluvio-aeolian interaction of the tropical latitude, ephemeral braided river dominated Koigab Fan, Skeleton Coast, NW Namibia. In: *Fluvial Sedimentology VII* (Eds M. Blum and S. Marriott), *IAS Spec Publ.*
- Krapf, C.B.E., Stanistreet, I.G., Stollhofen, H., Werner, M., Zeller, C. and Svendsen, J.** (2002) The Cenozoic succession in the Uniabmond area, Skeleton Coast, NW Namibia. 16<sup>th</sup> International Sedimentological Congress Abstract Volume, 199.
- Krapf, C.B.E. and Stollhofen, H.** (2000): Fluvio-aeolian interaction in the Koigab Fan area – Skeleton Coast, Namibia. *Mitt. Ges. Geol. Bergbaustud. Österr.*, **43**, 76-77.
- Krapf, C. B E., Stollhofen, H., and Stanistreet, I.** (2000): Contrasting styles of fluvio-aeolian interaction between ephemeral river systems and dunes of the Skeleton Coast Erg, Namibia. In: *Abstract IGCP 413 Meeting: Linkages between fluvial, lacustrine and aeolian systems, Desert Study Centre Zzyzx, California* (Ed. N. Lancaster), p. 11-12.

- Krapf, C. B E., Stollhofen, H., and Stanistreet, I.** (2003): Contrasting styles of ephemeral river systems and their interaction with dunes of the Skeleton Coast erg (Namibia). *Quaternary International*, **104**, 41-52.
- Lancaster, N.** (1982) Dunes on the Skeleton Coast, Namibia (South West Africa): Geomorphology and grain size relationships. *Earth Surface Processes and Landforms*, **7**, 575-587.
- Lancaster, N.** (2002) How dry was dry? – Late Pleistocene palaeoclimates in the Namib Desert. *Quaternary Science Reviews*, **21**, 769-782.
- Lancaster, J., Lancaster, N. and Seeley, M.K.** (1984) Climate of the central Namib Desert. *Madoqua*, **14/1**, 5-61.
- Langford, R.P.** (1989) Fluvial-aeolian interactions: Part I, modern systems. *Sedimentology* **36**, 1023-1035.
- Langford, R.P. and Chan, M.A.** (1989) Fluvial-aeolian interactions: Part II, ancient systems. *Sedimentology*, **36**, 1037-1051.
- Laurent, M., Falgueres, C., Bahain, J.J., Rousseau, L. and Van Vliet-Lanoe, B.** (1998) ESR dating of quartz extracted from Quaternary and Neogene sediments; method, potential and actual limits. *Quaternary Science Review*, **17**, 1057-1062.
- Lecce, S.A.** (1990) The alluvial fan problem. In: *Alluvial fans – A field approach* (Eds A.H. Rachocki and M. Church), pp. 3-24, John Wiley & Sons, Chichester.
- Ledendecker, S.** (1992) Stratigraphie der Karoosedimente der Huabregion (NW-Namibia) und deren Korrelation mit zeitäquivalenten Sedimenten des Paranäbeckens (Südamerika) und des Großen Karoobeckens (Südafrika) unter besonderer Berücksichtigung der überregionalen geodynamischen und klimatischen Entwicklung Westgondwanas. *Göttinger Arb. Geol. Paläont.*, **54**, 1-87.
- Leggett, K.E.A.** (1998) *Hoanib River catchment study – Project proposal*. Desert Research Foundation of Namibia, Windhoek, 65 pp.
- Light, M.P.R., Maslanyi, M.P., Greenwood, R.J. and Banks, N.L.** (1993) Seismic sequence stratigraphy and tectonics offshore Namibia. In: *Tectonics and seismic sequence stratigraphy* (Eds G.D. Williams and A. Dobb), *Spec. Publ. geol. Soc. London*, **71**, 163-191.
- Lindesay, J. and Seely, M.** (1989) Aridity of the Namib – Causes, links and implications. In: *Proceedings of the Namib-Benguela interactions workshop* (Eds V. Shannon, M. Seely and J. Ward), *Occasional Report*, **41**, 12-15.
- Löffler, T. and Porada, H.** (1998) Tontüten (“Mud curls”) aus der Etjo Formation am Gr. Waterberg (Namibia) und dem Germanischen Buntsandstein - Über die Erhaltungs-

- bedingungen von aufgerollten Trockenriß-Segmenten. *Freiberger Forschungsheft*, **C 475**, 201-221.
- Loope, D.B., Swinehart, J.B. and Mason, J.P.** (1995) Dune-dammed paleovalleys of the Nebraska Sand Hills; intrinsic versus climatic controls on the accumulation of lake and marsh sediments. *Geological Society of America Bulletin*, **107**, 396-406.
- Mange, M.A. and Maurer, H.F.W.** (1991) *Schwerminerale in Farbe*. Stuttgart, Enke, 148 pp.
- Marsh, J.S., Ewart, A., Milner, S.C., Duncan, A.R. and Miller, R. McG.** (2001) The Etendeka Igneous Province: magma types and their stratigraphic distribution with implications for the evolution of the Paraná-Etendeka flood basalt province. *Bull. Volcanol.*, **62**, 464-486.
- Maud, R.R. and Botha, G.A.** (2000) Deposits of the South Eastern and Southern Coasts. In: *The Cenozoic of Southern Africa* (Eds T.C. Partridge and R.R. Maud), pp. 19-32. Oxford University Press, Oxford.
- McCarthy, T.S., Cooper, G.R.J., Tyson, P.D. and Ellery, W.N.** (2000) Seasonal flooding in the Okavango Delta, Botswana; recent history and future prospects. *South African Journal of Science*, **96**, 25-33.
- McPherson, J.G., Shanmugam, G. and Moiola, R.J.** (1987) Fan-deltas and braid deltas: Varieties of coarse-grained deltas. *Geological Society of American Bulletin*, **99**, 331-340.
- Messerli, B., Grosjean, M., Bonani, G., Buergi, A., Geyh, M.A., Graf, K., Ramseyer, K., Romero, H., Schotterer, U., Schreier, H. and Vuille, M.** (1993) Climate change and natural resource dynamics of the Atacama Altiplano during the last 18,000 years; a preliminary synthesis. In: *Mountain geocology and the Andes; resources management and sustainable development* (Eds J.D. Ives and P. Ives), *Mountain Research and Development*, **13 (2)**, 117-127.
- Miall, A.D.** (1977) A review of the braided-river depositional environment. *Earth Sci. Rev.*, **13**, 1-62.
- Miall, A.D.** (1978) Lithofacies types and vertical profile models in braided river deposits, a summary. *Canadian Society of Petroleum Geologists*, **5**, 597-604.
- Miller, R.McG.** (1983): The Pan-African Damara orogene of South West Africa/Namibia. In: *Evolution of the Damara orogene* (Ed. R.McG. Miller), *Spec. Publ. Geol. Surv. S. Afr.*, **11**, 273-280.
- Miller, R. McG.** (1988) Geological Map of Namibia, Sheet 2013 Cape Cross 1:250.000, Geological Survey of Namibia, Windhoek.



- Miller, R.M. and Schalk, K.E.L.** (1980) Geological Map of Namibia 1:1.000.000, Geological Survey of Namibia, Windhoek.
- Milner, S.C.** (1986) The geological and volcanological features of the quartz latites of the Etendeka Formation. *Communications of the Geological Survey of South West Africa /Namibia*, **2**, 109-116.
- Milner, S.C.** (1988) The geology and geochemistry of the Etendeka Formation Quartz Latites, Namibia. Unpubl. PhD thesis, Univ. Cape Town, 263 pp.
- Milner, S.C. and Duncan, A.R.** (1987) Geochemical characterisation of quartz latite units in the Etendeka Formation. *Communs. Geol. Surv. Namibia*, **3**, 83-90.
- Milner, S.C, Duncan, A.R. and Ewart, A.** (1992) Quartz latite rheoignimbrite flows of the Etendeka Formation, north-western Namibia. *Bull. Volcanol.*, **54**, 200-219.
- Milner, S.C., Duncan, A.R., Ewart, A.R. and Marsh, J.S.** (1994) Promotion of the Etendeka Formation to Group status: A new integrated stratigraphy. *Communs. geol. Surv. Namibia*, **9**, 5-11.
- Milner, S.C., Duncan, A.R., Whittingham, A.M. and Ewart, A.R.** (1995) Trans-Atlantic correlation of eruptive sequences and individual silicic volcanic units within the Paraná-Etendeka igneous province. *J. Volcanol. Geotherm. Res.*, **69**, 137-157.
- Mountney, N., Howell, J., Flint, S. and Jerram, D.** (1998) Aeolian and alluvial deposition within the Mesozoic Etjo sandstone formation, Northwest Namibia. *Journal of African Earth Sciences*, **27**, 175-192.
- Mukherji, A.B.** (1976) Terminal fans of inland streams in Sutlej-Yamuna plain. *Geomorphology*, **20**, 190-204.
- Nemec, W. and Steel, R.J.** (1988) What is a fan delta and how do we recognize it? In: *Fan Deltas: Sedimentological and tectonic settings* (Ed. R.J. Steel), pp. 3-13. Blackie, Glasgow.
- North, C.P. and Prosser, D.J.** (1993) Characterization of fluvial and aeolian reservoirs: problems and approaches. In: *Characterization of fluvial and aeolian reservoirs* (Eds C.P. North and D.J. Prosser), *Geol. Soc. London Spec. Publ.*, **71**, 1-6.
- Odin, G.S.** (1988) Green marine clays. Oolitic ironstone facies, verdine facies, glaucony facies and celadonite-bearing facies – a comparative study. *Developments in Sedimentology*, **45**, 445 pp.
- Partridge, T.C. and Maud, R.R.** (1989) The end-Cretaceous event: New evidence from the southern hemisphere. *South African Journal of Science*, **85**, 428-430.

- Partridge, T.C. and Maud, R.R.** (2000) Macro-scale geomorphic evolution of Southern Africa. In: *The Cenozoic of Southern Africa* (Eds T.C. Partridge and R.R. Maud), pp. 3-18. Oxford University Press, Oxford.
- Passchier, C.W., Trouw, R.A.J., Ribeiro, A. and Paciullo, F.V.P.** (2002) Tectonic evolution of the southern Kaoko Belt, Namibia. *Journal of African Earth Sciences*, **35(1)**, 61-75.
- Pether, J., Roberts, D.L. and Ward, J.** (2000) Deposits of the West Coast. In: *The Cenozoic of Southern Africa* (Eds T.C. Partridge and R.R. Maud), pp. 33-54. Oxford University Press, Oxford.
- Pfisterer, U., Blume, H.P. and Beyer, L.** (1996) Distribution, pattern genesis and classification of soils of an arid dune area in Northern Negev. *Zeitschrift für Pflanzenernährung und Bodenkunde*, **159**, 419-428.
- Pickford, M. and Senut B.** (1999) Geology and Palaeobiology of the Namib Desert Southwestern Africa. Volume 1: Geology and history of study. *Mems. Geol. Surv. Namibia*, **18**, 155 pp.
- Pierson, T.C. and Costa, J.E.** (1987) A rheologic classification of subaerial sediment-water flows. In: *Debris flows/avalanches; process, recognition, and migration* (Eds J.E. Coasta and G.F. Wieczorek), *Review in Engineering Geology*, **7**, 1-12.
- Pierson, T.C. and Scott, K.M.** (1985) Downstream dilution of a lahar; transition from debris flow to hyperconcentrated stream flow. *Water Resources Research*, **21**, 1511-1524.
- Porada, H.** (1989) Pan-African Rifting and Orogenesis in Southern to Equatorial Africa and Eastern Brazil. *Precambrian Res.*, **44**, 103-136.
- Raab, M.** (2000) The geomorphic response of the passive continental margin of northern Namibia to Gondwana break-up and global scale tectonics. Unpubl. PhD thesis, University of Göttingen, 253 pp. (online publication: <http://www.sub.uni-goettingen.de/>).
- Reading, H. G.** (1996) *Sedimentary Environments: Processes, facies and stratigraphy*. Blackwell Science, Oxford, 688 pp.
- Reading, H.G. and Collinson, J.D.** (1996) Clastic coasts. In: *Sedimentary Environments: Processes, facies and stratigraphy* (Ed. H.G. Reading), 3<sup>rd</sup> edn, pp. 154-231, Blackwell Science, Oxford.
- Reineck, H.E. and Singh, I.B.** (1986) *Depositional Sedimentary Environments*. Springer, Berlin, 551pp.

- Renne, P.R., Glen, J.M., Milner, S.C. and Duncan, A.R.** (1996) Age of Etendeka flood volcanism and associated intrusions in southwestern Africa. *Geology*, **24**, 659-662.
- Rust, B.R.** (1978) Depositional model for braided alluvium. In: *Fluvial sedimentology* (Ed. A.D. Miall), *Mem. Can. Soc. Petrol. Geol.*, **5**, 605-625.
- Rust, U.** (1987) Geomorphologische Forschungen im südwestafrikanischen Kaokofeld zum angeblichen vollariden quartären Kernraum der Namibwüste. *Erdkunde*, **41**, 118-133.
- Rust, U.** (1999) River-end deposits along the Hoanib River, northern Namib: archives of Late Holocene climatic variation on a subregional scale. *South African Journal of Science*, **95**, 205-208.
- SACS (South African Committee for Stratigraphy)** (1988) Stratigraphy of South Africa. Part 1: Lithostratigraphy of the Republic of South Africa, South West Africa/Namibia and the Republics of Bophuthatswana, Transkei and Venda. *Handbook Geol. Surv. S. Africa* 8, Pretoria, 690 pp.
- Scheffer, F.** (2002) *Lehrbuch der Bodenkunde. Scheffer/Schachtschabel*. 15. Aufl., Spektrum Akademischer Verlag, Heidelberg, 593 pp.
- Scheepers A.C.T. and Rust, I.C.** (1999) The Uniab River Fan: an unusual alluvial fan on the hyper-arid Skeleton Coast, Namibia. In: *Varieties of fluvial forms* (Eds A.J. Miller and A. Gupta), pp. 273-294, John Wiley & Sons, Chichester.
- Schlicker, B.** (2000a): Erläuterungen zur Geologischen Karte 1:25.000 des Koigab-Canyon und seiner Umgebung, Skelettküste, NW Namibia. Unpubl. diploma-map, Univ. Würzburg, 64 pp.
- Schlicker, B.** (2000b): Sedimentfracht und Teilablagerungsräume des Koigab-Reviers, Skelettküste, NW Namibia. Unpubl. Diploma-thesis, Univ. Würzburg, 109 pp.
- Seely, M.K.** (1978): The Namib dune desert; an unusual ecosystem. *Journal of Arid Environments*, **1(2)**, 117-128.
- Seth, B.** (1999) Crustal evolution of the Kaoko belt, NW Namibia – Geochemical and geochronological study of Archaen to Mesoproterozoic basement gneisses and Pan-African migmatites and granitoids. Unpubl. PhD thesis, Univ. Würzburg, 120 pp.
- Shannon, L.V., Boyd, A.J., Brundrit, G.B. and Taunton-Clark, J.** (1986) On the existence of an El Niño-type phenomenon in the Benguela System. *J. Marine Res.*, **44**, 495-520.
- Shannon, V., Seely, M. and Ward, J.** (1989) Proceedings of the Namib-Benguela interactions workshop. Gobabeb, SWA/Namibia, 28 to 30 Nov. 1988. *Occasional Report*, **41**, 38 pp.

- Siedner, G. and Mitchell, J.A.** (1976) Episodic Mesozoic volcanism in Namibia and Brazil: K-Ar-isochron study bearing on the opening of the South Atlantic. *Earth Planetary Science Letters*, **30**, 292-302.
- Stanistreet, I.G., Cairncross, B. and McCarthy, T.S.** (1993) Low sinuosity and meandering bedload rivers of the Okavango Fan; channel confinement by vegetated levees without fine sediment. *Sedimentary Geology*, **85/1-4**, 135-156.
- Stanistreet, I.G. and Charlesworth, E.G.** (2001) Damaran basement-cored fold nappes incorporating pre-collisional basins, Kaoko Belt, Namibia, and controls on Mesozoic supercontinental break-up. *S. Afr. J. Geol.*, **104**, 1-12.
- Stanistreet, I.G., Kukla, P.A. and Henry, G.** (1991) Sedimentary basinal response to a Late Precambrian Wilson Cycle: the Damara Orogen and Nama Foreland, Namibia. *J. Afr. Earth Sci.*, **13**, 141-156.
- Stanistreet, I. G. & McCarthy, T. S.** (1993) The Okavango Fan and the classification of subaerial fan systems. *Sedimentary Geology*, **85**, 115-133.
- Stanistreet, I.G. and Stollhofen H.** (1999): Onshore equivalents of the main Kudu gas reservoir in Namibia. In: *The Oil and Gas habitates of the South Atlantic* (Eds N. Cameron, R. Bate and V. Clure), *Spec. Publ. geol. Soc. London*, **135**, 345-365.
- Stanistreet, I.G. and Stollhofen, H.** (2002) Hoanib River flood deposits of Namib Desert interdunes as analogues for thin permeability barrier mudstone layers in aeolianite reservoirs. *Sedimentology*, **49**, 719-736.
- Stocken, C.G.** (1962) The diamond deposits of the Sperrgebiet, South West Africa: Excursion Guide of the 5<sup>th</sup> Congress of the Geological Society of South Africa, Pretoria, 15 pp.
- Stollhofen, H.** (1999): Karoo Syndrift-Sedimentation und ihre tektonische Kontrolle am entstehenden Kontinentalrand Namibias. *Zeitschrift Deutsche Geologische Gesellschaft*, **149**, 519-623.
- Stollhofen, H. and Stanistreet, I.G.** (1997) Fluvial aeolian interactions of the ephemeral Hoanib River and floods through the Namib desert sand sea, Skeleton Coast, NW Namibia.- Abstract 6<sup>th</sup> Int. Conf. on Fluvial Sedimentology, Cape Town, South Africa, 1997: 199.
- Stollhofen, H. and Stanistreet, I.G.** (1999) Fluvio-äolische Interaktionen in der nördlichen Namibwüste, NW-Namibia. *Terra Nostra*, **99/4**, 264-265.
- Stollhofen, H., Stanistreet, I.G. and Jacobeit, J.** (1999) ENSO-type induced flooding of ephemeral rivers and their interaction with dunes of the Namib desert sand sea,

- Skeleton Coast, Namibia. – Abstract 19<sup>th</sup> IAS Regional Meeting on Sedimentology, Copenhagen, Denmark, 1999: 246-247.
- Svendsen, J.B.** (2000) A sedimentological and stratigraphic investigation in the Skeleton Coast, Namib Desert, South Africa – Hydrocarbon potential in fluvio-aeolian sediments. *Unpubl. field report*. University of Aarhus, 39 pp.
- Svendsen, J.B., Stollhofen, H., Krapf, C.B.E. and Stanistreet, I.G.** (in press) Mass and hyperconcentrated flow deposits record dune field damming and catastrophic breakthrough of ephemeral Uniab River Skeleton Coast erg, Namibia. *Sedimentary Geology*.
- Sweeting, M.M. and Lancaster, N.** (1982) Solutional and wind erosion forms on limestone in the central Namib Desert. *Z. Geomorph. N.F.*, **26**, 197-207.
- Teller, J.T., Rutter, N. and Lancaster, N.** (1990) Sedimentology and paleohydrology of Late Quaternary lake deposits in the Northern Namib Sand Sea, Namibia. *Quaternary Science Reviews*, **9**, 343-364.
- Trask, P.D.** (1959) Effect of grain size on strength of mixtures of clay, sand, and water. *Geological Society of America Bulletin*, **70**, 569-579.
- Tucker, M.E.** (1988): *Techniques in Sedimentology*. Blackwell, Oxford, 394 pp.
- Tyson, P.D.** (1969) Atmospheric circulation and precipitation over Africa. *Environmental Studies Occasional Paper*, **2**, 1-22.
- Tyson, P.D.** (1986) *Climatic change and variability in southern Africa*. Oxford University Press, Cape Town, 220 pp.
- Tyson, P.D. and Partridge, T.C.** (2000) Evolution of Cenozoic climates. In: *The Cenozoic of Southern Africa* (Eds T.C. Partridge and R.R. Maud), pp. 371-387. Oxford University Press, Oxford.
- Van Zinderen Bakker, E.M.** (1984) Aridity along the Namibian coast. *Palaeoecology of Africa*, **15**, 201-209.
- Van Zyl, J.A. and Scheepers, A.C.T** (1991) Landforms and geomorphic processes of the Uniab River mouth area, Namibia. *South African Geographer*, **18(1/2)**, 31-45.
- Van Zyl, J.A. and Scheepers, A.C.T.** (1992) Quaternary sediments and the depositional environment of the lower Uniab River area, Skeleton Coast, Namibia. *S. Afr. J. Geol.*, **95(3/4)**, 108-115.
- Van-Zyl, J.A. and Scheepers A.C.T.** (1993) The geomorphic history and landforms of the Lower Koigab River, Namibia. *South African Geographer*, **20(1/2)**, 12-22.










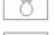



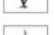
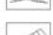


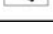


- Wanke, A.** (2000) Karoo-Etendeka Unconformities in NW Namibia and their tectonic implications. PhD thesis, Univ. Würzburg, 168 p. (online publication: <http://opus.bibliothek.uni-wuerzburg.de/opus/volltexte/2002/323/pdf/diss-wanke.pdf>)
- Ward, J.D.** (1987) The Cenozoic succession in the Kuiseb Valley, Central Namib Desert. *Mems. Geol. Surv. S.W.A./Namibia*, **9**, 124 pp.
- Ward, J.D.** (1988) Eolian, fluvial and pan (playa) facies of the Tertiary Tsondab sandstone formation in the central Namib Desert, Namibia. *Sedimentary Geology*, **55(1-2)**, 143-162.
- Ward, J.D.** (1989) Aeolianites of the Mesozoic Etjo Formation, Damaraland and Contemporary Dunes of the Skeleton Coast. Field Guide Dunes '89, Excursion 4B. 18.-21. Aug. 1989: 42 pp.
- Ward, J.D. and Martin, H.** (1987) A terrestrial conglomerate of cretaceous age – a new record from the Skeleton Coast, Namib Desert. *Communs. geol. Surv. S.W. Africa/Namibia*, **3**, 57-58.
- Ward, J.D. and Swart, R.** (1997) Flash-flood fluvial systems of the Central Namib Desert. Field Guide 6th Int. Conf. Fluv. Sedimentology, Cape Town, SA. 37 pp.
- Ward, J.D., Swart, R. and Bloem, A.** (1997) The Hunkab River Flood of 1995: An example of dune-river interaction from northwestern Namibia. – Abstract 6<sup>th</sup> Int. Conf. on Fluv. Sedimentology, Cape Town, South Africa, 1997: 223.
- Ward, J., Jacob, J., de Wit, M., Spaggiari, R. and Bluck, B.** (2002) Post-Gondwana evolution of the Vaal-Orange drainage system: Economic Implications. Exkursion Guide, 16<sup>th</sup> International Sedimentological Conference, Rand Afrikaans University, South Africa, 75 pp.
- Wells, N.A. and Dorr, J.A., Jr.** (1987a) Shifting of the Kosi River, northern India. *Geology*, **15**, 204-207.
- Wells, N.A. and Dorr, J.A., Jr.** (1987b): A reconnaissance of sedimentation on the Kosi alluvial fan of India. In: *Recent Developments in Fluvial Sedimentology* (Eds F.G. Erthridge, R.M. Flores and M. Harvey), Soc. Econ. Paleontol. Mineral., **39**, 51-62.
- Wescott, A. W.** (1990) The Yallahs Fan Delta: A coastal fan in a humid tropical climate. In: *Alluvial Fans – A Field Approach* (Eds A.H. Rachocki and M. Church), pp. 213-225. John Wiley & Sons. Chichester.
- Wescott, W.A. and Ethridge, F.G.** (1980) Fan-delta sedimentology and tectonic setting – Yallahs fan-delta, southeast Jamaica. *Bull. Amer. Assoc. Petrol. Geol.*, **64**, 374-399.
- Whitaker, A.** (1984) Dust transport by Bergwinds of the coast of South West Africa. Unpubl. B.Sc. (Hons.) Thesis, University of Cape Town, 31 pp.

- Woda, C.** (2000) Elektronen-Spin-Resonanz-Datierung von Quarz. Grundlagen, Systematik und Anwendungen unter Einbeziehung von Thermolumineszenz. Unpubl. PhD thesis, Naturwissenschaftlich-Mathematische Gesamtfakultät, Universität Heidelberg, 156 pp.
- Yeaton, R. I.** (1990) The structure and function of the Namib dune grassland: species interaction. *Journal of Arid Environments*, **18**, 343-349.
- Zeller, C.** (2000) Explanations to the Geological Map 1.25.000 of the Uniab Mond Area, Skeleton Coast, NW Namibia. Unpubl. diploma-map, Univ. Würzburg, 80pp.

# Appendix

**Appendix I:** Explanation of symbols in sedimentary logs

| <b>LEGEND</b>  |  |
|--|--|
| <b>Rocks</b>   |  |
|  Sand/Sandstone               |  Gravel/Conglomerate (matrix supported) |
|  Mud/Mudstone                 |  Gravel/Conglomerate (clast-supported)  |
| <b>Structures, Fossils etc.</b>  |  |
|  Massive, no apparent bedding |  Ball & pillow structures               |
|  Plane-bedding                |  Bioturbation                           |
|  Parallel lamination          |  Bivalves                               |
|  Low-angle cross-bedding      |  Caliche horizons                       |
|  Steep angle cross-bedding    |  <i>Stipagrostis</i>                    |
|  Through cross-beds           |  Rhizocretions                          |
|  Ripple cross lamination      |  Fossil bones                           |

**Appendix II: Clast size measurements at the Koigab Fan****A: Measurements on basalt clasts (location of sections see Fig. 4.11)**[*L: longest axis of clast*    *I: intermediate axis of clast*    *S: shortest axis of clast*]

| section | L     | I     | S   | section | L     | I     | S   | section | L    | I    | S   |
|---------|-------|-------|-----|---------|-------|-------|-----|---------|------|------|-----|
| A       | 8.40  | 8.40  | 4.6 | A       | 9.80  | 9.80  | 8   | B       | 7.5  | 7.5  | 4.2 |
| A       | 8.20  | 8.20  | 4.6 | A       | 10.00 | 10.00 | 4.1 | B       | 9.1  | 9.1  | 5.8 |
| A       | 7.50  | 7.50  | 2.5 | A       | 10.30 | 10.30 | 5.2 | B       | 6.8  | 6.8  | 2.6 |
| A       | 6.30  | 6.30  | 4.5 | A       | 7.70  | 7.70  | 4   | B       | 6.7  | 6.7  | 4.2 |
| A       | 5.80  | 5.80  | 4   | A       | 6.60  | 6.60  | 3.9 | B       | 7.1  | 7.1  | 2.8 |
| A       | 7.50  | 7.50  | 3.5 | A       | 4.80  | 4.80  | 4   | B       | 5.2  | 5.2  | 4.5 |
| A       | 7.10  | 7.10  | 4.2 | A       | 9.10  | 9.10  | 3.5 | B       | 8.7  | 8.7  | 7.9 |
| A       | 5.90  | 5.90  | 4.1 | A       | 11.50 | 11.50 | 6   | B       | 8.7  | 8.7  | 3.7 |
| A       | 7.00  | 7.00  | 3.6 | A       | 10.50 | 10.50 | 6.4 | B       | 8.2  | 8.2  | 4.3 |
| A       | 5.80  | 5.80  | 3.2 | A       | 12.00 | 12.00 | 8.5 | B       | 6.7  | 6.7  | 4.4 |
| A       | 6.30  | 6.30  | 2.8 | A       | 9.20  | 9.20  | 2.6 | B       | 6.3  | 6.3  | 3.7 |
| A       | 6.40  | 6.40  | 3.9 | A       | 9.60  | 9.60  | 6.2 | B       | 16.5 | 16.5 | 9.5 |
| A       | 3.80  | 3.80  | 2.6 | A       | 7.00  | 7.00  | 3.7 | B       | 8.7  | 8.7  | 3.2 |
| A       | 3.90  | 3.90  | 2.6 | A       | 5.60  | 5.60  | 3.2 | B       | 8.5  | 8.5  | 5.2 |
| A       | 3.20  | 3.20  | 2.3 | A       | 5.00  | 5.00  | 2.6 | B       | 6.5  | 6.5  | 3.9 |
| A       | 4.20  | 4.20  | 1.8 | A       | 5.70  | 5.70  | 3.4 | B       | 6.3  | 6.3  | 3.3 |
| A       | 2.70  | 2.70  | 1.9 | A       | 7.60  | 7.60  | 3.9 | B       | 12.5 | 12.5 | 9.5 |
| A       | 3.30  | 3.30  | 1.7 | A       | 6.80  | 6.80  | 2.4 | B       | 15   | 15   | 5.7 |
| A       | 2.90  | 2.90  | 1.5 | A       | 5.60  | 5.60  | 2.4 | B       | 5.3  | 5.3  | 4.3 |
| A       | 2.70  | 2.70  | 1.7 | A       | 6.50  | 6.50  | 4   | B       | 5.9  | 5.9  | 3.1 |
| A       | 7.70  | 7.70  | 2.6 | A       | 9.80  | 9.80  | 6.1 | B       | 6    | 6    | 2.6 |
| A       | 8.10  | 8.10  | 4.5 | A       | 9.60  | 9.60  | 5.4 | B       | 19.5 | 19.5 | 9.5 |
| A       | 6.30  | 6.30  | 3.1 | A       | 6.70  | 6.70  | 2.8 | B       | 7.2  | 7.2  | 4.7 |
| A       | 6.60  | 6.60  | 3.4 | A       | 5.90  | 5.90  | 3.4 | B       | 5.3  | 5.3  | 2.8 |
| A       | 4.20  | 4.20  | 3   | A       | 6.60  | 6.60  | 3.1 | B       | 4.8  | 4.8  | 3.3 |
| A       | 8.00  | 8.00  | 4.4 | A       | 6.60  | 6.60  | 1.7 | B       | 4.6  | 4.6  | 2.8 |
| A       | 7.30  | 7.30  | 3.4 | A       | 5.00  | 5.00  | 3.1 | C       | 10.2 | 10.2 | 7.5 |
| A       | 6.30  | 6.30  | 4.4 | A       | 5.40  | 5.40  | 2.1 | C       | 8.6  | 8.6  | 6.2 |
| A       | 5.50  | 5.50  | 3.4 | A       | 5.50  | 5.50  | 3.2 | C       | 6.2  | 6.2  | 3.6 |
| A       | 5.30  | 5.30  | 2.2 | A       | 4.90  | 4.90  | 3.3 | C       | 7.7  | 7.7  | 5.4 |
| A       | 10.30 | 10.30 | 5.7 | A       | 12.50 | 12.50 | 6.2 | C       | 6.7  | 6.7  | 4.3 |
| A       | 8.30  | 8.30  | 4.2 | A       | 7.70  | 7.70  | 4.6 | C       | 4.7  | 4.7  | 4.2 |
| A       | 7.50  | 7.50  | 3.6 | A       | 5.20  | 5.20  | 3.7 | C       | 11.5 | 11.5 | 8   |
| A       | 5.90  | 5.90  | 4   | A       | 4.10  | 4.10  | 1.3 | C       | 9.3  | 9.3  | 3.4 |
| A       | 3.40  | 3.40  | 1.8 | A       | 2.80  | 2.80  | 1.4 | C       | 7.6  | 7.6  | 2.3 |
| A       | 7.00  | 7.00  | 2.3 | B       | 8.2   | 8.2   | 5.2 | C       | 7.1  | 7.1  | 5.2 |
| A       | 5.70  | 5.70  | 3.1 | B       | 7.3   | 7.3   | 3.4 | C       | 7    | 7    | 3.6 |
| A       | 4.60  | 4.60  | 2.9 | B       | 5.2   | 5.2   | 4.2 | C       | 7.2  | 7.2  | 4.7 |
| A       | 4.40  | 4.40  | 2.5 | B       | 4.2   | 4.2   | 2.1 | D       | 6.8  | 6.8  | 4.2 |
| A       | 3.60  | 3.60  | 2.5 | B       | 9.2   | 9.2   | 6.6 | D       | 5.9  | 5.9  | 2.5 |
| A       | 11.80 | 11.80 | 7.9 | B       | 6.7   | 6.7   | 3.1 | D       | 5.1  | 5.1  | 2.2 |
| A       | 9.70  | 9.70  | 4.6 | B       | 5.6   | 5.6   | 2.8 | D       | 5.6  | 5.6  | 2.3 |
| A       | 9.70  | 9.70  | 4.3 | B       | 4.6   | 4.6   | 2.6 | D       | 2.8  | 2.8  | 2.4 |
| A       | 6.80  | 6.80  | 4   | B       | 8.5   | 8.5   | 6.6 | D       | 7.6  | 7.6  | 4.9 |
| A       | 6.80  | 6.80  | 2.9 | B       | 11.6  | 11.6  | 4.9 | D       | 4.5  | 4.5  | 1.8 |
| A       | 8.30  | 8.30  | 3.4 | B       | 9     | 9     | 5.7 | D       | 3.7  | 3.7  | 2.7 |
| A       | 6.30  | 6.30  | 3.3 | B       | 8.1   | 8.1   | 3   | D       | 3.7  | 3.7  | 2.2 |
| A       | 7.60  | 7.60  | 1.9 | B       | 16    | 16    | 12  | D       | 2.8  | 2.8  | 2.3 |
| A       | 4.90  | 4.90  | 3.1 | B       | 12.2  | 12.2  | 8.2 | D       | 7.4  | 7.4  | 3.7 |
| A       | 4.20  | 4.20  | 2.8 | B       | 7.5   | 7.5   | 5   | D       | 5.6  | 5.6  | 4.5 |



| section | L    | I    | S   | section | L   | I   | S   | section | L    | I    | S   |
|---------|------|------|-----|---------|-----|-----|-----|---------|------|------|-----|
| D       | 6.4  | 6.4  | 2.8 | E       | 4.5 | 4.5 | 2.9 | F       | 8.2  | 8.2  | 3.4 |
| D       | 4.3  | 4.3  | 3.5 | E       | 5.3 | 5.3 | 3.3 | F       | 4.4  | 4.4  | 2.2 |
| D       | 4.2  | 4.2  | 2.1 | E       | 5.6 | 5.6 | 3.9 | F       | 5.7  | 5.7  | 1.9 |
| D       | 6.4  | 6.4  | 4.3 | E       | 4   | 4   | 3.1 | F       | 4    | 4    | 1.9 |
| D       | 5.3  | 5.3  | 2.5 | E       | 3.7 | 3.7 | 2.9 | F       | 2.9  | 2.9  | 1.5 |
| D       | 4.4  | 4.4  | 2.3 | E       | 4.5 | 4.5 | 2.5 | F       | 7.3  | 7.3  | 3.7 |
| D       | 10.4 | 10.4 | 3.9 | E       | 9.7 | 9.7 | 3.9 | F       | 7.7  | 7.7  | 2   |
| D       | 8.3  | 8.3  | 3   | E       | 5.4 | 5.4 | 3.4 | F       | 14.5 | 14.5 | 7.5 |
| D       | 6.4  | 6.4  | 4.6 | E       | 4.9 | 4.9 | 3.4 | F       | 10.2 | 10.2 | 9.2 |
| D       | 6.7  | 6.7  | 4.1 | E       | 5   | 5   | 2.4 | G       | 11.5 | 11.5 | 7.5 |
| D       | 4.7  | 4.7  | 3.2 | E       | 5   | 5   | 2.4 | G       | 7.5  | 7.5  | 3.4 |
| D       | 7.6  | 7.6  | 5.6 | E       | 8   | 8   | 3.9 | G       | 5.5  | 5.5  | 2   |
| D       | 6    | 6    | 5.1 | E       | 4.3 | 4.3 | 3   | G       | 4.5  | 4.5  | 2   |
| D       | 6.2  | 6.2  | 5.2 | E       | 4.8 | 4.8 | 2.6 | G       | 2.9  | 2.9  | 1.9 |
| D       | 6.9  | 6.9  | 3.5 | E       | 4.5 | 4.5 | 2.7 | G       | 12.5 | 12.5 | 7   |
| D       | 6.1  | 6.1  | 4.5 | E       | 3.8 | 3.8 | 1.9 | G       | 10.3 | 10.3 | 5.5 |
| D       | 8    | 8    | 4.1 | E       | 7.2 | 7.2 | 4   | G       | 13.5 | 13.5 | 5.5 |
| D       | 5.1  | 5.1  | 2.7 | E       | 6.6 | 6.6 | 3.7 | G       | 7.7  | 7.7  | 5.4 |
| D       | 5.1  | 5.1  | 2.6 | E       | 6   | 6   | 2.5 | G       | 6.5  | 6.5  | 3.9 |
| D       | 3.6  | 3.6  | 2.2 | E       | 3.9 | 3.9 | 2.5 | H       | 16   | 16   | 6.5 |
| D       | 3.8  | 3.8  | 1.7 | E       | 2.6 | 2.6 | 1.4 | H       | 14   | 14   | 7.5 |
| D       | 12.5 | 12.5 | 5.5 | E       | 6.2 | 6.2 | 1.7 | H       | 13.5 | 13.5 | 7.5 |
| D       | 8.1  | 8.1  | 3.2 | E       | 5.4 | 5.4 | 2.8 | H       | 11   | 11   | 6   |
| D       | 5.8  | 5.8  | 3.6 | E       | 4.6 | 4.6 | 2.3 | H       | 7.4  | 7.4  | 3.7 |
| D       | 5.2  | 5.2  | 3.8 | E       | 3.9 | 3.9 | 2.3 | H       | 7.2  | 7.2  | 5.6 |
| D       | 5    | 5    | 2.2 | E       | 3.4 | 3.4 | 1.4 | H       | 11   | 11   | 4.3 |
| D       | 7.6  | 7.6  | 6   | E       | 4.7 | 4.7 | 2.7 | H       | 11.3 | 11.3 | 6.8 |
| D       | 6    | 6    | 4.6 | E       | 4.4 | 4.4 | 2.2 | H       | 10.8 | 10.8 | 7.2 |
| D       | 4.9  | 4.9  | 3.4 | E       | 3.9 | 3.9 | 2   | H       | 11.2 | 11.2 | 5   |
| D       | 4.2  | 4.2  | 2.7 | E       | 4.3 | 4.3 | 2.2 | H       | 8.9  | 8.9  | 3.4 |
| D       | 4.6  | 4.6  | 2.8 | E       | 3.2 | 3.2 | 2.2 | H       | 7.7  | 7.7  | 5.4 |
| E       | 14   | 14   | 6.5 | F       | 6.6 | 6.6 | 3.3 | H       | 7.3  | 7.3  | 4.1 |
| E       | 6.7  | 6.7  | 4.4 | F       | 6.3 | 6.3 | 3.9 | H       | 7.6  | 7.6  | 3.3 |
| E       | 6.9  | 6.9  | 3.7 | F       | 6.4 | 6.4 | 4.3 | H       | 5.3  | 5.3  | 3.9 |
| E       | 5.9  | 5.9  | 2.9 | F       | 4.7 | 4.7 | 2.2 | H       | 10.4 | 10.4 | 6.3 |
| E       | 5.5  | 5.5  | 2.7 | F       | 5.8 | 5.8 | 4.2 | H       | 8.7  | 8.7  | 5.3 |
| E       | 7.5  | 7.5  | 6.2 | F       | 9.3 | 9.3 | 7.5 | H       | 7.6  | 7.6  | 3.7 |
| E       | 8.2  | 8.2  | 6   | F       | 6.7 | 6.7 | 4.6 | H       | 7    | 7    | 4.8 |
| E       | 7.9  | 7.9  | 4.8 | F       | 8   | 8   | 3.3 | H       | 6.2  | 6.2  | 3.1 |
| E       | 6.2  | 6.2  | 5.8 | F       | 7.3 | 7.3 | 2.2 | I       | 12.3 | 12.3 | 5   |
| E       | 5.4  | 5.4  | 3.2 | F       | 5.3 | 5.3 | 3.2 | I       | 7.3  | 7.3  | 8   |
| E       | 9.1  | 9.1  | 3.7 | F       | 7.4 | 7.4 | 4.6 | I       | 12   | 12   | 5.2 |
| E       | 4.6  | 4.6  | 3.4 | F       | 7.6 | 7.6 | 4.7 | I       | 8.5  | 8.5  | 4   |
| E       | 4.8  | 4.8  | 2.6 | F       | 7.7 | 7.7 | 5   | I       | 6.5  | 6.5  | 4   |
| E       | 3.8  | 3.8  | 1.7 | F       | 7.6 | 7.6 | 4.6 |         |      |      |     |
| E       | 3.1  | 3.1  | 2.2 | F       | 4.9 | 4.9 | 2.8 |         |      |      |     |
| E       | 7.4  | 7.4  | 4.5 | F       | 8.2 | 8.2 | 4.3 |         |      |      |     |
| E       | 6.3  | 6.3  | 4   | F       | 8.2 | 8.2 | 4.3 |         |      |      |     |
| E       | 6    | 6    | 3.6 | F       | 5.2 | 5.2 | 2   |         |      |      |     |
| E       | 5.2  | 5.2  | 2.6 | F       | 4.3 | 4.3 | 1.9 |         |      |      |     |
| E       | 5.1  | 5.1  | 3.5 | F       | 3.6 | 3.6 | 2.2 |         |      |      |     |
| E       | 8.1  | 8.1  | 4.8 | F       | 3.8 | 3.8 | 2.3 |         |      |      |     |
| E       | 6.7  | 6.7  | 4.6 | F       | 3.6 | 3.6 | 2.3 |         |      |      |     |
| E       | 5.5  | 5.5  | 4.2 | F       | 2.8 | 2.8 | 1.3 |         |      |      |     |
| E       | 4.8  | 4.8  | 3.6 | F       | 2.4 | 2.4 | 1.6 |         |      |      |     |

**B: Measurements on quartz latite clasts (location of sections see Fig. 4.11)**

| section | L    | I    | S    | section | L    | I    | S    | section | L    | I    | S    |
|---------|------|------|------|---------|------|------|------|---------|------|------|------|
| A       | 26   | 14   | 13.5 | A       | 31   | 18   | 14.5 | B       | 28.5 | 16   | 13   |
| A       | 23   | 11   | 10   | A       | 34   | 15.5 | 9    | B       | 39   | 15   | 13   |
| A       | 23.5 | 18   | 9    | A       | 21   | 16   | 16   | B       | 20   | 15   | 15   |
| A       | 22   | 12   | 11   | A       | 25   | 19   | 14   | B       | 18   | 11   | 11   |
| A       | 22   | 17   | 13   | A       | 22   | 17.5 | 13.5 | B       | 22   | 17   | 16   |
| A       | 19   | 14.5 | 7.5  | A       | 26   | 14.5 | 7.5  | B       | 28   | 21   | 12   |
| A       | 22.5 | 16.5 | 10.5 | A       | 17   | 16   | 8.7  | B       | 20   | 14   | 10   |
| A       | 23   | 16   | 11.5 | A       | 34   | 12.5 | 10.5 | B       | 27   | 19   | 15.5 |
| A       | 18.5 | 10.5 | 6    | A       | 25   | 16.5 | 12.5 | B       | 27.5 | 23   | 15.5 |
| A       | 17.5 | 9.5  | 8    | A       | 36   | 19   | 10   | B       | 29   | 15.5 | 15   |
| A       | 29   | 13.5 | 10   | A       | 22   | 19   | 13   | B       | 19   | 16   | 14   |
| A       | 20   | 10.5 | 10   | A       | 23.5 | 18   | 14   | B       | 20.5 | 16   | 16   |
| A       | 16   | 10.5 | 10.5 | A       | 25.5 | 20   | 10   | B       | 18   | 12.5 | 11   |
| A       | 18   | 10   | 6    | A       | 24   | 19.5 | 15.5 | B       | 23.5 | 12   | 11   |
| A       | 17.5 | 9.5  | 6.5  | A       | 25   | 15.5 | 12.5 | B       | 23.5 | 15   | 14.5 |
| A       | 23.5 | 11.5 | 10.5 | A       | 23   | 15   | 14.5 | B       | 22   | 18.5 | 14   |
| A       | 20.5 | 13   | 7    | A       | 26   | 19   | 11.5 | B       | 24.5 | 14   | 12   |
| A       | 20   | 15   | 10.5 | A       | 30   | 18   | 16.5 | B       | 24   | 23   | 11   |
| A       | 12.5 | 6.5  | 4.5  | A       | 35   | 23   | 13   | B       | 24   | 16.5 | 12   |
| A       | 24.5 | 18   | 11.5 | A       | 22.5 | 18   | 7.5  | B       | 17   | 10.5 | 6    |
| A       | 25   | 25   | 21   | A       | 26   | 11.5 | 8.5  | B       | 15.5 | 12   | 6.5  |
| A       | 32   | 23.5 | 13   | A       | 25   | 14.5 | 8    | B       | 22   | 10   | 7    |
| A       | 38   | 22   | 10   | A       | 29   | 15.5 | 8.5  | B       | 31   | 14.5 | 13.5 |
| A       | 24.5 | 15.5 | 11   | A       | 18   | 15.5 | 11.5 | B       | 26.5 | 17.5 | 16   |
| A       | 38   | 23   | 15.5 | A       | 24   | 19.5 | 14   | B       | 29.5 | 14.5 | 6    |
| A       | 54   | 28.5 | 19   | A       | 16   | 16   | 9.5  | B       | 21   | 9    | 8.5  |
| A       | 35   | 24   | 9.5  | A       | 30   | 15   | 12   | B       | 20   | 12   | 4    |
| A       | 20   | 16.5 | 12   | A       | 17   | 12.5 | 10   | B       | 27.5 | 27.5 | 15   |
| A       | 36   | 20.5 | 17   | A       | 21.5 | 16   | 10   | B       | 26.5 | 26.5 | 11.5 |
| A       | 23   | 20.5 | 10   | A       | 23   | 18   | 10   | B       | 27.5 | 27.5 | 9.5  |
| A       | 21   | 13   | 11   | A       | 29   | 14.5 | 11   | B       | 18   | 18   | 8.5  |
| A       | 22   | 12   | 11   | A       | 40   | 21   | 10.5 | B       | 19   | 19   | 7    |
| A       | 15.5 | 7.5  | 5    | A       | 29   | 23   | 8.5  | C       | 12.9 | 8.2  | 5.9  |
| A       | 17   | 14   | 10.5 | A       | 25.5 | 14   | 9    | C       | 10.7 | 6.5  | 4.3  |
| A       | 20   | 7.5  | 7    | B       | 22   | 21   | 18.5 | C       | 9.2  | 6.1  | 6.1  |
| A       | 22   | 17   | 8.5  | B       | 16   | 9    | 4.2  | C       | 9    | 6.3  | 4.7  |
| A       | 20   | 8.5  | 7    | B       | 12.5 | 8.5  | 8.5  | C       | 6.2  | 5.9  | 4.5  |
| A       | 21   | 14.5 | 4    | B       | 16   | 11   | 4.8  | C       | 8.4  | 6.2  | 4.5  |
| A       | 14   | 12   | 6.5  | B       | 16.5 | 15   | 5.6  | C       | 7.8  | 4.2  | 3.9  |
| A       | 15   | 12.5 | 4    | B       | 11   | 8.8  | 4.6  | C       | 31.5 | 24   | 13.5 |
| A       | 36   | 14   | 13   | B       | 23   | 18   | 15.5 | C       | 26   | 18.5 | 18   |
| A       | 24.5 | 12   | 6    | B       | 24   | 18.5 | 14.5 | C       | 33   | 17.5 | 13   |
| A       | 25   | 10   | 9    | B       | 23   | 19   | 4    | C       | 24.5 | 15   | 10   |
| A       | 17   | 8.5  | 6.5  | B       | 23.5 | 11.5 | 10   | C       | 27.5 | 20   | 14.5 |
| A       | 18   | 11.5 | 9    | B       | 26   | 19   | 12   | C       | 40   | 23.5 | 12.5 |
| A       | 26   | 16   | 13.5 | B       | 19   | 14   | 9    | C       | 35   | 22   | 19   |
| A       | 21   | 18   | 16   | B       | 48   | 27   | 23   | C       | 13.5 | 8    | 4.1  |
| A       | 25.5 | 16.5 | 16   | B       | 29   | 21   | 14   | C       | 16   | 6.5  | 2.9  |
| A       | 38   | 22   | 16.5 | B       | 26   | 11.5 | 8.5  | C       | 12.5 | 10.5 | 6    |
| A       | 26   | 22   | 19   | B       | 27   | 21   | 17   | C       | 10.4 | 9    | 4.7  |
| A       | 28   | 15   | 12   | B       | 28.5 | 16.5 | 13   | C       | 8    | 6.6  | 5.4  |

| section | L    | I    | S    | section | L    | I    | S    | section | L    | I    | S    | section | L    | I    | S    |
|---------|------|------|------|---------|------|------|------|---------|------|------|------|---------|------|------|------|
| C       | 7.7  | 5.6  | 5.6  | D       | 17.5 | 14.5 | 10.5 | E       | 25   | 13   | 12   | H       | 41   | 23   | 5    |
| C       | 8.7  | 5.9  | 5.2  | D       | 16   | 7.5  | 2.5  | E       | 20   | 16   | 9    | H       | 31   | 23   | 4.5  |
| C       | 26   | 17   | 15   | D       | 14   | 10.5 | 8    | F       | 20   | 15   | 11.5 | H       | 21   | 18.5 | 13.5 |
| C       | 18.5 | 12.5 | 12   | D       | 12.5 | 10.5 | 9    | F       | 23   | 10.5 | 7.5  | H       | 46.5 | 38   | 28   |
| C       | 17   | 12.5 | 12   | D       | 18.5 | 10   | 7.5  | F       | 15   | 10.5 | 9.5  | H       | 55   | 48.5 | 13.5 |
| C       | 16   | 6.4  | 4.1  | D       | 9    | 7.5  | 6    | F       | 17   | 11.5 | 10.5 | H       | 31.5 | 23.5 | 12.5 |
| C       | 11.4 | 8    | 6.2  | E       | 10.5 | 8.6  | 6.7  | F       | 15.5 | 10.5 | 4.5  | H       | 24   | 20   | 4.5  |
| C       | 14   | 7.3  | 5.6  | E       | 12.5 | 5.8  | 4.7  | F       | 17.5 | 10   | 9.8  | H       | 25.5 | 14   | 9.5  |
| C       | 10.6 | 6.4  | 6.1  | E       | 8.7  | 7.6  | 3.5  | F       | 18.7 | 10   | 5.4  | H       | 41   | 18   | 14   |
| D       | 22.5 | 15   | 12.5 | E       | 12.9 | 9.8  | 8    | F       | 9.5  | 10   | 8    | H       | 36   | 30   | 19   |
| D       | 20   | 19   | 8.5  | E       | 13.2 | 4.4  | 4.3  | F       | 12.5 | 8.5  | 7.5  | H       | 23.5 | 13.5 | 12.5 |
| D       | 19.5 | 18   | 11.5 | E       | 26   | 14   | 12   | F       | 17   | 5.5  | 5    | H       | 53   | 53   | 31   |
| D       | 19.5 | 14   | 8    | E       | 23   | 15.5 | 14.5 | F       | 33   | 26   | 18   | H       | 27   | 23   | 11   |
| D       | 20   | 14   | 9    | E       | 18   | 15.5 | 12.2 | F       | 25.5 | 11.5 | 9    | H       | 40   | 35.5 | 15.5 |
| D       | 18   | 11   | 10   | E       | 31   | 17   | 14   | F       | 25   | 18   | 9    | I       | 146  | 97   | 34   |
| D       | 35   | 24.5 | 13.5 | E       | 21   | 14   | 13   | F       | 53   | 26   | 9.5  | I       | 132  | 92   | 55   |
| D       | 28   | 13   | 6    | E       | 24   | 10.5 | 9.5  | F       | 37   | 32   | 25   | I       | 47   | 47   | 43   |
| D       | 26   | 18   | 4.5  | E       | 19.5 | 13   | 5    | F       | 16   | 9.5  | 6.6  | I       | 220  | 170  | 88   |
| D       | 19.5 | 17.5 | 11   | E       | 17.5 | 8.2  | 2.1  | F       | 15.5 | 7.5  | 4.5  | I       | 71   | 60   | 21   |
| D       | 23   | 15   | 11   | E       | 18   | 10.6 | 4.3  | F       | 15   | 12.5 | 9.5  | I       | 144  | 96   | 70   |
| D       | 22.5 | 14.5 | 6.5  | E       | 15   | 11.6 | 2.8  | F       | 14   | 10.5 | 8.4  | I       | 108  | 61   | 39   |
| D       | 22   | 12.5 | 10.5 | E       | 15.5 | 5.3  | 4.2  | F       | 12.5 | 7.5  | 6    |         |      |      |      |
| D       | 14.5 | 10.5 | 9    | E       | 11.5 | 9    | 3.9  | F       | 19   | 12   | 9    |         |      |      |      |
| D       | 14.5 | 8.5  | 7.5  | E       | 11   | 4.7  | 2.3  | F       | 21.5 | 10.5 | 8    |         |      |      |      |
| D       | 15   | 7.5  | 7    | E       | 8    | 5.7  | 3.3  | F       | 16   | 10   | 2.5  |         |      |      |      |
| D       | 11   | 6.5  | 6    | E       | 6.6  | 4.2  | 2.7  | F       | 22   | 11.5 | 9.5  |         |      |      |      |
| D       | 13   | 11.5 | 10   | E       | 5.6  | 3.9  | 1.4  | F       | 16   | 9.5  | 6    |         |      |      |      |
| D       | 18.5 | 12.5 | 6    | E       | 20.5 | 13   | 9.8  | F       | 15   | 8    | 4.5  |         |      |      |      |
| D       | 18.5 | 16.5 | 9    | E       | 16.5 | 10.8 | 6.8  | F       | 24   | 12.5 | 11   |         |      |      |      |
| D       | 18   | 10   | 9    | E       | 9.4  | 8    | 7.1  | F       | 21.5 | 18.5 | 10.5 |         |      |      |      |
| D       | 18   | 10.5 | 7.5  | E       | 11.2 | 11.2 | 3.1  | F       | 18.5 | 15   | 10   |         |      |      |      |
| D       | 12   | 11   | 10.5 | E       | 22   | 14.5 | 13   | F       | 25   | 15.5 | 9.5  |         |      |      |      |
| D       | 10.5 | 9.5  | 5.5  | E       | 24   | 16   | 13.5 | F       | 19.5 | 14.5 | 4.5  |         |      |      |      |
| D       | 26   | 15.5 | 10.5 | E       | 12   | 10.5 | 9    | F       | 34   | 22.5 | 17   |         |      |      |      |
| D       | 23   | 11.5 | 9.5  | E       | 18.2 | 13.5 | 11.5 | F       | 34   | 10   | 7    |         |      |      |      |
| D       | 20.5 | 14   | 7.5  | E       | 25   | 20   | 17   | F       | 50   | 25   | 17.5 |         |      |      |      |
| D       | 20.5 | 7.5  | 7    | E       | 16.5 | 12   | 11   | F       | 25   | 18   | 9.5  |         |      |      |      |
| D       | 22   | 11   | 9    | E       | 17.5 | 14   | 11.5 | F       | 33   | 20.5 | 12   |         |      |      |      |
| D       | 20   | 11   | 10.5 | E       | 16.5 | 8.5  | 8    | F       | 41   | 21   | 20   |         |      |      |      |
| D       | 21.5 | 9    | 8    | E       | 15   | 14   | 13   | G       | 28   | 14.5 | 13.2 |         |      |      |      |
| D       | 18.5 | 13.5 | 13   | E       | 19.5 | 13   | 5.4  | G       | 17   | 11   | 4.3  |         |      |      |      |
| D       | 19   | 10   | 7    | E       | 17.8 | 11.5 | 3.3  | G       | 17.2 | 7    | 4.5  |         |      |      |      |
| D       | 14.5 | 13.5 | 11.5 | E       | 15   | 7.8  | 6.3  | G       | 15.5 | 7    | 6.5  |         |      |      |      |
| D       | 13   | 9.5  | 9.5  | E       | 14.5 | 9.5  | 4.7  | G       | 16.5 | 6.5  | 5.5  |         |      |      |      |
| D       | 21   | 7.5  | 5    | E       | 16.5 | 9.5  | 7.5  | G       | 23   | 16.5 | 15.5 |         |      |      |      |
| D       | 19   | 11   | 10.5 | E       | 10.2 | 9.4  | 3.5  | G       | 25   | 10   | 9    |         |      |      |      |
| D       | 17   | 9    | 7    | E       | 10.8 | 6.2  | 4.7  | G       | 27   | 12.5 | 10.5 |         |      |      |      |
| D       | 15   | 10   | 5.5  | E       | 9.7  | 7.3  | 4    | G       | 26   | 12.5 | 7.5  |         |      |      |      |
| D       | 9.5  | 9.5  | 6    | E       | 41.5 | 22.5 | 15   | G       | 23.5 | 10.2 | 6.5  |         |      |      |      |
| D       | 11   | 7    | 6.5  | E       | 26.5 | 22.5 | 12   | H       | 56   | 24   | 28   |         |      |      |      |
| D       | 36   | 26.5 | 14.5 | E       | 19   | 10.5 | 7    | H       | 40   | 29.5 | 19.5 |         |      |      |      |
| D       | 31.5 | 17   | 13.5 | E       | 18   | 11.5 | 11   | H       | 46   | 23   | 20   |         |      |      |      |
| D       | 20   | 19.5 | 12   | E       | 22   | 19   | 13   | H       | 39   | 37   | 24   |         |      |      |      |
| D       | 23   | 13   | 11   | E       | 28   | 14   | 10.5 | H       | 33.5 | 19.5 | 11   |         |      |      |      |
| D       | 20   | 19   | 15   | E       | 32   | 25   | 9.5  | H       | 41   | 22.5 | 9    |         |      |      |      |

## C: Measurements on quartz latite clasts (location of sections see Fig. 4.14)

| section | L    | I    | S    | section | L    | I    | S   | section | L    | I    | S   | section | L    | I    | S   |
|---------|------|------|------|---------|------|------|-----|---------|------|------|-----|---------|------|------|-----|
| 3,8     | 22   | 14,5 | 2,5  | 5,4     | 22,5 | 20   | 3   | 7,4     | 22   | 19   | 8   | 11,9    | 8,3  | 3,4  | 1,6 |
| 3,8     | 20   | 13   | 7,5  | 5,4     | 25   | 14   | 7   | 8,8     | 22   | 10   | 9   | 11,9    | 6,5  | 5    | 1,5 |
| 3,8     | 20,5 | 16,5 | 7,5  | 5,4     | 20   | 16   | 4   | 8,8     | 10,5 | 10   | 8   | 11,9    | 6    | 2,5  | 0,7 |
| 3,8     | 22,5 | 11,5 | 7    | 5,4     | 35   | 13   | 9   | 8,8     | 11   | 6,5  | 5   | 11,9    | 5,2  | 1,5  | 0,5 |
| 3,8     | 24   | 22,5 | 10   | 5,4     | 36   | 17   | 8   | 8,8     | 10,5 | 8,5  | 4,5 | 11,9    | 4    | 2,7  | 0,7 |
| 3,8     | 14,5 | 10   | 7,5  | 5,4     | 31   | 18   | 12  | 8,8     | 15   | 4,5  | 3,5 | 11,9    | 4,5  | 3    | 1   |
| 3,8     | 16   | 11   | 10   | 5,4     | 5    | 3,5  | 3   | 8,8     | 21,5 | 15   | 10  | 11,9    | 8    | 4,3  | 1,2 |
| 3,8     | 25,5 | 21   | 12   | 5,4     | 4    | 2,5  | 0,7 | 8,8     | 16   | 11   | 7,5 | 11,9    | 22   | 11,5 | 9   |
| 3,8     | 19   | 18,5 | 10   | 5,4     | 6,5  | 4,5  | 1,5 | 8,8     | 13   | 11   | 7   | 11,9    | 20   | 14   | 10  |
| 3,8     | 24   | 12,5 | 9    | 5,4     | 3    | 2,3  | 2   | 8,8     | 14   | 7,5  | 4   | 11,9    | 21   | 13   | 7   |
| 3,8     | 19,5 | 10   | 6    | 5,4     | 3    | 2,5  | 1,7 | 8,8     | 20   | 9,5  | 6   | 11,9    | 20   | 10   | 5   |
| 3,8     | 14,5 | 9,5  | 7,5  | 5,4     | 2,5  | 1,7  | 0,7 | 8,8     | 19   | 15   | 11  | 11,9    | 22   | 10   | 7,5 |
| 3,8     | 12,5 | 9,5  | 7    | 5,4     | 8    | 3,5  | 2   | 8,8     | 32   | 21   | 17  | 11,9    | 18   | 7,5  | 7   |
| 3,8     | 15   | 8,5  | 6    | 5,4     | 6    | 3,2  | 1,7 | 8,8     | 27   | 23   | 12  | 11,9    | 16,5 | 13   | 7   |
| 3,8     | 17   | 11   | 7    | 5,4     | 5,5  | 3    | 1,5 | 8,8     | 23   | 20   | 9   | 11,9    | 23   | 18   | 8   |
| 3,8     | 45   | 20   | 6    | 5,4     | 5    | 2,5  | 1,5 | 8,8     | 35   | 14   | 9   | 11,9    | 21   | 12   | 6   |
| 3,8     | 25,5 | 12,5 | 5    | 5,4     | 23   | 15   | 10  | 8,8     | 35   | 20   | 13  | 11,9    | 22   | 14   | 10  |
| 3,8     | 15   | 14   | 8,5  | 5,4     | 18   | 12,5 | 6,5 | 8,8     | 28   | 12   | 11  | 11,9    | 7,5  | 3,5  | 2   |
| 3,8     | 26   | 16,5 | 4    | 5,4     | 23   | 21,5 | 12  | 8,8     | 30   | 19   | 16  | 11,9    | 10   | 7,5  | 1,5 |
| 3,8     | 20   | 16   | 12   | 5,4     | 30   | 10   | 6   | 8,8     | 40   | 28   | 23  | 11,9    | 13   | 10   | 3   |
| 4,8     | 25,5 | 11,5 | 7    | 5,4     | 20   | 15   | 7   | 8,8     | 34   | 19   | 8   | 11,9    | 10   | 8    | 4   |
| 4,8     | 27,5 | 14,5 | 8    | 5,4     | 28   | 14,5 | 9   | 8,8     | 60   | 18   | 13  | 11,9    | 11   | 10   | 2   |
| 4,8     | 20   | 16   | 7,5  | 5,4     | 29   | 15   | 3   | 10,2    | 9,5  | 6,5  | 3   | 11,9    | 12   | 7    | 2,5 |
| 4,8     | 19   | 14,5 | 10   | 5,4     | 22   | 14,5 | 4   | 10,2    | 10   | 6    | 4   | 11,9    | 10,5 | 6,5  | 2,5 |
| 4,8     | 20,5 | 14   | 6    | 5,4     | 28   | 24   | 13  | 10,2    | 8,5  | 7    | 4   | 11,9    | 9,5  | 8    | 2   |
| 4,8     | 20   | 11   | 8    | 5,4     | 32   | 16   | 7   | 10,2    | 8    | 5,5  | 3,5 | 11,9    | 11   | 10   | 4,5 |
| 4,8     | 41,5 | 29,5 | 15   | 6,6     | 11   | 3,5  | 2   | 10,2    | 12   | 4,5  | 2   | 11,9    | 10   | 9    | 3,5 |
| 4,8     | 27,5 | 23,5 | 12   | 6,6     | 10   | 8,5  | 3,5 | 10,2    | 13,5 | 10   | 3   | 11,9    | 28   | 15   | 5   |
| 4,8     | 24   | 12   | 10   | 6,6     | 6,5  | 5,5  | 4   | 10,2    | 14   | 9,5  | 4   | 11,9    | 21   | 15   | 11  |
| 4,8     | 42   | 12   | 11   | 6,6     | 9    | 5    | 1,5 | 10,2    | 11,5 | 8,5  | 2,5 | 11,9    | 40   | 34   | 14  |
| 5,4     | 24,5 | 19,5 | 8    | 6,6     | 7    | 6    | 3,5 | 10,2    | 10,5 | 8,5  | 4,5 | 11,9    | 23   | 6,5  | 4,8 |
| 5,4     | 21   | 13,5 | 8    | 6,6     | 12   | 5    | 3   | 10,2    | 13   | 11   | 4,5 | 11,9    | 16   | 15,5 | 7   |
| 5,4     | 21,5 | 16   | 6,5  | 6,6     | 11   | 8,5  | 6,5 | 10,2    | 22   | 18   | 7   | 11,9    | 20   | 14   | 9   |
| 5,4     | 18   | 12   | 7,5  | 6,6     | 8,5  | 5,5  | 4   | 10,2    | 20   | 11   | 6   | 11,9    | 26   | 14   | 9   |
| 5,4     | 29   | 14   | 9    | 6,6     | 10   | 6    | 3,5 | 10,2    | 21   | 12   | 5   | 11,9    | 30   | 18   | 10  |
| 5,4     | 24   | 15   | 10   | 6,6     | 14   | 8,5  | 3   | 10,2    | 25   | 22   | 14  | 11,9    | 21   | 17   | 16  |
| 5,4     | 27   | 9    | 7    | 6,6     | 20,5 | 13   | 4   | 10,2    | 25   | 21   | 10  | 11,9    | 25   | 21   | 10  |
| 5,4     | 25   | 13,5 | 8,5  | 6,6     | 23   | 15   | 11  | 10,2    | 66   | 40   | 28  | 12,8    | 25   | 13   | 5   |
| 5,4     | 36   | 21   | 15   | 6,6     | 23   | 17   | 5   | 10,2    | 28   | 12   | 8   | 12,8    | 18   | 9    | 7   |
| 5,4     | 27   | 16   | 7    | 6,6     | 23   | 12   | 8,5 | 10,2    | 29   | 21   | 8   | 12,8    | 15   | 11   | 4   |
| 5,4     | 18,5 | 10,5 | 5,5  | 6,6     | 23   | 15   | 4,5 | 10,2    | 20   | 15   | 5   | 12,8    | 16   | 11   | 5   |
| 5,4     | 19,5 | 11   | 9,5  | 6,6     | 29   | 28   | 15  | 11,9    | 17   | 9    | 4   | 12,8    | 23   | 17   | 12  |
| 5,4     | 14,5 | 10   | 7    | 6,6     | 19,5 | 15   | 7   | 11,9    | 19   | 10   | 4   | 12,8    | 22   | 17   | 10  |
| 5,4     | 23   | 11,5 | 6,5  | 6,6     | 25   | 9    | 8   | 11,9    | 22,5 | 8,5  | 4,5 | 12,8    | 18   | 15   | 7   |
| 5,4     | 16   | 8    | 6    | 6,5     | 33   | 19   | 9   | 11,9    | 20   | 8,5  | 3,5 | 12,8    | 20   | 9    | 7   |
| 5,4     | 20   | 15   | 10,5 | 7,4     | 14,5 | 9,5  | 7,5 | 11,9    | 18   | 10   | 8   | 12,8    | 15   | 12   | 8   |
| 5,4     | 17,5 | 10   | 3,5  | 7,4     | 18   | 14,5 | 5   | 11,9    | 16   | 13   | 7,5 | 12,8    | 17   | 11   | 8   |
| 5,4     | 13   | 8,5  | 4,5  | 7,4     | 15   | 10   | 4   | 11,9    | 21   | 17,5 | 7   |         |      |      |     |
| 5,4     | 21,5 | 9,5  | 4    | 7,4     | 16   | 11   | 3,5 | 11,9    | 16   | 12   | 6,5 |         |      |      |     |
| 5,4     | 20,5 | 9,5  | 4    | 7,4     | 16,5 | 11,5 | 5,5 | 11,9    | 18   | 8,5  | 5   |         |      |      |     |
| 5,4     | 24   | 13   | 6    | 7,4     | 17,5 | 15   | 6,5 | 11,9    | 19   | 8,5  | 5   |         |      |      |     |
| 5,4     | 20   | 13   | 7    | 7,4     | 18,5 | 17   | 7   | 11,9    | 16,5 | 7    | 4,5 |         |      |      |     |
| 5,4     | 26   | 22   | 10   | 7,4     | 30   | 20   | 10  | 11,9    | 6,5  | 3    | 2,5 |         |      |      |     |
| 5,4     | 22,5 | 12   | 8    | 7,4     | 18   | 17   | 4,5 | 11,9    | 7    | 5,5  | 2,3 |         |      |      |     |

**Appendix III:** Grain size parameter of samples from of the Koigab River

A: channel sands (location of sections see Fig. 4.11)

| section | mean  | median | standard deviation | skewness |
|---------|-------|--------|--------------------|----------|
| A       | 1,74  | 1,72   | 1,22               | -0,3     |
| A       | 1,51  | 1,06   | 1,50               | -0,51    |
| A       | 1,89  | 1,65   | 1,20               | -0,44    |
| A       | 2,18  | 2,09   | 0,99               | -0,30    |
| A       | 1,89  | 1,83   | 1,00               | -0,30    |
| A       | 1,32  | 0,63   | 1,91               | -0,50    |
| B       | 0,32  | -0,24  | 2,08               | -0,34    |
| B       | -1,00 | -0,89  | 2,11               | 0,04     |
| B       | 1,64  | 1,18   | 1,55               | -0,46    |
| C       | 1,00  | 0,66   | 1,58               | -0,31    |
| C       | 1,51  | 0,95   | 1,65               | -0,51    |
| D       | 1,94  | 1,93   | 0,84               | -0,61    |
| D       | 0,00  | -0,14  | 1,89               | -0,611   |
| D       | 2,00  | 1,98   | 0,66               | -0,03    |
| D       | 0,74  | 0,06   | 2,32               | -0,40    |
| D       | 1,69  | 1,39   | 1,42               | -0,44    |
| D       | 2,06  | 2,08   | 0,74               | 0,10     |
| D       | 0,79  | -0,03  | 2,22               | -0,44    |
| D       | 1,56  | 1,29   | 1,35               | -0,42    |
| E       | 0,97  | 0,39   | 1,86               | -0,36    |
| E       | 1,29  | 0,59   | 2,03               | -0,46    |
| E       | 1,74  | 1,66   | 1,11               | -0,30    |
| E       | 1,43  | 1,08   | 1,44               | -0,35    |
| E       | 0,32  | 0,65   | 2,03               | -0,18    |
| E       | 1,74  | 1,71   | 1,06               | -0,15    |
| E       | 1,25  | 0,86   | 1,54               | -0,32    |
| E       | 1,32  | 0,79   | 1,61               | -0,45    |
| E       | 1,69  | 1,50   | 1,33               | -0,32    |
| F       | 1,32  | 0,83   | 1,61               | -0,43    |
| F       | 1,69  | 1,72   | 0,91               | -0,16    |
| F       | 2,25  | 2,20   | 0,91               | -0,20    |
| G       | -0,85 | -0,51  | 1,96               | 0,21     |
| G       | -1,68 | -1,22  | 2,34               | 0,24     |
| H       | 0,10  | -0,48  | 2,35               | -0,30    |
| H       | -1,81 | -1,70  | 1,81               | 0,23     |
| H       | -1,68 | -0,65  | 2,48               | 0,49     |
| I       | -1,63 | -0,99  | 2,31               | 0,39     |



**B: aeolian sands (location of sections see Fig. 4.11)**

| section | mean | median | standard deviation | skewness | kurtosis |
|---------|------|--------|--------------------|----------|----------|
| A       | 1,74 | 1,64   | 0,75               | 0,21     | 1,04     |
| A       | 2,12 | 2,06   | 0,83               | 0,20     | 1,09     |
| A       | 1,83 | 1,74   | 0,83               | -0,10    | 1,12     |
| A       | 1,68 | 1,60   | 0,55               | 0,25     | 1,05     |
| B       | 1,84 | 1,74   | 0,61               | 0,20     | 0,77     |
| B       | 2,05 | 2,12   | 0,57               | -0,14    | 0,80     |
| B       | 2,07 | 2,12   | 0,56               | -0,13    | 0,83     |
| C       | 1,72 | 1,64   | 0,54               | 0,21     | 1,03     |
| C       | 1,97 | 2,06   | 0,87               | -0,25    | 1,12     |
| C       | 1,86 | 1,79   | 0,60               | 0,16     | 0,79     |
| D       | 1,73 | 2,25   | 1,43               | -0,47    | 1,56     |
| D       | 1,78 | 1,69   | 0,60               | 0,15     | 0,95     |
| D       | 1,65 | 1,60   | 0,52               | 0,20     | 1,05     |
| D       | 2,61 | 2,56   | 1,21               | -0,10    | 1,28     |
| D       | 1,74 | 1,64   | 0,58               | 0,24     | 1,02     |
| E       | 1,89 | 1,79   | 0,69               | 0,27     | 0,95     |
| E       | 0,92 | 1,47   | 1,65               | -0,49    | 0,69     |
| E       | 0,94 | 1,60   | 1,67               | -0,57    | 0,60     |
| E       | 2,43 | 2,56   | 0,58               | -0,15    | 1,49     |
| F       | 2,01 | 1,94   | 0,73               | 0,24     | 0,99     |
| F       | 2,00 | 1,89   | 0,75               | 0,25     | 0,88     |
| F       | 2,23 | 2,18   | 1,09               | -0,02    | 1,11     |
| F       | 1,97 | 1,89   | 0,71               | 0,20     | 0,83     |
| F       | 1,89 | 1,79   | 0,70               | 0,27     | 0,94     |
| G       | 2,28 | 2,40   | 0,73               | -0,09    | 1,06     |
| G       | 2,68 | 2,56   | 0,72               | 0,16     | 1,25     |
| G       | 2,60 | 2,56   | 0,46               | 0,23     | 1,47     |
| G       | 2,77 | 2,64   | 0,62               | 0,23     | 1,08     |
| G       | 2,72 | 2,56   | 0,66               | 0,25     | 1,24     |
| H       | 2,93 | 2,84   | 0,65               | 0,22     | 0,95     |
| I       | 2,68 | 2,56   | 0,73               | 0,19     | 1,12     |

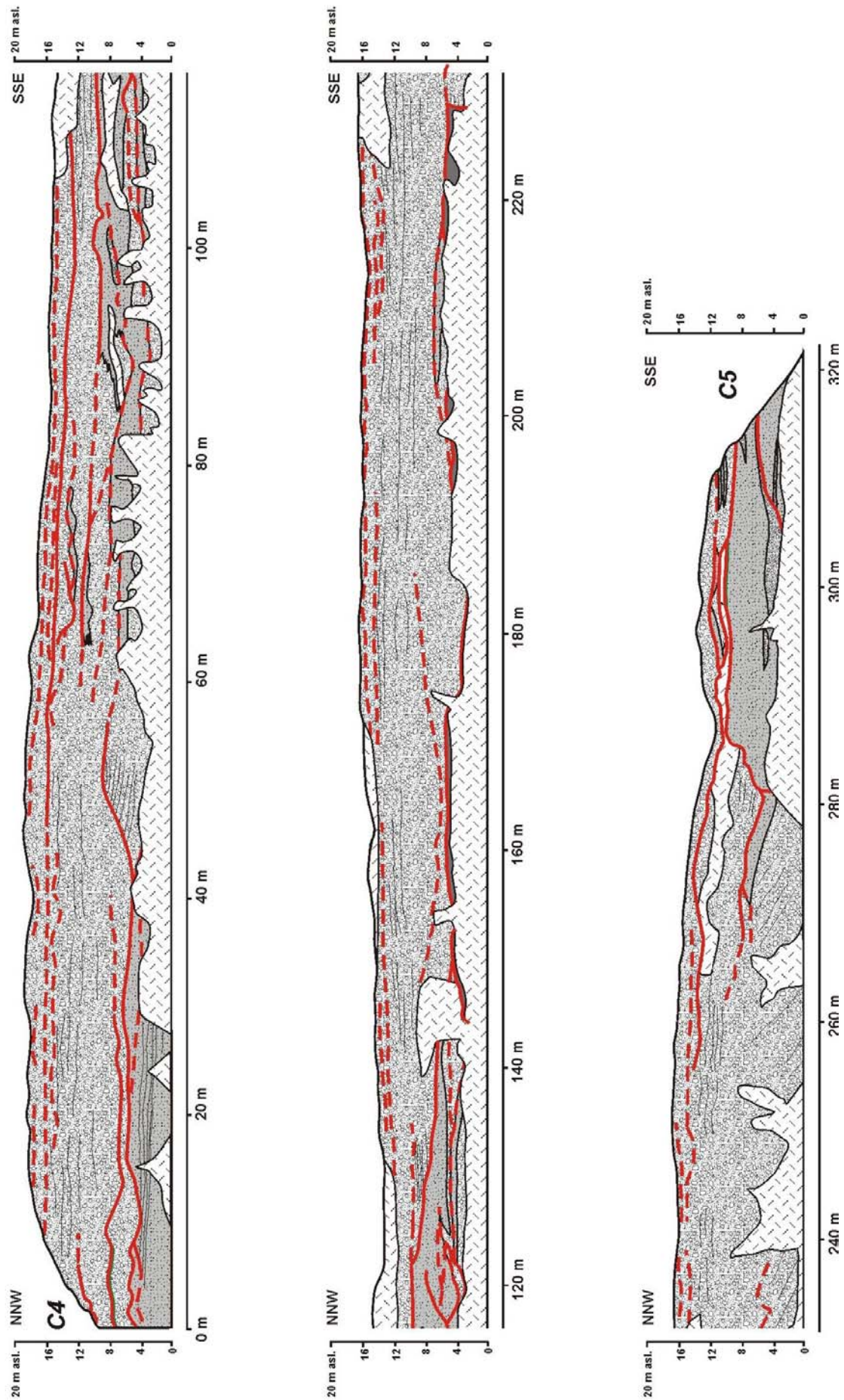
**Appendix VI: Grain size parameter of shrub coppice samples from the Koigab Fan (location of sections see Fig. 4.20)**

| section | mean | median | standard deviation | skewness | kurtosis |
|---------|------|--------|--------------------|----------|----------|
| 0       | 1,94 | 1,93   | 0,79               | -0,07    | 1,01     |
| 0       | 2,32 | 2,19   | 0,52               | -0,27    | 1,06     |
| 1       | 2,00 | 2,02   | 0,69               | 0,11     | 0,88     |
| 2,3     | 1,69 | 1,82   | 0,64               | 0,30     | 1,08     |
| 7,4     | 1,60 | 1,66   | 0,50               | 0,23     | 1,01     |
| 10,5    | 1,89 | 1,92   | 0,59               | 0,09     | 0,77     |
| 11,8    | 1,74 | 1,82   | 0,56               | 0,17     | 0,87     |
| 13,1    | 2,25 | 2,17   | 0,59               | -0,15    | 0,90     |
| 15      | 2,25 | 2,17   | 0,70               | -0,04    | 0,87     |
| 19,8    | 1,74 | 1,84   | 0,62               | 0,22     | 0,78     |
| 22,6    | 1,74 | 1,88   | 0,69               | 0,32     | 1,00     |
| 26,9    | 1,47 | 1,50   | 0,63               | 0,15     | 1,17     |

**Appendix VII:** Cross sections of the Uniabmond Fm. seacliff exposures

**A:** Cross section between channelmouths C4 and C5

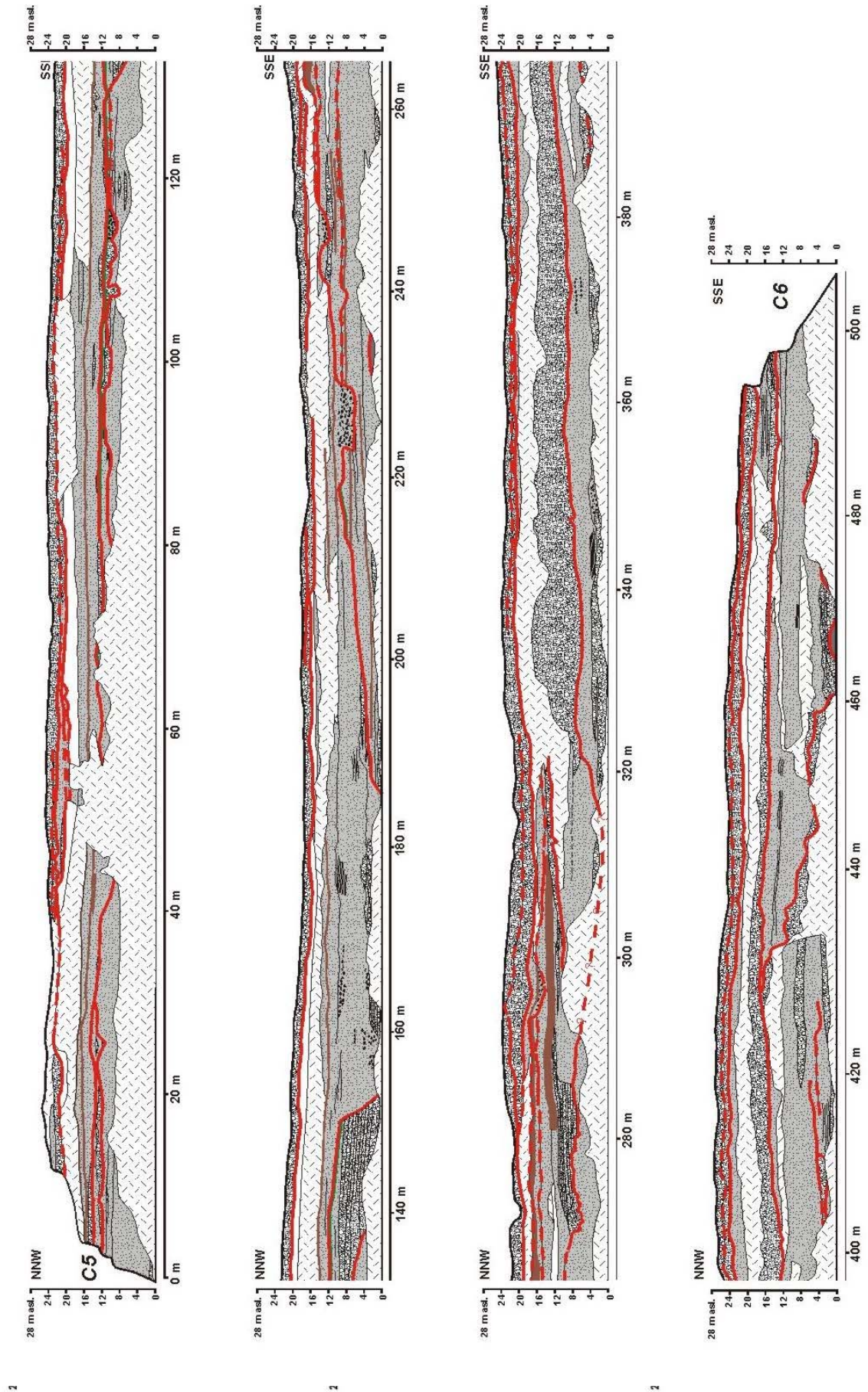
[see Appendix VII C for explanation of symbols]



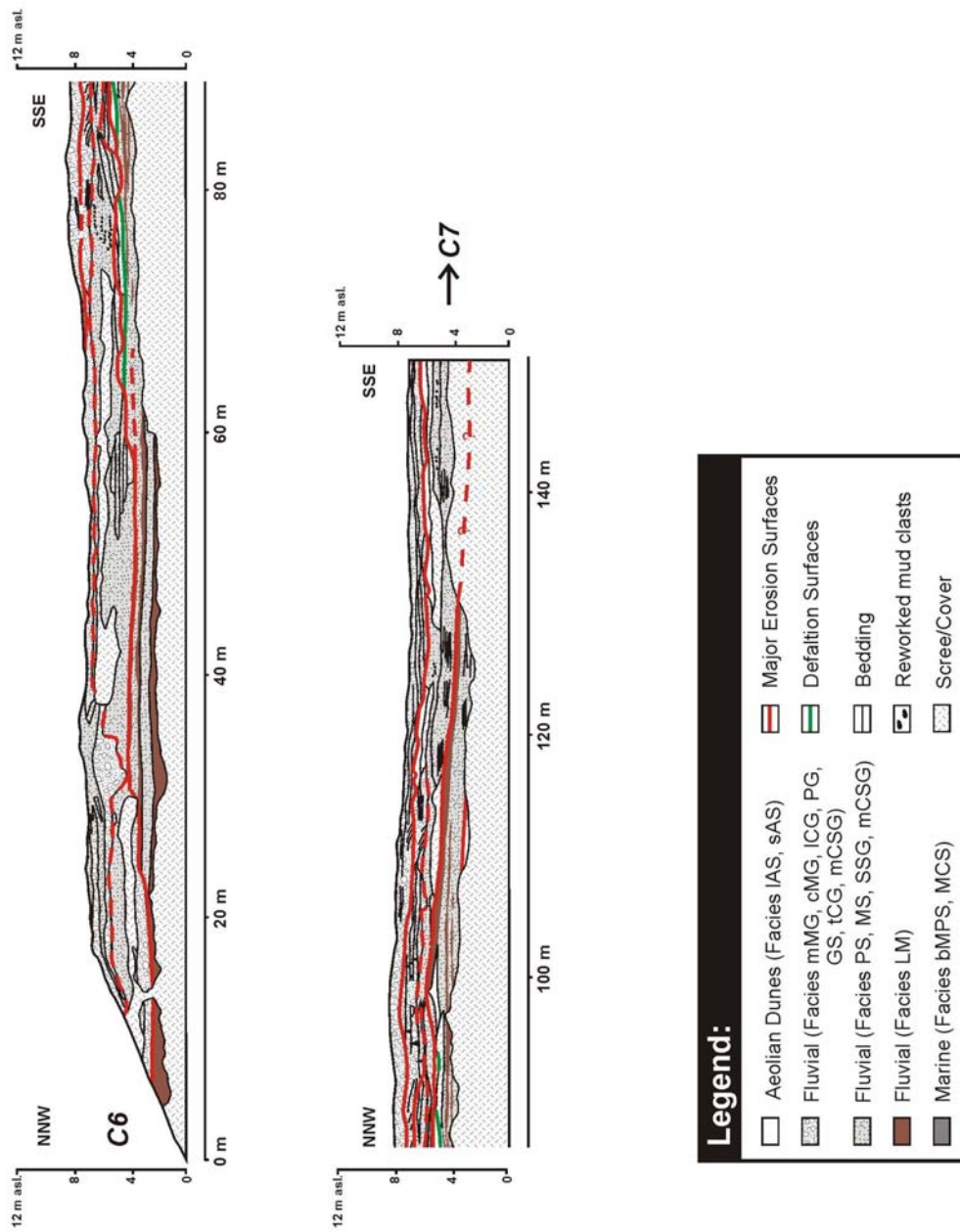


### B: Cross section between channelmouths C5 and C6

[see Appendix VII C for explanation of symbols]



C: Cross section from channelmouths C6 towards C7



**Circulum Vitae**

|               |                           |  |
|---------------|---------------------------|--|
| Name          | Carmen Barbara Elke Krapf |  |
| Geburtsdatum  | 12.02.1973                |  |
| Geburtsort    | Karlstadt                 |  |
| Wohnort       | Aachen                    |  |
| Familienstand | verheiratet               |  |
| Ausbildung    | 1979-1983                 | Grundschule Arnstein   |
|               | 1983-1992                 | Johann-Schöner Gymnasium Karlstadt   |
|               | 1992                      | Abitur   |
|               | 1992-1993                 | Studium Lehramt (LAG) Englisch-Erdkunde<br>Bayer. Julius Maximilians Universität, Würzburg   |
|               | 1993-1999                 | Studium Diplom-Geographie<br>Bayer. Julius Maximilians Universität, Würzburg   |
|               | 1995                      | Vordiplom im Fach Geographie   |
|               | 1999                      | Diplom im Fach Geographie  |
|               | 1999-2002                 | Stipendiatin im Graduiertenkolleg „Geowissenschaftliche Gemeinschaftsforschung in Afrika“<br>Bayer. Julius Maximilians Universität, Würzburg                           |
|               | 2002                      | dreimonatiges Promotionsstipendium des HWP<br>"Programm Chancengleichheit für Frauen in<br>Forschung und Lehre" der Bayer. Julius Maximilians<br>Universität, Würzburg |
|               | seit 10/2002              | Wissenschaftliche Angestellte am Geologischen<br>Institut des Lehrstuhls für Geologie und<br>Paläontologie der Rheinisch-Westfälische<br>Technische Hochschule, Aachen |

Würzburg, 25.02.2003



## **ERKLÄRUNG**

Hiermit erkläre ich, dass ich die vorliegende Dissertation in allen Teilen selbstständig angefertigt habe und keine anderen als die genannten Quellen und Hilfsmittel verwendet habe.

Würzburg, 25.02.2003

Carmen Krapf

Krapf, C.B.E. (2003): Ephemeral river systems at the Skeleton Coast, NW-Namibia - Sedimentological and geomorphological studies on the braided river dominated Koigab Fan, the Cenozoic succession in the Uniabmond area and comparative studies on fluvio-aeolian interaction between ephemeral rivers and the Skeleton Coast Erg. – Dissertation (Dr.rer.nat.) Univ. Würzburg, Germany, 201 pp., 7 Tables, 124 Figures.